**Phylogenomic Systematics of Lichenized Fungi at Multiple Taxonomic Levels**

BY

TODD J. WIDHELM

B.S., University of Nebraska at Omaha, 2005

M.S., University of Nebraska at Omaha, 2008

THESIS

Submitted as partial fulfillment of the requirements

for the degree of Doctor of Philosophy in Biological Sciences

in the Graduate College of the

University of Illinois at Chicago, 2019

Chicago, Illinois

Defense Committee:

Roberta Mason-Gamer, Chair and Advisor
Thorsten Lumbsch, Field Museum
Mary Ashley, Biological Sciences
Boris Igic, Biological Sciences
Stefan Green, DNA sequencing facility

This dissertation is dedicated to my parents Robin and Gary Widhelm for their love and support, and my wife Huini Wu who has been my source for inspiration making this dissertation possible.

## ACKNOWLEDGMENTS

I would like to thank my advisor Dr. Roberta Mason-Gamer for providing the opportunity to pursue a graduate degree and for her direction. I am incredibly grateful to Dr. Thorsten Lumbsch for providing superior guidance in lichen research. I also appreciate Dr. Robert Egan for introducing me to lichenology and for guidance during my master's degree. I also acknowledge Dr. Mary Ashley, Dr. Boris Igic, and Dr. Stefan Green for their support on graduate committees during this Ph.D. program.

The work presented in this dissertation was funded by the Field Museum, the American Bryological and Lichenological Society, and the University of Illinois at Chicago. I also acknowledge the teaching assistantships provided by the University of Illinois at Chicago during this Ph.D. program.

Support in the form of sample collection, molecular laboratory work, data analyses, and communication of the dissertation were aided by Felix Grewe, Jen-Pan Huang, Joel Mercado, Matt Nelsen, Steven D. Leavitt, Ekaphan Kraichak, Nicholas Crouch, Karolis Ramanauskas, Dawson White, Natalia Cortez Delgado, Natalia Ruiz, Francesca R. Bertoletti, Matt J. Asztalos, Bernard Goffinet, Robert Lücking, Bibiana Moncada, Nicolas Magain, Matt von Konrat, Juan Larrain, Peter de Lange, Dan Blanchon, Allison Knight, Gintaras Kantvilas, Taylor Quedenseley, Robert Harms, David Sutherland, and Emmanuël Sérusiaux.

I am also grateful for the support of my extended family and friends. The list of people that made a difference is much too long to put in this work. But I especially thank my wife Huini Wu, parents Robin and Gary Widhelm, and sister and brother-in-law Holly and Brandon Anderson for their love and support.

## CONTRIBUTION OF AUTHORS

**Chapter 2.** Multiple historical processes obscure phylogenetic relationships in a taxonomically difficult group (Lobariaceae, Ascomycota)

T.W. wrote the manuscript, prepared and sequenced the target capture samples, conducted phylogenetic analyses, and generated the figures and tables. T.W. collected some of the specimens in Australia, New Zealand, Chile, and the United States. F.G., J.H., R.L., B.G., R.M., and H.T.L aided with research design and writing the paper. F.G. provided bioinformatic guidance for bait design and dataset assembly. B.G. provided funding for baits. J.M and B.M. provided specimens for the study. All authors reviewed the manuscript.

**Chapter 3.** Oligocene origin and drivers of diversification in the genus *Sticta* (Lobariaceae, Ascomycota)

T.W. wrote the manuscript, performed laboratory work, conducted molecular analyses, and generated figures and tables. T.W. collected some of the specimens in Australia and the United States. J.M. provided specimens from the Caribbean. B.M. provided specimens from South America. E.S. provided specimens from Macronesia. J.H., R.L., B.G., R.M., and H.T.L helped with research design and writing the paper. N.C. provided assistance with statistical analyses. All authors reviewed the manuscript. F.B. and M.A. assisted with molecular laboratory work. All authors reviewed the manuscript.

**Chapter 4.** Using RADseq to understand the circum-Antarctic distribution of the lichenized fungus *Pseudocyphellaria glabra* (Ascomycota, Peltigeraceae)

T.W., F.G., J.H., and H.T.L. planned and designed the research. T.W., F.G., and H.T.L collected the specimens in Australia, New Zealand, and Chile T.W. performed laboratory work and molecular analyses, and generated figures and tables. T.W. wrote the manuscript with help from R.M. and H.T.L. K.R. performed RADseq data assemblies at the University of Illinois at Chicago. All authors reviewed the manuscript.

## CONTRIBUTION OF AUTHORS (continued)

**Chapter 5.** Picking holes in traditional species delimitations: an integrative taxonomic reassessment of the *Parmotrema perforatum* group (Parmeliaceae, Ascomycota)

T.W., R.E, S.L., and H.T.L planned and designed the research. T.W. and R.E. collected the specimens in Texas and Louisiana. T.W. performed laboratory work, conducted molecular analyses and generated figures and tables. T.W. wrote the manuscript with help from R.E., S.L., and H.T.L. E.K. helped with statistical analyses. F.B. and M.A. assisted with molecular laboratory work. All authors reviewed the manuscript.

## TABLE OF CONTENTS

**TABLE OF CONTENTS (continued)**

**TABLE OF CONTENTS (continued)**

## LIST OF TABLES

**LIST OF TABLES (continued)**

## LIST OF FIGURES

## LIST OF FIGURES (continued)

## LIST OF FIGURES (continued)

## LIST OF ABBREVIATIONS

| | |
|---|---|
| AIC | Akaike information criterion |
| AICc | Akaike information criterion corrected for small sample sizes |
| ASTRAL | Accurate Species TRee ALgorithm |
| BAMM | Bayesian Analysis of Macroevolutionary Mixtures |
| BEAST | Bayesian evolutionary analysis sampling trees |
| BI | Bayesian inference |
| BIC | Bayesian information criterion |
| BiSSE | Binary state speciation and extinction |
| BLAST | Basic local alignment search tool |
| BP&P | Bayesian Phylogenetics and Phylogeography |
| BPP | Bayesian posterior probability |
| BS | Bootstrap support |
| CAM | Campbell Island, New Zealand |
| CHI | Chile |
| CTR | Cretaceous Terrestrial Revolution |
| DA | Discriminant analysis |
| DAPC | Discriminant analysis of principal components |
| DEC | Dispersal-extinction-cladogenesis |
| DNA | Deoxyribonucleic acid |
| dNTP | Deoxyribose nucleoside triphosphate |
| ESS | Effective sampling size |
| F | Field Museum Herbarium |
| GLC | General lineage concept |
| *GPD* | Glyceraldehyde-3-phosphate-dehydrogenase |
| GTRGAMMA | General time reversible nucleotide substitution model with gamma distributed rate variation among sites |

## LIST OF ABBREVIATIONS (continued)

| | |
|---|---|
| GT | Horizontal gene transfer |
| IGS | Intergenic spacer |
| ILS | Incomplete lineage sorting |
| ITS | Internal transcribed spacer |
| JGI | Joint Genome Institute |
| K | Number of subpopulations |
| K-Pg | Cretaceous-Paleogene boundary |
| LDD | Long-distance dispersal |
| MAF | Minor allele frequency |
| MAFFT | Multiple alignment using fast Fourier transform |
| *MCM7* | DNA replication licensing factor |
| MCMC | Markov chain Monte Carlo |
| MDS | Multidimensional scaling |
| ML | Maximum likelihood |
| MMCO | Mid-Miocene climatic optimum |
| MPL | Maximum pseudo-likelihood |
| MSC | Multispecies coalescent |
| mtSSU | Mitochondrial small subunit |
| MUSCLE | MUltiple Sequence Comparison by Log-Expectation |
| Mya | Million years ago |
| NGS | Next-generation sequencing |
| nuLSU | Nuclear large subunit |
| NZN | New Zealand, North Island |
| NZS | New Zealand, South Island |

## LIST OF ABBREVIATIONS (continued)

| | |
|---|---|
| OMA | University of Nebraska at Omaha Herbarium |
| OTA | University of Otago Herbarium |
| PCA | Principal components analysis |
| PCR | Polymerase chain reaction |
| PHO | *Pseudocyphellaria homoeophylla* |
| PP | Posterior probability |
| RADseq | Restriction site-associated DNA sequencing |
| RAxML | Randomized Axelerated Maximum Likelihood |
| *RPB1* | RNA polymerase beta subunit one |
| SNP | Single nucleotide polymorphism |
| TAS | Tasmania, Australia |
| TLC | Thin-layer chromatography |
| *Tsr1* | Ribosome biogenesis protein |
| VIC | Victoria, Australia |
| WAG | Whelan And Goldman amino acid replacement model |
| q | Character state transition |
| μ | Extinction |
| λ | Speciation |

## SUMMARY

The past few decades has seen a surge in molecular data used to understand the evolution of lichenized fungi. Studies have been conducted to understand the taxonomic placement of lichenized fungi in the fungal kingdom, the diversification of higher-level taxonomic groups, the delimitation of species, and the genetic structure of populations. As in many other groups, the taxonomic value of morphological and chemical phenotypic characters for lichenized fungi are difficult to assess without other independent sources of data. Therefore, molecular data have provided a new line of evidence to critically evaluate the usefulness of phenotypic characters. Today lichenologists are using molecular data to test traditional hypotheses of homology based on phenotypic data. Generally, the findings are that many traditional systematic concepts are incongruent with molecular concepts, but a deeper understanding of the evolutionary history is gained. The first chapter in this dissertation introduces the evolution, taxonomy, and biogeography of lichenized fungi. The remaining chapters all use molecular data to understand the evolutionary relationships of lichenized fungi at different levels of taxonomy. Two chapters focus on the diversification of taxonomic groups above the species level, the next chapter focuses on population genetics, and the final chapter focuses on the delimitation of species boundaries.

Three chapters in this dissertation focus on the lobarioid clade in the family Peltigeraceae which until the past 10 years was not well studied. The lobarioid clade was once the family Lobariaceae, but it was recently synonymized with Peltigeraceae using a temporal banding approach. Temporal-banding is becoming a trend in higher-level classification of lichenized fungi and uses time-calibrated phylogenies to identify and define temporal bands for comparable ranks above the species level and aims for a more consistent taxonomic ranking system.

Chapter two, "Multiple historical processes obscure phylogenetic relationships in a taxonomically difficult group" is the first study in lichenized fungi to use target-capturing. Nearly 400 single-copy nuclear loci were sequenced to reconstruct the first time-calibrated phylogeny of the lobarioid clade of Peltigeraceae. The first molecular phylogeny reconstructed for this clade used three genetic loci, but could not resolve the nodes along the backbone, leaving the relationships of genera unresolved. Using two orders of magnitude more loci, this study aimed to resolve these relationships. The stem age of the lobariod clade was like other families found in previous research and the generic relationships became clearer, but the backbone was still resistant to resolution. Further investigation found evidence that this was can be explained by historic processes, including ancient hybridizations and rapid diversification that occurred near the Cretaceous-Paleogene boundary. Hundreds of individual gene trees had massive gene-tree discordance and evidence for ancient reticulate evolution. Due to these evolutionary processes, even with 400 loci, the generic relationships remain somewhat unresolved, but a clearer understanding of the processes influencing the evolution of the group was gained.

Chapter three, "Oligocene origin and drivers of diversification in the genus *Sticta*" used a five-locus time-calibrated phylogeny to understand the timing of diversification of the genus. This study was the first to reconstruct a time-calibrated, multi-locus phylogeny for the genus *Sticta.* Other genus-level studies in lichenized fungi that estimated divergence times among species at worldwide to regional scales found that most lichenized genera diversified within the last 40 Mya and in *Sticta*, the timing of diversification was similar. This dissertation chapter also used ancestral state reconstructions to understand the how photobiont association and Andean uplift influenced the diversification of the genus. An ancestral range reconstruction was also conducted to estimate where *Sticta* could have originated.

Chapter four is the final chapter on lobarioid species, "Using RADseq to understand the circum-Antarctic distribution of the lichenized fungus *Pseudocyphellaria glabra*" uses restriction-site-associated DNA sequencing (RADseq) to understand the biogeography and population genetics of a single species with a disjunct range, separated by oceans and seas, occurring in Australia, Chile, and New Zealand. The use of RADseq is challenging in lichenized fungi because isolation of DNA from a lichen thallus results in a metagenome composed mostly of the mycobiont DNA, but it also contains DNA of the photobiont and the microbiome. In this chapter, a reference genome was generated so *P. glabra* mycobiont RAD loci could be used to estimate patterns of genetic differentiation among populations collected in Australia, Chile, and New Zealand and to infer how major physical barriers such as the Pacific Ocean limit genetic exchange among populations.

Chapter five, "Picking holes in traditional species delimitations: an integrative taxonomic reassessment of the *Parmotrema perforatum* group" focuses on a species complex in another family, Parmeliaceae. This species delimitation study required the collection of population samples from eastern Texas and western Louisiana, where all six species live in sympatry. The aim was to use a seven-locus dataset and the integration of a variety of analytical methods determine if the genetic lineages inferred correlated with the traditional species circumscriptions based on secondary chemistry and mode of reproduction. Integrative taxonomy is increasingly used in lichenized fungi to assess species boundaries that were established using phenotypic characters and most studies find that traditional phenotype-based species delimitation vastly underestimated the number of species observed with the "general lineage concept" (GLC) of species. The GLC encourages the use of multiple sources of data to serve as independent lines of evidence in order to generate a robust hypothesis of species boundaries. In this final dissertation

chapter, multiple lines of evidence were used including concatenated maximum likelihood phylogeny reconstruction, Bayesian STRUCTURE analysis, multispecies coalescent species tree estimations, and the morphology conidia to determine species boundaries. The main result was that genetic lineages did not correspond directly with the traditional six-species delimitation based solely on secondary chemistry and reproductive mode. The genetic data discovered three lineages with a more complicated evolutionary history than traditionally assumed.

This dissertation outlines the work that was a training program on the latest research techniques in the field of lichenology. The research conducted encompassed most aspects that a professional systematist will encounter in a career. This includes planning field collection trips in the USA and foreign countries, which required obtaining grants and collection permits, preparation of logistical aspects, such as rental cars and accommodations, finding appropriate habitats, collecting and identifying specimens in the field, and finally, getting the specimens back safely so the research could be conducted. Once back in Chicago, the specimens were processed for deposition in the herbarium of the Field Museum, prepared for DNA isolation and sequencing, and analyzed on high performance servers. But the most challenging aspect was interpreting the results of the analyses, finding what was learned, and then framing the ideas in the context of what is already known, not just in the field of lichenology, but in the broader disciplines of systematics and evolutionary biology. The Biological Sciences PhD program at UIC and the collections and laboratories at the Field Museum provided excellent training for me to transform myself from an amateur lichen enthusiast, to a scientist that understands lichens in a much broader perspective.

# 1. Introduction

## 1.1 General Biology of Lichenized Fungi

Lichens are an example of mutualistic symbiosis between fungi and photosynthetic green algae or cyanobacteria. The photosynthetic symbiont (photobiont) provides the fungal partner (mycobiont) with carbohydrates, whereas the mycobiont protects the photobiont in the thallus – the physical form of the lichen. Lichenized fungi are ubiquitous and have a stunning diversity with nearly 20,000 described species (Jaklitsch et al. 2016; Lücking, Hodkinson, and Leavitt 2016). For over 200 years, beginning with Linnaeus, lichen taxonomists have been describing and classifying new species. Species were delineated by observing unique sets of fixed characteristics. Over this time span, major breakthroughs were made that increased understanding about lichens, including their symbiotic nature that was not fully recognized in classification until the 1950s (Santesson 1953). New knowledge influenced the classification of lichens and the taxonomy has been constantly shaped by new discoveries, advances in technology, and the use of new sets of characters, such as secondary metabolites (Hawksworth 1976; Lumbsch 1998).

Despite the accumulated knowledge and evolving classification, the taxonomy of lichenized fungi remains challenging. This is mostly due to a persistence of traditional classification that does not always correspond to species inferred with molecular data. Molecular approaches have been increasingly used to understand the phylogenetic relationships of lichenized fungi over the past three decades. Many molecular studies confirmed traditionally delimited species. However, many molecular studies find that the traditional characters are not always correlated with genetic clusters. This chapter introduces (1) the nature and evolution of

the lichen symbiosis, (2) the history of lichen taxonomy, (3) the traditional characters used to delimit lichen species, and (4) the biogeography of lichens.

### 1.1.1 The nature and evolution of the lichen symbiosis

The lichen symbiosis is one of many fungal associations with photoautotrophic organisms. Other fungal/photoautotrophic symbioses include mycorrhizal fungi that associate with plant roots and endophytic fungi that are found in the leaves of plants. Lichenization is a major lifestyle in the fungal kingdom where the fungal symbiont associates with microscopic green algae or cyanobacteria. Lichenized fungi make up nearly 20% of all described fungal species (Lumbsch and Rikkinen 2017). This nutritional strategy is not confined to a single monophyletic group. Rather, it and has evolved independently multiple times in the evolutionary history of fungi. Some lichenized groups can be closely related to non-lichenized fungi (Gargas et al. 1995; Schoch et al. 2009).

All terrestrial ecosystems have lichenized fungi. In harsh ecosystems such as alpine and arctic tundra and in the sub-Antarctic islands, lichens are dominant. Lichens are poikilohydric and this feature allows them to completely dry out and go dormant for extended periods of time (Lange and Tenhunen 1982). Upon rehydration, metabolic activity resumes. Poikilohydry is one explanation for this dominance in extreme habitats (Werth 2011). For example, there are hundreds of species of lichenized fungi in Antarctica compared to only two species of vascular plants (Øvstedal and Smith 2001). Lichens are also major components of biocrusts. These communities are also composed of cyanobacteria, bacteria, fungi, and bryophytes. All live together and form a crust that covers the soil in arid habitats (Belnap, Weber, and Büdel 2016).

Lichens form a persistent structure called a thallus that is mainly composed of mycobiont hyphae with a photobiont layer positioned below the upper cortex (Nash 2008). The photobiont

cells produce carbohydrates that the fungus consumes for metabolic processes. Mycobiont hyphae are in close contact with the photobiont and many lichens produce specific structures called haustoria that can penetrate the photobiont cell or invaginate the cell wall without penetration (the latter often referred to as appressoria) (Ahmadjian 1993; Honegger 1986). Photobionts can be a chlorophyte green alga or cyanobacterium (mostly *Nostoc* spp.) or both. When isolated and grown in pure culture, the mycobiont does not form a thallus as in the lichen symbiosis but has the appearance like a mold, while isolated photobionts are observed as green microbial colonies (Ahmadjian 1993). However, there is a growing body of evidence that lichens might not be as simple as a two or three partner symbiosis. Recent studies have found many species of bacteria and archaea present in lichen thalli (Bates, Garcia-Pichel, and Nash III 2010; Cardinale et al. 2012; Printzen et al. 2012), as well as lichenicolous fungi (Hawksworth 1994; Lawrey and Diederich 2003), and endolichenic fungi (Arnold et al. 2009; Spribille et al. 2016; U'Ren et al. 2010). Currently, it is unclear how these prokaryotic organisms and additional fungal taxa interact with the main fungal and photosynthetic partners in the lichen thallus, but it is hypothesized that they play a role in the symbiosis (Hodkinson and Lutzoni 2009).

### 1.1.2 Taxonomy of lichenized fungi

Lichen taxonomy has been constantly modified when new discoveries were made. In the 1860s, Schwendener recognized the dual nature of the lichen symbiosis (Honegger 2009). His discovery, that lichens were composed of fungal hyphae and algae was a breakthrough that took decades to catch on and was disputed among lichenologists at the time (Mitchell 2002). Before that and sometime after, lichens were classified as a separate group within cryptogams. This artificial taxonomic grouping also included bryophytes, ferns and algae, basically all plant and fungus-like organisms that are not seed plants. Linnaeus considered all lichens congeneric and

placed them all in the genus *Lichen* (Jørgensen 1991). Today, there are over 19,400 described species of lichenized fungi. Ninety-eight percent belong to the phylum Ascomycota, whereas the remaining two percent belong to Basidiomycota (Jaklitsch et al. 2016; Lücking, Hodkinson, and Leavitt 2016). Within Ascomycota, the largest class is Lecanoromycetes which includes around 15,000 species (Jaklitsch et al. 2016; Lücking, Hodkinson, and Leavitt 2016; Wijayawardene et al. 2018). In contrast to the large diversity of mycobiont species, the number of photobiont species is estimated to only be in the hundreds, although recent studies have indicated that numerous distinct lineages remain undescribed (Leavitt et al. 2015). This implies that many species of lichenized fungi share the same photobiont species. However, the taxonomy of symbiotic algae is still poorly known.

### 1.1.3 The morphological variation in lichenized fungi

Lichen thalli have a large diversity of forms and sizes used for classification (Nash 2008). Lichen thalli can be divided into three major growth forms. Crustose lichens are tightly appressed to their substrate. They have no lower surface and must be collected with the substrate. Foliose lichens are leaf-like and have a distinct upper and lower surface. Fruticose lichens are shrub-like and three-dimensional. All these major growth forms are found on all types of substrates, including tree bark, rocks, and soil. The photobiont influences the growth form of a lichen thallus. When both symbionts are grown in axenic cultures (pure cultures, free of other organisms), they both look nothing like they do when they are in symbiotic association. Another striking example is the photosymbiodemes in the genus *Sticta*, where a mycobiont species has two growth forms depending on the type of photobiont; the “chloromorph” as a foliose thallus and the “cyanomorph” as a fruticose thallus (James and Henssen 1976). In traditional taxonomy, these two growth forms of the same species were considered different genera but after thorough

morphological studies by James and Henssen (1976) and molecular data Armaleo and Clerc (1991) these morphotypes are regarded as one species. In addition to growth form, there are other vegetative characters of the thallus that are important for classification of lichenized fungi. Features of the upper cortex, the color of the lower surface, the presence of rhizines, root-like attachment structures, and their shape are additionally used to delimit species.

### 1.1.4 Reproduction in lichenized fungi

Reproductive structures have been used for classification of fungi since its beginning and lichenized fungi are no exception (Nash 2008). Lichenized fungi exhibit both sexual and asexual reproductive strategies. Most lichenized fungi are strictly sexual or mixed, while some are strictly asexual. Lichenized fungi produce either meiotic ascospores or basidiospores in ascomata or basidiomata, respectively. These meiospores usually do not carry photobiont cells when dispersed. Consequently, when a spore lands on a substrate and germinates, it must find an appropriate photosynthetic partner to associate with. The fact that asexual reproduction is common in lichens indicates that this is an issue. The most common types of asexual propagules in lichens are soredia and isidia. Soredia are algal cells wrapped in fungal hyphae and resemble a powder-like mass. Isidia are finger-like projections from the upper surface containing the photosynthetic layer. These asexual structures disperse both symbionts. In some cases, there are two morphologically identical species that differ in reproductive strategy. One is sexual and the other asexual forming a group often referred to as a "species pair" (Mattsson and Lumbsch 1989; Poelt 1972, 1970). The evolution and classification of species pairs have been studied and debated to this day. Some claim them to be separately evolving groups while others view them as conspecific (Buschbom and Mueller 2006; Robinson 1975; Tehler 1982; Mattsson and Lumbsch 1989; Poelt 1970).

The nature of sexual reproduction is poorly understood in lichenized fungi. Lichen fungi produce microscopic conidia. The morphology of conidia (= fungal mitospores) has been used for taxonomy in some groups. Conidia are the result of mitotic cell division and are hypothesized to act as spermatia or asexual spores (Vobis and Hawksworth 1981; Vobis 1980, 1977). When a conidium comes into contact with a hyphal receptory organ, the trichogyne, which is part of the female oogonium (=ascogonium), they fuse and form dikaryotic hyphae that grow in ascomata and form meiosporangia (Ahmadjian 1993; Letrouit-Galinou, Parguey-Leduc, and Janex-Favre 1994). Fusion requires the appropriate mating type. Some lichens are homothallic being able to fuse with the same mating type. This is like plants that can self-fertilize. Other lichens are heterothallic requiring a different mating type to fuse with. This is like self-incompatible plants. Lichenologists are just beginning to understand the genetic loci that regulate mating systems. Both types of mating systems, homothallic and heterothallic, have been observed in lichenized fungi (Honegger and Zippler 2007; Murtagh, Dyer, and Crittenden 2000; Scherrer, Zippler, and Honegger 2005).

### 1.1.5 Secondary chemistry in lichenized fungi

Fungi use several metabolic pathways to produce secondary metabolites. These compounds are used for classification, especially in lichenized fungi that often contain large amounts of substances, which allowed for characterization of the products even when analytical techniques were less sophisticated (Lumbsch 1998). There is a large diversity of secondary metabolites that are only found in lichen thalli and in total around 1000 substances have been isolated from lichens (Huneck and Yoshimura 1996). The importance of these products for the lichens is currently not well understood but several hypotheses have been formulated and there is evidence supporting a major role of cortical pigments in screening of UV light (McEvoy,

Solhaug, and Gauslaa 2007; McEvoy et al. 2006, 2004). These pigments include the yellow-green usnic acid or brilliant orange anthraquinones. Medullary compounds have been associated with controlling water saturation of the photobiont (Huneck 2002), or have been shown to have antimicrobial and antiherbivory properties (Nash 2008). The first use of secondary metabolites for taxonomy in lichens was by William Nylander who observed color changes when spotting calcium hypochlorite and potassium hydroxide on different parts of lichen thalli (Nylander 1866). The spot test could be used to sort lichens by the color reaction. Later, the use of chromatographic methods, including thin-layer chromatography (TLC) led to the discovery of more substances and patterns of occurrence of secondary metabolites. These observations led to a description of many new chemotypes or "chemospecies". Currently, most lichenologists agree that a fixed chemical difference needs to be correlated with other fixed characters to warrant recognition at the species level (Egan 1986). In some studies using molecular markers, chemical differences are diagnostic, fixed characters that correspond with the genetic data, while in others chemistry is variable within a population (Leavitt, Moreau, and Lumbsch 2015; Lumbsch 2007; Printzen 2010).

### 1.1.6 Ecology and biogeography of lichenized fungi

Lichenized fungi have a variety of distributional patterns at micro and macro levels (Galloway 2008). Most lichen thalli are sessile, being firmly attached to their substrate. They must disperse by means of their reproductive structures. Lichens are known to disperse over long distances and are among the first groups of organisms to colonize recently exposed land, such as volcanic islands (Brock 1973). Ascospores are microscopic and much smaller than asexual propagules, such as soredia and isidia. Being much smaller, they probably disperse over longer distances. Some studies suggest intercontinental dispersal facilitated by ascospores (Amo de Paz

et al. 2012; Buschbom 2007; Otálora et al. 2010; Ronnås et al. 2017). Asexual propagules have been shown to disperse at local distances. For example, in *Lobaria pulmonaria*, the mean dispersal for soredia is 200 m (Werth et al. 2006).

Lichenized fungi tend to have larger distributional ranges than seed plants (Leavitt and Lumbsch 2016; Werth 2011). Species with large distributional ranges are hypothesized to disperse over long distances and be ecological generalists. Many lichens show ecological affinities to particular macroclimates. For example, many dominant arctic lichens can be found at high elevation in alpine sites of lower latitudes (Poelt 1987). Furthermore, studies on species range distributions of different species of lichenized fungi have shown that species distributions are determined by ecological factors (Otte, Esslinger, and Litterski 2002, 2005). Widespread morphologically identical species can be composed of potentially isolated populations. The common occurrence of cryptic species is one of the major problems in lichen taxonomy (Lumbsch and Leavitt 2011; Crespo and Lumbsch 2010; Crespo and Pérez-Ortega 2009). Delimitation and classification these groups have proven challenging.

Some lichenized fungi have endemic distributions, i.e. they are only found in a restricted geographic range. These species are hypothesized to have dispersal limitations. Endemic lichen species are usually found in areas that also have endemic vascular plants, such as European (Otte, Esslinger, and Litterski 2002) and North American (Moberg and Nash 1999; Nash 2002) Mediterranean regions, Macaronesia (Simon et al. 2018; Sérusiaux et al. 2011), and the Galapagos Islands (Aptroot and Bungartz 2007). Besides restricted dispersal, there are other explanations for endemic distributions. Some mycobionts may be highly specialized to an endemic photobiont, restricting the range of the mycobiont. Also, some lichenized fungi may have strict microclimatic requirements that are only met in restricted microhabitats. In addition,

some species may have only recently come into existence – some genera of lichenized fungi have been shown to have a burst of diversification during the Pliocene and Pleistocene (Altermann et al. 2014; Lumbsch 2016). These lichens may have not had enough time to disperse and expand their range, exhibiting an endemic range.

Other lichens have disjunct ranges (Culberson 1972). Examples include bipolar species only or predominantly found at the polar regions of the planet (Du Rietz and Skottsberg 1940; Galloway and Aptroot 1995). Others are present on multiple continents and islands that surround Antarctica. Some species are disjunct throughout Fennoscandia, Newfoundland, and the Pacific Northwest. Intercontinental distributions bring up questions about the history of the species being examined. Was this species once widespread and now only fragments of the range exist today (vicariance), or is long-distance dispersal (LDD) the explanation for the disjunct distribution? Generally, vicariance is observed at higher levels of classification (Lücking 2003), such as species of the same genera or family. At the level of species, intercontinental distributions are usually interpreted as a result of LDD. Both processes play a role in the distributional patterns observed in lichenized fungi. In the southern Hemisphere, close to Antarctica, both are observed. Among major landmasses, lichen communities associated with temperate rainforests have the same genera. Typically, species are unique to each continent. However, the strong and sustained wind pattern that circles Antarctica is hypothesized to be responsible for the disjunct ranges of many lichen species that currently occur in Australia, New Zealand, and southern South America (Galloway 1988; Galloway 1979).

**1.2 References**

Ahmadjian, Vernon. *The Lichen Symbiosis*. Hoboken: John Wiley & Sons. (1993).

Altermann, Susanne, Steven D. Leavitt, Trevor Goward, Matthew P. Nelsen, and H. Thorsten

Lumbsch. "How do you solve a problem like *Letharia*? A new look at cryptic species in lichen-forming fungi using Bayesian clustering and SNPs from multilocus sequence data." *PLOS ONE* 9, no. 5 (2014): e97556.

Amo de Paz, Guillermo, Paloma Cubas, Ana Crespo, John A. Elix, and H. Thorsten Lumbsch. "Transoceanic dispersal and subsequent diversification on separate continents shaped diversity of the *Xanthoparmelia pulla* group (Ascomycota)." *PLOS ONE* 7, no. 6 (2012): e39683.

Aptroot, A., and F. Bungartz. "The lichen genus *Ramalina* on the Galapagos." *The Lichenologist* 39, no. 6 (2007): 519-542.

Armaleo, Daniele, and Philippe Clerc. "Lichen chimeras: DNA analysis suggests that one fungus forms two morphotypes." *Experimental Mycology* 15, no. 1 (1991): 1-10.

Arnold, A. Elizabeth, Jolanta Miadlikowska, K. Lindsay Higgins, Snehal D. Sarvate, Paul Gugger, Amanda Way, Valérie Hofstetter, Frank Kauff, and François Lutzoni. "A phylogenetic estimation of trophic transition networks for ascomycetous fungi: Are lichens cradles of symbiotrophic fungal diversification?." *Systematic Biology* 58, no. 3 (2009): 283-297.

Bates, Scott T., Ferran Garcia-Pichel, and Thomas H. Nash III. "Fungal components of biological soil crusts: Insights from culture-dependent and culture-independent studies" *Bibliotheca Lichenologica* 105 (2010): 197-210.

Belnap, Jayne, Bettina Weber, and Burkhard Büdel. *Biological Soil Crusts as an Organizing Principle in Drylands*. AG Switzerland: Springer. (2016): 3-13

Brock, Thomas D. "Primary colonization of Surtsey, with special reference to the blue-green

algae." *Oikos* (1973): 239-243.

Buschbom, Jutta. "Migration between continents: Geographical structure and long-distance gene flow in *Porpidia flavicunda* (lichen-forming Ascomycota)." *Molecular Ecology* 16, no. 9 (2007): 1835-1846.

Buschbom, Jutta, and Gregory M. Mueller. "Testing “species pair” hypotheses: Evolutionary processes in the lichen-forming species complex *Porpidia flavocoerulescens* and *Porpidia melinodes*." *Molecular Biology and Evolution* 23, no. 3 (2005): 574-586.

Cardinale, Massimiliano, Jana Steinová, Johannes Rabensteiner, Gabriele Berg, and Martin Grube. "Age, sun and substrate: triggers of bacterial communities in lichens." *Environmental Microbiology Reports* 4, no. 1 (2012): 23-28.

Crespo, Ana, and H. Thorsten Lumbsch. "Cryptic species in lichen-forming fungi." *IMA Fungus* 1, no. 2 (2010): 167-170.

Crespo, Ana, and Sergio Pérez-Ortega. "Cryptic species and species pairs in lichens: A discussion on the relationship between molecular phylogenies and morphological characters." *Anales del Jardín Botánico de Madrid*. 66, no. S1, (2009): 71-81.

Culberson, William Louis. "Disjunctive distributions in the lichen-forming fungi." *Annals of the Missouri Botanical Garden* 59, no. 2 (1972): 165-173.

Egan, Robert S. "Correlations and non-correlations of chemical variation patterns with lichen morphology and geography." *The Bryologist* (1986): 99-110.

Galloway, D. J. "Biogeographical elements in the New Zealand lichen flora." *Plants and Islands* (1979): 201-224.

Galloway, D. J., and A. Aptroot. "Bipolar lichens: A review." *Cryptogamic Botany* (1995).

Galloway, D. J. "Plate tectonics and the distribution of cool temperate Southern Hemisphere macrolichens." *Botanical journal of the Linnean Society* 96, no. 1 (1988): 45-55.

Galloway, D. J. "Lichen Biogeography." In *Lichen Biology*, Edited by T. H. Nash. Cambridge: Cambridge University Press. (2008): 315–35.

Gargas, Andrea, Paula T. DePriest, Martin Grube, and Anders Tehler. "Multiple origins of lichen symbioses in fungi suggested by SSU rDNA phylogeny." *Science* 268, no. 5216 (1995): 1492-1495.

Hawksworth, D. L. "Lichen-inhabiting fungi: A fascinating little-explored ecological niche." In *Aspects of African Mycology: Proceedings of the First Regional Conference on Mycology in Africa.* Louvain-la-Neuve: International Mycological Association. (1994): 69-75.

Hawksworth, D. L. "Lichen chemotaxonomy." In *Lichenology: Progress and Problems*, Edited by D. H. Brown, D. L. Hawksworth, and R. H. Bailey. Cambridge: Academic Press. (1976): 139–184.

Hodkinson, Brendan P., and François Lutzoni. "A microbiotic survey of lichen-associated bacteria reveals a new lineage from the Rhizobiales." *Symbiosis* 49, no. 3 (2009): 163-180.

Honegger, Rosmarie. "Ultrastructural studies in lichens: I. Haustorial types and their frequencies in a range of lichens with trebouxioid photobionts." *New Phytologist* 103, no. 4 (1986): 785-795.

Honegger, Rosmarie. "Simon Schwendener (1829-1919) and the dual hypothesis of lichens." *The Bryologist* 103, no. 2 (2000): 307-313.

Honegger, Rosmarie, and Undine Zippler. "Mating systems in representatives of Parmeliaceae, Ramalinaceae and Physciaceae (Lecanoromycetes, lichen-forming ascomycetes)." *Mycological Research* 111, no. 4 (2007): 424-432.

Huneck, S. "Die wasserabweisende Eigenschaft von Flechtenstoffen." *Bibliotheca Lichenologica* 86 (2002): 9-12.

Huneck, Siegfried, and Isao Yoshimura. "Identification of lichen substances." In *Identification of Lichen Substances*, Berlin, Heidelberg: Springer. (1996): 11-123.

Jaklitsch, Walter, Hans-Otto Baral, Robert Lücking, H. Thorsten Lumbsch, and Wolfgang Frey. *Syllabus of Plant Families-A. Engler's Syllabus der Pflanzenfamilien Part 1/2*. Edited by Wolfgang Frey. Stuttgart: Borntraeger Science Publishers. (2016).

James, P. W., and Aino Henssen. "Morphological and taxonomic significance of cephalodia." In *Lichenology: Progress and Problems; Proceedings of an International Symposium*. Cambridge: Academic Press. (1976).

Jørgensen, P. M. "Difficulties in lichen nomenclature." *Mycotaxon* (1991).

Lange, O. L., and J. D. Tenhunen. "Water relations and photosynthesis of desert lichens (Proceedings of the Symposia on Lichenology at the 13 International Botanical Congress, Sydney, Australia, Aug. 21-28. Part 2 Compiled by L. Kappen and RW Pogers)." *Journal of the Hattori Botanical Laboratory* 53 (1982): 309-313.

Lawrey, James D., and Paul Diederich. "Lichenicolous fungi: Interactions, evolution, and biodiversity." *The Bryologist* 106, no. 1 (2003): 80-121.

Leavitt, Steven D., and H. Thorsten Lumbsch. "Ecological biogeography of lichen-forming

fungi." In *Environmental and microbial relationships*, 15-37. Cham: Springer. (2016).

Leavitt, Steven D., Corrie S. Moreau, and H. Thorsten Lumbsch. "The dynamic discipline of species delimitation: Progress toward effectively recognizing species boundaries in natural populations." In *Recent Advances in Lichenology.* New Delhi: Springer. (2015): 11-44.

Leavitt, Steven D., Ekaphan Kraichak, Matthew P. Nelsen, Susanne Altermann, Pradeep K. Divakar, David Alors, Theodore L. Esslinger, Ana Crespo, and H. Thorsten Lumbsch. "Fungal specificity and selectivity for algae play a major role in determining lichen partnerships across diverse ecogeographic regions in the lichen-forming family Parmeliaceae (Ascomycota)." *Molecular Ecology* 24, no. 14 (2015): 3779-3797.

Letrouit-Galinou, M. A., A. Parguey-Leduc, and M. C. Janex-Favre. "Ascoma structure and ontogenesis in ascomycete systematics." In *Ascomycete Systematics*, Boston, Springer. (1994): 23-36

Lücking, Robert. "Takhtajan's floristic regions and foliicolous lichen biogeography: A compatibility analysis." *The Lichenologist* 35, no. 1 (2003): 33-53.

Lücking, Robert, Brendan P. Hodkinson, and Steven D. Leavitt. "The 2016 classification of lichenized fungi in the Ascomycota and Basidiomycota–Approaching one thousand genera." *The Bryologist* 119, no. 4 (2017): 361-417.

Lumbsch, H. Thorsten, and Steven D. Leavitt. "Goodbye morphology? A paradigm shift in the delimitation of species in lichenized fungi." *Fungal Diversity* 50, no. 1 (2011): 59.

Lumbsch, H. Thorsten, and Jouko Rikkinen. “Evolution of Lichens.” In *The Fungal Community: Its Organization and Role in the Ecosystem, Fourth Edition.* Boca Raton: CRC Press. (2017): 53–62.

Lumbsch, H. Thorsten. "Lichen-forming fungi, Diversification of." In *Encyclopedia of Evolutionary Biology,* Edited by Richard M. Kliman. Cambridge: Academic Press. (2016): 305-311.

Lumbsch, H. Thorsten. "Recent trends in phylogeny and classification of lichen-forming ascomycetes." In *Fungi: Multifaceted Microbes.* Delhi: Anamaya. (2007): 153-168.

Lumbsch, H. Thorsten. "Taxonomic use of metabolic data in lichen-forming fungi." In *Chemical Fungal Taxonomy.* New York: Marcel Dekker. (1998): 345-387.

Mattsson, Jan-Eric, and H. Thorsten Lumbsch. "The use of the species pair concept in lichen taxonomy." *Taxon* (1989): 238-241.

McEvoy, Maria, Line Nybakken, Knut Asbjørn Solhaug, and Yngvar Gauslaa. "UV triggers the synthesis of the widely distributed secondary lichen compound usnic acid." *Mycological Progress* 5, no. 4 (2006): 221-229.

McEvoy, Maria, Knut Asbjorn Solhaug, and Yngvar Gauslaa. "Solar radiation screening in usnic acid-containing cortices of the lichen *Nephroma arcticum*." *Symbiosis* 43, no. 3 (2007): 143-150.

McEvoy, Maria, Knut Asbjørn Solhaug, Line Nybakken, and Yngvar Gauslaa. “Induction of usnic acid synthesis by UV Irradiance in *Xanthoparmelia somloënsis*.” In *Lichens in Focus: IAL5 Book of Abstracts*, Edited by T. Randlane and A. Saag. Tartu: Tartu University Press. (2004): 46.

Mitchell, M. E. "Such a strange theory”: Anglophone attitudes to the discovery that lichens are composite organisms, 1871–1890." *Huntia* 11 (2002): 193-207.

Moberg, Roland, and T. H. Nash. "The genus *Heterodermia* in the Sonoran Desert area." *The Bryologist* 102 (1999): 1-14.

Murtagh, G. J., P. S. Dyer, and P. D. Crittenden. "Reproductive systems: sex and the single lichen." *Nature* 404, no. 6778 (2000): 564.

Nash, Thomas H. *Lichen Flora of the Greater Sonoran Desert Region*. Tempe: Lichens Unlimited. (2002).

Nash, Thomas H. *Lichen Biology*. Cambridge: Cambridge University Press. (2008).

Nylander, William. "Hypochlorite of lime and hydrate of potash, two new criteria in the study of lichens." *Botanical Journal of the Linnean Society* 9, no. 38 (1866): 358-365.

Otálora, Mónica AG, Isabel Martínez, Gregorio Aragón, and M. Carmen Molina. "Phylogeography and divergence date estimates of a lichen species complex with a disjunct distribution pattern." *American Journal of Botany* 97, no. 2 (2010): 216-223.

Otte, Volker, Theodore L. Esslinger, and Birgit Litterski. "Biogeographical research on European species of the lichen genus *Physconia*." *Journal of Biogeography* 29, no. 9 (2002): 1125-1141.

Otte, Volker, Theodore L. Esslinger, and Birgit Litterski. "Global distribution of the European species of the lichen genus *Melanelia* Essl." *Journal of Biogeography* 32, no. 7 (2005): 1221-1241.

Øvstedal, Dag Olav, and RI Lewis Smith. *Lichens of Antarctica and South Georgia: a guide to their identification and ecology*. Cambridge: Cambridge University Press. (2001).

Poelt, Josef. "Das Konzept der Artenpaare bei den Flechten." *Deutsche Botanische Gesellschaft,*

*neue Folge* 4 (1970): 187-198.

Poelt, J. "Taxonomische Behandlung von Artenpaaren bei den Flechten." *Botaniska Notiser* (1972).

Poelt, J. "Gesetz der relativen Standortskonstanz bei den Flechten." *Botanische Jahrbücher für Systematik, Pflanzengeschichte und Pflanzengeographie* (1987).

Printzen, Christian. "Lichen systematics: The role of morphological and molecular data to reconstruct phylogenetic relationships." In *Progress in Botany 71*. Berlin, Heidelberg, Springer. (2010): 233-275.

Printzen, Christian, Fernando Fernandez-Mendoza, Lucia Muggia, Gabriele Berg, and Martin Grube. "Alphaproteobacterial communities in geographically distant populations of the lichen *Cetraria aculeata*." *FEMS Microbiology Ecology* 82, no. 2 (2012): 316-325.

Du Rietz, Gustaf Einar, and Carl Skottsberg. *Problems of Bipolar Plant Distribution*. Stockholm: Almqvist & Wiksells. (1940).

Robinson, Harold. "Considerations on the evolution of lichens." *Phytologia* (1975).

Ronnås, Cecilia, Silke Werth, Otso Ovaskainen, Gergely Varkonyi, Christoph Scheidegger, and Tord Snäll. "Discovery of long-distance gamete dispersal in a lichen-forming ascomycete." *New Phytologist* 216, no. 1 (2017): 216-226.

Santesson, Rolf. “The New Systematics of Lichenized Fungi.” In *Proceedings of the 7th Internatlional Botanical Congress,* Stockholm. (1953): 809–10

Scherrer, Sandra, Undine Zippler, and Rosmarie Honegger. "Characterisation of the mating-type locus in the genus *Xanthoria* (lichen-forming ascomycetes, Lecanoromycetes)." *Fungal*

*Genetics and Biology* 42, no. 12 (2005): 976-988.

Schoch, Conrad L., Gi-Ho Sung, Francesc López-Giráldez, Jeffrey P. Townsend, Jolanta Miadlikowska, Valérie Hofstetter, Barbara Robbertse et al. "The Ascomycota tree of life: A phylum-wide phylogeny clarifies the origin and evolution of fundamental reproductive and ecological traits." *Systematic Biology* 58, no. 2 (2009): 224-239.

Sérusiaux, Emmanuël, Tim Wheeler, and Bernard Goffinet. "Recent origin, active speciation and dispersal for the lichen genus *Nephroma* (Peltigerales) in Macaronesia." *Journal of Biogeography* 38, no. 6 (2011): 1138-1151.

Simon, Antoine, Bernard Goffinet, Nicolas Magain, and Emmanuël Sérusiaux. "High diversity, high insular endemism and recent origin in the lichen genus *Sticta* (lichenized Ascomycota, Peltigerales) in Madagascar and the Mascarenes." *Molecular Phylogenetics and Evolution* 122 (2018): 15-28.

Spribille, Toby, Veera Tuovinen, Philipp Resl, Dan Vanderpool, Heimo Wolinski, M. Catherine Aime, Kevin Schneider et al. "Basidiomycete yeasts in the cortex of ascomycete macrolichens." *Science* 353, no. 6298 (2016): 488-492.

Tehler, Anders. "The species pair concept in lichenology." *Taxon* (1982): 708-714.

U'Ren, Jana M., François Lutzoni, Jolanta Miadlikowska, and A. Elizabeth Arnold. "Community analysis reveals close affinities between endophytic and endolichenic fungi in mosses and lichens." *Microbial Ecology* 60, no. 2 (2010): 340-353.

Vobis, G. "Studies on the germination of lichen conidia." *The Lichenologist* 9, no. 2 (1977): 131-136.

Vobis, G., and D. L. Hawksworth. "Conidial lichen-forming fungi." In *Biology of Conidial Fungi* 1. Edited by Garry T. Cole and Bryce Kendrick. Cambridge: Academic Press. (1981): 245-273.

Vobis, G. “Bau und Entwicklung der Flechten-Pycnidien und ihrer Conidien.” *Bibliotheca Lichenologica* 14, (1980): 141-215.

Werth, Silke. "Biogeography and phylogeography of lichen fungi and their photobionts." In *Biogeography of microscopic organisms: Is everything small everywhere?* Cambridge: Cambridge University Press, (2011): 191-208.

Werth, Silke, Helene H. Wagner, Felix Gugerli, Rolf Holderegger, Daniela Csencsics, Jesse M. Kalwij, and Christoph Scheidegger. "Quantifying dispersal and establishment limitation in a population of an epiphytic lichen." *Ecology* 87, no. 8 (2006): 2037-2046.

Wijayawardene, Nalin N., Kevin D. Hyde, H. Thorsten Lumbsch, Jian Kui Liu, Sajeewa SN Maharachchikumbura, Anusha H. Ekanayaka, Qing Tian, and Rungtiwa Phookamsak. "Outline of Ascomycota: 2017." *Fungal Diversity* 88, no. 1 (2018): 167-263.

## 2. Multiple historical processes obscure phylogenetic relationships in a taxonomically difficult group (Lobariaceae, Ascomycota)

Todd J. Widhelm, Felix Grewe, Jen-Pan Huang, Joel Mercado, Bernard Goffinet, Robert Lücking, Bibiana Moncada, Roberta Mason-Gamer, and H. Thorsten Lumbsch

### 2.1 Introduction

With the advent of next-generation sequencing (NGS) technology, the evolutionary relationships of many groups on the tree of life are increasingly resolved and our understanding of the diversification of these groups has been significantly improved (Rokas et al. 2003; Gee 2003; Hipp et al. 2014). However, in many groups, despite the use of NGS data, certain nodes have resisted unambiguous resolution. Conflicting topologies have been inferred from independent NGS data throughout the tree of life. For example, the placement of ctenophores and sponges has proven difficult as some studies place either sponges or ctenophores as sister to all other animals (Dunn et al. 2008; Simion et al. 2017). Phylogenomic reconstructions of birds also yielded conflicting relationships for the earliest divergence within Neoaves (Reddy et al. 2017), perhaps due to inferences from unequal data and taxon sampling: 42 Mbp from 48 bird genomes in Jarvis et al. (Jarvis et al. 2014) versus, 0.4 Mbp from 259 loci sampled from 198 species, in Prum et al. (Prum et al. 2015). In the plant kingdom, inferences from NGS datasets resolve *Amborella* either sister to all other angiosperms (Drew et al. 2014; Zhang et al. 2012) or sister to water lilies (Goremykin et al. 2015; Xi et al. 2014). Similarly, the Gnetales may be sister to pines, all conifers, or all seed plants (Burleigh and Mathews 2004).

Several reasons have been invoked to explain gene-tree discordance (Som 2015). Gene

duplication can cause problems in phylogenetic reconstruction if paralogous loci with different histories are not distinguished within taxa and erroneously analyzed as homologs between taxa (Maddison 1997; Martin and Burg 2002). Rapid diversifications may lead to the fixation of fewer substitutions and hence to difficulties in resolving phylogenetic relationships. When too many speciation events occur in a relatively short period of time, gene genealogies are not expected to be fully sorted among evolutionary lineages leading to incomplete lineage sorting (ILS). Species tree methods can be used to mitigate the effects of ILS, but computational constraints prohibit fully parameterized methods such as *BEAST (Bouckaert et al. 2014) to estimate a species tree directly from hundreds of loci. Instead, species trees for large datasets are estimated from reconstructed gene trees, which can underestimate the support of relationships since these methods use summary statistics or pseudolikelihood (Liu et al. 2015). Moreover, reticulate evolution, in the form of hybridization or horizontal gene transfer (HGT), can lead to incongruence among gene trees and obscure phylogenetic relationships (Xu 2000). Reticulations are not modeled in the commonly used species tree and concatenation approaches and hence specific, computationally intensive programs are needed to examine whether relationships of organisms are more complex than bifurcation (Nakhleh et al. 2005).

Reconstructing phylogenies can be done with either nucleotide and amino acid data and these sources of data can yield incongruent phylogenies (Liu et al. 2014). Nucleotide data can suffer from substitutional saturation at particular sites in a genome (Delsuc, Brinkmann, and Philippe 2005). Such homoplasy is difficult to model in tree reconstruction methods and hence result in phylogenetic signatures being erased (Philippe et al. 2011). In case of ancient divergences, amino acid sequences may be preferable, since they are less prone to saturation.

Fungi of Lobariaceae (recently also treated as a subfamily within Peltigeraceae (Kraichak

et al. 2018)) develop conspicuous foliose macrolichens. Nearly 400 species are currently accepted (Kirk et al. 2008), but the diversity is predicted to reach 800 species (Moncada and Lücking 2012). Inferences from variation in three loci failed to resolved either of the three traditional genera (i.e., *Lobaria*, *Pseudocyphellaria* and *Sticta*) as monophyletic, and were consequently broken up into several genera (e.g. *Crocodia, Parmostictina, Podostictina* and *Yarrumia* ) (Moncada, Lücking, and Betancourt-Macuase 2013). Despite the discovery of highly-supported, genus-level clades, the relationships among these new genera remain partially unresolved. None of the phenotypic traits, essential to traditional generic concepts in Lobariaceae, i.e., the presence and type of pores in the lower cortex, defined a clade wherein all descendants exhibit the particular traits: Pseudocyphellae and cyphellae no longer define a monophyletic *Pseudocyphellaria* and *Sticta* respectively. These pores have been shown to facilitate gas diffusion into the thallus (Nash 1996; Lange, Green, and Ziegler 1988; Green and Lange 2007) and may provide an adaptive advantage in temperate environments (Hale 1981). Cyphellae likely arose independently in *Dendriscosticta*, which is consistently resolved within the *Lobaria s.lat.* clade composed of genera lacking pores (Moncada, Lücking, and Betancourt-Macuase 2013). Phenotypic characters of the lichen association have been repeatedly shown to be poor phylogenetic predictors for the associated mycobiont (Lumbsch and Leavitt 2011; Printzen 2010; Jaklitsch et al. 2016), and the newly described genera, *Crocodia*, *Parmostictina*, *Podostictina*, and *Yarrumia,* represent morphological/ecological chimeric forms between *Pseudocyphellaria* and S*ticta*.

No study has yet critically estimated divergence times in Lobariaceae, but one study (Gaya et al. 2015) included three specimens from *Sticta*, *Lobaria* and *Pseudocyphellaria* in a fossil calibrated tree of eukaryotes. These samples were monophyletic and split from *Peltigera*

roughly 150 million years ago (Mya) and had a stem age of around 70 Mya. However, another study reported much earlier estimates, with the split from Peltigeraceae around 90 Mya and a stem age of nearly 50 Mya (Simon et al. 2018). Furthermore, two additional studies have estimated divergence times in *Lobaria* and *Sticta*, both reporting a stem age of nearly 30 Mya for each of the genera (Cornejo and Scheidegger 2018; Widhelm et al. 2018 – Chapter 3 in this dissertation).

We have reassessed phylogenetic relationships in Lobariaceae using 400 target captured nuclear protein coding loci, and a variety tree inference method to reconstruct relationships among genera. We sought to assess how historical processes may confound phylogenetic reconstructions and obscure relationships of major lineages within the family. Specifically, we addressed the effect of (1) data type (nucleotides and amino acids), (2) phylogeny reconstruction method (concatenation and species tree approaches), and (3) missing data. Furthermore, we examined our dataset for evidence of historical processes, such as (1) rapid diversification, and (2) reticulate evolution. Finally, we produced a fossil-calibrated phylogeny to estimate the timing of historical events during the diversification of Lobariaceae.

## 2.2 Methods

### 2.2.1 Taxon sampling

We sampled representatives of all the current and tentative genera in Lobariaceae. Our dataset includes representatives of the three major classic genera *Lobaria*, *Pseudocyphellaria*, *Sticta*, along with representative samples of the later segregated genera (*Anomolobaria*, *Crocodia*, *Dendriscosticta*, *Lobariella*, *Lobarina*, *Parmostictina*, *Podostictina*, *Ricasolia*, *Yarrumia*, and *Yoshimuriella* (Table I).

TABLE I. SAMPLES SEQUENCED USING TARGET CAPTURE IN THE CURRENT STUDY WITH VOUCHER DATA AND GENBANK ACCESSION NUMBERS.

| DNA # | *Genus* | *Species* | Collector | Voucher | Herbarium | Country | Genbank |
|---|---|---|---|---|---|---|---|
| 4005 | *Ricasolia* | *amplissima* | Tønsberg | 44719 | F | Norway | SAMN10602979 |
| 9930 | *Lobaria* | *pulmonaria* | Widhelm | TW4 | F | U.S. A | SAMN10602980 |
| 10048 | *Sticta* | *aff. fuliginosa* | McCune | 35727 | F | U.S. A | SAMN10602981 |
| 10049 | *Sticta* | *aff. limbata* | McCune | 35726 | F | U.S. A | SAMN10602982 |
| 14492 | *Sticta* | *beauvoisii* | Taylor Quedensely | *TQ16699* | F | U.S. A | SAMN10602983 |
| 14493 | *Sticta* | *carolinensis* | Taylor Quedensely | *TQ16700* | F | U.S. A | SAMN10602984 |
| 14532 | *Sticta* | *weigelii* | Joel Mercado-Diaz | 2284 | F | Puerto Rico | SAMN10602985 |
| 14538 | *Sticta* | *scabrosa* | Joel Mercado-Diaz | 2287 | F | Puerto Rico | SAMN10602986 |
| 14657 | *Sticta* | *aff.* | Joel Mercado-Diaz | 2378 | F | Puerto Rico | SAMN10602987 |
| 14665 | *Sticta* | *densiphyllidata* | Joel Mercado-Diaz | 2389 | F | Puerto Rico | SAMN10602988 |
| 14681 | *Pseudocyphellaria* | *glabra* | Lumbsch, Widhelm & Grewe | 2046 A | F | Australia | SAMN10602989 |
| 14829 | *Pseudocyphellaria* | *dissimilis* | Lumbsch, Widhelm & Grewe | 2173 | F | Australia | SAMN10602990 |
| 14830 | *Pseudocyphellaria* | *carpoloma* | Lumbsch, Widhelm & Grewe | 2074 D | F | Australia | SAMN10602991 |
| 14835 | *Pseudocyphellaria* | *crocata* | Lumbsch, Widhelm & Grewe | 2145 | F | Australia | SAMN10602992 |
| 14840 | *Pseudocyphellaria* | *neglecta* | Lumbsch, Widhelm & Grewe | 2031 | F | Australia | SAMN10602993 |
| 14845 | *Pseudocyphellaria* | *granulata* | Lumbsch, Widhelm & Grewe | 2469 | F | Australia | SAMN10602994 |
| 14850 | *Yarrumia* | *coronata* | Lumbsch, Widhelm & Grewe | 2042 | F | Australia | SAMN10602995 |
| 15144 | *Pseudocyphellaria* | *homoeophylla* | de Lange, Lucking & Moncada | ??? | F | New Zealand | SAMN10602996 |
| 15155 | *Sticta* | *sp.* | Coca | 43 | F | Colombia | SAMN10602997 |
| 15156 | *Sticta* | *sp.* | Coca | 47 | F | Colombia | SAMN10602998 |
| 15253 | *Dendriscosticta* | *platyphylla* | Goffinet | 13475 | CONN | Taiwan | SAMN10602999 |
| 15254 | *Lobaria* | *linita* | Simon | 147 | CONN | Canada | SAMN10603000 |
| 15256 | *Lobaria* | *sp.* | Goffinet | 13511 | CONN | Taiwan | SAMN10603001 |
| 15257 | *Lobaria* | *sp* | Goffinet | 13563 | CONN | Taiwan | SAMN10603002 |
| 15258 | *Nephroma* | *antarcticum* | Goffinet | 13963 | CONN | Chile | SAMN10603003 |
| 15261 | *Ricasolia* | *sp.* | Goffinet | 13062 | CONN | Taiwan | SAMN10603004 |
| 15271 | *Anomalobaria* | *anomala* | Simon | 150 | CONN | Canada | SAMN10603005 |
| 15272 | *Dendriscosticta* | *aff. wrightii* | Goffinet | 13227 | CONN | Taiwan | SAMN10603006 |
| 15273 | *Nephroma* | *plumbeum* | Goffinet | 12673 | CONN | Chile | SAMN10603007 |
| 15274 | *Lobarina* | *oregana* | Simon | 143 | CONN | Canada | SAMN10603008 |
| 15275 | *Lobariella* | *sp.* | Lucking | 41013a | BGBM | Colombia | SAMN10603009 |
| 15276 | *Lobariella* | *sp.* | Lucking | 41042 | BGBM | Colombia | SAMN10603010 |

TABLE I, CONTINUED

| DNA # | *Genus* | *Species* | Collector | Voucher | Herbarium | Country | Genbank |
|---|---|---|---|---|---|---|---|
| 15277 | *Lobariella* | *sp.* | Lucking | 41025 | BGBM | Colombia | SAMN10603011 |
| 15278 | *Yoshimuriella* | *subdissecta* | Moncada | 5369 | BGBM | Colombia | SAMN10603012 |
| 15279 | *Yoshimuriella* | *peltigera* | Moncada | 5389 | BGBM | Colombia | SAMN10603013 |
| 15280 | *Yoshimuriella* | *peltigera* | Moncada | 5322 | BGBM | Colombia | SAMN10603014 |
| 15313 | *Crocodia* | *poculifera* | de Lange, Lucking & Moncada | 39102 | F | New Zealand | SAMN10603015 |
| 15316 | *Yarrumia* | *colensoi* | de Lange, Lucking & Moncada | 38741 | F | New Zealand | SAMN10603016 |
| 15317 | *Yarrumia* | *coronata* | de Lange, Lucking & Moncada | 38974 | F | New Zealand | SAMN10603017 |
| 15678 | *Yoshimuriella* | *sp.* | Joel Mercado-Diaz | 2955 | F | Dominican Republic | SAMN10603018 |
| 15679 | *Yoshimuriella* | *sp.* | Joel Mercado-Diaz | 3072i | F | Dominican Republic | SAMN10603019 |
| 15680 | *Yoshimuriella* | *sp.* | Joel Mercado-Diaz | 3067b | F | Dominican Republic | SAMN10603020 |
| 15681 | *Yoshimuriella* | *sp.* | Joel Mercado-Diaz | 3133b | F | Dominican Republic | SAMN10603021 |
| 15682 | *Ricasolia* | *sp.* | Joel Mercado-Diaz | 2939 | F | Dominican Republic | SAMN10603022 |
| 15683 | *Ricasolia* | *sp.* | Joel Mercado-Diaz | 3031 | F | Dominican Republic | SAMN10603023 |
| 15684 | *Yoshimuriella* | *sp.* | Joel Mercado-Diaz | 2991a | F | Dominican Republic | SAMN10603024 |
| 15685 | *Ricasolia* | *sp.* | Joel Mercado-Diaz | 3038c | F | Dominican Republic | SAMN10603025 |
| 15686 | *Lobariella* | *sp.* | Joel Mercado-Diaz | 3063a | F | Dominican Republic | SAMN10603026 |
| 15687 | *Nephroma* | *sp.* | Joel Mercado-Diaz | 3122f | F | Dominican Republic | SAMN10603027 |
| 15688 | *Nephroma* | *sp.* | Joel Mercado-Diaz | 3104 | F | Dominican Republic | SAMN10603028 |
| 15841 | *Pseudocyphellaria* | *granulata* | Felix Grewe, Todd Widhelm, Matt von Konrat, Juan Larrain | 4117 | F | Chile | SAMN10603029 |
| 15842 | *Pseudocyphellaria* | *lecheri* | Felix Grewe, Todd Widhelm, Matt von Konrat, Juan Larrain | 4118 | F | Chile | SAMN10603030 |
| 15843 | *Parmostictina* | *obvoluta* | Felix Grewe, Todd Widhelm, Matt von Konrat, Juan Larrain | 4119 | F | Chile | SAMN10603031 |
| 15844 | *Pseudocyphellaria* | *crocata* | Felix Grewe, Todd Widhelm, Matt von Konrat, Juan Larrain | 4121 | F | Chile | SAMN10603032 |
| 15845 | *Pseudocyphellaria* | *crocata* | Felix Grewe, Todd Widhelm, Matt von Konrat, Juan Larrain | 4122 | F | Chile | SAMN10603033 |
| 15847 | *Podostictina* | *berberina* | Felix Grewe, Todd Widhelm, Matt von Konrat, Juan Larrain | 4124 | F | Chile | SAMN10603034 |
| 15848 | *Pseudocyphellaria* | *freycinetii* | Felix Grewe, Todd Widhelm, Matt von Konrat, Juan Larrain | 4125 | F | Chile | SAMN10603035 |
| 15849 | *Podostictina* | *flavicans* | Todd Widhelm, Matt von Konrat, Juan Larrain | 4389 | F | Chile | SAMN10603036 |
| 15850 | *Yarrumia* | *coronata* | de Lange, Lucking & Moncada | 38675 | F | New Zealand | SAMN10603037 |
| 15851 | *Yarrumia* | *colensoi* | de Lange, Lucking & Moncada | 38836 | F | New Zealand | SAMN10603038 |
| 15868 | *Pseudocyphellaria* | *coriifolia* | Todd Widhelm, Matt von Konrat, Juan Larrain | 4319 | F | Chile | SAMN10603039 |
| 15869 | *Pseudocyphellaria* | *intricata* | Todd Widhelm, Matt von Konrat, Juan Larrain | 4353 | F | Chile | SAMN10603040 |
| 15870 | *Sticta* | *hypochroa* | Todd Widhelm, Matt von Konrat, Juan Larrain | 4354 | F | Chile | SAMN10603041 |
| 15871 | *Sticta* | *caulescens* | Todd Widhelm, Matt von Konrat, Juan Larrain | 4357 | F | Chile | SAMN10603042 |
| 15872 | *Sticta* | *sp.* | Todd Widhelm, Matt von Konrat, Juan Larrain | 4358 | F | Chile | SAMN10603043 |

TABLE I, CONTINUED

| DNA # | *Genus* | *Species* | Collector | Voucher | Herbarium | Country | Genbank |
|---|---|---|---|---|---|---|---|
| 15873 | *Podostictina* | *encoensis* | Todd Widhelm, Matt von Konrat, Juan Larrain | 4401 | F | Chile | SAMN10603044 |
| 15874 | *Pseudocyphellaria* | *haywardiosum* | Peter de Lange | 12586 | F | New Zealand | SAMN10603045 |
| 15875 | *Pseudocyphellaria* | *haywardiosum* | Peter de Lange | 12587 | F | New Zealand | SAMN10603046 |
| 15876 | *Pseudocyphellaria* | *cinnamomea* | Mark Moorhouse | | F | New Zealand | SAMN10603047 |
| 15877 | *Pseudocyphellaria* | *lividofusa* | Peter de Lange | 13259 | F | New Zealand | SAMN10603048 |
| 15878 | *Pseudocyphellaria* | *pubescens* | Mark Moorhouse | | F | New Zealand | SAMN10603049 |
| 15879 | *Sticta* | *latifrons* | | CH2534 | F | New Zealand | SAMN10603050 |
| 15880 | *Sticta* | *fuliginosa* | | CH2547 | F | New Zealand | SAMN10603051 |
| 15881 | *Sticta* | *fuliginosa* | Peter de Lange | 13163 | F | New Zealand | SAMN10603052 |
| 15882 | *Sticta* | *cinereoglauca* | | CH2547 | F | New Zealand | SAMN10603053 |
| 15884 | *Pseudocyphellaria* | *sp.* | Todd Widhelm, Matt von Konrat, Juan Larrain | 4405 | F | Chile | SAMN10603054 |
| 15885 | *Parmostictina* | *hirsuta* | Todd Widhelm, Matt von Konrat, Juan Larrain | 4417 | F | Chile | SAMN10603055 |
| 15886 | *Pseudocyphellaria* | *sp.* | Todd Widhelm, Matt von Konrat, Juan Larrain | 4440 | F | Chile | SAMN10603056 |
| 15887 | *Podostictina* | *vaccina* | Todd Widhelm, Matt von Konrat, Juan Larrain | 4443 | F | Chile | SAMN10603057 |
| 15888 | *Crocodia* | *aurata* | Felix Grewe, Todd Widhelm | 3496 | F | New Zealand | SAMN10603058 |
| 15889 | *Nephroma* | *australe* | Felix Grewe, Todd Widhelm | 3516 | F | New Zealand | SAMN10603059 |
| 15890 | *Pseudocyphellaria* | *carpoloma* | Felix Grewe, Todd Widhelm | 3192 | F | New Zealand | SAMN10603060 |
| 15891 | *Pseudocyphellaria* | *carpoloma* | Felix Grewe, Todd Widhelm | 3617 | F | New Zealand | SAMN10603061 |
| 15892 | *Pseudocyphellaria* | *chloroluca* | Felix Grewe, Todd Widhelm, Dan Blanchon, Peter de Lange | 3044 | F | New Zealand | SAMN10603062 |
| 15893 | *Pseudocyphellaria* | *corbettii* | Felix Grewe, Todd Widhelm | 3190 | F | New Zealand | SAMN10603063 |
| 15894 | *Pseudocyphellaria* | *crocata* | Allison Knight | 69193a | OTA | New Zealand | SAMN10603064 |
| 15895 | *Podostictina* | *degelii* | Felix Grewe, Todd Widhelm | 3594 | F | New Zealand | SAMN10603065 |
| 15896 | *Pseudocyphellaria* | *disimilis* | Felix Grewe, Todd Widhelm | 3019 | F | New Zealand | SAMN10603066 |
| 15897 | *Pseudocyphellaria* | *episticta* | Felix Grewe, Todd Widhelm | 3498 | F | New Zealand | SAMN10603067 |
| 15898 | *Pseudocyphellaria* | *montagnei* | Felix Grewe, Todd Widhelm | 3507 | F | New Zealand | SAMN10603068 |
| 15899 | *Pseudocyphellaria* | *rufovirescens* | Felix Grewe, Todd Widhelm | 3219 | F | New Zealand | SAMN10603069 |
| 15900 | *Sticta* | *filix* | Felix Grewe, Todd Widhelm, Dan Blanchon, Peter de Lange | 3074 | F | New Zealand | SAMN10603070 |
| 15901 | *Sticta* | *latifrons* | Felix Grewe, Todd Widhelm | 3274 | F | New Zealand | SAMN10603071 |
| 15902 | *Sticta* | *lacera* | Felix Grewe, Todd Widhelm | 3255 | F | New Zealand | SAMN10603072 |
| 15903 | *Pseudocyphellaria* | *corbettii* | Felix Grewe, Todd Widhelm, Dan Blanchon, Peter de Lange | 3105 | F | New Zealand | SAMN10603073 |
| 15904 | *Sticta* | *subcaperata* | Felix Grewe, Todd Widhelm | 3310 | F | New Zealand | SAMN10603074 |

### 2.2.2 Bait design

We designed baits for target capture using Markerminer (Chamala et al. 2015), a bioinformatics pipeline that finds single copy loci in the genome using genome and transcriptome data as inputs. Markerminer is designed for use with angiosperms, and has databases for 15 angiosperm genomes, but other genome databases can be added for customized use of the program. We used the *Lobaria pulmonaria* genome and the gene annotation file (Lobpul1_AssemblyScaffolds_Repeatmasked.fasta and Lobpul1_GeneCatalog_20170213.gff3) from JGI (https://jgi.doe.gov/) to develop a custom database. The result is a simplified reference genome that only contains gene regions and the introns are hard-masked as "N"s in the sequence.

We assembled transcriptome data (published in Meiser et al. 2017) from *Evernia prunastri*, *Pseudevernia furfuracea* and *Lasallia pustulata* using Trinity (Grabherr et al. 2011). The resulting transcriptomes and the custom *L. pulmonaria* database were used to identify clusters of single-copy gene transcripts present in the transcriptome assemblies. Next, these were aligned and filtered against the *L. pulmonaria* reference proteome from JGI (Lobpul1_GeneCatalog_proteins_20170213.aa.fasta) using BLAST. These single-copy genes were re-aligned to the intron hard-masked genome and intron-exon boundaries were identified.

Markerminer identified and aligned 1,714 single-copy genes to the hard-masked *L. pulmonaria* reference genome. We selected loci that had at least one exon of at least 500 bp and indicated clear intron-exon boundaries on the hard-masked alignment. The designed baits were collected as 800 separate fasta DNA sequence files from the *L. pulmonaria* and *E. prunastri* (400 each). These sequences were provided to Arbor Biosciences (Ann Arbor, MI, USA) for MYbaits bait design. These filtered baits covered 92% of the desired target positions with at least one bait, therefore all 800 target sequences are represented with at least one bait. One hundred nucleotide-

long baits were designed with two times tiling density resulting in 18,139 raw unfiltered baits. Following Arbor Biosciences recommended filtering process (baits passing “Moderate” BLAST filtering), 17,941 baits were retained for target-capturing.

### 2.2.3 Library preparation

DNA was obtained using the ZR Fungal/Bacterial DNA MiniPrep™ (Zymo Research, Irvine, CA, USA) or by a cetyl trimethylammonium bromide (CTAB) extraction protocol. The concentration of all DNA isolates was quantified with the Qubit (Thermo Fisher Scientific, Waltham, MA, USA). Two hundred ng of meta-genomic DNA was normalized to a final volume of 52.5 µL in resuspension buffer. Fragments of DNA around 500 bp were generated with M220 Focused-ultrasonicator™ (Woburn, MA, USA) and then 50 µL was cleaned up with 80 µL SeraPure beads which are an inexpensive alternative to commercially purchased magnetic beads (Glenn et al. 2016). The Adapterama dual-indexing system (Glenn et al. 2016) was used to uniquely barcode all samples using the KAPA Hyper Prep Kit (KAPABiosystems, Wilmington, MA, USA). Twenty-five µL of the sheared, cleaned bead elution was used in a 30 µL end-repair and A-tailing reaction followed by a 55 µL ligation to attach the Adapterama stubby y-yolk adapter. The ligation products were subjected to bead-based size selection with SeraPure bead to enrich for fragments of around 550 bp which was eluted in 22 µL of RSB. Twenty µL of the elution was used in a limited-cycle (9-11 cycles) polymerase chain reaction (PCR) to attach the barcoded iTru5 and iTru7 Adapterama primers. Subsequently, the PCR products were cleaned with 1X SeraPure beads and eluted in 43 µL of nuclease-free, PCR-grade water. DNA concentrations of all samples were quantified with a Qubit fluorometer (Thermo Fisher Scientific, Waltham, MA, USA) and a subset were checked for proper size distribution of fragments on the Bioanalyzer (Agilent, Santa Clara, CA, USA).

Samples were pooled by phylogenetic relatedness, corresponding to major clades of the previous Lobariaceae three-locus phylogeny (Moncada, Lücking, and Betancourt-Macuase 2013), for hybridization with RNA baits. For each sample, 100-200 ng of DNA was mixed with all samples of each of the five pools and then concentrated in a heated vacuum centrifuge. Pools were hybridized with reagents provided with the baits from Arbor Biosciences for ~20 h at 65°C. After incubation, the baits were attached to streptavidin beads and then washed according to the Arbor Biosciences protocol followed by a post-wash enrichment PCR cycle with KAPA Hifi Hotstart ReadyMix. Each pool went through 11 cycles of PCR except for the outgroup (*Nephroma* samples), which was subjected to 14 cycles. These were cleaned with 1X SeraPure beads and the DNA concentration was quantified on the Qubit and size of distribution of the DNA fragments in the pools were observed on the Bioanalyzer. These pools were mixed together to have 3 ng of DNA per sample in the final 96-sample pool which was used for sequencing at the Field Museum's Pritzker Laboratory with a single 300-cycle v2 MiSeq reagent kit (Illumina, San Diego, CA, USA).

### 2.2.4 Data processing

The MiSeq run (300 cycles using V2 chemistry) produced 15,835,491 150-bp paired-end reads, which were demultiplexed and adapter-trimmed by Illumina BaseSpace. The raw reads were downloaded to the Field Museum server and quality trimmed with Trimmomatic (Bolger, Lohse, and Usadel 2014) using a quality cutoff of 15 in a 4-bp sliding window, discarding any reads under 35 bp. Only paired, trimmed reads were used in downstream analyses, which is an average of 158,443 reads per sample remaining after trimming with a range from 7929 to 317,874 reads (Table XVIII, Appendix A). These sequences were used for the read files using the program HybPiper (Johnson et al. 2016) which assembles gene regions and extracts exon

sequences for each sample. We generated a target file from the *L. pulmonaria* transcriptome on JGI (Lobpul1_GeneCatalog_proteins_20170213.aa.fasta) that has the complete amino acid sequences of each of the 400 target genes that were used for bait design. The sorted, trimmed reads of each sample were mapped to the targets using the default BLASTX (Camacho et al. 2009) option, which we found recovered much more data (a more complete dataset), especially for the outgroup (*Nephroma* taxa) than the BWA option that uses a nucleotide target file. Upon completion of the HybPiper assembly, the 399 gene sequences (one gene did not produce any sequences) were extracted using retrieve_sequences.py and then batch aligned using MAFFT (Katoh and Standley 2013).

HybPiper will flag a gene if it identifies multiple sequences spanning at least 85% of the gene length (Johnson et al. 2016). When this occurs at a specific gene, HybPiper will choose only one of the sequences, first by selecting the sequence with the highest depth of sequencing and then, if all sequences are similar in coverage, it uses the closest match to the specified target sequence file. For the paralog warning genes, all the copies were extracted (paralog_retriever.py), aligned and phylogenetically analyzed to check the patterns of paralogy for each of these flagged genes. However, paralogous sequences could be present in some datasets that did not have a warning. For example, if one or more taxa yield only one sequence that is paralogous to the others. Furthermore, multiple copies could be alleles or a duplication that postdates a bifurcation which HybPiper would flag, but this case would not cause problems with phylogenetic inference. Future studies will need to use more thorough analyses to have a detailed understanding of how paralogs are influencing phylogenetic reconstructions.

### 2.2.5 Concatenation of datasets

Multiple nucleotide alignments of single genes were concatenated with FASconCAT-G

(Kück and Longo 2014). One alignment contained 376 loci and 96 tips (376x96nuc) and had 438,036 nucleotide positions with 13.75% gaps and undetermined characters. Only genes that had at least 48 sequences (50% sample representation) were used. Another reduced dataset (297x17nuc) with only 17 taxa, representing all Lobariaceae genera and the well supported subclades in *Sticta* and *Pseudocyphellaria* was generated in HybPiper. With this dataset 297 of the genes had all 17 sequences and these alignments were used to generated gene trees and a concatenated alignment with 338,019 nucleotide positions and 4.04% gaps and undetermined characters. We also generated the same concatenated datasets with amino acid sequences using FASconCAT-G. The dataset with 376 loci and 96 tips (376x96aa) and had 145,467 amino acid positions with 6.34% missing data and 7.26% indels. Finally, the reduced dataset (297x17aa) of 297 loci and 17 tips had 112,265 amino acid positions with no missing data, but it did contain 3.89% indels. A summary of all datasets can be found in table II.

TABLE II. SUMMARY OF DATASETS ANALYZED IN THE CURRENT STUDY.

| | **Dataset** | **# loci** | **# tips** | **Positions** | **missing data** |
|---|---|---|---|---|---|
| | | | *nucleotide data* | | |
| 50% sample representation | 397x96nuc | 397 | 96 | 438036 | 13.75% |
| Complete, simplified | 297x17nuc | 297 | 17 | 338019 | 0.00% |
| | | | *amino acid data* | | |
| 50% sample representation | 397x96aa | 397 | 96 | 145467 | 6.34% |
| Complete, simplified | 297x17aa | 297 | 17 | 112265 | 0.00% |

### 2.2.6 Maximum likelihood and species tree analyses

For all full and reduced datasets, concatenated phylogenies and all single gene trees were estimated using the RAxML (Stamatakis 2014) rapid hill climbing algorithm and performing 100 bootstrap replicates. All single gene alignments and all partitions of each concatenated dataset had substitution model selection using either the GTRGAMMA or PROTGAMMA -AUTO models for nucleotide and amino acid models of sequences respectively. Since concatenated datasets can be prone to false positive topologies (Heled and Drummond 2010; Kubatko and Degnan 2007), we also analyzed our datasets with the multi-species coalescent model the program Accurate Species Tree Algorithm (ASTRAL 5.6.1) (Mirarab and Warnow 2015). For the ASTRAL analyses, we inferred species trees from single, fully resolved, and unrooted gene trees mentioned above. Branch support was reported as local posterior probabilities (i.e., the support for a quadripartition).

### 2.2.7 Analysis of gene-tree discordance and tree space

Regardless of the data type or tree building approach, all of the datasets produced backbones with short internal branches. During rapid diversification, speciation and gene flow occur simultaneously in a relatively short period of time, which can lead to high levels of gene-tree discordance. Discordance among gene-trees can be the result of incomplete lineage sorting (ILS), reticulate evolution, and homoplasy. The coalescent model implemented in ASTRAL, accounts for ILS, but this approach was still unable to completely resolve the deep divergences in the backbone of the amino acid and nucleotide datasets. Although this does not completely rule out ILS as a source of gene-tree discordance, it does suggest that other historical processes, such as homoplasy or reticulate evolution, which are not accounted for in ASTRAL, were potentially contributing to the poorly resolved backbones in our reconstructions. To conduct

analyses on and visualize the gene-tree discordance the best trees from the RAxML analyses for each gene were converted to ultrametric trees using the chronos() function in the R package APE (Paradis, Claude, and Strimmer 2004) with a lambda = 1. This was done using the program SumTrees (Sukumaran and Holder 2015) implemented in DendroPy 4.0.0 (Sukumaran and Holder 2010) to find if there was a common tree topology among the reduced (297x17) amino acid and nucleotide datasets. DensiTree 2.2.5 (Bouckaert 2010) was used to visualize the discordance of gene-tree topologies.

Tree space of the reduced datasets (297x17nuc and 297x17aa) were described using multidimensional scaling (MDS) in R using the customized topclustMDS function described elsewhere. These datasets were used because complete trees (all having 17 tips) were required. Gene trees were loaded into R using the APE package (Paradis, Claude, and Strimmer 2004), then MDS scaling and functions in the cluster package (Maechler 2018) were used to identify the most appropriate number of clusters and the identity of loci comprising each cluster.

### 2.2.8 Tests for reticulate evolution

Another known source of poor backbone node support in phylogenies is reticulate evolution. This process is not modeled in the most used phylogenomic inference programs such as RAxML or ASTRAL as the output can only be bifurcating. A current program, PhyloNet (Than, Ruths, and Nakhleh 2008), does model this process, and we used it to investigate whether parts of the relationships in the Lobariaceae phylogeny are better supported with a model of reticulate evolution rather than a strictly bifurcating tree. PhyloNet identifies reticulation events using a multi-species network coalescent model that accounts for ILS and reticulate evolution. We first used the maximum pseudo-likelihood approach (InferNetwork_MPL option) on the 297x17nuc dataset, specifying the -po option which optimizes the branch lengths and inheritance

probabilities under full likelihood for the returned species networks. We conducted six analyses with reticulation scenarios ranging from zero to five and then ten with each analysis conducting ten runs and inferring five networks. The zero-reticulation scenario served as a null model and we then increased the reticulation events step-wise to five reticulations to see how each increase fit to the data by calculating AIC for each network. Finally, we conducted a ten-reticulation analysis to see if more than five reticulations could be recovered from our dataset.

Although the MPL approach is computationally fast, under certain conditions, the true reticulation history may not be identifiable (Yu and Nakhleh 2015). Thus, using the drop.tip() function in the R package APE (Paradis, Claude, and Strimmer 2004), we produce a five-tip dataset that contain only *Crocodia*, *Podostictina*, *Pseudocyphellaria*, *Sticta*, and *Yarrumia (*the genera that were usually involved in the reticulations of the MPL analyses), so that we could apply a fully parameterized ML approach (InferNetwork_ML). Due to the taxing computational demands of the fully parameterized ML option of PhyloNet, we only tested zero to three reticulations (using the -po option described above), because the best fitting scenarios in the MPL analyses included three reticulations (see results). Each analysis conducted five runs and produced one network and the total log probabilities were used to calculate AIC to assess model fit.

### 2.2.9 Dated phylogeny of Lobariaceae

The program MCMCTree 1.2 (Yang 2007; Yang and Rannala 2005) was used to infer divergence times in Lobariaceae. The ML tree (376x96aa), inferred with amino acids and congruent with the one inferred in ASTRAL was used for the dating analyses and the concatenated amino acid matrix. We used CODEML to generate the Hessian matrix using an empirical rate matrix with gamma rates among sites (WAG+Gamma). Using this matrix, we ran

MCMCTree with appropriate rates under the approximate method. Settings were set as follows: independent-rates model, time unit at 100 Ma, sampling fraction at ρ=0.1, and the birth and death rates at λ=μ=1. We ran the analyses with gaps and ambiguities removed (cleandata = 0). The gamma prior for the substitution model was set at six transitions to two transversions rate ratio. The gamma shape parameter for variable rates among sites was set as α = 1 The Dirichlet-gamma prior was set to α = 2 and β = 20 for a diffuse prior. The MCMC was run for 40,000 iterations, with samples taken every other iteration, after a 5% burnin. Two runs were conducted to check for consistency.

We calibrated the phylogeny with the only known fossil from the family, obtained from a 12-24 Myr-old Miocene deposit from northern California. The fossil is an impression that resembles the genus *Lobaria*. A recent study by Cornejo and Scheidegger (Cornejo and Scheidegger 2018), used a molecular clock-calibrated phylogeny of *Lobaria*, to estimate the age of the fossil impression and found that it fits into the time frame of *Lobaria* diversification and placed it near the crown of the genus. Based on that, we calibrated the 376x96aa concatenated phylogeny with the impression fossil, by placing it on the branch between *L. linita* and the remaining *Lobaria* species, with a range of 12 to 24 million years.

## 2.3 Results

### 2.3.1 Efficiency of sequencing data recovery and assembly of datasets

Following the read assembly via Hybpiper (Johnson et al. 2016) we recovered 390.65 of the 400 target genes per sample (337.67 with 75% coverage). Most coverage (all 400 genes mapped and 398 having 75% coverage) was achieved for *Lobaria pulmonaria* which was used as the reference in HybPiper and for the bait design. The lowest coverage was in *Sticta cinereoglauca* and *Pseudocyphellaria crocata* for which only 386 and 387 targets were

recovered and only with partial coverage to the extent that at 75% coverage only 32 and 0 genes were recovered (Table XVIII, Appendix A, [hybpiper blastx stats]). This is probably due to the DNA extract quality reducing the hybridization of these sample to the baits. Of the 400 loci sequenced in this study, 138 generated a paralog warning (an average of 14.125 paralogs per sample) involving between one and 95 samples (average 11 taxa with multiple sequences at a given locus). The trees produced after running the HybPiper script paralog_retriever.py to obtain all paralogous sequences for all flagged loci exhibited two patterns: (1) the two sequences retrieved would cluster and form a clade or (2) the two sequences would be resolved in two very different clades, separated by a long branch, which is indicative of an ancestral gene duplication event (data not shown). In all 138 cases, HybPiper selected only one sequence that was most like the target sequence.

### 2.3.2 Topological patterns among data types and phylogeny reconstruction methods

Initially we generated a nucleotide dataset (376x96nuc; Figure 1A) where all included loci had at least 50% specimen representation (at least 48 sequences regardless of recovered length in HybPiper), which was the case for 376 of the 400 loci. All Lobariaceae formed a well-supported (100% bootstrap support) clade and the tree had a well-supported backbone with the lowest nodes having a bootstrap support value of 73% (Figure 1A). The earliest diverging clade included samples of *Podostictina* forming a sister-group relationship to the remaining Lobariaceae. The next split reflects the divergence of *Lobaria* and its closely related genera (*Anomolobaria*, *Dendriscosticta*, *Lobariella*, *Lobarina*, *Ricasolia*, and *Yoshimuriella*). The following split gives rise to the clade composed of two sister genera, *Sticta* and *Yarrumia*. The most derived split among genera yields *Crocodia* sister to *Pseudocyphellaria* (Figure 1A).

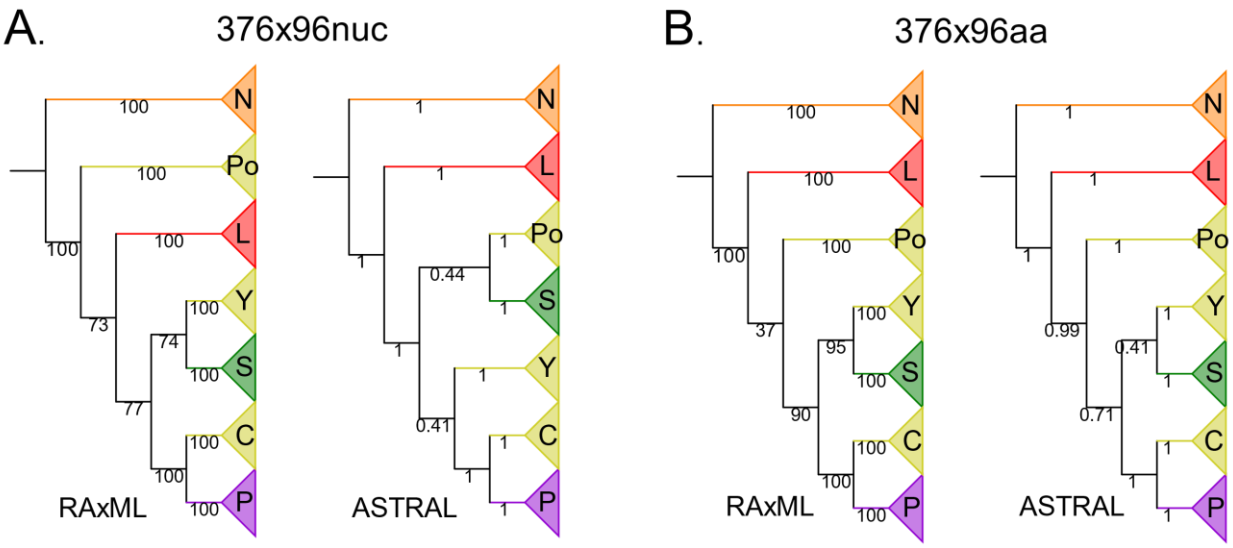


Figure 1 Tree topologies estimated with nucleotide (A) and amino acid (B) data and different tree reconstruction methods (RAxML concatenated vs. ASTRAL species tree). Nodal support, either as bootstrap (RAxML) or local posterior probability (ASTRAL) is depicted under the branches. Abbreviations are as follows: N = *Nephroma* (outgroup); L = *Lobaria s. lat*. clade (also including *Anomolobaria, Dendriscosticta, Lobariella, Lobarina, Ricasolia,* and *Yoshimuriella*); Po = Podostictina; S = *Sticta*; Y = *Yarrumia*; C = *Crocodia*; P = *Pseudocyphellaria*.

Subsequently, we analyzed amino acid sequences from the same dataset (376x96aa; Figures. 1B and 2). Again, the calculated tree supported Lobariaceae as a well-supported monophyletic clade, but the tree resulted in even lower backbone support (37%) for the unique ancestry to the *Podostictina* clade, and the clade including *Sticta*, *Yarrumia*, *Crocodia* and *Pseudocyphellaria*. (Figures. 1B and 2).

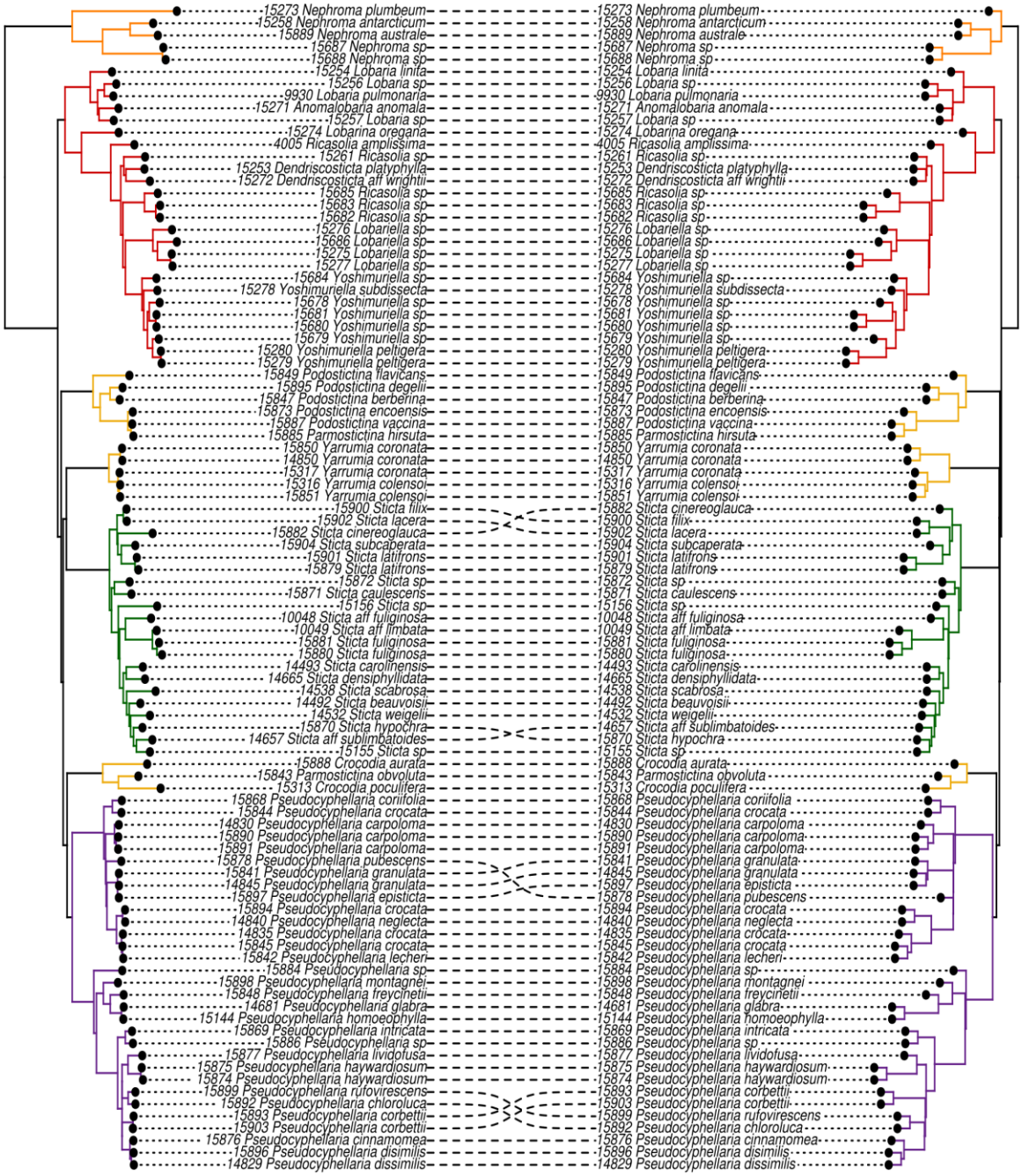


Figure 2. Congruence of topologies inferred with concatenation (A: RAxML) and species tree approaches (B: ASTRAL) from dataset composed of 376 amino acid sequences. Nodal support for the backbone is depicted in Figure 2B. The colors of branches are assigned to clades as follows: Orange: *Nephroma* (outgroup); Red: *Anomolobaria, Dendriscosticta, Lobaria, Lobariella, Lobarina, Ricasolia, Yoshimuriella*; Yellow: *Crocodia, Parmostictina, Podostictina*, and *Yarrumia* (not monophyletic); Green: *Sticta*; Purple: *Pseudocyphellaria.*

The species tree inferred in ASTRAL with nucleotide sequences conflicted with the same dataset reconstructed from concatenated data in RAxML (376x96nuc; Figure 1A), while the amino acid species tree produced in ASTRAL-II had the same backbone topology as the concatenated amino acid tree (376x96aa; Figures. 1B and 2B). However, in the amino acid tree reconstruction from ASTRAL, two nodes were poorly supported; one associated with the splitting of *Podostictina* (0.71 local posterior probability) and another associated with the branching of *Sticta* and *Yarrumia*, both still forming a monophyletic clade (0.41 local posterior probability). The nucleotide species tree had a similar topology as the amino acid species tree, except that *Yarrumia* was sister to *Crocodia* and *Pseudocyphellaria* with poor support (0.41 local posterior probability). *Podostictina* and *Sticta* formed a poorly supported clade (0.44 local posterior probability) (Figure 1A).

### 2.3.3 Evidence for rapid diversification and gene-tree discordance

The short backbone branches leading to *Crocodia*, *Parmostictina*, *Podostictina*, *Pseudocyphellaria*, *Sticta*, and *Yarrumia* occurred within a 5-million-year period, which is suggestive of a rapid diversification. To investigate the cause for inconsistent phylogenetic tree results based on potential rapid diversification and gene-tree discordance, we created a pruned dataset (Figure 3) (297x17). This created a complete matrix without missing data which was analyzed with RAxML and ASTRAL based on nuclear and amino acid translations. All four trees differed in their backbone branching patterns (Figure 3A), with incongruent clades receiving strong support. *Podostictina* and *Yarrumia* were the major sources of incongruence, as they were recovered in different relationships depending on the data type and analysis.

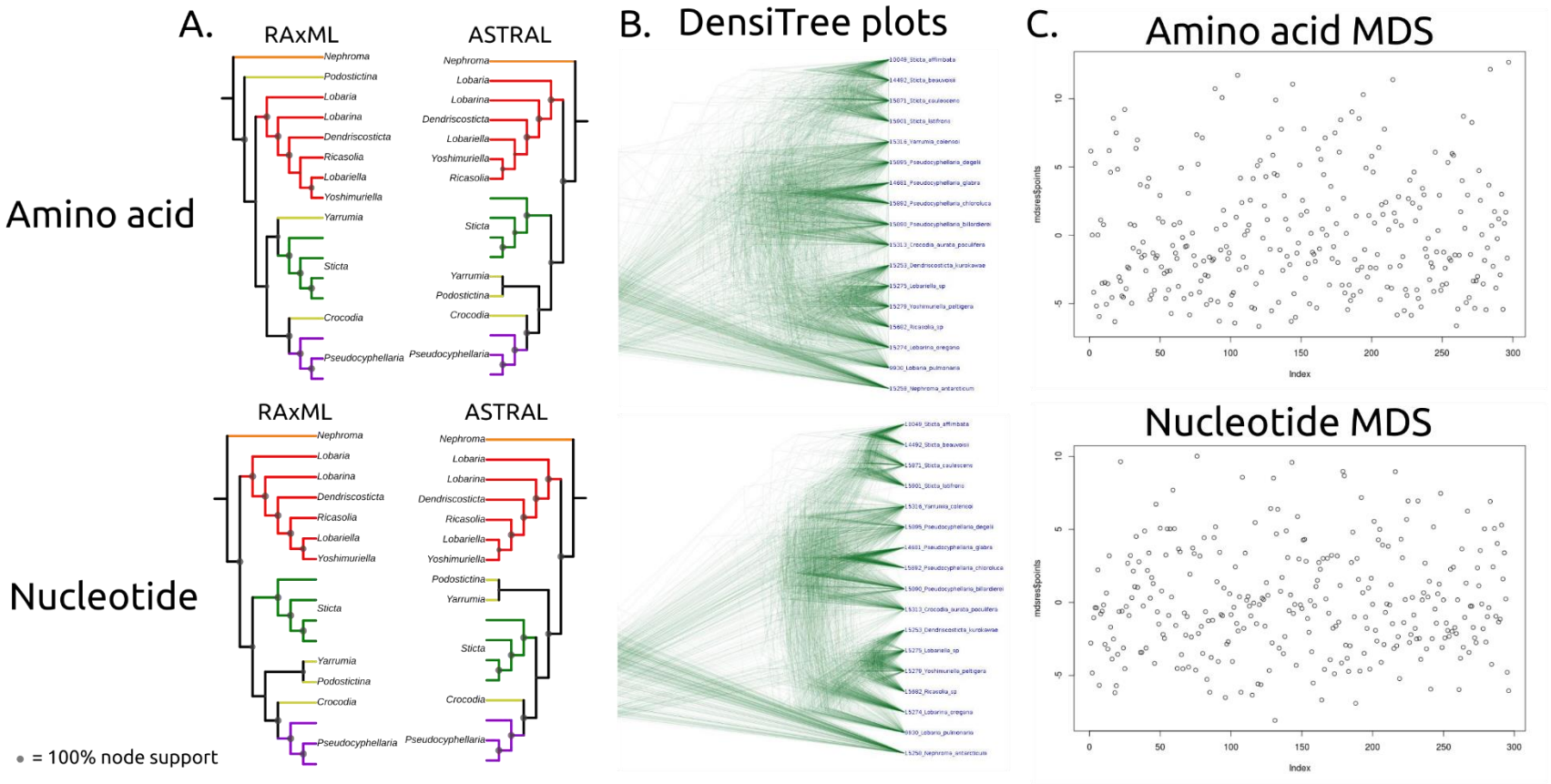


Figure 3. Poor support, incongruence of relationships of genera and gene tree discordance in Lobariaceae with (A.) different methods (RAxML vs. ASTRAL) and different datatypes (amino acid vs. nucleotide) of the reduced dataset of 297 loci and 17 tips with no missing data. Nodal support is depicted by the size of the gray circles in the nodes, with larger circles being higher supported. (B.) DensiTree plots of the gene trees used to produce the 297x17 datasets. (C.) Dimension one of multi-dimensional scaling (MDS) plots of one-to-one Robinson Foulds distances of 297 trees produced from amino acid and nucleotide sequences.

Removing these genera from the dataset, especially *Podostictina*, increased congruence and node support among all trimmed datasets (Figure 21, Appendix A). To find the most common topology we used SumTrees, which recovered 297 unique topologies of each tree reconstruction from the pruned nucleotide and amino acid datasets (Figure 21 & Figure 22, Appendix A). We visualized this gene-tree discordance by using DensiTree, which creates a figure by overlaying all 297 gene trees. Although both datasets recovered clear groupings representing well supported clades, the backbone is depicted as a diffuse cloud of branches (Figure 3B). Using the pairwise Robinson-Foulds distances (topological distances) of gene-trees and MDS, we found that clustering of topologies was not significant and that both the amino acid and nucleotide datasets exhibited a diffuse pattern in all dimensions (Figure 3C). This suggests that the gene-trees in both datasets have no dominant topology.

### 2.3.4 Evidence for reticulate evolution in Lobariaceae

We used the same pruned 297x17nuc dataset to infer evidence of reticulate evolution in Lobariaceae by using PhyloNet. Although, the maximum pseudo-likelihood (MPL) option (InferNetwork_MPL) in PhyloNet indicated that a three-reticulation model had the best fit to our data, none of the networks produced by PhyloNet had three reticulations (Table III). At most, two reticulations were inferred (Figure 4). The reticulations reconstructed in the networks generally originated in the ancestral nodes or branches of samples from *Crocodia*, *Podostictina*, *Pseudocyphellaria*, *Sticta* and *Yarrumia.* Using a full likelihood approach (InferNetwork_ML) on 17 taxa is too computationally heavy for most servers so we produced a dataset with only *Crocodia*, *Podostictina*, *Pseudocyphellaria*, *Sticta*, and *Yarrumia*. As with the MPL approach, the three-reticulation scenario had the best fit to the data in the ML analysis (Table IV and Figure 21, Figure 22, Appendix A).

TABLE III. LIKELIHOOD AND AIC SCORES FOR ALL RETICULATION SCENARIOS USING THE MPL APPROACH.

| Reticulations | k | Total log probability | AIC | |
|---|---|---|---|---|
| **0** | **32** | -4,772.61 | 9,609.22 | |
| | | -4,772.93 | 9,545.87 | |
| | | -4,773.10 | 9,546.21 | |
| | | -4,774.06 | 9,548.11 | |
| | | -4,774.08 | 9,548.16 | |
| | | **-4,773.36** | **9,546.71** | Average |
| **1** | **33** | -4,757.90 | 9,581.80 | |
| | | -4,766.82 | 9,533.64 | |
| | | -4,770.67 | 9,541.33 | |
| | | -4,773.04 | 9,546.08 | |
| | | -4,774.05 | 9,548.10 | |
| | | **-4,768.50** | **9,536.99** | Average |
| **2** | **34** | -4,749.11 | 9,566.22 | |
| | | -4,771.13 | 9,542.27 | |
| | | -4,771.34 | 9,542.68 | |
| | | -4,772.93 | 9,545.87 | |
| | | -4,774.05 | 9,548.11 | |
| | | **-4,767.71** | **9,535.43** | Average |
| **3** | **35** | -4,687.22 | 9,444.44 | |
| | | -4,743.86 | 9,487.72 | |
| | | -4,760.41 | 9,520.82 | |
| | | -4,772.93 | 9,545.87 | |
| | | -4,773.04 | 9,546.07 | |
| | | **-4,747.49** | **9,494.98** | Average |
| **4** | **36** | -4,769.16 | 9,610.31 | |
| | | -4,770.96 | 9,541.91 | |
| | | -4,771.03 | 9,542.07 | |
| | | -4,771.78 | 9,543.57 | |
| | | -4,772.94 | 9,545.87 | |
| | | **-4,771.17** | **9,542.35** | Average |

TABLE III, CONTINUED

| Reticulations | k | Total log probability | AIC | |
|---|---|---|---|---|
| **5** | **37** | -4,770.67 | 9,615.33 | |
| | | -4,772.11 | 9,544.21 | |
| | | -4,773.10 | 9,546.21 | |
| | | -4,774.05 | 9,548.11 | |
| | | -4,774.07 | 9,548.15 | |
| | | **-4,772.80** | **9,545.60** | Average |
| **10** | **42** | -4,770.66 | 9,625.33 | |
| | | -4,770.96 | 9,541.92 | |
| | | -4,772.93 | 9,545.87 | |
| | | -4,773.04 | 9,546.07 | |
| | | -4,773.32 | 9,546.63 | |
| | | **-4,772.18** | **9,544.36** | Average |

TABLE IV. LIKELIHOOD AND AIC SCORES FOR ALL RETICULATION SCENARIOS USING THE ML APPROACH.

| Reticulations | k | Total log probability | AIC |
|---|---|---|---|
| 0 | 7 | -1435.24 | 2870.48 |
| 1 | 8 | -1366.30 | 2734.60 |
| 2 | 9 | -1335.74 | 2675.48 |
| 3 | 10 | -1328.20 | 2662.40 |

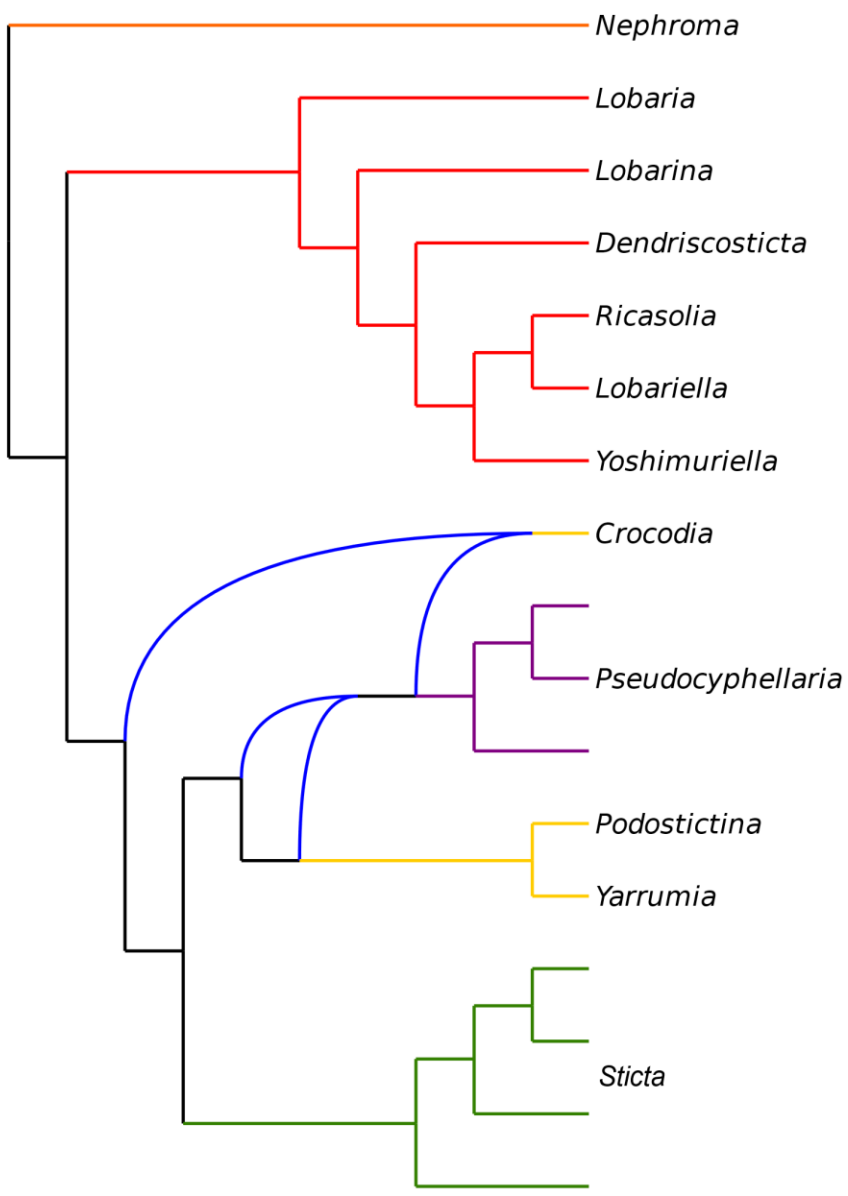


Figure 4. PhyloNet network showing one of the most likely reticulation scenarios.

### 2.3.5 Timing of divergence in Lobariaceae

Both runs of MCMCTree converged on similar estimations. The average stem age of Lobariaceae was estimated to be 64.4 Mya (91.9-43.4 Mya). Crown divergences of the major clades in Lobariaceae are as follows: *Lobaria s. lat* clade (which also includes *Anomolobaria*, *Dendriscosticta*, *Lobariella*, *Lobarina*, *Ricasolia*, and *Yoshimuriella*), 57.6 Mya (84.0-38.1 Mya); *Podostictina*, 29.5 Mya (53.0-14.2 Mya); *Yarrumia*, 12.4 Mya (21.2-5.9 Mya); *Sticta*, 25.2 Mya (39.9-15.2 Mya); *Crocodia*, 33.4 Mya (56.0-16.7 Mya); and *Pseudocyphellaria*, 54.1 Mya (78.7-35.2 Mya). The results of one of the runs is depicted in Figure 5 and detailed output of the analysis is in Figure 23, Appendix A.

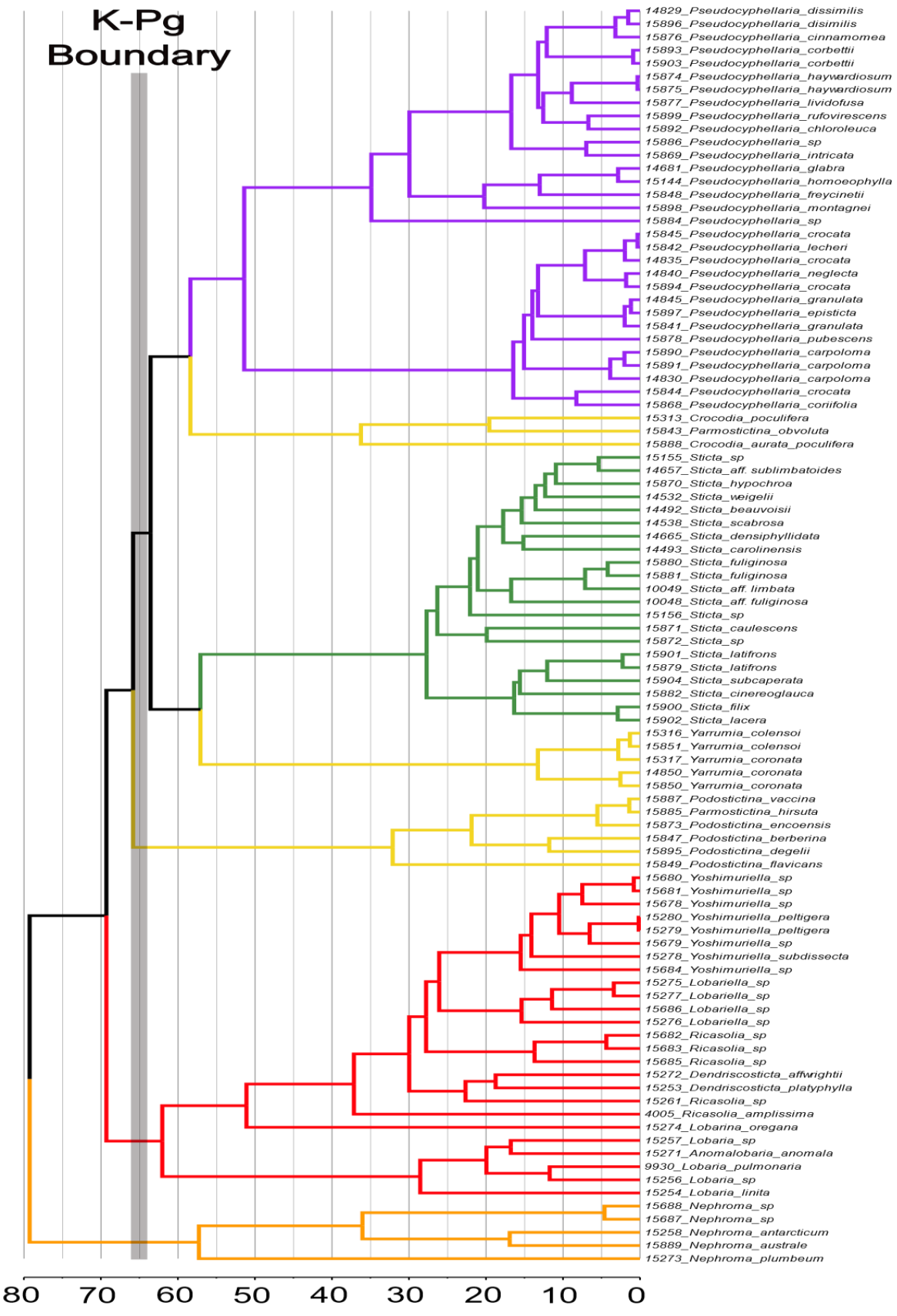
K-Pg
Boundary
14829_Pseudocyphellaria_dissimilis
15896_Pseudocyphellaria_disimilis
15876_Pseudocyphellaria_cinnamomea
15893_Pseudocyphellaria_corbettii
15903_Pseudocyphellaria_corbettii
15874_Pseudocyphellaria_haywardiosum
15875_Pseudocyphellaria_haywardiosum
15877_Pseudocyphellaria_lividofusa
15899_Pseudocyphellaria_rufovirescens
15892_Pseudocyphellaria_chloroleuca
15886_Pseudocyphellaria_sp
15869_Pseudocyphellaria_intricata
14681_Pseudocyphellaria_glabra
15144_Pseudocyphellaria_homoeophylla
15848_Pseudocyphellaria_freycinetii
15898_Pseudocyphellaria_montagnei
15884_Pseudocyphellaria_sp
15845_Pseudocyphellaria_crocata
15842_Pseudocyphellaria_lecheri
14835_Pseudocyphellaria_crocata
14840_Pseudocyphellaria_neglecta
15894_Pseudocyphellaria_crocata
14845_Pseudocyphellaria_granulata
15897_Pseudocyphellaria_episticta
15841_Pseudocyphellaria_granulata
15878_Pseudocyphellaria_pubescens
15890_Pseudocyphellaria_carpoloma
15891_Pseudocyphellaria_carpoloma
14830_Pseudocyphellaria_carpoloma
15844_Pseudocyphellaria_crocata
15868_Pseudocyphellaria_coriifolia
15313_Crocodia_poculifera
15843_Parmostictina_obvoluta
15888_Crocodia_aurata_poculifera
15155_Sticta_sp
14657_Sticta_aff._sublimbatoides
15870_Sticta_hypochroa
14532_Sticta_weigelii
14492_Sticta_beauvoisii
14538_Sticta_scabrosa
14665_Sticta_densiphyllidata
14493_Sticta_carolinensis
15880_Sticta_fuliginosa
15881_Sticta_fuliginosa
10049_Sticta_aff._limbata
10048_Sticta_aff._fuliginosa
15156_Sticta_sp
15871_Sticta_caulescens
15872_Sticta_sp
15901_Sticta_latifrons
15879_Sticta_latifrons
15904_Sticta_subcaperata
15882_Sticta_cinereoglauca
15900_Sticta_filix
15902_Sticta_lacera
15316_Yarrumia_colensoi
15851_Yarrumia_colensoi
15317_Yarrumia_coronata
14850_Yarrumia_coronata
15850_Yarrumia_coronata
15887_Podostictina_vaccina
15885_Parmostictina_hirsuta
15873_Podostictina_encoensis
15847_Podostictina_berberina
15895_Podostictina_degelii
15849_Podostictina_flavicans
15680_Yoshimuriella_sp
15681_Yoshimuriella_sp
15678_Yoshimuriella_sp
15280_Yoshimuriella_peltigera
15279_Yoshimuriella_peltigera
15679_Yoshimuriella_sp
15278_Yoshimuriella_subdissecta
15684_Yoshimuriella_sp
15275_Lobariella_sp
15277_Lobariella_sp
15686_Lobariella_sp
15276_Lobariella_sp
15682_Ricasolia_sp
15683_Ricasolia_sp
15685_Ricasolia_sp
15272_Dendriscosticta_affwrightii
15253_Dendriscosticta_platyphylla
15261_Ricasolia_sp
4005_Ricasolia_amplissima
15274_Lobarina_oregana
15257_Lobaria_sp
15271_Anomalobaria_anomala
9930_Lobaria_pulmonaria
15256_Lobaria_sp
15254_Lobaria_linita
15688_Nephroma_sp
15687_Nephroma_sp
15258_Nephroma_antarcticum
15889_Nephroma_australe
15273_Nephroma_plumbeum
80
70
60
50
40
30
20
10
0

Figure 5. A chronogram estimated by Bayesian relaxed molecular clock implemented in MCMCTree. The ML tree inferred with concatenated amino acid sequences (376x96aa - congruent with the ASTRAL species tree) was used a scaffold for the dating analysis. The grey vertical bar depicts the K-Pg boundary. The timescale is in units of millions of years. Colors of clades: Orange: *Nephroma* (outgroup); Red: *Anomolobaria, Dendriscosticta, Lobaria, Lobariella, Lobarina, Ricasolia, Yoshimuriella*; Yellow: *Crocodia, Parmostictina, Podostictina,* and *Yarrumia* (not monophyletic); Green: *Sticta*; Purple: *Pseudocyphellaria*.

TABLE V. NODE AGES ESTIMATED IN MCMCTREE WITH MINIMUM AND MAXIMUM STANDARD DEVIATIONS IN MILLIONS OF YEARS.

| **Clades** | **Run 1** | | | **Run 2** | | | **Averaged runs** | | |
|---|---|---|---|---|---|---|---|---|---|
| | **age** | **minimum** | **max** | **age** | **minimum** | **max** | **age** | **minimum** | **max** |
| Lobariaceae | ***69.3*** | 53.4 | 89 | ***59.4*** | 33.4 | 94.7 | ***64.4*** | 43.4 | 91.9 |
| *Nephroma* | ***57.3*** | 36.6 | 86 | ***53.9*** | 31.2 | 84.6 | ***55.6*** | 33.9 | 85.3 |
| *"Lobaria* clade*"* | ***62*** | 46.7 | 81.6 | ***53.2*** | 29.5 | 86.4 | ***57.6*** | 38.1 | 84.0 |
| *Lobaria* | ***28.5*** | 20 | 42.5 | ***25.2*** | 14.7 | 41.1 | ***26.9*** | 17.4 | 41.8 |
| *Dendriscosticta* | ***22.7*** | 13.9 | 35.2 | ***19.2*** | 9.6 | 37.4 | ***21.0*** | 11.8 | 36.3 |
| *Ricasolia* | ***13.7*** | 7.7 | 21.1 | ***11.4*** | 5 | 20.4 | ***12.6*** | 6.4 | 20.8 |
| *Lobariella* | ***15.4*** | 9.4 | 22.2 | ***12.9*** | 6.1 | 21.8 | ***14.2*** | 7.8 | 22.0 |
| *Yoshimuriella* | ***15.5*** | 10.2 | 21.6 | ***13.1*** | 6.6 | 21.7 | ***14.3*** | 8.4 | 21.7 |
| *Podostictina* | ***32.1*** | 16.8 | 54.6 | ***26.8*** | 11.5 | 51.3 | ***29.5*** | 14.2 | 53.0 |
| *Yarrumia* | ***13.3*** | 6.8 | 21.7 | ***11.5*** | 5 | 20.6 | ***12.4*** | 5.9 | 21.2 |
| *Sticta* | ***27.7*** | 18.5 | 43.2 | ***22.6*** | 11.8 | 36.6 | ***25.2*** | 15.2 | 39.9 |
| *Crocodia* | ***36.2*** | 20 | 56.3 | ***30.6*** | 13.4 | 55.6 | ***33.4*** | 16.7 | 56.0 |
| *Pseudocyphellaria* | ***58.4*** | 43.2 | 76.2 | ***49.8*** | 27.2 | 81.1 | ***54.1*** | 35.2 | 78.7 |

## 2.4 Discussion

We produced the first target enrichment dataset of a lineage of lichenized fungi with a goal of resolving the higher-level relationships in Lobariaceae and found that the evolutionary history exhibited rapid diversification and that we could not confidently reconstruct the relationships assuming a strictly bifurcating tree. The phylogenetic positions in which certain lineages are resolved differs when using (1) number of loci or (2) different tree reconstruction methods (Figure 1). However, more slowly-evolving amino acid sequence data yielded more consistent results, especially with the 376-locus dataset, where the RAxML and ASTRAL backbone branching patterns were identical (Figure 2). This topology was highly supported in ASTRAL, but the node leading to *Podostictina* clade in RAxML was poorly supported (Figure 1B). An increasing number of studies are producing datasets of hundreds, even thousands of loci, and are finding that certain nodes in the tree of life that are still very challenging to resolve with our current inference methods (Reddy et al. 2017; Prum et al. 2015; Jarvis et al. 2014; Xi et al. 2014; Goremykin et al. 2015; Dunn et al. 2008; Simion et al. 2017; Burleigh and Mathews 2004). We found no exception in Lobariaceae. However, even though phylogenetic relationship among genera remained uncertain (c.f., Moncada, Lücking, and Betancourt-Macuase 2013), we were able to further study the factors that are preventing resolution. As a result, our study is the first on lichenized fungi to investigate the underlying mechanisms – namely rapid diversification and reticulations – that may lead to poorly-resolved relationships.

Regardless of the dataset or analysis, the genera were separated by short branches, suggesting a rapid diversification resulting in the genera that were previously placed within *Pseudocyphellaria* (including *Crocodia, Podostictina,* and *Yarrumia*) and *Sticta* (i.e., *Dendriscosticta*). Short branches can be difficult to resolve with confidence, even with large

subgenomic datasets (Wiens et al. 2008). Rapid diversifications can also lead to conflicting topologies among individual gene trees (Maddison 1997). This is consistent with our study, even in our reduced dataset (297x17) with 297 unique rooted topologies (Figure 3). The multi-species coalescent-based species tree approach can account for ILS (Liu and Edwards 2009). However, species trees with short, deep branches, such as those recovered in this study, can result in uninformative gene-trees, and the gene trees may result in erroneous species tree reconstruction (Huang et al. 2010). The inconsistency in phylogenetic reconstruction and low support for certain branching patterns revealed in our study suggest that the short branches in our trees confound species tree approaches in this case. The only time we found a consensus between the two methods was when we used the largest amino acid data set (376x96aa), but node support, was low for some of these relationships (Figures. 1B and 2).

Concatenation of genetic loci has a long history in phylogenetics, but it has also been known to produce highly supported yet conflicting results, especially in the area of tree space known as the "anomaly zone" (Kubatko and Degnan 2007) (when most gene trees in the genome do not reflect the true speciation history). Furthermore, concatenated analyses cannot account for the different evolutionary histories at different loci, which can also produce misleading topologies (Degnan and Rosenberg 2006). They can also be extremely sensitive to outlier loci (Lacey et al. 2018). The probability of sampling an outlier locus increases as the amount of data increases, and it is therefore expected that the effect of such loci will be stronger in larger subgenomic data set (Lacey et al. 2018).

Models that incorporate reticulations always had better fit to the data than models assuming a strictly bifurcating tree (Figure 4, Tables III and IV). Furthermore, in most phylogenetic networks generated, the taxa with labile topological positions (*Podostictina*, *Sticta*

and *Yarrumia*) were usually associated with the reticulations in the network. Reticulation events can confound both concatenated ML and coalescent-based species tree approaches, causing incongruence and poorly supported relationships (Som 2015; Nakhleh et al. 2005). This could also contribute to the inconsistency among phylogenetic reconstructions and poor nodal supports found in our study. Additionally, the effects of reticulation and rapid diversification may not be independent. Reticulations have been hypothesized to promote subsequent rapid diversification events in cichlids (Meier et al. 2017), yeasts (Leducq et al. 2016), and fungal pathogens (Stukenbrock 2016). Reticulate evolution is most likely to induce rapid diversification when parental lineages occupy highly dissimilar ecological niches but are only moderately genetically differentiated (Kagawa and Takimoto 2018). Recombination among distinct yet compatible evolutionary lineages may generate novel phenotypes to exploit new niches. Although we have shown that reticulate models have a better fit, it is unclear whether they led to a rapid diversification (suggested by the short and poorly supported nodes) in Lobariaceae as the two are not mutually exclusive. Rapid radiations could also increase the chances of reticulate evolution, because so many closely related taxa may not have had the chance to develop effective reproductive barriers before secondary contact occurred in nature. Reticulate evolution may characterize the evolution of a number of lichenized fungi. Hybridization has been invoked to account for patterns in secondary chemistry in *Hypotrachyna* (Culberson and Hale 1973), and among gene-tree incongruence in *Cladonia* (Jana et al. 2013) and *Lobaria* (Cornejo, Chabanenko, and Scheidegger 2018) were seen as compatible with reticulation. In *Letharia* a reticulate evolutionary history was proposed based on patterns of recombination in nuclear DNA markers (Kroken and Taylor 2001). The other form of reticulate evolution, horizontal gene transfer (HGT), has been discovered with fungal genes being found in the *Trebouxia* photobionts

(Beck et al. 2015), and with polyketide synthases of actinobacterial origin being found in lichenized fungi (Schmitt and Lumbsch 2009), but HGT has not yet been reported among lichenized fungi and is not hypothesized in this study.

Our topology (376x96aa data sets in Figure 1B and 2) was similar to that of Moncada, Lücking, and Betancourt-Macuase (2013) with the main exceptions being the relationships of *Sticta* and of genera previously segregated from *Pseudocyphellaria* (e.g. *Crocodia, Parmostictina, Podostictina,* and *Yarrumia*). In the previous study (Moncada, Lücking, and Betancourt-Macuase 2013), *Parmostictina*, *Podostictina* and *Crocodia* formed a well-supported clade (*Yarrumia* was not included in their analysis) sister to *Pseudocyphellaria.* In our analyses, the *Crocodia* and *Pseudocyphellaria* still formed a sister-group relationship in all datasets, but the relationships of *Parmostictina* and *Podostictina* were poorly supported and differed depending on data type and method of inference: it could be placed sister to either all Lobariaceae, to (*Crocodia* + *Pseudocyphellaria* + *Sticta* + *Yarrumia*), to *Yarrumia,* or only to *Sticta* (Figures. 1, 2, and 3). The erratic placement of *Parmostictina* and *Podostictina,* when using different data types and inference methods, exhibits patterns found in other unrelated groups of organisms with unresolved phylogenetic relationships, such as the deep, poorly supported nodes leading to ctenophores and sponges (Dunn et al. 2008; Simion et al. 2017), *Amborella* (Xi et al. 2014; Goremykin et al. 2015; Drew et al. 2014; Zhang et al. 2012), and Gnetales (Mathews 2009; Burleigh and Mathews 2004). Another relationship that was often but not always recovered was the *Sticta* and *Yarrumia* sister relationship.

Our time-calibrated phylogeny recovered a nearly 70 Mya stem age of Lobariaceae which is in agreement with the estimate of Gaya et al. (Gaya et al. 2015) but not with Simon et al. (Simon et al. 2018) where a 50 Mya stem age was reported. Furthermore, our crown age

estimates agree with other dated phylogenies generated for the genera *Sticta* (Widhelm et al. 2018 – Chapter 3 in this dissertation) and *Lobaria* (Cornejo and Scheidegger 2018), both of which have crown ages around 30 Mya. The timing of the rapid and reticulate Lobariaceae divergence is near the end of the Cretaceous around 70–60 Mya. The Cretaceous Terrestrial Revolution (Vermeij 2011; Benton 2010) (CTR) occurred between 100 and 70 Mya and is associated with the massive diversification event that gave rise to the angiosperms (Lidgard and Crane 1988, 1990). The increase in angiosperm diversity in the late Cretaceous created new ecological opportunities (Schuettpelz and Pryer 2009; Schneider et al. 2004) and these may have triggered bursts of diversification in spore-dispersing plants (Schuettpelz and Pryer 2009; Schneider et al. 2004; Feldberg et al. 2014; Laenen et al. 2014) mammals (Meredith et al. 2011), and ants (Moreau et al. 2006). Secondary diversification pulses following the CTR and rise of angiosperms are especially linked to the evolution of epiphytism and has been demonstrated in leafy liverworts (Feldberg et al. 2014) and ferns (Schuettpelz and Pryer 2009; Schneider et al. 2004). Most Lobariaceae species are epiphytic and the rapid diversification event seen in our study could be another example of a subsequent pulse in divergence linked to the CTR. The rapid diversification of Lobariaceae was also associated with the Cretaceous-Paleogene (K-Pg) boundary around 66 Mya. Mass extinctions associated with K-Pg boundary may have reduced competition and provided an opportunity for surviving lineages to radiate (Renne et al. 2013). The macrolichen growth form is associated with multiple diversification rate increases following the K-Pg boundary (Huang et al. 2018). Lobariaceae, a lineage composed solely of macrolichens, may have also experienced a similar diversification rate increase as in other clades of lichenized fungi.

Since the application of genetic data to reconstructing the evolutionary relationships of lichenized fungi, our understanding of the diversification of most lineages has significantly improved. Single and multiple locus phylogenies have discovered many relationships that were obscured by homoplasy in phenotypic characters. With the advent of next-generation sequencing (NGS) technology, only a handful of studies have been conducted on groups of lichenized fungi to resolve phylogenetic relationships (Leavitt et al. 2016; Grewe et al. 2017). In traditional phylogenetic studies, fungal-specific primers got around the issue of mixed genomes in DNA isolations, but with genomic studies, the only way to get purely fungal DNA is to culture the fungal symbiont. The ability of lichenized fungi to be cultured varies among groups and it has not been successful in many. Regardless, over ten genomes have been sequenced and are available for study. Recently, studies using purely fungal reference genomes from cultured lichenized fungi have gotten around the issue of using metagenomic DNA isolations, by applying a mapping step that pulls out the fungal reads for use in phylogenomic analyses (Grewe et al. 2017).

**2.5 Conclusion**

This study is the first to apply the target capturing approach in lichenized fungi to investigate historical processes influencing the evolution of major clades in Lobariaceae. Although we were not able to confidently resolve certain relationships, we were able to investigate why certain nodes remained unresolved, and we have a more thorough understanding of the evolutionary history of the group. We provide evidence for rapid diversification and reticulate evolution in our data set, which would not be possible to infer with only a few loci. However, it is still not clear what the relative effects of rapid diversification and reticulations are on gene tree discordance and difficulties in species tree reconstruction. We encourage the

phylogenetic study of taxonomic groups with uncertain phylogenetic relationships so, as a scientific community, we can understand how historical processes are most likely to obscure relationships in the tree of life. Resolution of some nodes in the tree of life may not always be possible with increasing datasets, but a detailed understanding of the evolutionary events that confound the history of a group are the next best steps to take to make informed decisions about their taxonomic classification.

**2.6 References**


Beck, A., P. K. Divakar, N. Zhang, M. C. Molina, and L. Struwe. "Evidence of ancient horizontal gene transfer between fungi and the terrestrial alga *Trebouxia*." *Organisms Diversity & Evolution* 15, no. 2 (2015): 235-248.

Benton, Michael J. "The origins of modern biodiversity on land." *Philosophical Transactions of the Royal Society B: Biological Sciences* 365, no. 1558 (2010): 3667-3679.

Bolger, Anthony M., Marc Lohse, and Bjoern Usadel. "Trimmomatic: A flexible trimmer for Illumina sequence data." *Bioinformatics* 30, no. 15 (2014): 2114-2120.

Bouckaert, Remco, Joseph Heled, Denise Kühnert, Tim Vaughan, Chieh-Hsi Wu, Dong Xie, Marc A. Suchard, Andrew Rambaut, and Alexei J. Drummond. "BEAST 2: A software platform for Bayesian evolutionary analysis." *PLoS Computational Biology* 10, no. 4 (2014): e1003537.

Bouckaert, Remco R. "DensiTree: Making sense of sets of phylogenetic trees." *Bioinformatics* 26, no. 10 (2010): 1372-1373.

Burleigh, J. Gordon, and Sarah Mathews. "Phylogenetic signal in nucleotide data from seed plants: Implications for resolving the seed plant tree of life." *American Journal of*

*Botany* 91, no. 10 (2004): 1599-1613.

Camacho, Christiam, George Coulouris, Vahram Avagyan, Ning Ma, Jason Papadopoulos, Kevin Bealer, and Thomas L. Madden. "BLAST+: Architecture and applications." *BMC Bioinformatics* 10, no. 1 (2009): 421.

Chamala, Srikar, Nicolás García, Grant T. Godden, Vivek Krishnakumar, Ingrid E. Jordon-Thaden, Riet De Smet, W. Brad Barbazuk, Douglas E. Soltis, and Pamela S. Soltis. "MarkerMiner 1.0: A new application for phylogenetic marker development using angiosperm transcriptomes." *Applications in Plant Sciences* 3, no. 4 (2015): 1400115.

Cornejo, Carolina, Svetlana Chabanenko, and Christoph Scheidegger. "Are species-pairs diverging lineages? A nine-locus analysis uncovers speciation among species-pairs of the *Lobaria meridionalis*-group (Ascomycota)." *Molecular Phylogenetics and Evolution* 129 (2018): 48-59.

Cornejo, Carolina, and Christoph Scheidegger. "Estimating the timescale of *Lobaria* diversification." *The Lichenologist* 50, no. 1 (2018): 113-121.

Culberson, Chicita F., and Mason E. Hale. "Chemical and morphological evolution in *Parmelia* sect. *Hypotrachyna*: Product of ancient hybridization?." *Brittonia* 25, no. 2 (1973): 162-173.

Degnan, James H., and Noah A. Rosenberg. "Discordance of species trees with their most likely gene trees." *PLoS Genetics*2, no. 5 (2006): e68.

Delsuc, Frédéric, Henner Brinkmann, and Hervé Philippe. "Phylogenomics and the reconstruction of the tree of life." *Nature Reviews Genetics* 6, no. 5 (2005): 361.

Drew, Bryan T., Brad R. Ruhfel, Stephen A. Smith, Michael J. Moore, Barbara G. Briggs,

Matthew A. Gitzendanner, Pamela S. Soltis, and Douglas E. Soltis. "Another look at the root of the angiosperms reveals a familiar tale." *Systematic Biology* 63, no. 3 (2014): 368-382.

Dunn, Casey W., Andreas Hejnol, David Q. Matus, Kevin Pang, William E. Browne, Stephen A. Smith, Elaine Seaver et al. "Broad phylogenomic sampling improves resolution of the animal tree of life." *Nature* 452, no. 7188 (2008): 745.

Feldberg, Kathrin, Harald Schneider, Tanja Stadler, Alfons Schäfer-Verwimp, Alexander R. Schmidt, and Jochen Heinrichs. "Epiphytic leafy liverworts diversified in angiosperm-dominated forests." *Scientific Reports* 4 (2014): 5974.

Gaya, Ester, Samantha Fernández-Brime, Reinaldo Vargas, Robert F. Lachlan, Cécile Gueidan, Martín Ramírez-Mejía, and François Lutzoni. "The adaptive radiation of lichen-forming Teloschistaceae is associated with sunscreening pigments and a bark-to-rock substrate shift." *Proceedings of the National Academy of Sciences* 112, no. 37 (2015): 11600-11605.

Gee, Henry. "Evolution: Ending incongruence." *Nature* 425, no. 6960 (2003): 782.

Glenn, Travis C., Roger Nilsen, Troy J. Kieran, John W. Finger, Todd W. Pierson, Kerin E. Bentley, Sandra Hoffberg et al. "Adapterama I: Universal stubs and primers for thousands of dual-indexed Illumina libraries (iTru & iNext)." *BioRxiv* (2016): 049114.

Goremykin, V. V., S. V. Nikiforova, D. Cavalieri, M. Pindo, and Peter Lockhart. "The root of flowering plants and total evidence." *Systematic Biology* 64, no. 5 (2015): 879-891.

Grabherr, Manfred G., Brian J. Haas, Moran Yassour, Joshua Z. Levin, Dawn A. Thompson, Ido Amit, Xian Adiconis et al. "Trinity: Reconstructing a full-length transcriptome without a genome from RNA-Seq data." *Nature Biotechnology* 29, no. 7 (2011): 644.

Green, T. G. A., and Otto L. Lange. "Ecophysiological adaptations of the lichen genera *Pseudocyphellaria* and *Sticta* to south temperate rainforests." *The Lichenologist* 23, no. 3 (1991): 267-282.

Grewe, Felix, Jen-Pen Huang, Steven D. Leavitt, and H. Thorsten Lumbsch. "Reference-based RADseq resolves robust relationships among closely related species of lichen-forming fungi using metagenomic DNA." *Scientific Reports* 7, no. 1 (2017): 9884.

Hale, Mason E. "Pseudocyphellae and pored epicortex in the Parmeliaceae: Their delimitation and evolutionary significance." *The Lichenologist* 13, no. 1 (1981): 1-10.

Heled, J., and A. J. Drummond. 2010. “Bayesian inference of species trees from multilocus data.” *Molecular Biology and Evolution* 27 (3): 570–80.

Hipp, Andrew L., Deren Eaton, Jeannine Cavender-Bares, Elisabeth Fitzek, Rick Nipper, and Paul S. Manos. "A framework phylogeny of the American oak clade based on sequenced RAD data." *PLOS ONE* 9, no. 4 (2014): e93975.

Huang, Huateng, Qixin He, Laura S. Kubatko, and L. Lacey Knowles. "Sources of error inherent in species-tree estimation: Impact of mutational and coalescent effects on accuracy and implications for choosing among different methods." *Systematic Biology* 59, no. 5 (2010): 573-583.

Huang, Jen-Pan, Ekaphan Kraichak, Steven D. Leavitt, Matthew P Nelsen, and H. Thorsten Lumbsch. “Accelerated diversification in three diverse clades of morphologically complex lichen-forming fungi after the K-Pg boundary.” *BMC Evolutionary Biology,* under review. (2019).

Jaklitsch, Walter, Hans-Otto Baral, Robert Lücking, H. Thorsten Lumbsch, and Wolfgang Frey.

*Syllabus of Plant Families-A. Engler's Syllabus der Pflanzenfamilien Part 1/2*. Edited by Wolfgang Frey. Stuttgart: Borntraeger Science Publishers. (2016).

Jarvis, Erich D., Siavash Mirarab, Andre J. Aberer, Bo Li, Peter Houde, Cai Li, Simon Ho et al. "Whole-genome analyses resolve early branches in the tree of life of modern birds." *Science* 346, no. 6215 (2014): 1320-1331.

Johnson, Matthew G., Elliot M. Gardner, Yang Liu, Rafael Medina, Bernard Goffinet, A. Jonathan Shaw, Nyree JC Zerega, and Norman J. Wickett. "HybPiper: Extracting coding sequence and introns for phylogenetics from high-throughput sequencing reads using target enrichment." *Applications in Plant Sciences* 4, no. 7 (2016): 1600016.

Kagawa, Kotaro, and Gaku Takimoto. "Hybridization can promote adaptive radiation by means of transgressive segregation." *Ecology Letters* 21, no. 2 (2018): 264-274.

Katoh, Kazutaka, and Daron M. Standley. "MAFFT multiple sequence alignment software version 7: Improvements in performance and usability." *Molecular Biology and Evolution* 30, no. 4 (2013): 772-780.

Kirk, Paul M., Paul F. Cannon, D. W. Minter, and J. A. Stalpers. *Dictionary of the fungi 10th edition.* Wallingford: CAB International. (2008).

Kraichak, Ekaphan, Jen-Pan Huang, Matthew Nelsen, Steven D. Leavitt, and H. Thorsten Lumbsch. "A revised classification of orders and families in the two major subclasses of Lecanoromycetes (Ascomycota) based on a temporal approach." *Botanical Journal of the Linnean Society* 188, no. 3 (2018): 233-249.

Kroken, Scott, and John W. Taylor. "Outcrossing and recombination in the lichenized fungus *Letharia*." *Fungal Genetics and Biology* 34, no. 2 (2001): 83-92.

Kubatko, Laura Salter, and James H. Degnan. "Inconsistency of phylogenetic estimates from concatenated data under coalescence." *Systematic Biology* 56, no. 1 (2007): 17-24.

Kück, Patrick, and Gary C. Longo. "FASconCAT-G: Extensive functions for multiple sequence alignment preparations concerning phylogenetic studies." *Frontiers in Zoology* 11, no. 1 (2014): 81.

Knowles, L. Lacey, Huateng Huang, Jeet Sukumaran, and Stephen A. Smith. "A matter of phylogenetic scale: Distinguishing incomplete lineage sorting from lateral gene transfer as the cause of gene tree discord in recent versus deep diversification histories." *American Journal of Botany* 105, no. 3 (2018): 376-384.

Laenen, B., B. Shaw, H. Schneider, B. Goffinet, Emmanuel Paradis, A. Désamoré, J. Heinrichs et al. "Extant diversity of bryophytes emerged from successive post-Mesozoic diversification bursts." *Nature Communications* 5 (2014): 5134.

Lange, O. L., T. G. A. Green, and H. Ziegler. "Water status related photosynthesis and carbon isotope discrimination in species of the lichen genus *Pseudocyphellaria* with green or blue-green photobionts and in photosymbiodemes." *Oecologia*75, no. 4 (1988): 494-501.

Leavitt, Steven D., Felix Grewe, Todd Widhelm, Lucia Muggia, Brian Wray, and H. Thorsten Lumbsch. "Resolving evolutionary relationships in lichen-forming fungi using diverse phylogenomic datasets and analytical approaches." *Scientific Reports* 6 (2016): 22262.

Leducq, Jean-Baptiste, Lou Nielly-Thibault, Guillaume Charron, Chris Eberlein, Jukka-Pekka Verta, Pedram Samani, Kayla Sylvester, Chris T. Hittinger, Graham Bell, and Christian R. Landry. "Speciation driven by hybridization and chromosomal plasticity in a wild yeast." *Nature Microbiology* 1, no. 1 (2016): 15003.

Lidgard, Scott, and Peter R. Crane. "Quantitative analyses of the early angiosperm radiation." *Nature* 331, no. 6154 (1988): 344.

Lidgard, Scott, and Peter R. Crane. "Angiosperm diversification and Cretaceous floristic trends: A comparison of palynofloras and leaf macrofloras." *Paleobiology* 16, no. 1 (1990): 77-93.

Liu, Liang, and Scott V. Edwards. "Phylogenetic analysis in the anomaly zone." *Systematic Biology* 58, no. 4 (2009): 452-460.

Liu, Liang, Zhenxiang Xi, Shaoyuan Wu, Charles C. Davis, and Scott V. Edwards. "Estimating phylogenetic trees from genome-scale data." *Annals of the New York Academy of Sciences* 1360, no. 1 (2015): 36-53.

Liu, Yang, Cymon J. Cox, Wei Wang, and Bernard Goffinet. "Mitochondrial phylogenomics of early land plants: Mitigating the effects of saturation, compositional heterogeneity, and codon-usage bias." *Systematic Biology* 63, no. 6 (2014): 862-878.

Lumbsch, H. Thorsten, and Steven D. Leavitt. "Goodbye morphology? A paradigm shift in the delimitation of species in lichenized fungi." *Fungal Diversity* 50, no. 1 (2011): 59.

Maddison, Wayne P. "Gene trees in species trees." *Systematic Biology* 46, no. 3 (1997): 523-536.

Maechler, Martin. "Finding groups in data": Cluster analysis extended Rousseeuw et. al." R Package version 2.0.6 (2018).

Martin, Andrew P., and Theresa M. Burg. "Perils of paralogy: Using HSP70 genes for inferring organismal phylogenies." *Systematic Biology* 51, no. 4 (2002): 570-587.

Mathews, Sarah. "Phylogenetic relationships among seed plants: Persistent questions and the limits of molecular data." *American Journal of Botany* 96, no. 1 (2009): 228-236.

Meier, Joana I., David A. Marques, Salome Mwaiko, Catherine E. Wagner, Laurent Excoffier, and Ole Seehausen. "Ancient hybridization fuels rapid cichlid fish adaptive radiations." *Nature Communications* 8 (2017): 14363.

Meiser, Anjuli, Jürgen Otte, Imke Schmitt, and Francesco Dal Grande. "Sequencing genomes from mixed DNA samples-evaluating the metagenome skimming approach in lichenized fungi." *Scientific Reports* 7, no. 1 (2017): 14881.

Meredith, Robert W., Jan E. Janečka, John Gatesy, Oliver A. Ryder, Colleen A. Fisher, Emma C. Teeling, Alisha Goodbla et al. "Impacts of the Cretaceous Terrestrial Revolution and KPg extinction on mammal diversification." *Science* 334, no. 6055 (2011): 521-524.

Mirarab, Siavash, and Tandy Warnow. "ASTRAL-II: Coalescent-based species tree estimation with many hundreds of taxa and thousands of genes." *Bioinformatics* 31, no. 12 (2015): i44-i52.

Moncada, Bibiana, and Robert Lücking. "Ten new species of *Sticta* and counting: Colombia as a hot spot for unrecognized diversification in a conspicuous macrolichen genus." *Phytotaxa* 74 (2012): 1-29.

Moncada, Bibiana, Robert Lücking, and Luisa Betancourt-Macuase. "Phylogeny of the Lobariaceae (lichenized Ascomycota: Peltigerales), with a reappraisal of the genus *Lobariella*." *The Lichenologist* 45, no. 2 (2013): 203-263.

Moreau, Corrie S., Charles D. Bell, Roger Vila, S. Bruce Archibald, and Naomi E. Pierce. "Phylogeny of the ants: Diversification in the age of angiosperms." *Science* 312, no. 5770 (2006): 101-104.

Nakhleh, Luay, Tandy Warnow, C. Randal Linder, and Katherine St John. "Reconstructing

reticulate evolution in species—Theory and practice." *Journal of Computational Biology* 12, no. 6 (2005): 796-811.

Nash, Thomas H. *Lichen biology*. Cambridge, Cambridge University Press, (1996).

Paradis, Emmanuel, Julien Claude, and Korbinian Strimmer. "APE: Analyses of phylogenetics and evolution in R language." *Bioinformatics* 20, no. 2 (2004): 289-290.

Philippe, Hervé, Henner Brinkmann, Dennis V. Lavrov, D. Timothy J. Littlewood, Michael Manuel, Gert Wörheide, and Denis Baurain. "Resolving difficult phylogenetic questions: Why more sequences are not enough." *PLoS Biology* 9, no. 3 (2011): e1000602.

Printzen, Christian. "Lichen systematics: The role of morphological and molecular data to reconstruct phylogenetic relationships." In *Progress in Botany 71*, Berlin, Heidelberg: Springer. (2010): 233-275.

Prum, Richard O., Jacob S. Berv, Alex Dornburg, Daniel J. Field, Jeffrey P. Townsend, Emily Moriarty Lemmon, and Alan R. Lemmon. "A comprehensive phylogeny of birds (Aves) using targeted next-generation DNA sequencing." *Nature* 526, no. 7574 (2015): 569.

Reddy, Sushma, Rebecca T. Kimball, Akanksha Pandey, Peter A. Hosner, Michael J. Braun, Shannon J. Hackett, Kin-Lan Han et al. "Why do phylogenomic data sets yield conflicting trees? Data type influences the avian tree of life more than taxon sampling." *Systematic Biology* 66, no. 5 (2017): 857-879.

Renne, Paul R., Alan L. Deino, Frederik J. Hilgen, Klaudia F. Kuiper, Darren F. Mark, William S. Mitchell, Leah E. Morgan, Roland Mundil, and Jan Smit. "Time scales of critical events around the Cretaceous-Paleogene boundary." *Science* 339, no. 6120 (2013): 684-687.

Rokas, Antonis, Barry L. Williams, Nicole King, and Sean B. Carroll. "Genome-scale approaches to resolving incongruence in molecular phylogenies." *Nature* 425, no. 6960 (2003): 798.

Schmitt, Imke, and H. Thorsten Lumbsch. "Ancient horizontal gene transfer from bacteria enhances biosynthetic capabilities of fungi." *PLOS ONE* 4, no. 2 (2009): e4437.

Schneider, Harald, Eric Schuettpelz, Kathleen M. Pryer, Raymond Cranfill, Susana Magallón, and Richard Lupia. "Ferns diversified in the shadow of angiosperms." *Nature* 428, no. 6982 (2004): 553.

Schuettpelz, Eric, and Kathleen M. Pryer. "Evidence for a Cenozoic radiation of ferns in an angiosperm-dominated canopy." *Proceedings of the National Academy of Sciences*106, no. 27 (2009): 11200-11205.

Simion, Paul, Herve Philippe, Denis Baurain, Muriel Jager, Daniel J. Richter, Arnaud Di Franco, Beatrice Roure et al. "A large and consistent phylogenomic dataset supports sponges as the sister group to all other animals." *Current Biology* 27, no. 7 (2017): 958-967.

Simon, Antoine, Bernard Goffinet, Nicolas Magain, and Emmanuël Sérusiaux. "High diversity, high insular endemism and recent origin in the lichen genus *Sticta* (lichenized Ascomycota, Peltigerales) in Madagascar and the Mascarenes." *Molecular Phylogenetics and Evolution* 122 (2018): 15-28.

Som, Anup. "Causes, consequences and solutions of phylogenetic incongruence." *Briefings in Bioinformatics* 16, no. 3 (2014): 536-548.

Stamatakis, Alexandros. "RAxML version 8: A tool for phylogenetic analysis and post-analysis of large phylogenies." *Bioinformatics* 30, no. 9 (2014): 1312-1313.

Stukenbrock, Eva H. "The role of hybridization in the evolution and emergence of new fungal plant pathogens." *Phytopathology* 106, no. 2 (2016): 104-112.

Sukumaran, J., and M. T. Holder. "SumTrees: Phylogenetic tree summarization. 4.0.0." *Program and documentation available from the authors at: https://github. com/jeetsukumaran/Dendrophy* (2015).

Sukumaran, Jeet, and Mark T. Holder. "DendroPy: A Python library for phylogenetic computing." *Bioinformatics* 26, no. 12 (2010): 1569-1571.

Than, Cuong, Derek Ruths, and Luay Nakhleh. "PhyloNet: A software package for analyzing and reconstructing reticulate evolutionary relationships." *BMC Bioinformatics* 9, no. 1 (2008): 322.

Vermeij, Geerat J. "The energetics of modernization: the last one hundred million years of biotic evolution." *Paleontological Research* 15, no. 2 (2011): 54-62.

Widhelm, Todd J., Francesca R. Bertoletti, Matt J. Asztalos, Joel A. Mercado-Díaz, Jen-Pan Huang, Bibiana Moncada, Robert Lücking et al. "Oligocene origin and drivers of diversification in the genus *Sticta* (Lobariaceae, Ascomycota)." *Molecular Phylogenetics and Evolution* 126 (2018): 58-73.

Wiens, John J., Caitlin A. Kuczynski, Sarah A. Smith, Daniel G. Mulcahy, Jack W. Sites Jr, Ted M. Townsend, and Tod W. Reeder. "Branch lengths, support, and congruence: Testing the phylogenomic approach with 20 nuclear loci in snakes." *Systematic Biology* 57, no. 3 (2008): 420-431.

Xi, Zhenxiang, Liang Liu, Joshua S. Rest, and Charles C. Davis. "Coalescent versus concatenation methods and the placement of *Amborella* as sister to water lilies." *Systematic*

*Biology* 63, no. 6 (2014): 919-932.

Xu, Shizhong. "Phylogenetic analysis under reticulate evolution." *Molecular Biology and Evolution* 17, no. 6 (2000): 897-907.

Yang, Ziheng. "PAML 4: Phylogenetic analysis by maximum likelihood." *Molecular Biology and Evolution* 24, no. 8 (2007): 1586-1591.

Yang, Ziheng, and Bruce Rannala. "Bayesian estimation of species divergence times under a molecular clock using multiple fossil calibrations with soft bounds." *Molecular Biology and Evolution* 23, no. 1 (2005): 212-226.

Yu, Yun, and Luay Nakhleh. "A maximum pseudo-likelihood approach for phylogenetic networks." *BMC Genomics* 16, no. 10 (2015): S10.

Zhang, Ning, Liping Zeng, Hongyan Shan, and Hong Ma. "Highly conserved low-copy nuclear genes as effective markers for phylogenetic analyses in angiosperms." *New Phytologist* 195, no. 4 (2012): 923-937.

## 3. Oligocene origin and drivers of diversification in the genus *Sticta* (Lobariaceae, Ascomycota)

Todd J. Widhelm, Francesca R. Bertoletti, Matt J. Asztalos, Joel A. Mercado-Díaz, Jen Pan Huang, Bibiana Moncada, Robert Lücking, Nicolas Magain, Emmanuël Sérusiaux, Bernard Goffinet, Nicholas Crouch, Roberta Mason-Gamer, H. Thorsten Lumbsch

This chapter is a reprint (with minimal formatting) of an original article published in the journal *Molecular Phylogenetics and Evolution*. The citation is as follows:

Widhelm, Todd J., Francesca R. Bertoletti, Matt J. Asztalos, Joel A. Mercado-Díaz, Jen-Pan Huang, Bibiana Moncada, Robert Lücking et al. "Oligocene origin and drivers of diversification in the genus *Sticta* (Lobariaceae, Ascomycota)." *Molecular Phylogenetics and Evolution* 126 (2018): 58-73.

### 3.1 Introduction

One of the main challenges evolutionary biologists face is identifying the mechanisms that influence the distribution of biodiversity through time and space. As molecular data have become widely available and models for molecular evolution have been well developed, many studies have placed estimates on the timing of diversification through relaxed molecular clock methods (Rutschmann 2006). These time trees have been used for downstream analyses, such as lineage through time plots, and indicated changes in diversification rates across the branches and through time. Furthermore, these time trees have also been used to study different drivers of diversification (Morlon 2014; Ng and Smith 2014; Vamosi and Vamosi 2011; van der Niet and

Johnson 2012). Intrinsic factors, in the form of symbiont associations can give groups the ability to exploit new habitats and resources, allowing them to radiate into new niches (Janson et al. 2008; Stanley 1981). Extrinsic factors, such as tectonic activity, can cause habitat fragmentation and barriers between populations, letting genetic drift and differential selection act on isolated populations (Badgley et al. 2017). Sometimes associated with tectonic activity, climatic changes can increase diversification by promoting range shifts, which can place unique selective pressures on new immigrant populations, allowing divergent selection to affect speciation (Badgley et al. 2017; Hoorn et al. 2010). In most groups, many factors play a role, but it is not clear which exert greater influence in shaping biodiversity. Some drivers of diversification might play a larger role in some groups, while different drivers could be more important in others. In most cases, drivers of diversification are in a dynamic balance (Vamosi and Vamosi 2011). With sampling throughout the entire range of a group of organisms, it may be possible to tease apart the contribution of all drivers and determine the contribution of each to the evolution of organisms on a case-by-case basis (Vamosi and Vamosi 2011; van der Niet and Johnson 2012).

Recent studies have utilized molecular methods and the few available fossils to gain a better understanding of the diversification of groups of lichenized fungi (Amo de Paz et al. 2012, 2011; Blanco et al. 2004; Del-Prado et al. 2016, 2013, Divakar et al. 2012, 2015; Leavitt, Esslinger, and Lumbsch 2012; Leavitt, Moreau, and Lumbsch 2015; Leavitt, Lumbsch, et al. 2013; Leavitt et al. 2012; Magain et al. 2016; Molina et al. 2017). Lichens are a form of symbiotic mutualism where fungi (mycobionts: mostly ascomycetes) form a close association with photosynthetic green algae or cyanobacteria (photobionts). Most of these studies have focused on the family Parmeliaceae, while other families have received less attention (Gaya et al. 2015; Leavitt, Lumbsch, et al. 2013; Leavitt, Esslinger, and Lumbsch 2012; Otálora et al. 2010;

Prieto and Wedin 2013; Sérusiaux et al. 2011). Lobariaceae is a large family of lichenized fungi where phylogenetic relationships are just beginning to be understood. (Moncada, Coca, and Lücking 2013; Moncada, Lücking, and Betancourt-Macuase 2013; Moncada, Lücking, and Coca 2013) investigated relationships in Lobariaceae, and showed that the classification at the genus level did not accurately explain the branching patterns observed when using molecular data and new genera were segregated within the family. The genus *Sticta* was found to include two unrelated lineages; viz. *Sticta sensu stricto* and the *S. wrightii* group, which was reclassified as *Dendriscosticta*. *Sticta sensu stricto* is one of the largest genera in Lobariaceae, but the species diversity is only beginning to be understood. (Kirk et al. 2008) listed 114 species for *Sticta*, but (Moncada, Lücking, and Suárez 2014) after extensive sampling in the Colombian Andes, suggested that the actual global diversity might be four to five times higher. With so much diversity recently revealed, we began to investigate which drivers of diversification played a major role in shaping the diversity of *Sticta* through time and over the landscape.

Long-distance dispersal has been documented in many groups of lichens (Amo de Paz et al. 2012; Buschbom 2007; Del-Prado et al. 2013; Leavitt, Moreau, and Lumbsch 2015; Otálora et al. 2010) and collection records indicate that *Sticta* has colonized oceanic islands throughout the world, suggesting a high dispersal rate in the genus. A recent study (Simon et al. 2018) found evidence for a rapid radiation of *Sticta* in the Western Indian Ocean Islands (Madagascar, Reunion, and Mauritius), but little work has been done on islands in the Pacific, such as Hawaii, where it is unclear whether the species are derived from a single colonization followed by a radiation, or from multiple colonizations of unrelated species on the archipelago. Recent collections in Hawaii allowed us to test which scenario is more likely and where colonizers originated.

Species in *Sticta* associate with two types of photobionts, cyanobacteria and green algae, which makes the genus a unique study system where biotic interactions can be tested for effects on diversification. In the case of photosymbiodemes, one species of mycobiont can form associations with both photobiont types. The two types, chloro-morphs (containing green algae) and cyano-morphs (containing cyanobacteria, usually *Nostoc* spp.), can be so different morphologically, that specimens of the same mycobiont species were previously classified as different genera (e.g., *Dendrisocaulon* spp.) until morphological and molecular data confirmed that one taxon associates with both types of photobiont (Armaleo and Clerc 1991; James and Henssen 1976; Ranft et al. 2018). While photosymbiodemes are often found on separate thalli, there are records of both morphs attached on the same thallus (Dughi 1944, 1936; James and Henssen 1976; F. Moreau 1956). The photosymbiodemic state is thought to be limited to only a few taxa in *Sticta* and it is hypothesized that most species are primarily found in association with only one type of photobiont (either cyanobacteria or green-algal photobionts). Many more species in *Sticta* associate with cyanobacteria compared to green-algae, which invokes the question: Does the cyanobacterial association increase the net diversification rate compared to green-algal associations?

External factors may also be influencing diversification in *Sticta*. A majority of the known *Sticta* species are found in South America (Moncada, Lücking, and Suárez 2014). The Andes has been the site of major radiations in many groups of organisms (Hoorn et al. 2010; Lagomarsino et al. 2016; Madriñán, Cortés, and Richardson 2013; Nürk et al. 2015). Furthermore, a recent study by Magain et a1. (Magain et al. 2016) found a recent radiation in the lichen genus *Peltigera* in the Andes. The uplift of the Andes began between 66 and 33 million years ago, with a rapid increase in elevation during the late Miocene and early Pliocene (10-4

Mya). The uplift of mountains influences local and regional climate, creates fragmented habitats, and facilitates immigration of some species, promoting diversification of many groups simultaneously (Badgley et al. 2017; Hoorn et al. 2010). The pattern of high Andean diversity invokes another question of the study: Could the mountain building processes in the Andes have increased the diversification of *Sticta* species in this region relative to others?

With sampling throughout most of the known ranges of *Sticta* and a five gene dataset we produced the first robust time-calibrated phylogeny for the genus. We used this phylogeny to carry out the following aims: (1) estimate the age and ancestral range of *Sticta*, (2) infer the colonization history of Hawaii (3) determine if primary photobiont (green-algal and cyanobacterial) associations affect diversification, and (4) investigate if tectonic activity in the Andes has affected diversification. Note that the two hypothesized mechanisms that may affect the changes in biodiversity patterns through time and space in *Sticta* - i.e., (1) the effect of association with different photobionts and (2) the effect of recent Andean uplifting — are not mutually exclusive. Different mechanisms could have functioned contemporaneously or at different times in the past. Our study investigates some of the mechanisms that are likely to have a significant effect on shaping the biodiversity of *Sticta*.

## 3.2. Materials and Methods

### 3.2.1 Taxon sampling

Sampling was conducted in Africa, Madagascar, Europe, Canary Islands, Azores, Australasia, North America, the Colombian Andes, Ecuador, Brazil, Central America, the Caribbean, and Hawaii (Galloway 1997; Magain and Sérusiaux 2015; Moncada, Reidy, and Lücking 2014; Moncada, Coca, and Lücking 2013; Moncada, Lücking, and Coca 2013; Moncada and Lücking 2012; Simon et al. 2018). We selected 222 *Sticta* specimens from the major clades

of the ITS phylogeny of (Moncada, Lücking, and Suárez 2014) representing 132 species-level lineages that were identified by phylogenetic binning approach that allows for type specimens lacking DNA sequence data, to be assigned to clades on a molecular phylogeny via a phenotype data matrix of morphological, anatomical, and chemical characters (Berger, Stamatakis, and Lücking 2011; Parnmen, Lücking, and Lumbsch 2012) (Table VI). This level of sampling has more lineages than listed in the latest official count on species in *Sticta* (Kirk et al. 2008), but it is likely a subset of the global diversity, as areas of Africa, Asia, and Indonesia have not been thoroughly sampled yet. There are nearly 120 described species in *Sticta* (Kirk et al. 2008), but, recent studies (Magain and Sérusiaux 2015; Moncada, Lücking, and Suárez 2014; Moncada, Coca, and Lücking 2013; Moncada, Lücking, and Coca 2013; Moncada and Lücking 2012; Simon et al. 2018) have demonstrated that the diversity of the genus is underestimated and that there may be 400 to 500 species-level lineages in the genus. With the knowledge of this recently observed diversity, great care has been taken to properly determine species and some samples in this study have been challenging to assign. Those have been marked with a cf., *aff.* or just *S. sp* in their name since they are most likely new to science. For assignment of character states in downstream analyses, we assumed these to be new species and used the distribution and photobiont data from the collected material for these specimens.

TABLE VI. SPECIMEN SAMPLING AND GENBANK ACCESSION NUMBERS.

| ID | Taxon | Country of collection | ITS | *MCM7* | mtSSU | nuLSU | *RPB1* |
|---|---|---|---|---|---|---|---|
| DNA9930 | *Lobaria pulmonaria* | U.S.A. | MG367435 | MF984336 | MG754091 | MG063078 | MG754080 |
| LG0688 | *Pseudocyphellaria citrina* | Canary Islands | JQ735976 | - | JQ736009 | JQ735993 | KT281770 |
| DNA5022 | *Sticta aff. cordillerana* | Colombia | KC732553 | MF984252 | MG754120 | MG062963 | - |
| DNA7246 | *Sticta aff. andreana* | Costa Rica | MG367402 | MF984284 | - | MG063062 | - |
| DNA10048 | *Sticta aff. fuliginosa* | U.S.A. | MG367377 | MF984203 | - | - | MG754081 |
| DNA14466 | *Sticta aff. fuliginosa 1* | Australia | MG754192 | MF984305 | MG754180 | MG062943 | - |
| DNA7382 | *Sticta aff. granatensis* | Ecuador | MG367416 | - | MG754117 | MG062990 | - |
| DNA7226 | *Sticta aff. laciniosa* | Costa Rica | MG367401 | MF984240 | - | MG062988 | - |
| JM110 | *Sticta aff. laminobeauvosii* | Puerto Rico | MG367370 | MF984332 | - | MG062978 | - |
| DNA10049 | *Sticta aff. limbata* | U.S.A. | MG367378 | MF984292 | - | - | - |
| DNA13781 | *Sticta aff. martinii* | New Zealand | MG367383 | MF984270 | MG754172 | MG063018 | - |
| DNA13814 | *Sticta aff. martinii 1* | New Zealand | MG367384 | MF984227 | MG754171 | MG063019 | - |
| DNA14262 | *Sticta aff. martinii 2* | New Zealand | MG754193 | MF984223 | MG754187 | MG063021 | - |
| DNA7259 | *Sticta aff. orinoquensis* | Costa Rica | - | MF984264 | MG754121 | MG063077 | - |
| DNA7345 | *Sticta aff. peltigerella* | Colombia | MG367410 | MF984216 | MG754158 | MG063049 | - |
| DNA4932 | *Sticta aff. phyllidiata* | Colombia | KC732476 | MF984295 | - | - | - |
| JM111 | *Sticta aff. sinuosa* | Puerto Rico | MG367371 | MF984330 | - | - | - |
| DNA5541 | *Sticta aff. subscrobiculata* | Colombia | KC732639 | - | MG754096 | MG062985 | - |
| DNA6288 | *Sticta aff. subtomentella* | Colombia | KC732730 | MF984259 | - | MG063059 | - |
| DNA7260 | *Sticta aff. tomentosa* | Costa Rica | MG367406 | MF984315 | MG754157 | MG063051 | - |
| DNA5467 | *Sticta aff. weigelii* | Colombia | MG367390 | MF984299 | MG754103 | MG062983 | - |
| DNA6227 | *Sticta aff. weigelii 1* | Colombia | KC732710 | MF984320 | MG754165 | MG062980 | - |
| DNA7224 | *Sticta aff. zahlbruckneri* | Costa Rica | MG367400 | MF984318 | - | MG062991 | - |
| DNA5030 | *Sticta albocyphellata* | Colombia | KC732557 | - | MG754114 | MG062937 | - |

TABLE VI, CONTINUED

| ID | Taxon | Country of collection | ITS | *MCM7* | mtSSU | nuLSU | *RPB1* |
|---|---|---|---|---|---|---|---|
| DNA8197 | *Sticta albohypoarbuscula* | Hawaii | MG367434 | MF984210 | MG754094 | MG062923 | - |
| LG0992 | *Sticta ambavillaria* | Reunion | JQ735978 | - | JQ736011 | JQ735995 | - |
| DNA7373 | *Sticta andensis* | Colombia | KC732548 | MF984317 | MG754134 | MG062956 | - |
| DNA4985 | *Sticta arachnofuliginosa* | Colombia | KC732524 | MF984306 | - | MG062946 | - |
| DNA5443 | *Sticta arachnosylvatica* | Colombia | KC732580 | MF984309 | MG754154 | MG062948 | - |
| DNA5599 | *Sticta arbuscula* | Colombia | KC732682 | - | - | MG063046 | - |
| DNA7253 | *Sticta arbusculofuliginosa* | Costa Rica | MG367404 | MF984218 | MG754156 | MG063050 | - |
| DNA5424 | *Sticta arbusculotomentosa 1* | Colombia | KC732572 | MF984220 | - | MG063041 | - |
| LG3747 | *Sticta atlantica* | Ireland | KT281734 | - | KT281690 | KT281645 | - |
| LG3858 | *Sticta atlantica 1* | Azores | KT281737 | - | KT281693 | KT281648 | KT281784 |
| DNA4999 | *Sticta atroandensis* | Colombia | KC732533 | MF984310 | - | MG062952 | MG754082 |
| DNA14282 | *Sticta babingtonii* | New Zealand | MF373808 | MF984256 | MG754167 | MG063012 | - |
| DNA14493 | *Sticta beauvoisii 2* | U.S.A | MG754194 | MF984244 | - | MG062957 | - |
| LG3303 | *Sticta beauvoisii* | U.S.A. | KT281725 | - | KT281681 | KT281636 | KT281787 |
| DNA6211 | *Sticta beauvoisii 1* | Colombia | KC732707 | MF984328 | - | MG062958 | - |
| DNA6357 | *Sticta borinquensis* | Puerto Rico | MG367397 | MF984263 | - | MG062976 | - |
| DNA4914 | *Sticta brevior* | Colombia | MG367386 | - | MG754108 | MG062929 | - |
| DNA13507 | *Sticta caliginosa* | New Zealand | MF373760 | MF984229 | MG754135 | MG063035 | - |
| DNA13782 | *Sticta caliginosa 1* | New Zealand | MF373767 | - | MG754136 | MG063036 | - |
| LG3741 | *Sticta canariensis* | Ireland | KT281733 | - | KT281689 | KT281644 | KT281779 |
| LG1333 | *Sticta canariensis (cyanomorph)* | Canary Islands | KT281700 | - | KT281658 | KT281612 | KT281752 |
| LG0962 | *Sticta caperata* | Reunion | JQ735979 | - | JQ736012 | JQ735996 | KT281745 |
| DNA14494 | *Sticta carolinensis 1* | U.S.A | - | MF984234 | MG754116 | MG063074 | - |
| LG3302 | *Sticta carolinensis* | U.S.A. | KT281724 | - | KT281680 | KT281635 | KT281786 |

TABLE VI, CONTINUED

| ID | Taxon | Country of collection | ITS | *MCM7* | mtSSU | nuLSU | *RPB1* |
|---|---|---|---|---|---|---|---|
| DNA6237 | *Sticta cf. lhermineri* | Colombia | MG367393 | MF984331 | - | MG063009 | - |
| DNA5560 | *Sticta cf. ocaniensis* | Colombia | KC732654 | - | - | MG062997 | - |
| DNA5027 | *Sticta cf. sinuosa* | Colombia | KC732554 | MF984296 | - | MG062977 | - |
| JM112 | *Sticta ciliata* | Puerto Rico | MG367375 | MF984323 | - | MG063038 | - |
| LG1605 | *Sticta ciliata 1* | Rwanda | KT281717 | - | KT281673 | KT281629 | KT281763 |
| LG2751 | *Sticta ciliata 2* | Canary Islands | KT281712 | - | KT281668 | KT281624 | - |
| LG3099 | *Sticta ciliata 3* | Azores | KT281715 | - | KT281671 | KT281627 | KT281762 |
| LG3406 | *Sticta ciliata 4* | Canary Islands | KT281713 | - | KT281669 | KT281625 | KT281780 |
| LG3539 | *Sticta ciliata 5* | France | KT281718 | - | KT281674 | KT281630 | KT281774 |
| LG3542 | *Sticta ciliata 6* | France | KT281714 | - | KT281670 | KT281626 | KT281772 |
| LG3781 | *Sticta ciliata 7* | Ireland | KT281716 | - | KT281672 | KT281628 | KT281773 |
| LG3830 | *Sticta ciliata 8* | Canary Islands | KT281719 | - | KT281675 | KT281631 | KT281775 |
| DNA6336 | *Sticta ciliosylvativa* | Colombia | MG367395 | MF984205 | - | MG063060 | - |
| DNA12977 | *Sticta cinereoglauca* | New Zealand | MG367380 | MF984224 | - | MG063027 | - |
| DNA13835 | *Sticta cinereoglauca 1* | New Zealand | MF373794 | MF984242 | MG754139 | MG063028 | - |
| DNA13863 | *Sticta cinereoglauca 2* | New Zealand | MF373798 | MF984241 | MG754140 | MG063029 | - |
| DNA5526 | *Sticta cometia* | Colombia | KC732626 | MF984222 | MG754178 | MG062927 | - |
| DNA4977 | *Sticta cometiella* | Colombia | KC732517 | MF984221 | MG754177 | MG062926 | - |
| DNA6179 | *Sticta delicatula* | Colombia | MG367391 | MF984237 | MG754119 | MG062998 | - |
| DNA13506 | *Sticta dendroides (cyanomorph)* | New Zealand | - | MF984233 | - | MG063073 | - |
| DNA13875 | *Sticta dendroides (cyanomorph) 1* | New Zealand | MF373799 | MF984272 | MG754188 | MG063025 | - |
| DNA13881 | *Sticta dendroides (cyanomorph) 2* | New Zealand | MF373805 | MF984253 | - | MG063026 | - |
| DNA6358 | *Sticta densiphyllidiata* | Puerto Rico | MG367398 | MF984239 | - | MG062987 | - |
| LG0945 | *Sticta dichotoma* | Reunion | JQ735981 | - | JQ736014 | JQ735998 | KT281743 |

TABLE VI, CONTINUED

| ID | Taxon | Country of collection | ITS | *MCM7* | mtSSU | nuLSU | *RPB1* |
|---|---|---|---|---|---|---|---|
| LG0984 | *Sticta dichotoma 2* | Reunion | JQ735982 | - | JQ736015 | JQ735999 | KT281746 |
| DNA5550 | *Sticta dilatata* | Colombia | KC732647 | - | MG754125 | MG063057 | - |
| DNA4945 | *Sticta dioica* | Colombia | KC732486 | - | - | MG062973 | - |
| DNA5015 | *Sticta dioica 1* | Colombia | KC732546 | MF984246 | MG754105 | MG062974 | MG754083 |
| LG1040 | *Sticta duplolimbata* | Reunion | JQ735984 | - | JQ736001 | JQ736017 | KT281751 |
| LG0919 | *Sticta duplolimbata 2* | Rwanda | KT281696 | - | KT281654 | KT281651 | KT281741 |
| DNA12973 | *Sticta filix* | New Zealand | MG367379 | MF984228 | - | MG063010 | - |
| DNA13779 | *Sticta filix 1* | New Zealand | MF373766 | - | - | MG063011 | - |
| DNA4907 | *Sticta fuliginoides 4* | Wales | KC732454 | MF984215 | - | MG063047 | - |
| LG1421 | *Sticta fuliginoides* | France | KT281701 | - | KT281659 | KT281613 | KT281753 |
| LG3012 | *Sticta fuliginoides 1* | Canary Islands | KT281722 | - | KT281678 | KT281634 | KT281765 |
| LG3551 | *Sticta fuliginoides 2* | France | KT281729 | - | KT281685 | KT281640 | KT281777 |
| LG3733 | *Sticta fuliginoides 3* | Ireland | KT281732 | - | KT281688 | KT281643 | KT281781 |
| LGS4 | *Sticta fuliginoides 5* | Wales | KT281738 | - | KT281694 | KT281649 | KT281785 |
| DNA6226 | *Sticta Sp. 3* | Colombia | KC732709 | MF984304 | - | MG063048 | - |
| DNA7395 | *Sticta fuliginosa 9* | Brazil | MG367419 | MF984303 | MG754184 | MG062939 | - |
| DNA8112 | *Sticta fuliginosa 10* | Hawaii | MG367426 | - | MG754185 | MG062941 | - |
| DNA8114 | *Sticta fuliginosa 11* | Hawaii | MG367427 | MF984300 | MG754186 | MG062944 | - |
| DNA8162 | *Sticta fuliginosa 12* | Hawaii | MG367432 | MF984301 | MG754182 | MG062942 | - |
| LG1611 | *Sticta fuliginosa 2* | Rwanda | KT281702 | - | KT281660 | KT281614 | KT281754 |
| LG1952 | *Sticta fuliginosa 3* | South Africa | KT281703 | - | KT281661 | KT281615 | KT281755 |
| LG3010 | *Sticta fuliginosa 4* | Canary Islands | KT281721 | - | KT281677 | KT281633 | KT281776 |
| LG3100 | *Sticta fuliginosa 5* | Azores | KT281704 | - | KT281662 | KT281616 | KT281756 |
| LG3537 | *Sticta fuliginosa 6* | France | KT281727 | - | KT281683 | KT281638 | KT281766 |
| LG3729 | *Sticta fuliginosa 7* | Ireland | KT281731 | - | KT281687 | KT281642 | KT281768 |
| LG795 | *Sticta fuliginosa* | Madagasgar | KT281695 | - | KT281653 | KT281609 | KT281740 |
| LGS9 | *Sticta fuliginosa 8* | Wales | KT281739 | - | - | KT281650 | KT281769 |

TABLE VI, CONTINUED

| ID | Taxon | Country of collection | ITS | *MCM7* | mtSSU | nuLSU | *RPB1* |
|---|---|---|---|---|---|---|---|
| LG0989 | *Sticta fuliginosa 1* | Reunion | KT281698 | - | KT281656 | KT281610 | KT281747 |
| DNA5568 | *Sticta fuscotomentosa* | Colombia | KC732661 | MF984280 | MG754126 | MG063070 | - |
| DNA4959 | *Sticta gallowayana* | Colombia | KC732496 | MF984285 | - | MG062934 | MG754087 |
| DNA5475 | *Sticta globulifuliginosa* | Colombia | KC732608 | - | - | MG062924 | - |
| DNA5444 | *Sticta guascensis* | Colombia | KC732581 | MF984289 | MG754150 | MG062928 | - |
| DNA5457 | *Sticta gyalocarpa* | Colombia | KC732594 | MF984327 | MG754111 | MG063043 | MG754089 |
| DNA7250 | *Sticta gyalocarpoides* | Costa Rica | MG367403 | MF984326 | - | MG063044 | - |
| DNA5477 | *Sticta hirsutofuliginosa* | Colombia | KC732610 | MF984311 | MG754152 | MG062950 | - |
| DNA6199 | *Sticta humboldtii* | Colombia | KC732702 | MF984312 | MG754118 | MG062951 | - |
| DNA5586 | *Sticta hypoglabra* | Colombia | KC732667 | MF984322 | MG754104 | MG063001 | - |
| DNA5549 | *Sticta impressula* | Colombia | KC732646 | MF984287 | MG754110 | MG062931 | - |
| DNA7291 | *Sticta inversa* | Colombia | MG367407 | MF984213 | - | - | - |
| DNA6339 | *Sticta isidioimpressula* | Colombia | KC732761 | MF984219 | - | MG062936 | - |
| DNA4982 | *Sticta isidiokunthii* | Colombia | KC732522 | MF984288 | MG754189 | MG062930 | MG754088 |
| DNA8081 | *Sticta isidiopedunculata* | Hawaii | MG367425 | MF984211 | MG754137 | MG063037 | - |
| DNA5607 | *Sticta jaguirreana* | Colombia | MG754195 | - | MG754162 | MG062999 | - |
| DNA7223 | *Sticta laciniata* | Costa Rica | MG367399 | - | MG754179 | MG062984 | - |
| DNA7301 | *Sticta laevis* | Colombia | MG367409 | MF984206 | - | MG063052 | - |
| DNA5589 | *Sticta laselvae* | Colombia | KC732673 | MF984269 | MG754145 | MG063008 | - |
| DNA13538 | *Sticta latifrons* | New Zealand | MF373763 | MF984230 | MG754173 | MG063015 | - |
| DNA13876 | *Sticta latifrons (cyanomorph)* | New Zealand | MF373800 | - | - | MG063016 | - |
| DNA5460 | *Sticta leucoblepharis* | Colombia | KC732597 | MF984276 | - | MG063063 | - |
| DNA8131 | *Sticta limbata 6* | Hawaii | MG367428 | MF984298 | MG754181 | MG062940 | - |
| LG2230 | *Sticta limbata* | Canary Islands | KT281706 | - | KT281664 | KT281618 | KT281758 |
| LG2690 | *Sticta limbata 1* | Scotland | KT281707 | - | KT281665 | KT281619 | KT281759 |
| LG2749 | *Sticta limbata 2* | Canary Islands | KT281708 | - | KT281666 | KT281620 | KT281760 |

TABLE VI, CONTINUED

| ID | Taxon | Country of collection | ITS | *MCM7* | mtSSU | nuLSU | *RPB1* |
|---|---|---|---|---|---|---|---|
| LG3105 | *Sticta limbata 3* | Azores | KT281709 | - | KT281667 | KT281621 | - |
| LG3170 | *Sticta limbata 7* | Canada | KT281710 | - | - | KT281622 | - |
| LG3544 | *Sticta limbata 4* | France | KT281728 | - | KT281684 | KT281639 | KT281767 |
| LG3868 | *Sticta limbata 5* | Azores | KT281711 | - | - | KT281623 | KT281761 |
| DNA5028 | *Sticta lobarioides* | Colombia | KC732555 | MF984238 | MG754113 | MG062992 | - |
| DNA4939 | *Sticta lobulata* | Colombia | KC732482 | MF984271 | MG754098 | MG062960 | - |
| DNA6279 | *Sticta lobulata 1* | Colombia | KC732727 | - | - | MG062961 | - |
| DNA5436 | *Sticta lumbschii* | Colombia | KC732575 | MF984212 | MG754124 | MG063055 | - |
| DNA5569 | *Sticta macrocyphellata* | Colombia | KC732662 | MF984313 | - | MG063056 | - |
| DNA5511 | *Sticta macrogyalocarpa* | Colombia | KC732619 | - | MG754092 | MG063045 | MG754090 |
| LG0946 | *Sticta macrophylla* | Reunion | JQ735985 | - | JQ736018 | JQ736002 | KT281744 |
| DNA5539 | *Sticta macrothallina* | Colombia | KC732629 | MF984208 | MG754122 | MG063034 | - |
| DNA5562 | *Sticta macrothallina 1* | Colombia | KC732637 | - | MG754107 | MG063033 | - |
| DNA5529 | *Sticta macrothallina (cyanomorph)* | Colombia | KC732655 | MF984314 | MG754106 | MG063032 | - |
| DNA4975 | *Sticta maculofuliginosa* | Colombia | KC732514 | MF984235 | - | - | - |
| DNA8052 | *Sticta maculohyposcrobiculata* | Hawaii | MG367423 | MF984302 | MG754093 | MG062922 | - |
| LG1023 | *Sticta marginalis* | Reunion | JQ735980 | - | JQ736013 | JQ735997 | KT281748 |
| DNA7378 | *Sticta marilandia* | Ecuador | MG367415 | MF984251 | MG754160 | MG062971 | - |
| DNA13522 | *Sticta menziesii* | New Zealand | MF373761 | MF984225 | MG754191 | MG063013 | - |
| DNA13829 | *Sticta menziesii 1* | New Zealand | MF373788 | MF984254 | - | MG063014 | - |
| DNA13430 | *Sticta menziesii (cyanomorph)* | New Zealand | - | MF984255 | - | MG063075 | - |
| DNA13883 | *Sticta menziesii (cyanomorph) 1* | New Zealand | - | MF984257 | - | MG063076 | - |
| DNA5474 | *Sticta microisidiata* | Colombia | KC732607 | MF984324 | MG754144 | MG063039 | - |

TABLE VI, CONTINUED

| ID | Taxon | Country of collection | ITS | *MCM7* | mtSSU | nuLSU | *RPB1* |
|---|---|---|---|---|---|---|---|
| DNA6186 | *Sticta microisidiata 1* | Colombia | KC732699 | MF984325 | - | MG063040 | - |
| DNA5446 | *Sticta minutula* | Colombia | KC732583 | MF984297 | - | MG063042 | - |
| DNA5003 | *Sticta montana* | Colombia | KC732537 | MF984248 | MG754099 | MG062967 | MG754084 |
| DNA5010 | *Sticta montana 1* | Colombia | MG367388 | MF984249 | MG754100 | MG062970 | MG754086 |
| DNA5017 | *Sticta montana 2* | Colombia | KC732548 | MF984247 | MG754101 | MG062966 | - |
| DNA5605 | *Sticta montana 3* | Colombia | KC732688 | MF984321 | MG754161 | MG062969 | - |
| DNA6229 | *Sticta montana 4* | Colombia | KC732712 | - | - | MG062975 | - |
| DNA6326 | *Sticta montana 5* | Colombia | KC732753 | MF984250 | MG754159 | MG062972 | MG754085 |
| DNA6327 | *Sticta montana 6* | Colombia | MG367394 | MF984245 | MG754163 | MG062968 | - |
| DNA5524 | *Sticta neopulmonarioides* | Colombia | KC732625 | MF984204 | MG754115 | - | - |
| DNA5528 | *Sticta neopulmonarioides1* | Colombia | KC732628 | - | - | MG062989 | - |
| DNA5537 | *Sticta neopulmonarioides (cyanomorph)* | Colombia | KC732636 | MF984236 | - | MG062993 | - |
| DNA5557 | *Sticta neopulmonarioides (cyanomorph) 1* | Colombia | KC732651 | - | - | MG062994 | - |
| DNA5558 | *Sticta neopulmonarioides (cyanomorph) 2* | Colombia | KC732652 | - | - | MG062995 | - |
| DNA5021 | *Sticta papillata* | Colombia | KC732552 | MF984232 | MG754123 | MG063053 | - |
| DNA7371 | *Sticta papillata 1* | Colombia | MG367414 | MF984283 | MG754133 | MG063054 | - |
| DNA5019 | *Sticta parahumboldtii* | Colombia | KC732550 | MF984308 | MG754151 | MG062949 | - |
| DNA4921 | *Sticta paralimbata* | Colombia | KC732466 | - | - | MG062959 | - |
| DNA4958 | *Sticta phyllidiofuliginosa* | Colombia | KC732495 | MF984329 | - | - | - |
| DNA5456 | *Sticta phyllidiokunthii* | Colombia | KC732593 | MF984291 | MG754112 | MG062932 | - |
| DNA5540 | *Sticta phyllidiokunthii (chloromorph)* | Colombia | KC732638 | MF984286 | MG754109 | MG062933 | - |
| DNA6346 | *Sticta plumbeociliata* | Colombia | KC732767 | MF984290 | - | MG062935 | - |

TABLE VI, CONTINUED

| ID | Taxon | Country of collection | ITS | *MCM7* | mtSSU | nuLSU | *RPB1* |
|---|---|---|---|---|---|---|---|
| DNA4934 | *Sticta pseudobeauvoisii* | Colombia | KC732478 | MF984265 | MG754143 | MG063007 | - |
| DNA7254 | *Sticta pseudodilatata* | Costa Rica | MG367405 | MF984214 | MG754127 | MG063058 | - |
| DNA6299 | *Sticta pseudohumboldtii* | Colombia | KC732736 | MF984307 | - | MG062947 | - |
| DNA4922 | *Sticta pseudolimbata* | Colombia | KC732467 | MF984316 | MG754142 | MG062955 | - |
| DNA5556 | *Sticta pseudolobaria* | Colombia | KC732650 | - | - | MG062996 | - |
| DNA6276 | *Sticta pseudosylvatica* | Colombia | KC732724 | MF984335 | - | MG062953 | - |
| DNA6198 | *Sticta puracensis* | Colombia | KC732701 | MF984243 | MG754175 | - | - |
| DNA4953 | *Sticta rhizinata* | Colombia | KC732491 | - | MG754097 | MG062962 | - |
| DNA7357 | *Sticta roseocyphellata* | Colombia | MG367412 | MF984207 | MG754176 | MG062938 | - |
| JM121 | *Sticta scabrosa* | Puerto Rico | MG367374 | MF984334 | - | MG063002 | - |
| DNA4948 | *Sticta scabrosa 1* | Colombia | MG367387 | MF984258 | - | - | - |
| DNA8042 | *Sticta scabrosa/hawaiiensis* | Hawaii | MG367422 | - | MG754148 | MG063003 | - |
| DNA8150 | *Sticta scabrosa/hawaiiensis 1* | Hawaii | MG367429 | MF984266 | MG754147 | MG063004 | - |
| DNA8152 | *Sticta scabrosa/hawaiiensis 2* | Hawaii | MG367431 | MF984267 | MG754149 | MG063005 | - |
| DNA8195 | *Sticta scabrosa/hawaiiensis 3* | Hawaii | MG367430 | MF984268 | MG754146 | MG063006 | - |
| JM114 | *Sticta schizophylliza* | Puerto Rico | MG367376 | MF984281 | - | MG063071 | - |
| DNA6356 | *Sticta schizophylliza 1* | Puerto Rico | KC732774 | MF984282 | MG754190 | MG063072 | - |
| DNA5405 | *Sticta sp.* | Brazil | KC732568 | MF984319 | - | MG062954 | - |
| DNA7297 | *Sticta sp.1* | Colombia | MG367408 | MF984209 | MG754174 | MG063061 | - |
| DNA7351 | *Sticta sp.* | Colombia | MG367411 | - | MG754153 | - | - |
| DNA7384 | *Sticta sp.* | Brazil | MG367417 | - | - | MG063000 | - |
| DNA7389 | *Sticta sp. 2* | Brazil | MG367418 | MF984294 | MG754183 | MG062945 | - |
| DNA8047 | *Sticta sp.* | Hawaii | MG754196 | - | MG754095 | MG062921 | - |

TABLE VI, CONTINUED

| ID | Taxon | Country of collection | ITS | *MCM7* | mtSSU | nuLSU | *RPB1* |
|---|---|---|---|---|---|---|---|
| LG2229 | *Sticta sp.* | Canary Islands | KT281705 | - | KT281663 | KT281617 | KT281757 |
| LG2752 | *Sticta sp.* | Canary Islands | KT281720 | - | KT281676 | KT281632 | KT281764 |
| LG3173 | *Sticta sp.* | Canada | KT281723 | - | KT281679 | - | - |
| JM130 | *Sticta sp. nov.* | Puerto Rico | MG367373 | MF984275 | - | MG062986 | - |
| DNA13526 | *Sticta squamata* | New Zealand | MG367381 | MF984260 | MG754138 | MG063030 | - |
| DNA13528 | *Sticta squamata* | New Zealand | MG367382 | MF984226 | MG754168 | MG063031 | - |
| DNA4925 | *Sticta squamifera* | Colombia | KC732470 | MF984217 | - | MG062965 | - |
| DNA14462 | *Sticta stipitata* | Australia | MG754197 | MF984274 | MG754141 | MG063024 | - |
| DNA13537 | *Sticta subcaperata* | New Zealand | MG754198 | MF984231 | MG754169 | MG063017 | - |
| DNA13860 | *Sticta subcaperata 1* | New Zealand | MG754199 | - | MG754170 | MG063023 | - |
| DNA13861 | *Sticta subcaperata 2* | New Zealand | MG754200 | MF984273 | - | MG063022 | - |
| DNA13864 | *Sticta subcaperata 3* | New Zealand | MG367385 | MF984261 | - | MG063020 | - |
| DNA5579 | *Sticta subfilicinella* | Colombia | KT354937 | - | - | MG063064 | - |
| LG1038 | *Sticta sublimbata 1* | Reunion | KT281699 | - | KT281657 | KT281611 | KT281750 |
| LG0885 | *Sticta sublimbata* | DR Congo | JQ735986 | - | JQ736019 | JQ736003 | KT281771 |
| DNA6292 | *Sticta sublimbatoides* | Colombia | KC732732 | MF984333 | - | MG062964 | - |
| LG3536 | *Sticta sylvatica* | France | KT281726 | - | KT281682 | KT281637 | KT281788 |
| LG3723 | *Sticta sylvatica 1* | Great Britain | KT281730 | - | KT281686 | KT281641 | KT281778 |
| LG3780 | *Sticta sylvatica 2* | Ireland | KT281735 | - | KT281691 | KT281646 | KT281782 |
| LG3837 | *Sticta sylvatica 3* | France | KT281736 | - | KT281692 | KT281647 | KT281783 |
| DNA5608 | *Sticta tomentosa* | Colombia | KC732690 | MF984279 | MG754128 | MG063065 | - |
| DNA8041 | *Sticta tomentosa/hawaiiensis* | Hawaii | MG367420 | - | MG754130 | MG063066 | - |
| DNA8078 | *Sticta tomentosa/hawaiiensis 1* | Hawaii | MG367424 | MF984278 | MG754131 | MG063069 | - |
| DNA8079 | *Sticta tomentosa/hawaiiensis 2* | Hawaii | MG367421 | MF984277 | MG754132 | MG063067 | - |

TABLE VI, CONTINUED

| ID | Taxon | Country of collection | ITS | *MCM7* | mtSSU | nuLSU | *RPB1* |
|---|---|---|---|---|---|---|---|
| DNA8184 | *Sticta tomentosa/hawaiiensis 3* | Hawaii | MG367433 | - | MG754129 | MG063068 | - |
| LG0925 | *Sticta umbilicariaeformis* | Rwanda | KT281697 | - | KT281655 | KT281652 | KT281742 |
| LG1037 | *Sticta variabilis* | Reunion | JQ735987 | - | JQ736020 | JQ736004 | KT281749 |
| DNA5593 | *Sticta viviana* | Colombia | KC732680 | - | MG754155 | MG062925 | - |
| DNA4940 | *Sticta weigelii* | Colombia | KC732483 | MF984262 | MG754102 | MG062982 | - |
| DNA6187 | *Sticta weigelii 1* | Colombia | MG367392 | MF984293 | MG754166 | MG062979 | - |
| DNA7358 | *Sticta weigelii 2* | Colombia | MG367413 | - | MG754164 | MG062981 | - |

### 3.2.2 DNA isolation, polymerase chain reaction (PCR) amplification, and sequencing

DNA was isolated from small portions of thallus using the ZR Fungal/Bacterial DNA MiniPrep'" (Zymo Research, Irvine, CA, USA). The internal transcribed spacer (ITS ~ 550 bp, N = 219), ribosomal DNA from the mitochondrial small subunit (mtSSU ~ 800 bp, N = 153) and the nuclear large subunit (nuLSU ~ 550 bp, N = 212) were amplified, along with two low-copy nuclear protein coding genes: DNA replication licensing factor (*MCM7* ~ 600 bp, N = 134) and RNA polymerase beta subunit one (RPBI ~ 1000 bp, N = 60). All PCR amplifications were carried out using MyTaq$^{TM}$ Red DNA Polymerase (Bioline, Taunton, MA, USA). Primers and PCR conditions are summarized in Table VII. Due to poor sequencing results using previously described primers (Mangold et al. 2008; Vilgalys and Hester 1990; Zoller, Scheidegger, and Sperisen 1999), new *Sticta*-specific primers were developed for these loci (Table VII) which increased amplification success. Products that produced high quality PCR bands in agarose gel

electrophoresis were cleaned with ExoSAP-IT (USB, Cleveland, OH, USA), following the manufacturer's instructions. Cycle sequencing reactions were carried out using BigDye v3.1 (Applied Biosystems, Foster City, CA, USA) and products were cleaned using an alcohol precipitation method. Sequencing of amplified products was conducted with an ABI 3730 automated sequencer (Applied Biosystems) at the Field Museum in Chicago, IL, USA.

TABLE VII. Polymerase chain reaction primers and annealing temperatures used in this study.

| Marker | Primer Name | Forward Primer Sequence | Annealing Temperature (C) | Reference |
|---|---|---|---|---|
| ITS | ITS1F | CTTGGTCATTTAGAGGAAGTAA | 48 | Zoller et al. (1999) |
| | ITS4 | TCCTCCGCTTATTGATATGC | | |
| ITS | ITS_*Sticta*_F | GATTTTGTGGGTGGTGGTGC | 53 | This study |
| | ITS_*Sticta*_R | TTAACCTCGCGTTCGGTTCA | | |
| mtSSU | mrSSU1 | AGCAGTGAGGAATATTGGTC | 50 | Zoller et al. (1999) |
| | mrSSU3 | ATGTGGCACGTCTATAGCCC | | |
| mtSSU | mtSSU_*Sticta*_F | CTTGGAGGAATGAAAAGCAATAGC | 43 | This study |
| | mtSSU_*Sticta*_R | TGATGACTTGTCATGTTCCCTCT | | |
| nuLSU | AL2R | GCGAGTGAAGCGGCAACAGCTC | 55 | Mangold et al. (2008) |
| | LR3 | GGTCCGTGTTTCAAGAC | | Vilgalys & Hester (1990) |
| nuLSU | nuLSU_*Sticta*_F | CCAACAGGGATTGCCTCAGT | 53 | This study |
| | nuLSU_*Sticta*_R | ATTACGCCAGCATCCTAGCC | | |
| *MCM7* | MCM7_*Sticta*_F | AAGCCATCGGTGCAGGTAAA | 65 | This study |
| | MCM7_*Sticta*_R | CGATTTAGCCACACCAGGGT | | |

### 3.2.3 Sequence alignment

Sequences were assembled and edited using Geneious 8.1.7 (Kearse et al. 2012). All sequences were confirmed as being *Sticta* using Genbank's BLASTn suite (Benson et al. 2013). Multiple sequence alignment was conducted using the MAFFT 7.017 (Katoh and Standley 2013) plugin in Geneious 8.1.7 under default settings. Alignments of ITS and mtSSU were reduced by deleting ambiguously aligned regions using the Gblocks 0.91b server (Castresana 2000), selecting all options for less stringent selection (allowing for smaller final blocks, gap positions within the final blocks, and less strict flanking positions). Each single locus alignment was

analyzed using the RaxML 8.2.11 (Stamatakis 2014) plugin in Geneious, each with 100 bootstrap replicates to check for any well-supported conflict among the single locus trees. Four separate concatenated alignments were produced to see how missing data and number of tips affect the estimation of divergence times in *Sticta*. Three alignments were concatenated in Generous with five loci (ITS, *MCM7*, mtSSU, nuLSU, and *RPB1*) having 224, 196, and 118 samples and decreasing amounts of missing loci respectively (Table VIII). A three-locus concatenated dataset containing sequences of ITS, mtSSU and nuLSU of 147 samples was assembled, producing a dataset with no missing loci. The software JModelTest 2.1.10 (Darriba et al. 2012) was used to determine the best-fit nucleotide substitution models for each locus in each of the four alignments (Table VIII).

TABLE VIII. ALIGNMENT INFORMATION AND NUCLEOTIDE EVOLUTION MODELS USED FOR ANALYSES.

| # of specimens | missing loci | Locus | Aligned length | # in matrix | jModelTest AIC model selection |
|---|---|---|---|---|---|
| | | ITS | 450 | 218 | TIM1+I+G |
| | | *MCM7* | 616 | 133 | TrN+I+G |
| **224** | 30.54% | mtSSU | 673 | 155 | TPM1uf+I+G |
| | | nuLSU | 558 | 211 | GTR+I+G |
| | | *RPB1* | 1111 | 61 | TIM3+G |
| | | ***Total*** | ***3408*** | ***778*** | |
| | | ITS | 452 | 194 | TIM1+I+G |
| | | *MCM7* | 616 | 123 | TrNef+I+G |
| **196** | 26.22% | mtSSU | 673 | 153 | TIM3+I+G |
| | | nuLSU | 558 | 192 | TIM2+I+G |
| | | *RPB1* | 1111 | 61 | TrN+G |
| | | ***Total*** | ***3410*** | ***723*** | |
| | | ITS | 452 | 116 | TIM1+I+G |
| | | *MCM7* | 616 | 86 | TVMef+I+G |
| **118** | 26.95% | mtSSU | 673 | 87 | TIM3+I+G |
| | | nuLSU | 558 | 115 | TIM2+I+G |
| | | *RPB1* | 1111 | 27 | TrN+G |
| | | ***Total*** | ***3410*** | ***431*** | |
| | | ITS | 450 | 147 | GTR+G |
| **147** | 0.00% | mtSSU | 673 | 147 | TPM3uf+I+G |
| | | nuLSU | 558 | 147 | TIM2+I+G |
| | | ***Total*** | ***1681*** | ***441*** | |

### 3.2.4 Phylogenetic analyses, molecular dating and calibrations

Divergence time estimates were estimated in BEAST 2.1 (Bouckaert et al. 2014) using the four concatenated matrices described above (Table VIII). We used secondary calibrations from (Gaya et al. 2015) who estimated a chronogram of Eukaryotes using five loci; the tree was calibrated using eight fossils, two molecular-based calibrations, and forced monophyly at some nodes. The chronogram has representative specimens from the Lobariaceae, with *Lobaria scrobiculata* diverging from *Pseudocyphellaria anomala* and *Sticta beauvoisii* nearly 62.5 ± 20 Mya and *Sticta* diverged from *Pseudocyphellaria* nearly 40 ± 20 Mya. These estimates were used to calibrate the four alignments at the out-group nodes of *Lobaria pulmonaria* and *Pseudocyphellaria crinita*.

Input files were prepared in BEAUti (Bouckaert et al. 2014). For each analysis, clock models and trees were linked for the five loci and the model of DNA evolution, inferred in JModelTest (Table VIII) were strictly used (transitions were not estimated) for site models while nucleotide frequencies were estimated for each locus. In each analysis, a relaxed lognormal molecular clock was applied, and each run began with a random starting tree.

Different priors (yule, calibrated yule and birth/death) were initially tested in exploratory analyses with the 118-specimen dataset to examine their effect on the estimation of divergence times. For comparison of the four alignments we only used a yule prior, which assumes a constant speciation rate per lineage. *Sticta* was monophyletic in exploratory Bayesian and ML analyses, thus *Sticta* was forced to be monophyletic and the node calibration was set to a lognormal distribution at 40 Mya (M parameter = 3.69; S parameter = 0.4). Another calibration forced the monophyly of *Pseudocyphellaria crinita* plus all *Sticta* specimens and was set under a lognormal distribution to 62.5 Mya (M parameter = 4.135; S parameter = 0.4). Each analysis was

run in triplicate for 100,000,000 generations with log and tree samples saved every 10,0000th generation. We used Tracer 1.6 (Rambaut et al. 2014) to estimate run convergence, determine the burn-in cutoff (10% for each analysis), and to obtain effective sampling sizes (ESS) of the estimated parameters (an ESS > 200 was considered appropriate for use in this study). Posterior probabilities of the nodes were calculated with the sampled trees after the burn-in. If all replicates converged, one of the runs was used to produce a maximum-clade-credibility tree in TreeAnnotator 2 (Rambaut and Drummond 2013).

In addition to using secondary calibrations from (Gaya et al. 2015), we analyzed the 118-specimen dataset using a molecular evolution rate of $2.43 \times 10^{9}$ substitution/site/year (s/s/y) for the ITS locus that were established by (Leavitt et al. 2012) for the Parmeliaceae. Although the Parmeliaceae is distantly related to the Lobariaceae, we assumed that the rates were comparable, as similar rates of molecular evolution ($2.52 \times 10^{9}$ sys/y) have been reported in the distantly related powdery-mildews by (Takamatsu and Matsuda 2004). Analyses were run in triplicate as described above on the 118-specimen dataset.

### 3.2.5 Biogeographic analyses and ancestral area reconstruction

We used character mapping on the 118-tip time-calibrated phylogeny to investigate major radiations and major dispersal events of *Sticta*. Species were coded as present or absent from four broad geographic regions (New World, Old World, Australasian, and Hawaii). The data for this geographic character coding was determined by searching for geographic ranges in species descriptions in the literature (Brodo, Sharnoff, and Sharnoff 2001; Galloway 2007, 2006, 1998, 1997, 1994; Galloway, Stenroos, and Ferraro 1995; Galloway and Thomas 2001; Magain and Sérusiaux 2015; McDonald, Miadlikowska, and Lutzoni 2003; Moncada, Lücking, and Suárez 2014; Moncada, Coca, and Lücking 2013; Moncada, Lücking, and Betancourt-Macuase 2013;

Moncada and Lücking 2012; Nash et al. 2004; Simon et al. 2018; Smith et al. 2009; Suarez and Lucking 2013). To reconstruct the ancestral ranges for the major clades, we used a dispersal-extinction-cladogenesis (DEC) model implemented in Lagrange (Ree and Smith 2008) using the same four-region character coding. In the continuous-time DEC model, range expansion is achieved through dispersal while range contraction is caused by extinction. Due to the highly dispersive nature of lichens and the cosmopolitan distribution of some species (*S. fuliginosa*, *S. limbata*, and *S. tomentosa*), max range sizes and dispersal were unconstrained. The most probable ancestral range of each major clade was mapped onto the phylogeny.

### 3.2.6 Diversification Analyses

We investigated diversification dynamics with the software Bayesian Analysis of Macroevolutionary Mixtures (BAMM; (Rabosky 2014)). BAMM can detect heterogeneity in speciation and extinction rates along the branches of a time-calibrated phylogeny using reversible MCMC, which explores all possible rate shift configurations and returns the posterior distribution. We used the 118-tip time-calibrated phylogeny as input and adjusted for incomplete sampling at the clade level using the "SamplesProbsFilename" argument in the control file (Clades I, II, and III, 75%; Clade IV, 50%; Clade V, 12.5%; *Pseudocyphellaria,* 0.5%; Lobaria 1%; see result section for the clade I, II, III, and IV). We also ran the analysis without the outgroup, removed with the drop.tips() function in the R package APE (Paradis, Claude, and Strimmer 2004) and obtained similar results. The BAMMtools v. 2.1.5 package in R (Rabosky et al. 2014) was used to determine the priors for the tree with the setBAMMPriors() command. We ran two parallel chains of 10,000,000 generations, sampling every 5O00th tree. Further analyses of the BAMM output files ("mcmcout" and "eventdata") were examined in the BAMMtools v. 2.1.5 package in R. Twenty percent of trees were discarded as burnin and ESS values were

estimated using the coda v. 0.18-1 package in R using the "mcmcout" file as an input. The "eventdata" file was used to visualize phylorate plots which depict diversification rates along the branches. Net diversification rate through time plots were generated using the plotRateThroughTime() function.

### 3.2.7 Binary state speciation and extinction (BiSSE) analyses

#### *3.2.7.1 Primary photobiont association*

To investigate how primary photobiont association affects diversification in *Sticta*, we performed a BiSSE analysis (Maddison, Midford, and Otto 2007), implemented in the R package diversitree (FitzJohn 2012). Primary photobiont, the photobiont (green algal or cyanobacterial) that is most frequently found to associate with a species, was determined by a literature search of species descriptions (Brodo, Sharnoff, and Sharnoff 2001; Galloway 2007, 2006, 1998, 1997, 1994; Galloway, Stenroos, and Ferraro 1995; D J Galloway and Thomas 2001; Magain and Sérusiaux 2015; McDonald, Miadlikowska, and Lutzoni 2003; Moncada, Reidy, and Lücking 2014; Moncada, Coca, and Lücking 2013; Moncada, Lücking, and Betancourt-Macuase 2013; Moncada and Lücking 2012; Nash et al. 2004; Smith et al. 2009; Suarez and Lucking 2013). In the case of species that are yet to be described, the authors were contacted in order to determine primary photobiont (Robert Lücking, personal communication). Although some species form photosymbiodemes, each of these species are mostly in association with one photobiont or another and these were scored accordingly in the BiSSE analyses. The BiSSE model estimates state-specific rates of character transition (q01 and ql0), speciation (λ) and extinction (μ). Species primarily associated with cyanobacteria were assigned "0" and species with green algal associations were assigned "1". Since this dataset has a large asymmetry in character state (93 cyanobacterial species to 25 green algal species) and less than 300 tips, there is a potential that

there is not enough power in the data to accurately estimate differences in parameters in BiSSE (Davis, Midford, and Maddison 2013). To see how sensitive the results are to changes in the data, we randomized the character state assignment on the phylogeny, keeping the same ratio (See section on measuring Type I error below). Initial runs were conducted with no adjustment for sampling, but since the estimated amount of species in *Sticta* is conservatively estimated to be nearly 400 species (Robert Lücking, personal communication), we adjusted for incomplete sampling by entering a fraction of 30% and 29% sampled species for cyanobacterial and green algal species respectively.

We estimated parameters on an unconstrained model, where all parameters (q01, q10, λ1, μ0 and μ1) were allowed to take any value and a fully constrained model, where all parameters were equal (q01 = q10, λ0= λ1, and μ0 = μ1). To test for irreversible transition between primary photobiont, we set speciation and extinction rates to take on any value for both states and then compared models were transitions were allowed in only one direction (q01 = 0 and q10 = 0) to models that had transitions equal (q01 = q10) and the full model where transitions take on any value. Equilibrium frequencies of speciation, extinction and transition rates were estimated using Markov chain Monte Carlo (MCMC) sampling using the full model described above. We conducted the estimation with a ten-percent burnin (10,000 MCMC steps) and then 1,000,000 step-process to estimate posterior distributions.

#### ***3.2.7.2 Andean tectonic influence on diversification***

To gain a better understanding of the large New World radiation of *Sticta* (mostly in Clades I, II, and III), for which we suspected that Andean tectonic activity played a major role, we assigned Andean species “1” and extra-Andean taxa “0”. As above, model testing was

conducted and exploratory analyses were performed with and without sampling adjustment, each having similar outcomes.

#### *3.2.7.3 Measuring type I error in datasets*

BiSSE analyses can be biased by small sample sizes and asymmetry in character states (Davis, Midford, and Maddison 2013), and is prone to high Type I error rates (Rabosky and Goldberg 2015). To test the sensitivity of our results to both sample size and tip imbalance, we permuted the data 500 times to generate simulated data sets. To each of these simulated data sets we estimated the fit of a model where speciation rates were allowed to vary between states to a model where they were constrained to be equal. We compared to the fit of the two models using likelihood ratio tests. We defined Type I error rate as the proportion of simulated data sets where the free-speciation model was estimated to better explain the data.

## 3.3 Results

### 3.3.1 Molecular data

A total of 497 sequences were generated for this study and the other 281 sequences were used in previous studies. Details on number of taxa, unambiguously aligned sites, missing data and JModelTest AIC model selections are summarized in Table VIII. Gblocks removed 233 and 413 ambiguously aligned sites from the ITS and mtSSU datasets respectively. All alignments (individual and combined) are deposited in Treebase (S21378).

### 3.3.2 Phylogenetic analyses

There was no well-supported conflict among the single-locus trees using RAxML, and concatenated datasets were produced for further analyses. The five-locus datasets analyzed with a Bayesian approach (118, 196, 224-tips) recovered congruent topologies (Figure 6). *Sticta* is a well-supported monophyletic clade in relation to the outgroup species *Pseudocyphellaria crinita*

and *Lobaria pulmonaria*. Within *Sticta*, five well-supported, major clades were recovered. Clades I, II, and III cluster in a well-supported clade sister to clade IV, which contains most of the accessions from Australia and New Zealand. Clade V is sister to the rest of *Sticta*. Backbone support for these five-locus datasets are poor, so phylogenetic relationships among clades should be interpreted with caution. The three-locus data set (147 tips) had different relationships among the major clades where clades IV and V are merged and monophyletic with clades I and III. Clade II is sister to the rest of the specimens. As with the five-locus datasets, backbone support of the three-locus tree was poor. The placement of *Sticta macrothaliana* is ambiguous, but both ML and Bayesian analyses of all datasets suggest that this species forms a distinct lineage.

### 3.3.3 Divergence time analyses

To see how different priors influence the estimation of divergence times using secondary calibrations, we used the 118-tip dataset to compare the models in BEAST 2.0 (Table IX). Both the yule and births/death models estimated similar divergence times for the calibrated nodes (~ 30.85 mya for *Sticta* and 46.5 mya for *Pseudocyphellaria* and *Sticta*). The calibrated yule model estimated a similar origin for *Sticta* (30.2 mya), but it recovered an earlier divergence of *Pseudocyphellaria* and *Sticta* from *Lobaria* (65.2 mya). The ITS rate calibrated analysis (2.43 $\times 10^9$ s/s/y) had similar estimates for the origin of *Sticta* (32.3 mya), but similar to the calibrated yule analysis, the ITS rate estimated the divergence of *Pseudocyphellaria* and *Sticta* to be 63.3 mya.

TABLE IX. DIVERGENCE TIMES ESTIMATED WITH THE 118-TIP DATASET USING RATE CALIBRATED YULE AND SECONDARY CALIBRATIONS WITH YULE, CALIBRATED YULE, AND BIRTH/DEATH PRIORS SET IN BEAST.

| Analysis | *Sticta* (Mya) | *Pseudocyphellaria and Sticta* (Mya) |
|---|---|---|
| ITS rate calibrated (Yule) | 32.3 | 63.3 |
| **Analyses using secondary calibrations** | | |
| Yule prior | 30.8 | 46.6 |
| Calibrated Yule prior | 30.2 | 65.2 |
| Birth/Death prior | 30.9 | 46.7 |

Effective sample sizes (ESS), estimated in Tracer, were all well over 200 for all parameters in both the yule and calibrated yule analyses, but in the birth/death and rate calibrated runs, some of the tree likelihoods for individual loci and the combined tree likelihood and posterior were lower than 200. Since a yule prior is a more appropriate model of recent diversification among species level lineages (Drummond et al. 2006), and ESS values were all higher than 200, this prior was used for comparing the four datasets with different amounts of missing data and tips.

All four datasets are compared in Table X. The average origin of *Sticta* is estimated to be 30.0 mya and the origin of *Pseudocyphellaria* and *Sticta* 45.2 mya. All datasets suggest a Miocene dominated diversification of the five major clades in *Sticta* (Table X, Figure 6), but the larger datasets (196 and 224 tips) show diversification throughout and after the Miocene.

TABLE X. DIVERGENCE TIME ESTIMATIONS FROM FOUR DIFFERENT CONCATENATED ALIGNMENTS

| Dataset | Max loci | Min loci | # Tips | *Sticta* only (Mya) | *Sticta*+*Pseudocyphellaria* (Mya) |
|---|---|---|---|---|---|
| Gappy | 5 | 2 | 224 | *32.1* | *44.5* |
| Less gappy | 5 | 3 | 196 | *30.2* | *44.4* |
| Nonredundant | 5 | 3 | 118 | *30.8* | *46.6* |
| Complete | 3 | 3 | 147 | *26.8* | - |

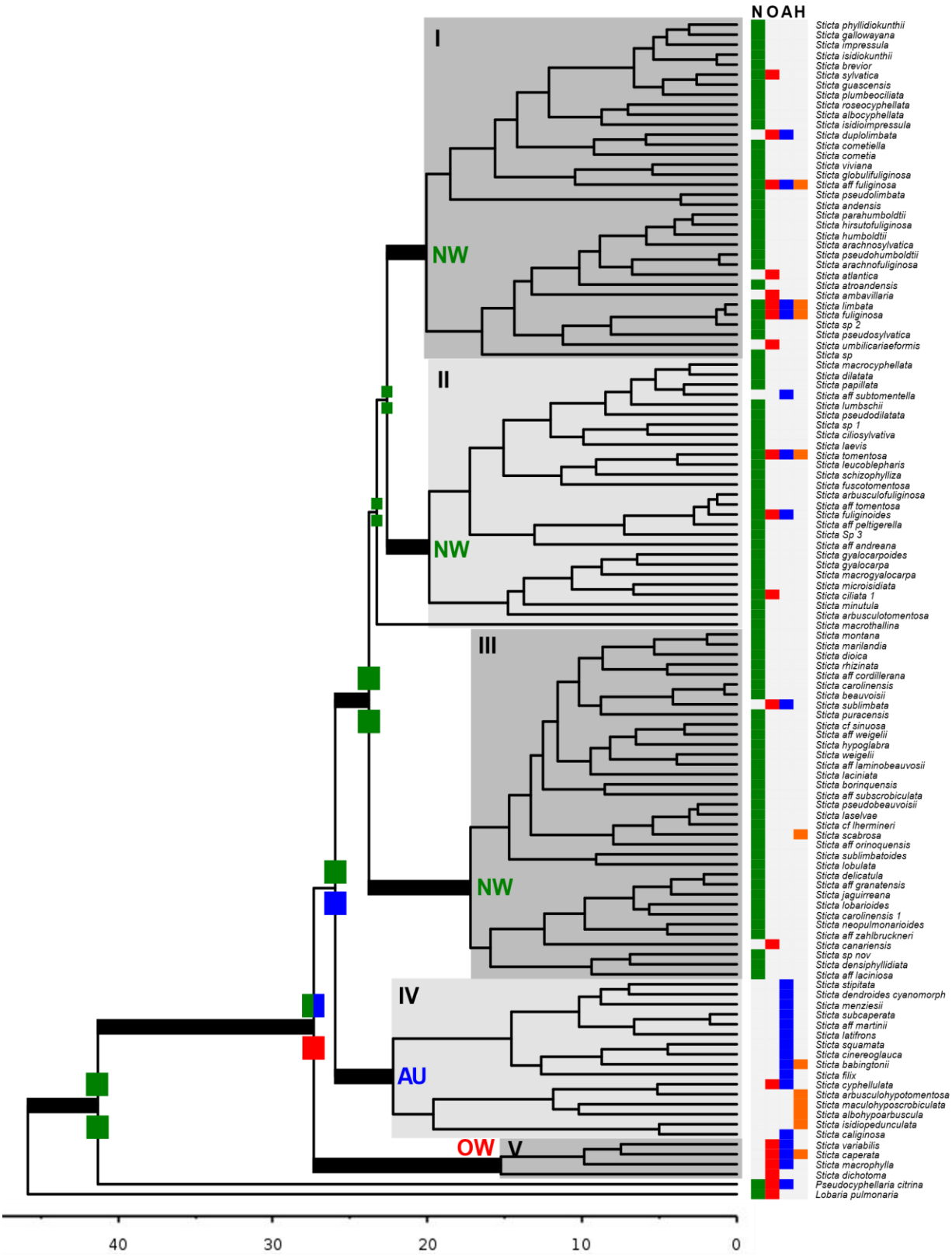
NOAH
I
II
III
IV
V
NW
NW
NW
AU
OW
Sticta phyllidiokunthii
Sticta gallowayana
Sticta impressula
Sticta isidiokunthii
Sticta brevior
Sticta sylvatica
Sticta guascensis
Sticta plumbeociliata
Sticta roseocyphellata
Sticta albocyphellata
Sticta isidioimpressula
Sticta duplolimbata
Sticta cometiella
Sticta cometia
Sticta viviana
Sticta globulifuliginosa
Sticta aff fuliginosa
Sticta pseudolimbata
Sticta andensis
Sticta parahumboldtii
Sticta hirsutofuliginosa
Sticta humboldtii
Sticta arachnosylvatica
Sticta pseudohumboldtii
Sticta arachnofuliginosa
Sticta atlantica
Sticta atroandensis
Sticta ambavillaria
Sticta limbata
Sticta fuliginosa
Sticta sp 2
Sticta pseudosylvatica
Sticta umbilicariaeformis
Sticta sp
Sticta macrocyphellata
Sticta dilatata
Sticta papillata
Sticta aff subtomentella
Sticta lumbschii
Sticta pseudodilatata
Sticta sp 1
Sticta ciliosylvativa
Sticta laevis
Sticta tomentosa
Sticta leucoblepharis
Sticta schizophylliza
Sticta fuscotomentosa
Sticta arbusculofuliginosa
Sticta aff tomentosa
Sticta fuliginoides
Sticta aff peltigerella
Sticta Sp 3
Sticta aff andreana
Sticta gyalocarpoides
Sticta gyalocarpa
Sticta macrogyalocarpa
Sticta microisidiata
Sticta ciliata 1
Sticta minutula
Sticta arbusculotomentosa
Sticta macrothallina
Sticta montana
Sticta marilandia
Sticta dioica
Sticta rhizinata
Sticta aff cordillerana
Sticta carolinensis
Sticta beauvoisii
Sticta sublimbata
Sticta puracensis
Sticta cf sinuosa
Sticta aff weigelii
Sticta hypoglabra
Sticta weigelii
Sticta aff laminobeauvosii
Sticta laciniata
Sticta borinquensis
Sticta aff subscrobiculata
Sticta pseudobeauvoisii
Sticta laselvae
Sticta cf lhermineri
Sticta scabrosa
Sticta aff orinoquensis
Sticta sublimbatoides
Sticta lobulata
Sticta delicatula
Sticta aff granatensis
Sticta jaguirreana
Sticta lobarioides
Sticta carolinensis 1
Sticta neopulmonarioides
Sticta aff zahlbruckneri
Sticta canariensis
Sticta sp nov
Sticta densiphyllidiata
Sticta aff laciniosa
Sticta stipitata
Sticta dendroides cyanomorph
Sticta menziesii
Sticta subcaperata
Sticta aff martinii
Sticta latifrons
Sticta squamata
Sticta cinereoglauca
Sticta babingtonii
Sticta filix
Sticta cyphellulata
Sticta arbusculohypotomentosa
Sticta maculohyposcrobiculata
Sticta albohypoarbuscula
Sticta isidiopedunculata
Sticta caliginosa
Sticta variabilis
Sticta caperata
Sticta macrophylla
Sticta dichotoma
Pseudocyphellaria citrina
Lobaria pulmonaria
40
30
20
10
0

Figure 6. Time-calibrated chronogram of the phylogeny of the genus *Sticta* including 118 tips. Grey boxes circumscribe the major clades I, II, III, IV, and V. Highly supported branches (bootstrap support > 70 and posterior probability > 90) are depicted as thick branches. Four columns of character states for occurrence are coded at the tips of the phylogeny (NW = New World, OW = Old World, AU = Australasian, HA = Hawaii). Ancestral ranges, estimated with the DEC model in Lagrange, are mapped onto the branches indicating species range divergence at the nodes.

### 3.3.4 Biogeographic Analysis

The 118-tip dataset was used for biogeographic and diversification analyses because it is pruned to have only one individual per species and always had ESS values higher than 200 for all estimated parameters in the BEAST analysis. Geographic character states are mapped onto the 118-tip phylogeny in Figure 6. Geographic structure can be observed; Clades I, II, and III are dominated by New World taxa, suggesting a major radiation in the New World. Similarly, an Australasian radiation of lesser scale, is found in Clade IV. Old World species mostly are found in Clade V, but there seems to be numerous dispersal event from the New World to the Old World. A striking pattern of long-distance dispersal is observed in Hawaiian species, which are represented in every major clade, demonstrating the remarkable dispersal ability of the genus.

Ancestral range reconstructions estimated with the DEC model are mapped onto the phylogeny in Figure 6. Clades I, II and III have ancestral ranges in the New World, Clade IV in Australasia, and Clade V in the Old World. The reconstruction suggests a New World origin for *Sticta*, but this should be interpreted with caution, as backbone support was poor for certain nodes.

### 3.3.5 Diversification analysis

The ESS obtained from two parallel runs in BAMM were similar and well over 200 and indicated that both runs converged. In the time-calibrated phylogeny of *Sticta*, there were no distinct rate shifts, with the posterior distribution of the number of shifts suggesting zero shifts with a frequency of 0.97. Exploratory analyses run without adjustment for incomplete sampling detected rate shifts in the tree on the ancestral node of *Sticta*. The mean phylorate plot (Figure 7) shows a pattern of decreasing speciation rates through time, but this decrease in rate is low, starting at just below 0.2 lineages per million years and only decreasing slightly through time. On the other hand, extinction rates remained close to zero throughout time.

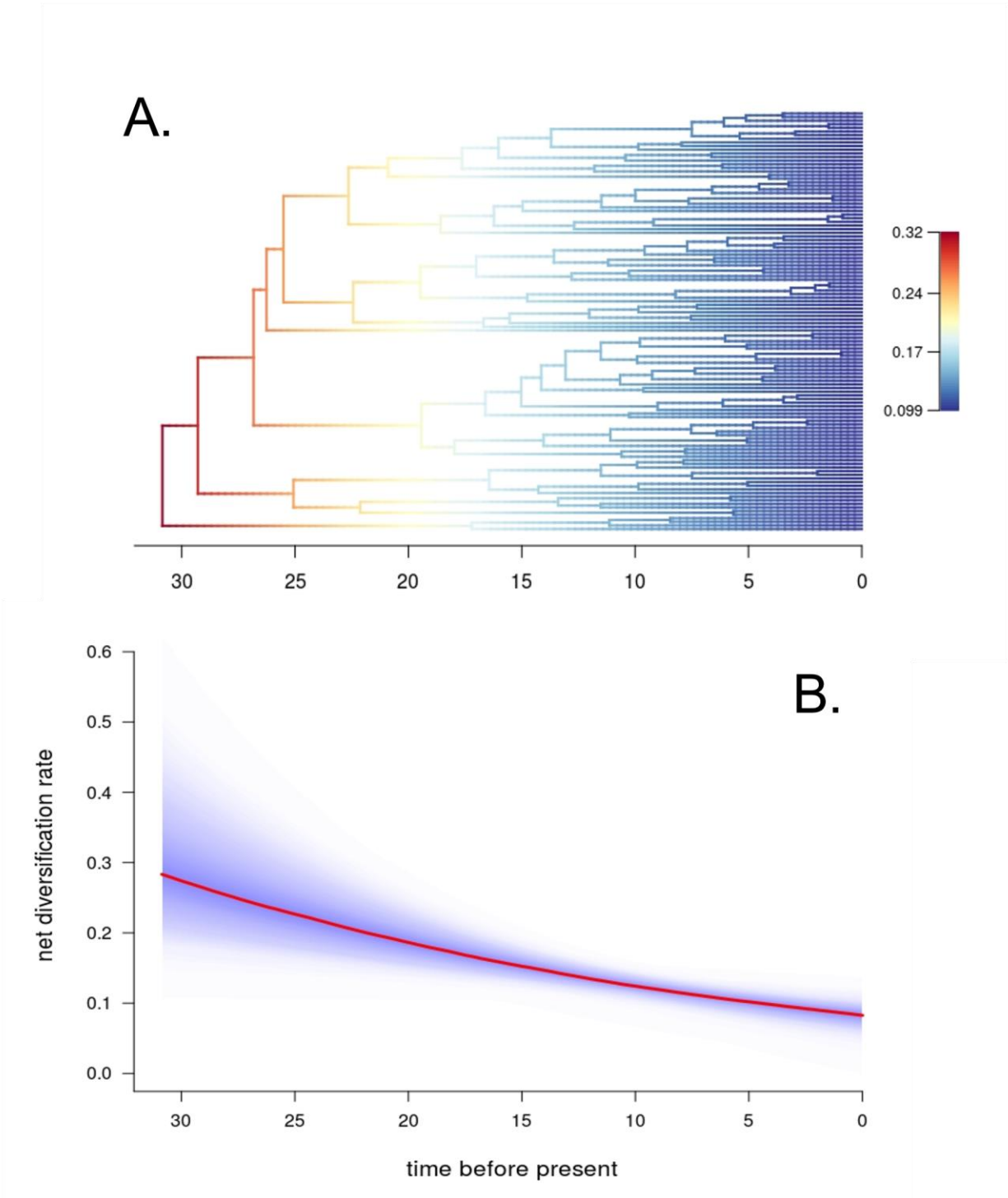


Figure 7. BAMM mean phylorate plot on (A) unrooted *Sticta* phylogeny of 116 tips and (B) a net diversification through time plot.

### 3.3.6 Binary state speciation and extinction (BiSSE) analyses

#### *3.3.6.1 Primary photobiont association*

Model testing results, including estimated speciation, extinction and transition parameters, for analyses adjusted for sampling and unadjusted are listed in Table XI. Sampling adjustment had no effect on the model selection, but the diversification parameters are different. The distribution of character states on the 118-tip tree is visualized in Figure 8A. All the major clades contain both green algal and cyanobacterial species. Clades I and II are composed mostly of primarily cyanobacterial species, but each major clade has one green algal species. Clade III is the largest and it contains nine green algal species. Clades IV and V are composed mostly of green algal taxa, but they both contain cyanobacterial species too.

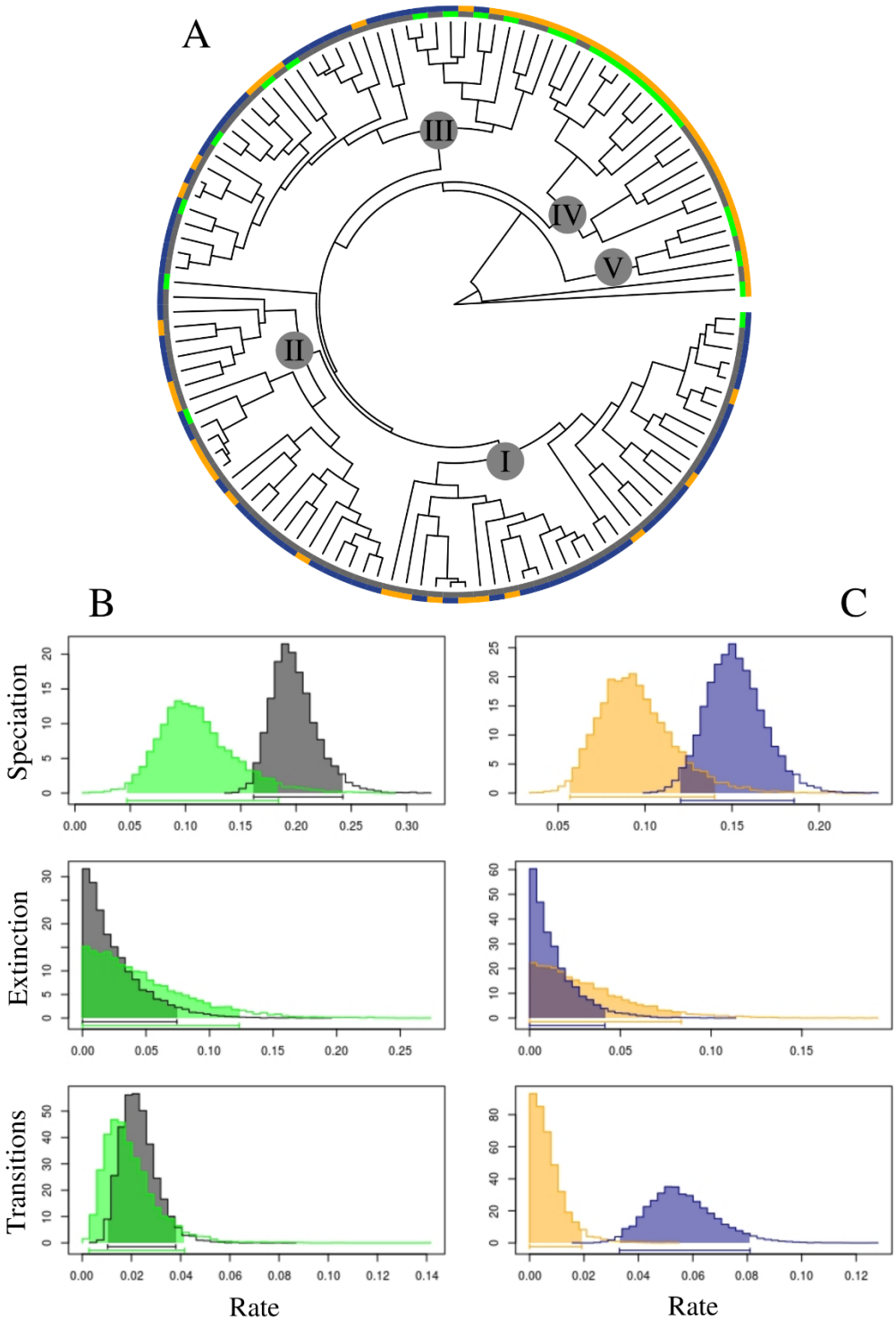


Figure 8. (A) Distribution of character states for photobiont association and Andean tectonic influence mapped onto the tips of the 118-tip phylogeny with the five well-supported major clades labeled at the nodes. Photobiont: Green-algal associations shown in green; cyanobacterial associations shown in grey. Andean tectonic influence: Andean species shown in blue and non-

Andean species shown in orange. (B) Posterior distributions (95%) from a BiSSE MCMC analysis of photobiont associations. The plots are as follows; top = speciation rate, middle = extinction rates, and bottom = transitions. Cyanobacterial associations ("1") are depicted in grey and green-algal associations ("0") are in green. (C) Posterior distributions (95%) from a BiSSE MCMC analysis of Andean tectonic associations. The plots are as follows; top = speciation rate, middle = extinction rates, and bottom = transitions. Andean species ("1") are depicted in blue and non-Andean species ("0") are in orange.

Regardless of the sampling setting in diversitree, adjusted and unadjusted analyses were congruent (Table XI). Speciation rates were higher for the cyanobacterial state (0) than the green algal state (1), suggesting that cyanobacterial species have a higher speciation rate than green algal species, but there was slight overlap of the posterior distributions (Figure 8B). Both extinction and transition rates were mostly overlapping, indicating that extinction and transitions between primary photobiont are similar regardless of the primary photobiont association.

The "no extinction" and "free-speciation" models had similar likelihoods and AIC scores and fit the tree and state assignments with the highest likelihoods (Table XI). Additionally, these two models produced the same estimates for diversification parameters. Even though it has the best fit, the no extinction model, when testing for Type I error (the inability to determine whether speciation rates are different between photobiont associations), would freeze and all iterations could not be completed, therefore we chose to use the free-speciation model, which only allows for the speciation rates to vary.

TABLE XI. BISSE MODEL TESTING FOR PHOTOBIONT ASSOCIATION WITH ESTIMATIONS OF SPECIATION, EXTINCTION, AND TRANSITION RATES FOR EACH MODEL (CYANOBACTERIAL = '0', GREEN-ALGAL = '1').

| No sampling adjustment | | | | speciation | | extinction | | transitions | |
|---|---|---|---|---|---|---|---|---|---|
| **Model** | **Df** | **lnLik** | **AIC** | **λ0** | **λ1** | **μ0** | **μ1** | **q01** | **q10** |
| No extinction (μ0=0, μ1=0) | 4 | -447.38 | 902.77 | 0.10 | 0.04 | 0.00 | 0.00 | 0.02 | 0.02 |
| Free speciation (λ0 and λ1 take on any value) | 4 | -447.47 | 902.95 | 0.10 | 0.04 | 0.00 | 0.00 | 0.02 | 0.02 |
| Equal transition rates (q01=q10) | 5 | -447.47 | 904.95 | 0.10 | 0.04 | 0.00 | 0.00 | 0.02 | 0.02 |
| Full BiSSE (λ0, λ1, μ0, μ1, q01, q10 take on any value) | 6 | -447.39 | 906.77 | 0.10 | 0.04 | 0.00 | 0.00 | 0.02 | 0.02 |
| Fully constrained (λ0=λ1, μ0=μ1, q01=q10) | 3 | -451.31 | 908.62 | 0.09 | 0.09 | 0.00 | 0.00 | 0.02 | 0.02 |
| Mk2 (λ0=λ1, μ0=μ1) | 4 | -451.17 | 910.33 | 0.09 | 0.09 | 0.00 | 0.00 | 0.02 | 0.03 |
| unidirectional, green to cyano, (q10=0) | 5 | -451.11 | 912.22 | 0.10 | 0.03 | 0.00 | 0.02 | 0.02 | 0.00 |
| unidirectional, cyano to green, (q01=0) | 5 | -460.64 | 931.28 | 0.07 | 0.10 | 0.00 | 0.00 | 0.00 | 0.06 |
| Sampling adjustment (cyano 30%, green 29%) | | | | speciation | | extinction | | transitions | |
| **Model** | **Df** | **lnLik** | **AIC** | **λ0** | **λ1** | **μ0** | **μ1** | **q01** | **q10** |
| No extinction (μ0=0, μ1=0) | 4 | -437.64 | 883.28 | 0.18 | 0.08 | 0.00 | 0.00 | 0.02 | 0.02 |
| Free speciation (λ0 and λ1 take on any value) | 4 | -437.68 | 883.37 | 0.18 | 0.08 | 0.00 | 0.00 | 0.02 | 0.02 |
| Equal transition rates (q01=q10) | 5 | -437.68 | 885.35 | 0.18 | 0.08 | 0.00 | 0.00 | 0.02 | 0.02 |
| Full BiSSE (λ0, λ1, μ0, μ1, q01, q10 take on any value) | 6 | -437.54 | 887.09 | 0.18 | 0.10 | 0.00 | 0.03 | 0.02 | 0.01 |
| Fully constrained (λ0=λ1, μ0=μ1, q01=q10) | 3 | -444.16 | 894.31 | 0.16 | 0.16 | 0.00 | 0.00 | 0.02 | 0.02 |
| Mk2 (λ0=λ1, μ0=μ1) | 4 | -444.03 | 896.07 | 0.16 | 0.16 | 0.00 | 0.00 | 0.02 | 0.03 |
| unidirectional, green to cyano, (q10=0) | 5 | -443.29 | 896.57 | 0.18 | 0.08 | 0.00 | 0.06 | 0.03 | 0.00 |
| unidirectional, cyano to green, (q01=0) | 5 | -454.00 | 918.00 | 0.20 | 0.17 | 0.09 | 0.00 | 0.00 | 0.08 |

In each of the 500 iterations of randomized tip state assignments, the free-speciation model was compared to the fully constrained model using a likelihood ratio test and no matter how the states were distributed, the free-speciation model was better. Therefore, given the phylogeny and the state assignments, our results appear to be driven by Type I error (Table XIX, Appendix B).

#### ***3.3.6.2 Andean tectonic influence on diversification***

Clades I, II, and III contain mostly New World species, of which, most were collected in the Andes which was tectonically active during the diversification of *Sticta* (Hoorn et al. 2010). We coded the specimens that were collected in the tectonically active region as "1" and those outside as "0". Model testing results are summarized in Table XII. Adjusting for incomplete sampling did not change which models had the best fit [No extinction (p0 = 0, pl = 0) and Unidirectional, Andean to extra-Andean (ql0 = 0)), but speciation and q10 parameters increased with the adjustment. In the adjusted analysis, which we used to test for Type I error, speciation and transitions are identical in the three most likely models [No extinction (p0 = 0, pt = 0); Unidirectional, Unidirectional, Andean to extra-Andean, (q01 = 0); and Full BiSSE (TO, Al, p0, q1, q0l, ql0 take on any value)]. As mentioned above, the "No extinction" model is not likely, so we used the "Unidirectional, Andean to extra-Andean, (q01 = 0)" model for testing Type I error. The distribution of Andean species is depicted in Figure 8A. Clades I, II and III contain all of the 67 Andean taxa plus six extra-Andean species. The other 51 extra-Andean taxa are found in clades IV and V and evenly distributed throughout the other three clades. Posterior distributions (95%) found Andean taxa to have a higher speciation rate and a tendency for transitions from Andean to extra-Andean state (Figure 8C). As in the photobiont association analysis, the "no extinction" model had the highest likelihood, but when using it to iterate through random

arrangements of state assignments, it would freeze as some arrangements were to computationally problematic. This was the same for the full model as well. The Unidirectional (q01) model did not have this problem and could successfully iterate through 500 arrangements of tip assignments, having a two percent Type I error rate (Table XX, Appendix B).

TABLE XII. BISSE MODEL TESTING FOR ANDEAN ASSOCIATION WITH ESTIMATIONS OF SPECIATION, EXTINCTION, AND TRANSITION RATES FOR EACH MODEL (NON-ANDEAN = '0', ANDEAN = '1').

| No sampling adjustment | | | | speciation | | extinction | | transitions | |
|---|---|---|---|---|---|---|---|---|---|
| **Model** | **Df** | **lnLik** | **AIC** | **λ0** | **λ1** | **μ0** | **μ1** | **q01** | **q10** |
| No extinction (μ0=0, μ1=0) | 4 | -461.4112 | 930.8224 | 0.04 | 0.11 | 0.00 | 0.00 | 0.00 | 0.04 |
| Unidirectional, Andean to extra-Andean, (q01=0) | 5 | -461.4115 | 932.8229 | 0.04 | 0.11 | 0.00 | 0.00 | 0.00 | 0.04 |
| Full BiSSE (λ0, λ1, μ0, μ1, q01, q10 take on any value) | 6 | -461.4112 | 934.8225 | 0.04 | 0.11 | 0.00 | 0.00 | 0.00 | 0.04 |
| Free speciation (λ0 and λ1 take on any value) | 4 | -466.3794 | 940.7589 | 0.09 | 0.09 | 0.00 | 0.00 | 0.01 | 0.03 |
| Equal transition rates (q01=q10) | 5 | -466.3797 | 942.7594 | 0.09 | 0.09 | 0.00 | 0.00 | 0.03 | 0.03 |
| Mk2 (λ0=λ1, μ0=μ1) | 4 | -469.4712 | 946.9425 | 0.05 | 0.11 | 0.00 | 0.00 | 0.03 | 0.03 |
| Fully constrained (λ0=λ1, μ0=μ1, q01=q10) | 3 | -471.6897 | 949.3795 | 0.05 | 0.11 | 0.00 | 0.00 | 0.03 | 0.03 |
| Unidirectional, extra-Andean to Andean, (q10=0) | 5 | -488.693 | 987.3861 | 0.10 | 0.08 | 0.00 | 0.07 | 0.06 | 0.00 |

| Sampling adjustment (extra-Andean 43%, Andean 75%) | | | | speciation | | extinction | | transitions | |
|---|---|---|---|---|---|---|---|---|---|
| **Model** | **Df** | **lnLik** | **AIC** | **λ0** | **λ1** | **μ0** | **μ1** | **q01** | **q10** |
| No extinction (μ0=0, μ1=0) | 4 | -460.1327 | 928.2653 | 0.08 | 0.14 | 0.00 | 0.00 | 0.00 | 0.05 |
| Unidirectional, Andean to extra-Andean, (q01=0) | 5 | -460.1022 | 930.2044 | 0.08 | 0.14 | 0.01 | 0.00 | 0.00 | 0.05 |
| Full BiSSE (λ0, λ1, μ0, μ1, q01, q10 take on any value) | 6 | -460.1025 | 932.205 | 0.08 | 0.14 | 0.01 | 0.00 | 0.00 | 0.05 |
| Mk2 (λ0=λ1, μ0=μ1) | 4 | -464.3601 | 936.7201 | 0.12 | 0.12 | 0.00 | 0.00 | 0.00 | 0.04 |
| Fully constrained (λ0=λ1, μ0=μ1, q01=q10) | 3 | -469.1124 | 944.2247 | 0.12 | 0.12 | 0.00 | 0.00 | 0.04 | 0.04 |
| Free speciation (λ0 and λ1 take on any value) | 4 | -468.5143 | 945.0287 | 0.10 | 0.13 | 0.00 | 0.00 | 0.04 | 0.04 |
| Equal transition rates (q01=q10) | 5 | -468.4796 | 946.9591 | 0.10 | 0.14 | 0.00 | 0.01 | 0.04 | 0.04 |
| Unidirectional, extra-Andean to Andean, (q10=0) | 5 | -479.3274 | 968.6548 | 0.15 | 0.11 | 0.00 | 0.13 | 0.06 | 0.00 |

## 3.4 Discussion

We investigated the diversification history of *Sticta* by sampling throughout most of the global range of the genus and constructed a time-calibrated phylogeny. The results suggest an Oligocene origin of *Sticta* and a pattern of relatively higher diversification followed by a slowdown in the present. Collections from Hawaii suggest a high long-distance dispersal rate of the *Sticta*. We also investigated the effects of photobiont association and found that the significant association between speciation rate and cyanobacterial photobionts may result from Type I Error. Additionally, we looked into the effect of Andean uplifting and found that speciation rate is higher among *Sticta* species associated with the Andes. The significant results here are robust even when the effect of sampling bias is considered. In the following sections, we will discuss the timing and geographic location of diversification in *Sticta* and then discuss how intrinsic and extrinsic factors affect diversification.

### 3.4.1 Oligocene origin, Miocene diversification, and frequent long-distance dispersal in *Sticta*

The time tree (Figure 6) shows that *Sticta* originated in the late Oligocene and radiated into five major clades during the Miocene. The Miocene diversification is para11e1 with other groups of lichens (Amo de Paz et al. 2012; Leavitt et al. 2012; Leavitt, Esslinger, and Lumbsch 2012) and for diversification of many other groups of organisms (Finarelli and Badgley 2010; Nürk et al. 2015; Shaw et al. 2010). In the early Miocene, global temperatures increased until the MMCO (Flower and Kennett 1994). During this time of elevated temperature, ranges for many tropical and sub-tropical organisms expanded towards the poles and into higher elevations. After the MMCO, these tropical ranges retracted back to the equator and into lower elevations, opening up new habitats and niche space for more temperate organisms. Most species of *Sticta*

inhabit temperate rain forests and higher elevations (cooler temperatures) in tropical regions (Moncada, Lücking, and Suárez 2014). These new temperate spaces may have been the ranges where the major lineages of *Sticta* diversified during the Miocene.

*Sticta* species inhabit all continents, except Antarctica, and occur on many oceanic islands. Our results suggested that *Sticta* originated in the New World, but this should be interpreted with caution, as our sampling on the 118-tip phylogeny is not complete and adding more taxa to the tree could influence the result. Additionally, the branch support for the backbone is not resolved on some of the nodes (Figure 6). Also, exploratory analyses that divided up ranges into eight ranges, produced ambiguous results on the origin of the genus, but suggested that either South America, Australia or Madagascar to be potential ancestral ranges (data not shown).

Clade IV is composed of all New Zealand and Australian specimens. This suggests that shortly after the continental separation of Australia, Antarctica and South America, before they assumed their current positions, a lineage of *Sticta* became isolated in the Australasian region. Species of this lineage tend to inhabit temperate rain forest ecosystems of New Zealand, and South Eastern Australia and Tasmania. One member of Clade IV was found in Hawaii, which is interesting since prevailing winds are not in favor of Australasian to Hawaii dispersal and could potentially be a case of avian or ocean current mediated dispersal (Gillespie et al. 2012).

### 3.4.2 High long-distance dispersal rate of *Sticta*

Hawaiian *Sticta* species in Figure 6, represent up to five independent colonization events. Each colonization of Hawaii originated from one of the five major clades, indicating a high long-distance dispersal ability for species of this genus. Microscopic ascospores and asexual propagules can be carried on the wind during storms and on the feathers and feet of migratory

birds, and even on floating vegetation rafts that become dislodged from land, carrying lichens on ocean currents to other landmasses (Gillespie et al. 2012). Similar to the results in *Sticta*, a previous research on Hawaiian *Pseudocyphellaria* (Moncada, Reidy, and Lücking 2014) also found multiple colonization events (some of which are suspected to be anthropogenic). Furthermore, a study of *Porpidia flavicunda* in North Eastern Canada, Greenland, and Scandinavia suggested frequent and recurrent dispersal across the northern Atlantic (Buschbom 2007) and a study on the *Xanthoparmelia pulla* group (Amo de Paz et al. 2012) found evidence for multiple long-distance dispersal events and subsequent radiation on different continents. Other studies on lichens, however, have found radiations after a single colonization. For example, a study of *Lobariella* found a radiation after from a single colonization in the Hawaiian archipelago (Lücking, Moncada, and Smith 2017) and another found a radiation in Madagascar and the Mascarenes (Simon et al. 2018). It is still unclear why some groups of lichens seem to have high dispersal rates while other do not and our current understanding of distributional ranges in lichens and the factors shaping those are still in its infancy (Leavitt and Lumbsch 2016; Lumbsch 2016). Further investigation into the traits associated with long-distance dispersal would be an interesting line of research for future studies.

### 3.4.3 Decrease in net diversification over time

BAMM analysis revealed higher diversification rates on the backbone branches of the phylogeny, with rates decreasing towards the present (Figure 7). There were no distinct rate shifts detected by BAMM, only a trend of cooling diversification rates toward present time in every clade, suggesting that all clades diversify at the same rate in *Sticta*. With such high dispersal rates, *Sticta* may have quickly spread throughout the world, filling all available niche space with species and has reached its carrying capacity, but this is a difficult claim to confirm as

thorough sampling has not been conducted in all parts of the world. Another explanation for a slowing of net diversification rates is the changing climate during the Miocene. Diversification rates for *Sticta* were relatively high leading up to the MMCO (~ 18-14 mya) and then they began to decrease after this warmer period. This may indicate that the climatic changes during the Miocene influenced *Sticta* by continuously and gradually slowing down net diversification. However, as Figure 6 shows that *Sticta* diversified mostly during the Miocene, which is a similar scenario observed in the lichen genus *Melanohalea*, that is thought to have increased diversification rates caused by a drier climate and changes in vegetation patterns that occurred during the Miocene (Leavitt et al. 2012; Leavitt, Esslinger, and Lumbsch 2012). Our BAMM result may be misleading due to incomplete sampling. Even though we adjusted for incomplete sampling at the lineage level, this adjustment does not capture the complexity of branching that may be found in under-sampled lineages. Increasing the sampling on the phylogeny may tell a more accurate story and find rate shifts associated with undiscovered radiations.

### 3.4.4 Binary state speciation and extinction (BiSSE) analyses

#### *3.4.4.1 Primary photobiont association*

Species interactions play a large role in evolution, potentially through increasing the diversification of each partner in the group (Janson et al. 2008; Moran 2007; Stanley 1981). In *Sticta*, cyanobacterial species tend to be found in wetter conditions while green-algal mycobionts of *Sticta* tend to be found in relatively dryer micro climates (James and Henssen 1976). On the phylogeny, there are many more cyanobacterial species than green-algal (93:25 ratio, Figure 8A). Adjusting for incomplete sampling was challenging since BiSSE can only be adjusted by assuming one fraction for the entire tree, or by state (cyanobacterial vs green-algal photobiont). Exploratory analyses of different adjustments were compared to the unadjusted and there was no

large difference between them. The trend was that cyanobacterial associations have a higher, but not significantly higher speciation rate; there was no difference in extinction and transitions (Figure 8B). Moreover, when we randomized the tip assignments of "1" and "0", keeping the same ratio (93 cyanobacterial to 25 green-algal), the free-speciation model always out competed the fully-constrained model in 500 iterations, indicating that the high tip-ratio bias makes it unable to determine if photobiont association is responsible for higher diversification rates in cyanobacterial species. It is expected that some distributions of tip assignments will support the fully constrained model instead of a model where values of speciation are allowed to take on any value. Therefore, the statistical results obtained from the dataset for photobiont association are driven by Type I error.

The presence of photosymbiodemes in *Sticta*, where a single taxon can associate with both cyanobacterial or green-algal photobionts, may explain why we were unable to detect an effect on diversification rate. The ability to form photosymbiodemes is present throughout the phylogeny, and it is hypothesized that many species are photosymbiodemic and we have just missed the other morph (Moncada, Coca, and Lücking 2013). Another reason photobiont associations do not have an effect is that lichen fungi appear to be flexible in their association with particular photobiont genotypes that are geographically or ecologically adapted, allowing the fungus to inhabit multiple habitats by switching to a locally adapted photobiont population (Fernandez-Mendoza et al. 2011; Nelsen and Gargas 2009; Werth and Sork 2014) . It is still unclear if primary photobiont association has any effect in influencing diversification of species in *Sticta* and if this can explain the dominance of cyanobacterial species in the genus. Increased taxon sampling and a closer look for undiscovered photosymbiodemes will help to elucidate this in the future.

#### ***3.4.4.2 Andean tectonic influence on diversification***

Three of the five major clades recovered in *Sticta* are composed mostly of species that occur in the tectonically active Andes and it has been hypothesized that a major radiation occurred there (Moncada, Lücking, and Suárez 2014). In our study, we hypothesized that Andean species have a higher diversification rates than species occurring outside of the Andes. Our result from BiSSE analysis (Figure 8, Table XII) found that speciation rates are higher (not significantly) in Andean species and found a pattern of transitions from the Andean (tectonically active region) to extra-Andean state (tectonically passive region). Randomization of tip character state assignments while maintaining the same ratio (67 Andean to 51 extra-Andean) found that the fully constrained model would out compete the full model in 11% of the iterations, demonstrating that some configurations will select a much different model of diversification, which implies that the results here were less likely due to Type I error. Our result is congruent with a similar study using BiSSE (Lagomarsino et al. 2016) that found Andean bellflowers (Campanulaceae) to have higher speciation rates than their lowland counterparts. Many other studies have attributed Andean uplift to diversifications in many groups (for a review see: (Hoorn et al. 2010)). Furthermore, a study of the lichen genus *Peltigera* found a recent and rapid radiation that was associated with the Andes (Magain et al. 2016).

If *Sticta* species were present during Andean uplift periods, coupled with high dispersal rates, a significant diversification event could have been triggered by increasing the carrying capacity of the Andes, allowing for more species of *Sticta* in the region. While the uplift was occurring, many new microhabitats were produced, and the dispersal ability of *Sticta* could have allowed for colonization of many unique habitats in a relatively short span of evolutionary time. Moreover, species associate with both green-algae and cyanobacteria in the Andes region and

photobiont shifts, due to different ecological requirements of the symbiont could have caused divergence.

### 3.5. Conclusions

We used molecular markers and Bayesian time-calibrated trees to determine that *Sticta* originated in the New World during the Oligocene and diversified throughout the Miocene epoch. Furthermore, we provide evidence that *Sticta* has a high dispersal rate with Hawaiian collections that show multiple independent colonizations of the islands. We also attempted to tease apart the individual contribution of drivers of *Sticta* diversification.

Species interactions have been found to influence diversification in plant-pollenator systems, phytophagous insects, and reef building corals (Janson et al. 2008; Stanley 1981; van der Niet and Johnson 2012) , but there are still many gaps in our knowledge in other groups. In *Sticta*, the diversification process did not seem to be influenced by photobiont associations and it is still unclear why there are so many more species that associate with cyanobacteria than green-algae. Further sampling may be able to uncover how photobionts affect diversification of the mycobionts in *Sticta*. However, more sampling may also discover that more species form photosymbiodemes that we currently know.

Researchers, uncertain in the effect of intrinsic factors on diversification have invoked geographical and climatic explanations to explain heterogeneity in biodiversity. *Sticta* is undergoing a slowdown in diversification, which might be associated with cooling climate, but it is unclear whether climate-induced range shifts occurred and if this decrease in net diversification is due to limits on global carrying capacity.

Our results do suggest that Andean tectonic activity, does influence diversification of species in *Sticta* by increasing the speciation rate which is congruent with the growing body of

evidence that the Andes is a hotspot for diversification, not only in lichens, but in almost all groups studied there. This could be explained by the fragmentation and turnover of habitats during the uplift of the Andes, coupled with the incredible dispersal ability of the *Sticta*, which creates the perfect conditions for founder events leading to many isolated populations being selected by different factors on an ever-changing landscape.

Our study adds to the small but growing base of knowledge of the timing and placement of diversification in groups of lichenized fungi by investigating the genus *Sticta*. Furthermore, we investigated the effect of drivers of diversification in *Sticta,* which is relatively rare in the study of lichen evolution and adds not only to the knowledge of lichens, but to the overall knowledge of evolution in the tree of life.

**3.6 References**

Amo de Paz, Guillermo, Paloma Cubas, Ana Crespo, John A. Elix, and H. Thorsten Lumbsch. "Transoceanic dispersal and subsequent diversification on separate continents shaped diversity of the *Xanthoparmelia pulla* group (Ascomycota)." *PLOS ONE* 7, no. 6 (2012): e39683.

Amo de Paz, Guillermo, Paloma Cubas, Pradeep K. Divakar, H. Thorsten Lumbsch, and Ana Crespo. "Origin and diversification of major clades in parmelioid lichens (Parmeliaceae, Ascomycota) during the Paleogene inferred by Bayesian analysis." *PLOS ONE* 6, no. 12 (2011): e28161.

Armaleo, Daniele, and Philippe Clerc. "Lichen chimeras: DNA analysis suggests that one fungus forms two morphotypes." *Experimental Mycology* 15, no. 1 (1991): 1-10.

Badgley, Catherine, Tara M. Smiley, Rebecca Terry, Edward B. Davis, Larisa RG DeSantis, David L. Fox, Samantha SB Hopkins et al. "Biodiversity and topographic complexity:

Modern and geohistorical perspectives." *Trends in Ecology & Evolution* 32, no. 3 (2017): 211-226.

Benson, D. A., M. Cavanaugh, K. Clark, I. Karsch-Mizrachi, D. J. Lipman, J. Ostell, and E. W. Sayers. "*GenBank Nucleic Acids Res* 41 (D1)." *D36–D42* (2013).

Berger, Simon A., Alexandros Stamatakis, and Robert Lücking. "Morphology-based phylogenetic binning of the lichen genera *Graphis* and *Allographa* (Ascomycota: Graphidaceae) using molecular site weight calibration." *Taxon* 60, no. 5 (2011): 1450-1457.

Blanco, Oscar, Ana Crespo, John A. Elix, David L. Hawksworth, and H. Thorsten Lumbsch. "A molecular phylogeny and a new classification of parmelioid lichens containing *Xanthoparmelia*-type lichenan (Ascomycota: Lecanorales)." *Taxon* 53, no. 4 (2004): 959-975.

Bouckaert, Remco, Joseph Heled, Denise Kühnert, Tim Vaughan, Chieh-Hsi Wu, Dong Xie, Marc A. Suchard, Andrew Rambaut, and Alexei J. Drummond. "BEAST 2: A software platform for Bayesian evolutionary analysis." *PLoS Computational Biology* 10, no. 4 (2014): e1003537.

Brodo, Irwin M., Sylvia Duran Sharnoff, and Stephen Sharnoff. *Lichens of North America*. New Haven: Yale University Press. (2001).

Buschbom, Jutta. "Migration between continents: Geographical structure and long-distance gene flow in *Porpidia flavicunda* (lichen-forming Ascomycota)." *Molecular Ecology* 16, no. 9 (2007): 1835-1846.

Castresana, J. "Selection of conserved blocks from multiple alignments for their use in

phylogenetic analysis." *Molecular Biology and Evolution* 17, no. 4 (2000): 540-552.

Darriba, Diego, Guillermo L. Taboada, Ramón Doallo, and David Posada. "jModelTest 2: More models, new heuristics and parallel computing." *Nature Methods* 9, no. 8 (2012): 772.

Davis, Matthew P., Peter E. Midford, and Wayne Maddison. "Exploring power and parameter estimation of the BiSSE method for analyzing species diversification." *BMC Evolutionary Biology* 13, no. 1 (2013): 38.

Del-Prado, Ruth, Oscar Blanco, H. Thorsten Lumbsch, Pradeep K. Divakar, John A. Elix, M. Carmen Molina, and Ana Crespo. "Molecular phylogeny and historical biogeography of the lichen-forming fungal genus *Flavoparmelia* (Ascomycota: Parmeliaceae)." Taxon 62, no. 5 (2013): 928-939.

Del-Prado, Ruth, Pradeep Kumar Divakar, H. Thorsten Lumbsch, and Ana M. Crespo. "Hidden genetic diversity in an asexually reproducing lichen forming fungal group." *PLOS ONE* 11, no. 8 (2016): e0161031.

Divakar, Pradeep K., Ana Crespo, Mats Wedin, Steven D. Leavitt, David L. Hawksworth, Leena Myllys, Bruce McCune et al. "Evolution of complex symbiotic relationships in a morphologically derived family of lichen-forming fungi." *New Phytologist* 208, no. 4 (2015): 1217-1226.

Divakar, Pradeep K., Ruth Del-Prado, H. Thorsten Lumbsch, Mats Wedin, Theodore L. Esslinger, Steven D. Leavitt, and Ana Crespo. "Diversification of the newly recognized lichen-forming fungal lineage *Montanelia* (Parmeliaceae, Ascomycota) and its relation to key geological and climatic events." *American Journal of Botany* 99, no. 12 (2012): 2014-2026.

Drummond, Alexei J., Simon YW Ho, Matthew J. Phillips, and Andrew Rambaut. "Relaxed phylogenetics and dating with confidence." *PLoS Biology* 4, no. 5 (2006): e88.

Dughi, R. "Etude comparée du *Dendriscocaulon bolacinum* Nyl. et de la céphalodie fruticuleuse du *Ricasolia amplissima* (Scop.) Leight." *Bulletin de la Société Botanique de France* 83, no. 89 (1936): 671-693.

Dughi, R. "Sur Les Relations, La Position Systématique et l'extension Du Genre *Dendriscocaulon*." *Annales de La Faculté Des Sciences de Marseille* 2, no. 14 (1944): 147–57.

Fernández-Mendoza, F., S. Domaschke, M. A. García, P. Jordan, María P. Martín, and Christian Printzen. "Population structure of mycobionts and photobionts of the widespread lichen *Cetraria aculeata*." *Molecular Ecology* 20, no. 6 (2011): 1208-1232.

Finarelli, John A., and Catherine Badgley. "Diversity dynamics of Miocene mammals in relation to the history of tectonism and climate." *Proceedings of the Royal Society B: Biological Sciences* 277, no. 1694 (2010): 2721-2726.

FitzJohn, Richard G. "Diversitree: Comparative phylogenetic analyses of diversification in R." *Methods in Ecology and Evolution* 3, no. 6 (2012): 1084-1092.

Flower, Benjamin P., and James P. Kennett. "The middle Miocene climatic transition: East Antarctic ice sheet development, deep ocean circulation and global carbon cycling." *Palaeogeography, Palaeoclimatology, Palaeoecology* 108, no. 3-4 (1994): 537-555.

Galloway, D. J. "Studies on the lichen genus *Sticta* (Schreber) Ach. IV. New Zealand

Species." *The Lichenologist* 29, no. 2 (1997): 105-168.

Galloway, D. J. "Studies on the lichen genus *Sticta* (Schreber) Ach.: I. Southern South American species." *The Lichenologist* 26, no. 3 (1994): 223-282.

Galloway, D. J. *Flora of New Zealand Lichens. Revised second edition including lichen-forming and lichenicolous fungi. Volumes 1 and 2*. Lincoln, Manaaki Whenua Press. (2007): 261.

Galloway, D. J., and M. A. Thomas. "Sticta." In *Flora of Australia* 58 (2001): 78-97.

Galloway, D. J. "Studies on the lichen genus *Sticta* (Schreber) Ach.: V. Australiuan species." *Tropical Bryology* (1998): 117-160.

Galloway, D. J. "Notes on the holotype of *Sticta damaecornis* β *weigelii* Ach. (= *Sticta weigelii*)." *The Lichenologist* 38, no. 1 (2006): 89-92.

Galloway, D. J., Soili Stenroos, and Lidia I. Ferraro. *Lichenes Peltigerales: Lobariaceae y Stictaceae*. Vol. 13, no. 6. Buenos Aires: Consejo Nacional de Investigaciones Científicas y Técnicas. (1995).

Gaya, Ester, Samantha Fernández-Brime, Reinaldo Vargas, Robert F. Lachlan, Cécile Gueidan, Martín Ramírez-Mejía, and François Lutzoni. "The adaptive radiation of lichen-forming Teloschistaceae is associated with sunscreening pigments and a bark-to-rock substrate shift." *Proceedings of the National Academy of Sciences* 112, no. 37 (2015): 11600-11605.

Gillespie, Rosemary G., Bruce G. Baldwin, Jonathan M. Waters, Ceridwen I. Fraser, Raisa Nikula, and George K. Roderick. "Long-distance dispersal: A framework for hypothesis testing." *Trends in Ecology & Evolution* 27, no. 1 (2012): 47-56.

Hoorn, Carina, F. P. Wesselingh, H. Ter Steege, M. A. Bermudez, A. Mora, J. Sevink, Isabel

Sanmartín et al. "Amazonia through time: Andean uplift, climate change, landscape evolution, and biodiversity." *Science* 330, no. 6006 (2010): 927-931.

James, P. W., and Aino Henssen. "Morphological and taxonomic significance of cephalodia." In *Lichenology: Progress and Problems; Proceedings of an International Symposium*. Cambridge: Academic Press. (1976).

Janson, Eric M., John O. Stireman III, Michael S. Singer, and Patrick Abbot. "Phytophagous insect–microbe mutualisms and adaptive evolutionary diversification." *Evolution* 62, no. 5 (2008): 997-1012.

Katoh, Kazutaka, and Daron M. Standley. "MAFFT multiple sequence alignment software version 7: Improvements in performance and usability." *Molecular Biology and Evolution* 30, no. 4 (2013): 772-780.

Kearse, Matthew, Richard Moir, Amy Wilson, Steven Stones-Havas, Matthew Cheung, Shane Sturrock, Simon Buxton et al. "Geneious Basic: An integrated and extendable desktop software platform for the organization and analysis of sequence data." *Bioinformatics* 28, no. 12 (2012): 1647-1649.

Kirk, P. M., P. F. Cannon, D. W. Minter, and J. A. Stalpers. *Dictionary of the Fungi*. Wallingford: CAB International. (2008).

Lagomarsino, Laura P., Fabien L. Condamine, Alexandre Antonelli, Andreas Mulch, and Charles C. Davis. "The abiotic and biotic drivers of rapid diversification in Andean bellflowers (Campanulaceae)." *New Phytologist* 210, no. 4 (2016): 1430-1442.

Leavitt, Steven D., and H. Thorsten Lumbsch. "Ecological biogeography of lichen-forming

fungi." In *Environmental and microbial relationships*. Cham: Springer. (2016): 15-37.

Leavitt, Steven D., Pradeep K. Divakar, Yoshihito Ohmura, Li-song Wang, Theodore L. Esslinger, and H. Thorsten Lumbsch. "Who's getting around? Assessing species diversity and phylogeography in the widely distributed lichen-forming fungal genus *Montanelia* (Parmeliaceae, Ascomycota)." *Molecular Phylogenetics and Evolution* 90 (2015): 85-96.

Leavitt, Steven D., Theodore L. Esslinger, Pradeep K. Divakar, and H. Thorsten Lumbsch. "Miocene and Pliocene dominated diversification of the lichen-forming fungal genus *Melanohalea* (Parmeliaceae, Ascomycota) and Pleistocene population expansions." *BMC Evolutionary Biology* 12, no. 1 (2012a): 176.

Leavitt, Steven D., Theodore L. Esslinger, and H. Thorsten Lumbsch. "Neogene-dominated diversification in neotropical montane lichens: Dating divergence events in the lichen-forming fungal genus *Oropogon* (Parmeliaceae)." *American Journal of Botany* 99, no. 11 (2012b): 1764-1777.

Leavitt, Steven D., Fernando Fernández-Mendoza, Sergio Pérez-Ortega, Mohammad Sohrabi, Pradeep K. Divakar, Jan Vondrák, H. Thorsten Lumbsch, and Larry L. St Clair. "Local representation of global diversity in a cosmopolitan lichen-forming fungal species complex (*Rhizoplaca*, Ascomycota)." *Journal of Biogeography* 40, no. 9 (2013a): 1792-1806.

Leavitt, Steven D., H. Thorsten Lumbsch, Soili Stenroos, and Larry L. St Clair. "Pleistocene speciation in North American lichenized fungi and the impact of alternative species circumscriptions and rates of molecular evolution on divergence estimates." *PLOS ONE* 8, no. 12 (2013b): e85240.

Lücking, Robert, Bibiana Moncada, and Clifford W. Smith. "The genus *Lobariella* (Ascomycota: Lobariaceae) in Hawaii: Late colonization, high inferred endemism and three new species resulting from “micro-radiation”." *The Lichenologist* 49, no. 6 (2017): 673-691.

Lumbsch, H. T. "Lichen-forming fungi, Diversification of." In Encyclopedia of Evolutionary Biology, edited by Richard M. Kliman. Cambridge: Academic Press. (2016): 305-311.

Maddison, Wayne P., Peter E. Midford, and Sarah P. Otto. "Estimating a binary character's effect on speciation and extinction." *Systematic Biology* 56, no. 5 (2007): 701-710.

Madriñán, Santiago, Andrés J. Cortés, and James E. Richardson. "Páramo is the world's fastest evolving and coolest biodiversity hotspot." *Frontiers in Genetics* 4 (2013): 192.

Magain, Nicolas, J. Miadlikowska, Bernard Goffinet, Emmanuël Sérusiaux, and François Lutzoni. "Macroevolution of specificity in cyanolichens of the genus *Peltigera* section *polydactylon* (Lecanoromycetes, Ascomycota)." *Systematic Biology* 66, no. 1 (2016): 74-99.

Magain, Nicolas, and Emmanuël Sérusiaux. "Dismantling the treasured flagship lichen *Sticta fuliginosa* (Peltigerales) into four species in Western Europe." *Mycological Progress* 14, no. 10 (2015): 97.

Mangold, Armin, María P. Martín, Robert Lücking, and H. Thorsten Lumbsch. "Molecular phylogeny suggests synonymy of Thelotremataceae within Graphidaceae (Ascomycota: Ostropales)." *Taxon* 57, no. 2 (2008): 476-486.

McDonald, Tami, Jolanta Miadlikowska, and François Lutzoni. "The lichen genus *Sticta* in the Great Smoky Mountains: A phylogenetic study of morphological, chemical, and molecular data." *The Bryologist* 106, no. 1 (2003): 61-80.

Molina, M. Carmen, Pradeep K. Divakar, Trevor Goward, Ana M. Millanes, H. Thorsten Lumbsch, and Ana Crespo. "Neogene diversification in the temperate lichen-forming fungal genus *Parmelia* (Parmeliaceae, Ascomycota)." *Systematics and biodiversity* 15, no. 2 (2017): 166-181.

Moncada, Bibiana, Luis Fernando Coca, and Robert Lücking. "Neotropical members of *Sticta* (lichenized Ascomycota: Lobariaceae) forming photosymbiodemes, with the description of seven new species." *The Bryologist* 116, no. 2 (2013): 169-201.

Moncada, Bibiana, and Robert Lücking. "Ten new species of *Sticta* and counting: Colombia as a hot spot for unrecognized diversification in a conspicuous macrolichen genus." *Phytotaxa* 74 (2012): 1-29.

Moncada, Bibiana, Robert Lücking, and Luisa Betancourt-Macuase. "Phylogeny of the Lobariaceae (lichenized Ascomycota: Peltigerales), with a reappraisal of the genus *Lobariella*." *The Lichenologist* 45, no. 2 (2013): 203-263.

Moncada, Bibiana, Robert Lücking, and Luis Fernando Coca. "Six new apotheciate species of *Sticta* (lichenized Ascomycota: Lobariaceae) from the Colombian Andes." *The Lichenologist* 45, no. 5 (2013): 635-656.

Moncada, Bibiana, Robert Lücking, and Alejandra Suárez. "Molecular phylogeny of the genus *Sticta* (lichenized Ascomycota: Lobariaceae) in Colombia." *Fungal Diversity* 64, no. 1 (2014): 205-231.

Moncada, Bibiana, Brendon Reidy, and Robert Lücking. "A phylogenetic revision of Hawaiian *Pseudocyphellaria sensu lato* (lichenized Ascomycota: Lobariaceae) reveals eight new species and a high degree of inferred endemism." *The Bryologist* 117, no. 2 (2014): 119-

161.

Moran, Nancy A. "Symbiosis as an adaptive process and source of phenotypic complexity." *Proceedings of the National Academy of Sciences* 104, no. suppl 1 (2007): 8627-8633.

Moreau, F. "Sur la théorie biomorphogénique des lichens." *Revue Bryologique et Lichénologique* 25 (1956): 183-186.

Morlon, Hélène. "Phylogenetic approaches for studying diversification." *Ecology Letters* 17, no. 4 (2014): 508-525.

Nash, Thomas H., B. D. Ryan, Paul Diederich, C Gries, and Frank Bungartz. *Lichen Flora of the Greater Sonoran Desert Region II*. Tempe: Lichens Unlimited. (2004).

Nelsen, Matthew P., and Andrea Gargas. "Symbiont flexibility in *Thamnolia vermicularis* (Pertusariales: Icmadophilaceae)." *The Bryologist* 112, no. 2 (2009): 404-418.

Ng, J., and Stacey D. Smith. "How traits shape trees: New approaches for detecting character state-dependent lineage diversification." *Journal of Evolutionary Biology* 27, no. 10 (2014): 2035-2045.

Nürk, Nicolai M., Simon Uribe-Convers, Berit Gehrke, David C. Tank, and Frank R. Blattner. "Oligocene niche shift, Miocene diversification – cold tolerance and accelerated speciation rates in the St. John's Worts (*Hypericum*, Hypericaceae)." *BMC Evolutionary Biology* 15, no. 1 (2015): 80.

Otálora, Mónica AG, Isabel Martínez, Gregorio Aragón, and M. Carmen Molina. "Phylogeography and divergence date estimates of a lichen species complex with a disjunct distribution pattern." *American Journal of Botany* 97, no. 2 (2010): 216-223.

Paradis, Emmanuel, Julien Claude, and Korbinian Strimmer. "APE: Analyses of phylogenetics and evolution in R language." *Bioinformatics* 20, no. 2 (2004): 289-290.

Parnmen, Sittiporn, Robert Lücking, and H. Thorsten Lumbsch. "Phylogenetic classification at generic level in the absence of distinct phylogenetic patterns of phenotypical variation: A case study in Graphidaceae (Ascomycota)." *PLOS ONE* 7, no. 12 (2012): e51392.

Prieto, María, and Mats Wedin. "Dating the diversification of the major lineages of Ascomycota (Fungi)." *PLOS ONE* 8, no. 6 (2013): e65576.

Rabosky, Daniel L. "Automatic detection of key innovations, rate shifts, and diversity-dependence on phylogenetic trees." *PLOS ONE* 9, no. 2 (2014): e89543.

Rabosky, Daniel L., and Emma E. Goldberg. "Model inadequacy and mistaken inferences of trait-dependent speciation." *Systematic Biology* 64, no. 2 (2015): 340-355.

Rabosky, Daniel L., Michael Grundler, Carlos Anderson, Pascal Title, Jeff J. Shi, Joseph W. Brown, Huateng Huang, and Joanna G. Larson. "BAMM tools: An R package for the analysis of evolutionary dynamics on phylogenetic trees." *Methods in Ecology and Evolution* 5, no. 7 (2014): 701-707.

Rambaut, A., and A. J. Drummond. "TreeAnnotator v2. 0.4." (2013).

Rambaut, A., M. A. Suchard, D. Xie, and A. J. Drummond. "Tracer v1. 6. 2014." (2015).

Ranft, Hannah, Bibiana Moncada, Peter J. de Lange, H. Thorsten Lumbsch, and Robert Lücking. "The *Sticta filix* morphodeme (Ascomycota: Lobariaceae) in New Zealand with the newly recognized species *S. dendroides* and *S. menziesii*: Indicators of forest health in a threatened island biota?." *The Lichenologist* 50, no. 2 (2018): 185-210.

Ree, R. H., and S. A. Smith. "Lagrange: Software for likelihood analysis of geographic range evolution." *Systematic Biology* 57 (2008): 4-14.

Rutschmann, Frank. "Molecular dating of phylogenetic trees: A brief review of current methods that estimate divergence times." *Diversity and Distributions* 12, no. 1 (2006): 35-48.

Sérusiaux, Emmanuël, Tim Wheeler, and Bernard Goffinet. "Recent origin, active speciation and dispersal for the lichen genus *Nephroma* (Peltigerales) in Macaronesia." *Journal of Biogeography* 38, no. 6 (2011): 1138-1151.

Shaw, A. Jonathan, Nicolas Devos, Cymon J. Cox, Sandra B. Boles, Blanka Shaw, Alex M. Buchanan, Lynette Cave, and Rodney Seppelt. "Peatmoss (*Sphagnum*) diversification associated with Miocene Northern Hemisphere climatic cooling?." *Molecular Phylogenetics and Evolution* 55, no. 3 (2010): 1139-1145.

Simon, Antoine, Bernard Goffinet, Nicolas Magain, and Emmanuël Sérusiaux. "High diversity, high insular endemism and recent origin in the lichen genus *Sticta* (lichenized Ascomycota, Peltigerales) in Madagascar and the Mascarenes." *Molecular Phylogenetics and Evolution* 122 (2018): 15-28.

Smith, C W, A Aptroot, B J Coppins, A Flechter, O L Gilbert, P W James, and P A Wolseley. *The Lichens of Great Britain and Ireland*. London: British Lichen Society. (2009).

Stamatakis, Alexandros. "RAxML version 8: A tool for phylogenetic analysis and post-analysis of large phylogenies." *Bioinformatics* 30, no. 9 (2014): 1312-1313.

Stanley Jr, George D. "Early history of scleractinian corals and its geological consequences." *Geology* 9, no. 11 (1981): 507-511.

Suarez, Alejandra, and Robert Lücking. "*Sticta viviana* (lichenized Ascomycota: Peltigerales: Lobariaceae), a new species from Colombian paramos." *The Lichenologist* 45, no. 2 (2013): 153-157.

Takamatsu, Susumu, and Sanae Matsuda. "Estimation of molecular clocks for ITS and 28S rDNA in Erysiphales." *Mycoscience* 45, no. 5 (2004): 340-344.

Vamosi, Jana C., and Steven M. Vamosi. "Factors influencing diversification in angiosperms: At the crossroads of intrinsic and extrinsic traits." *American Journal of Botany* 98, no. 3 (2011): 460-471.

van der Niet, Timotheüs, and Steven D. Johnson. "Phylogenetic evidence for pollinator-driven diversification of angiosperms." *Trends in Ecology & Evolution* 27, no. 6 (2012): 353-361.

Vilgalys, Rytas, and Mark Hester. "Rapid genetic identification and mapping of enzymatically amplified ribosomal DNA from several *Cryptococcus* species." *Journal of Bacteriology* 172, no. 8 (1990): 4238-4246.

Werth, Silke, and Victoria L. Sork. "Ecological specialization in Trebouxia (Trebouxiophyceae) photobionts of *Ramalina menziesii* (Ramalinaceae) across six range-covering ecoregions of western North America." *American Journal of Botany* 101, no. 7 (2014): 1127-1140.

Zoller, Stefan, Christoph Scheidegger, and Christoph Sperisen. "PCR primers for the amplification of mitochondrial small subunit ribosomal DNA of lichen-forming ascomycetes." *The Lichenologist* 31, no. 5 (1999): 511-516.

## 4. Using RADseq to understand the circum-Antarctic distribution of the lichenized fungus *Pseudocyphellaria glabra* (Ascomycota, Peltigeraceae)

Todd J Widhelm, Felix Grewe, Jen-Pan Huang, Karolis Ramanauskas, Roberta Mason-Gamer, H. Thorsten Lumbsch

### 4.1 Introduction

Disjunct distributions across vast physical barriers have intrigued scientists because there are clear geographic constrains which physically divide a species into multiple populations. Furthermore, these populations do not always comprise a single randomly mating unit, but are subdivided into smaller entities which can be arranged spatially, temporally, or ecologically (Excoffier 2004). Therefore, a major goal of population genomics is to estimate patterns of genetic structure in natural populations to infer the underlying ecological and evolutionary processes such as migration, extinction, and speciation, that contribute to the observed genetic diversity. Advances in population genomics have generated new ways to approach this study question (Davey and Blaxter 2010). Population genetic structure is characterized by the number of subpopulations within a population, the frequencies of genetic variants in each subpopulation, and the degree of genetic isolation of the subpopulations (Chakraborty 1993). Understanding the genetic structure of a species' populations can uncover whether some have been isolated for long periods of time and the spatial scale at which populations are differentiated (Werth 2010). A better understanding of population genetic structure can also have important implications for the conservation of threatened species and the spread of invasive species.

Many species of lichenized fungi have large distributional ranges and some can be distributed across multiple continents being isolated by large bodies of water. The floras of major landmasses in the Southern Hemisphere, such as New Zealand, Southern South America, and

Eastern Australia share many taxonomic groups. This pattern is seen in flowering plants (Winkworth et al. 2002, 2015), ferns (Parris 2001), bryophytes (Miller 1982), and lichens (Galloway 1991). Almost 100 species of lichens are shared between Australia and New Zealand and over 40 species are shared among Australia, New Zealand and southern South America (Galloway 1991; Nash 2008). These Southern Hemisphere disjunct distributions could be the result of two possible processes, vicariance (the breakup of Gondwanaland that separated and isolated ancestral biotas) or long-distance, transoceanic dispersal.

The breakup of Gondwanaland occurred between 155-80 Mya (Stevens 1980) and predates the ages of most species-level lineages, but at the genus and family level, vicariance could explain the many shared groups among southern landmasses (Galloway 1988; Moncalvo and Buchanan 2008). Molecular data suggest that many southern hemisphere plant distributions have arisen only within the last 10 million years (Winkworth et al. 2002). Studies have shown the importance of dispersal for species that have intercontinental distributions (Sanmartín and Ronquist 2004; McGlone 2005; Moreira-Muñoz 2007). The West Wind Drift is a meteorological phenomenon causing cyclonic weather systems to move eastward in a clockwise motion around Antarctica. This pattern was initiated during the Miocene when Australia and South America separated from Antarctica and the eastward flow intensified during the Tertiary and was probably the strongest during the Pleistocene glacial periods (2 mya – 14,000 ya) and to this day it is a dominant weather pattern (Winkworth et al. 2002). These winds are four times as strong as their counterparts in the Northern Hemisphere and play an important role in dispersal (Raven 1973). The floristic similarities of southern landmasses have been shown to be direction-dependent and driven by this wind pattern (Muñoz et al. 2004). Given these strong wind patterns, many scientists assume that dispersal explains the current distribution patterns of species more than the

vicariance hypothesis.

Lichens are symbiotic organisms consisting of a fungus and a photosynthetic green algae or cyanobacteria or both simultaneously. In austral lichen taxa, Galloway (2008) describes two types of mycobiotas, namely the paleoaustral lichens, primitive Gondwanan groups that have poor dispersal abilities, and neoaustral lichens that dispersed after the breakup of Gondwanaland, producing large quantities of vegetative propagules that allow for long-distance dispersal via birds, ocean currents, or the West Wind Drift. *Pseudocyphellaria glabra* has a disjunct range (Figure 9), occurring in Southeastern Australia, New Zealand, Chile, Argentina, and subantarctic islands and is considered a neoaustral lichen species (Galloway 2008). In New Zealand, *P. glabra* has the widest range and ecological tolerance of all *Pseudocyphellaria* species (Galloway 2007). It can be found in all forest types, but is most abundant in the wettest of temperate rain forests. It is a large foliose species that is mostly epiphytic, but is also found on moss covered rocks (Figure 10). The species has been hypothesized to be neoaustral and have dispersed after fragmentation of Gondwanaland between the Oligocene and the present (Galloway 1991). The species reproduces sexually with microscopic ascospores and vegetatively with phyllidia which can be present in copious quantities. Both reproductive strategies could be the mode of dispersal via West Wind Drift, birds, and ocean currents.

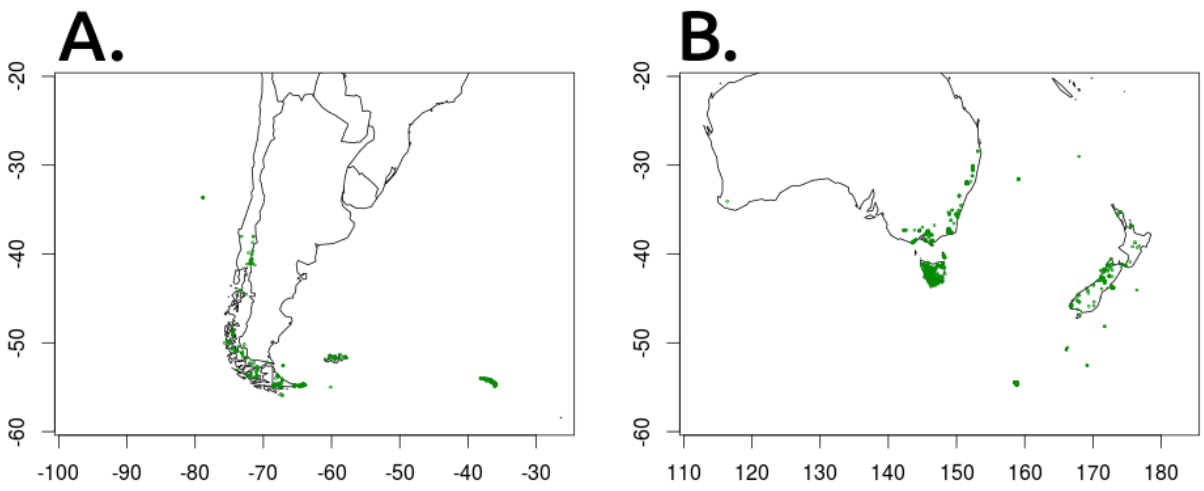


Figure 9. Global distribution of *P. glabra* in (A) southern South America and (B) Australia and New Zealand from GBIF collection records. Degrees longitude are displayed on the X-axes and latitude on the Y-axes.

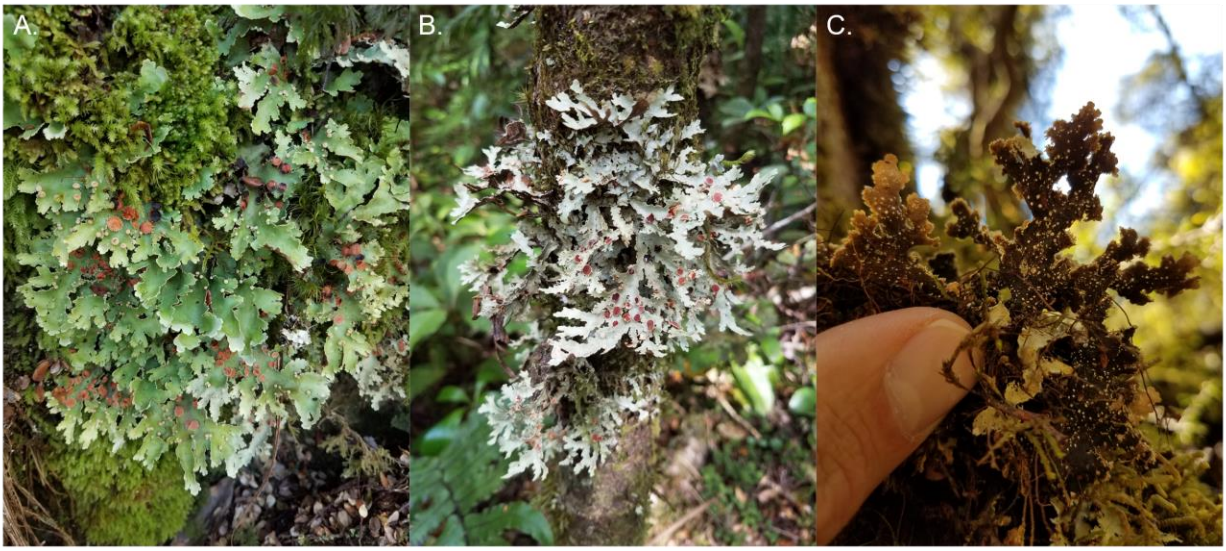


Figure 10. Natural habit of *P. glabra* (A) when hydrated, (B), in dry conditions, and (C) the lower cortex.

The disjunct distribution of *P. glabra* (Figure 9) makes it an excellent study system for understanding the pattern of genetic differentiation among populations sampled from different landmasses, and how major physical barriers (Pacific Ocean, Tasman Sea, Bass Strait, and Cook Strait) limit genetic exchange among populations. We specifically set out to test two hypotheses: (1) if large bodies of water isolate populations of *P. glabra*, then these populations will be genetically distinct, and (2) given the strong wind patterns in southern hemisphere, *P. glabra* populations on different landmasses will be connected by frequent and ongoing long-distance dispersal (i.e. gene-flow). To address this issue, we collected 286 samples from southeast Australia, North and South Islands of New Zealand, and Chile. We used restriction site-associated DNA sequencing data (RADseq) for phylogeographic and population genetic analyses in order to understand how the genetic variation of *P. glabra* is distributed across Australia, New Zealand, and Chile and to understand if large bodies of water correspond to major breaks in gene flow.

## 4.2 Materials and methods

### 4.2.1 Sampling

Fresh population samples of *P. glabra* were collected in the Australian states of Tasmania and Victoria (TAS and VIC), throughout the North and South Islands of New Zealand (NZN and NZS), and in Chile (CHI) during three field trips from 2015 to 2017 (See Figure 3B for collection locality maps). Additional samples were obtained from historical museum collections including one sample from Campbell Island (CAM) south of New Zealand. The sister species *P. homoeophylla* was also collected in New Zealand. A total of 286 specimens were sampled. At each site, if possible, at least 20 individual thalli were collected on separate trees. All specimens were vouchered in FMNH. (TABLE XXI, Appendix C).

### 4.2.2 DNA isolation and quality assessment

Genomic DNA was extracted from a roughly one cm2 portion of vegetative tissue. The tissues were disrupted using liquid nitrogen and a mortar and pestle and then the DNAs were isolated using ZR Fungal/Bacterial DNA MiniPrepTM kit (Zymo Research, Irvine, CA, USA) following manufacturer's directions except that macerated tissues were incubated at 65℃ for one hour in lysis buffer before proceeding to the isolation steps. The concentration of isolated DNA was determined using the AccuBlue (Biotium, Inc., Fremont, CA, USA) kit and the Tecan plate reader (Tecan Group Ltd., Männedorf, Switzerland). The quality of isolated DNA was assessed by gel electrophoresis.

### 4.2.3 Metagenomic DNA sequencing and mycobiont reference genome assembly

Metagenomic DNA from sample VIC 2287A (DNA# 14816) was sequenced at the University of Illinois at Chicago Sequencing Core on an Illumina (Illumina Inc, San Diego, CA, USA) NextSeq500 platform. Trimmomatic (Bolger, Lohse, and Usadel 2014) was used to remove poor quality reads and adapter sequences. Bases were trimmed when the average quality of 4-base sliding windows was below 15 and bases at the start and end of reads had a quality below 10. All trimmed reads shorter than 25 bp were filtered out (LEADING:10 TRAILING:10 SLIDING-WINDOW:4:15 MINLEN:25). After quality filtering, a total of 14 gigabases (Gb) of trimmed paired-end reads resulted. The trimmed reads were assembled using SPAdes 3.5.0 (Bankevich et al. 2012) with default parameter settings. The assembled metagenome was used as an input for MetaWatt Binner version 3.5.3 (Strous et al. 2012) which was used to cluster contigs that originated from the mycobiont population of DNA data. The MetaWatt binning procedure uses multivariate statistics of tetranucleotide frequencies combined with the use of interpolated Markov models. Because MetaWatt was originally designed only for prokaryotic organisms, we

produced a custom database of 10 axenically cultured lichen-forming fungal genomes available on NCBI to identify contigs of Lecanoromycetes origin. To create the custome database, we performed gene prediction using AUGUSTUS version 2.5.5 (Stanke and Morgenstern 2005) on all 10 genomes. Amino acid sequences of the generated gene models were used by MetaWatt for the identification of bins. Only reads identified as Lecanoromycetes were selected from the metagenomic contigs resulting in 1,149 contigs ranging from 9,960 bp to 84,423 bp in length. Finally, we created a Bowtie2 (Langmead and Salzberg 2012) database from the selected scaffolds for the mapping approach to filter for mycobiont RAD loci.

#### 4.2.4 RADseq library prep and Illumina sequencing

Restriction site associated DNA libraries were prepared and sequenced from whole DNA isolations at the University of Wisconsin-Madison Biotechnology Center. DNA concentration was verified using the Quant-iT™ PicoGreen® dsDNA kit (Life Technologies, Grand Island, NY). Libraries were prepared as in Elshire et al (2011) with minimal modification; in short, 50 ng of DNA was digested using the 5-bp cutter ApeKI (New England Biolabs, Ipswich, MA) after which barcoded adapters amenable to Illumina sequencing were added by ligation with T4 ligase (New England Biolabs, Ipswich, MA). 192 adapter-ligated samples were pooled and amplified to provide library quantities amenable for sequencing, and adapter dimers were removed by SPRI bead purification. Quality and quantity of the finished libraries were assessed using the Agilent Bioanalyzer High Sensitivity Chip (Agilent Technologies, Inc., Santa Clara, CA) and Qubit® dsDNA HS Assay Kit (Life Technologies, Grand Island, NY), respectively. Libraries were standardized to 2nM. Cluster generation was performed using HiSeq SR Cluster Kit v3 cBot kits (Illumina Inc, San Diego, CA, USA). Flowcells were sequenced using single read, 100bp sequencing and HiSeq SBS Kit v4 (50 Cycle) (Illumina Inc.) on a HiSeq2500 sequencer. Images

were analyzed using the standard Illumina Pipeline, version 1.8.2.

### 4.2.5 RADseq data assembly

The raw reads of *P. glabra* and *P. homoeophylla* from the HiSeq2500 sequencing were processed and assembled as described earlier for metagenomic datasets of lichens (Grewe et al. 2017). This process used ipyRAD (Eaton and Overcast 2016) to demultiplex raw reads and pyRAD (Eaton and Ree 2013) for the remaining steps. An additional mapping step is conducted after the generation of consensus sequences (pyRAD step 5) that used Bowtie2 to filter for mycobiont loci with a reference sequence. Raw Illumina RAD sequences are referred to as 'read' and the clustered reads per individual sample as 'loci'; the final matrices are alignments of homologous loci from multiple samples with nucleotide substitutions referred to as 'SNP'. In pyRAD, we set the datatype to genotype-by-sequencing (gbs), ploidy to haploid (1), a similarity threshold for the clustering of reads within and between individuals to 90% (.90) and a minimum coverage of four samples per locus (4). For the reference-based filtering of RAD loci, we used Bowtie2 with adjusted parameters to allow one permitted mismatch (−N 1), a seed length of 20 (−L 20), up to 20 seed extension attempts (−D 20) and a maximum "re-seeding" of 3 (−R 3). Following an initial round with all sequenced samples, we re-ran step 7 of pyRAD and excluded 70 samples with less than 1000 recovered loci (1000min_full dataset). A reduced dataset was generated for population genetic analyses without the 13 P. homoephylla samples with minimum of four samples per locus (1000min_no_PHO). We used the filtered pyRAD output files from these datasets, such as unlinked_snps, alleles and vcf, for further phylogenetic and population genomic analyses as described earlier for lichen RADseq datasets (Grewe et al. 2018).

### 4.2.6 Phylogenetic analysis

A maximum likelihood (ML) phylogenetic analysis was conducted in RAxML version

8.1.16 (Stamatakis 2014) using the concatenated unlinked SNPs files for the 1000min_full dataset generated by pyRAD which contained all *P. glabra* and *P. homoeophylla* samples with at least 1000 loci (216 samples total). We used the GTRGAMMA model approximation for the ML tree search with 100 bootstrap replicates using the rapid bootstrapping algorithm. The resulting phylogenetic tree was rooted with the *P. homoeophylla* clade and drawn to scale with the online interface of Interactive Tree Of Life (https://itol.embl.de/).

### 4.2.7 Identification of panmictic clusters

The differences in the population structure of *P. glabra* samples between different landmass populations (1000min_no_PHO; TAS, VIC, NZN, NZS, and CHI; 202 samples total) was calculated by creating a reduced dataset that included all sites with a minor allele frequency larger than 0.05 and greater than 50% coverage using vcftools version 0.1.15 (Danecek et al. 2011). We converted the reduced file to a genind object using the adegenet version 2.0.2 R package. The genind object was further modified to account for haploid genomes and the population membership for samples based on landmass were assigned. This modified genind object was used for population genetic analyses in R.

We estimated Gst (Nei 1973), G'st (Hedrick 2005) and Jost's D (Jost 2008) using the R package mmod version 1.3.3 (Winter 2012) to ascertain the degree of population subdivision among landmass populations. Gst measures gene diversity within and between subpopulations and is useful when mutation rate is low compared to the migration rate. G'st and Jost's D, on the other hand, are important when mutation rate is higher than or equal to migration rate (Whitlock 2011). All measures were used to quantify genomic differentiation. The average per site indices were calculated pairwise among landmass populations and inferred genetic clusters.

We used the Discriminant Analysis of Principal Components (DAPC) to estimate the

genetic structure of 202 *P. glabra* samples (1000min_no_PHO genind datasets) from different landmasses. The DAPC was implemented in the adegenet version 2.1.1 R package (Jombart, Devillard, and Balloux 2010). Initially, data were transformed using a principal components analysis (PCA) and then components of PCA were submitted to a discriminant analysis (DA). We used the function a.score in the adegenet R package using the smart procedure as a criterion for choosing the optimal number of PCs in the PCA step of DAPC. The smart procedure selects an evenly distributed number of PCs in a pre-defined range and computes the a-score for each. Next, the a-score results are interpolated using splines to predict an approximate optimal number of PCs. For the DAPC we used the first six PCs and all four DA-eigenvalues. The results of the analyses were visualized in two ways; one showing genetic variation in genomic space and the other in a STRUCTURE-like plot that shows the predicted group membership.

### 4.2.8 Estimation of shared ancestry

With the 1000min_no_PHO dataset (202 samples, not including *P. homoeophylla*) we inferred population structure based on nearest neighbor haplotype co-ancestry using the programs RADpainter and fineRADstructure (Malinsky et al. 2018). The fineRADstructure package uses the program RADpainter (Malinsky et al. 2018) to infer a co-ancestry matrix from RADseq data and the Markov chain Monte Carlo (MCMC) clustering algorithm fineSTRUCTURE (Lawson et al. 2012). The alleles output file from pyRAD was converted with the python script finerad_input.py (https://github.com/edgardomortiz/fineRADstructure-tools; last accessed December 3, 2018) with a minimum number of 101 samples (50%) in a locus. The output of the analyses was visualized with the R script fineRADstructurePlot.R provided by the fineRADstructure package.

## 4.3 Results

### 4.3.1 Reference genome assembly and RADseq results

We assembled a draft reference genome of *P. glabra* to filter for mycobiont RAD loci. The Illumina NextSeq sequencing of the whole *P. glabra* (2287A VIC) thallus resulted in 42,803,904 metagenomic paired-end reads. First, we trimmed these raw data which reduced the paired-end reads to 40,247,418 (94% of raw data). The trimmed read pairs were then assembled into 1,038,157 scaffolds (N50 = 189,136 bp; L50 count of 513 Kb) with a total size of 494 Mbp (including 1,866 scaffolds of sizes larger than 10 Kb). Further metagenomic binning identified 30.65 Mbp of the assembly as mycobiont derived from which we selected 1,142 scaffolds (N50 = 401 bp; L50 count of 17.123 KB) with sizes larger than 10 kb. The sorted draft genome of *P. glabra* had a total size of 19.36 Mbp.

We included 286 specimens of *P. glabra* from 3 RADseq libraries. The sequence read number of each sample varied from 6,901 for sample 15528_CHI to 3,286,909 for sample 15953_NZN with an average sequence read number of 994,295.95 (sd = 535,452.64). The number of loci (within sample clusters) that pyRAD generated from these sequences directly correlated with the initial number of sequences (R2 = 0.75, TABLE XXII, Appendix C). An average of 16.92% (sd = 7.51%) of all loci mapped to the mycobiont reference genome and, of these, an average of 96.58% (sd = 2.88%) were included into the final pyRAD dataset. The numbers of loci before and after the mapping were directly correlated (R2 = 0.83, TABLE XXII, Appendix C). In addition, the number of mapped loci were strongly correlated to the number of loci included in the final dataset (R2 = 0.99, Table XXII, Appendix C). Seventy samples of *P. glabra* had less than 1,000 loci in the final dataset and were removed from the analysis. All remaining 216 samples in the final dataset had on average of 5073.16 (sd = 3263.88) loci

(TABLE XXII, Appendix C).

### 4.3.2 Phylogenetic analysis

The ML tree (Figure 11A) was estimated from the 1000min_full RADseq matrix with 21,937 distinct alignment patterns and 79.48% missing data. The phylogenetic analyses recovered a well-supported clade containing all *P. glabra* samples sister to the *P. homoeophylla* clade. Four samples of *P. glabra* from Victoria are early divergent and form a well-supported clade. The remaining samples from all landmasses are recovered in two well-supported (100% bootstrap support) clades (Clades A and B) that also contained other well-supported subclades. Clade A contains *P. glabra* individuals from both Islands of New Zealand and Chile (NZN, NZS, and CHI). Samples from Chile in Clade 2 form their own well-supported (100% bootstrap support) clade that is sister to the New Zealand clade (75% bootstrap support). Clade B contains *P. glabra* individuals from every major landmass (TAS, VIC, NZN, NZS, CAM, and CHI). Australian samples in Clade B (TAS and VIC) form a well-supported subclade (100% bootstrap support). Similarly, Chilean samples (CHI) in Clade B also form a well-supported (91% bootstrap support) monophyletic clade. The New Zealand (NZN and NZS) samples in Clade 1 are polyphyletic, forming three lineages with no well-supported geographic clusters corresponding to the North or South Islands. The one individual from Campbell Island is in a well-supported (88% bootstrap support) clade with one individual from the South Island of New Zealand.

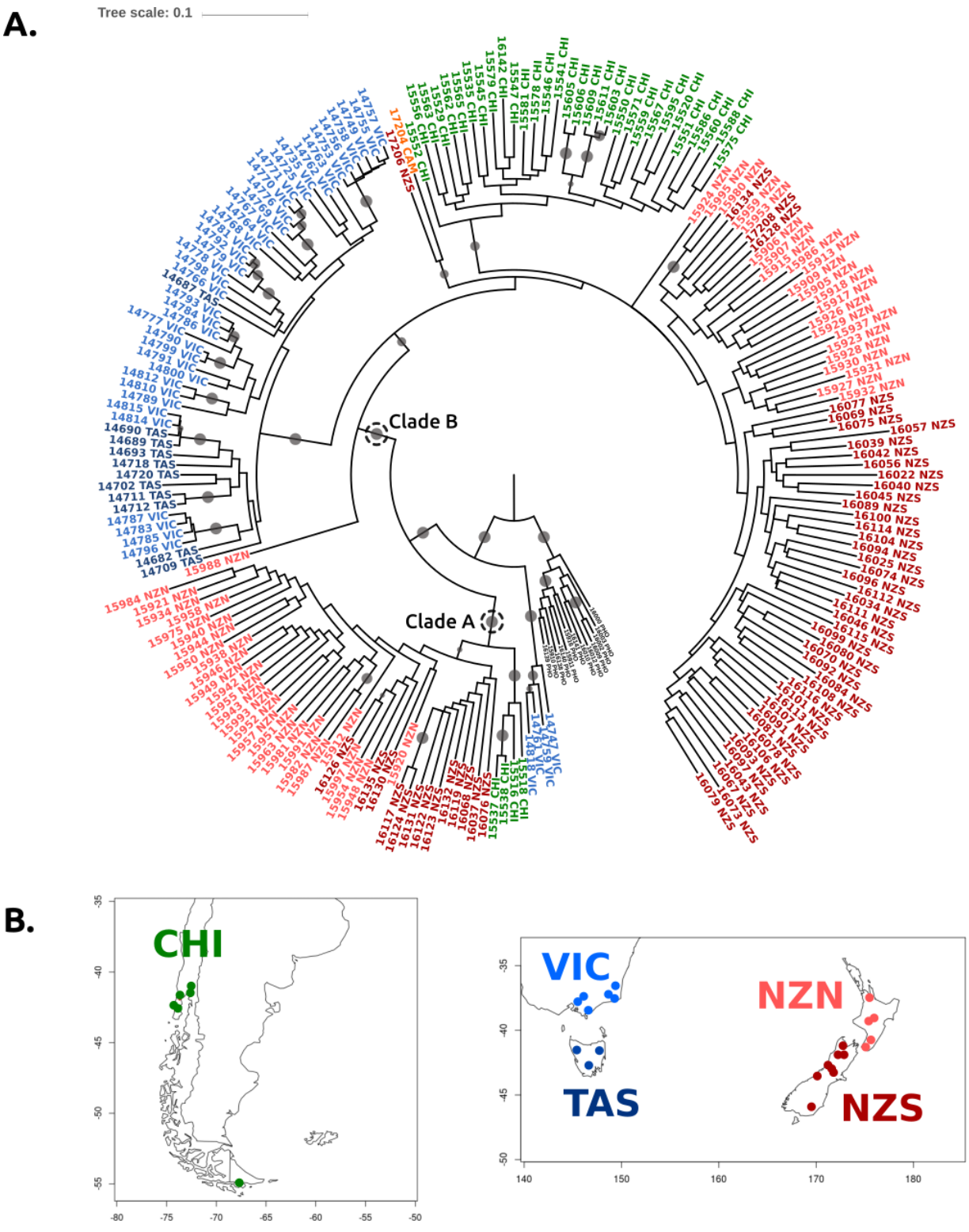


Figure 11. Phylogenetic tree (A) inferred from from *P. glabra*, and *P. homoeophylla* RADseq data. The population collection sites from all major land masses are shown on the maps (B) and

represented by colors on the tips (TAS=dark blue, VIC=light blue, CHI=green, NZN=dark red, NZS=light red, CAM=orange, PHO & PFR=black). Bootstrap values between 70-100% are indicated at the nodes by the size of the grey circles. The unit of branch length is substitutions per site.

### 4.3.3 Population subdivision analyses

We determined the degree to which populations from different landmasses (TAS, VIC, NZN, NZS, and CHI) are subdivided by Gst, G'st and D measurements. For these analyses, we included only SNPs with a MAF greater than 0.05 and more than 50% coverage. This reduced the RADseq dataset to a total of 2,255 SNPs. The average pairwise values of Gst, G'st and D measures for each population are reported in Table XIII. Average values for Gst, G'st and D that approach 1 indicate that genomes from different populations are completely isolated, but the highest values recovered were slightly above 0.5 for Hendricks G'st for TAS and CHI. Hendrick's G'st reported higher values among populations in general, while Nei's Gst and Jost's D were lower in comparison. All measure indicated that no population was completely isolated from any other population.

TABLE XIII. MEAN PAIRWISE MEASURES OF POPULATION SUBDIVISION FOR THE FIVE MAJOR POPULATIONS OF *P. GLABRA*.

| | Pairwise Nei's Gst | | | |
|---|---|---|---|---|
| | CHI | NZN | NZS | TAS |
| NZN | 0.14616298 | | | |
| NZS | 0.11546406 | 0.06814561 | | |
| TAS | 0.27533185 | 0.21892748 | 0.19753898 | |
| VIC | 0.23198384 | 0.17710142 | 0.1544978 | 0.06126183 |
| | Pairwise Hendrick's G'st | | | |
| | CHI | NZN | NZS | TAS |
| NZN | 0.3309072 | | | |
| NZS | 0.2644481 | 0.1701334 | | |
| TAS | 0.5198048 | 0.4508762 | 0.4077721 | |
| VIC | 0.4638908 | 0.3863554 | 0.3384012 | 0.137628 |
| | Pairwise Jost's D | | | |
| | CHI | NZN | NZS | TAS |
| NZN | 0.10183161 | | | |
| NZS | 0.07241562 | 0.04875867 | | |
| TAS | 0.15491221 | 0.14304747 | 0.11619887 | |
| VIC | 0.1400209 | 0.12222243 | 0.09661457 | 0.0250716 |

### 4.3.4 Discriminant analysis of principal components

The same 2,255 SNPs dataset used in the population subdivision analyses was also used to differentiate the genomes by their variation in a non-parametric approach with a DAPC (Figure 12). The DAPC combines a PCA with a DA for a separation of genomes based on their variance

between groups rather than the total variance of the sample. We used sampling location to designate populations (landmass populations), three clusters representing Chile, New Zealand and Australia were clearly separated in genomic space, but subclusters representing TAS and VIC were overlapping as were subclusters representing NZN and NZS (Figure 12A). Furthermore, there is evidence for admixture between Chile and New Zealand and between Australia and New Zealand, but not between Chile and Australia (Figure 12B).

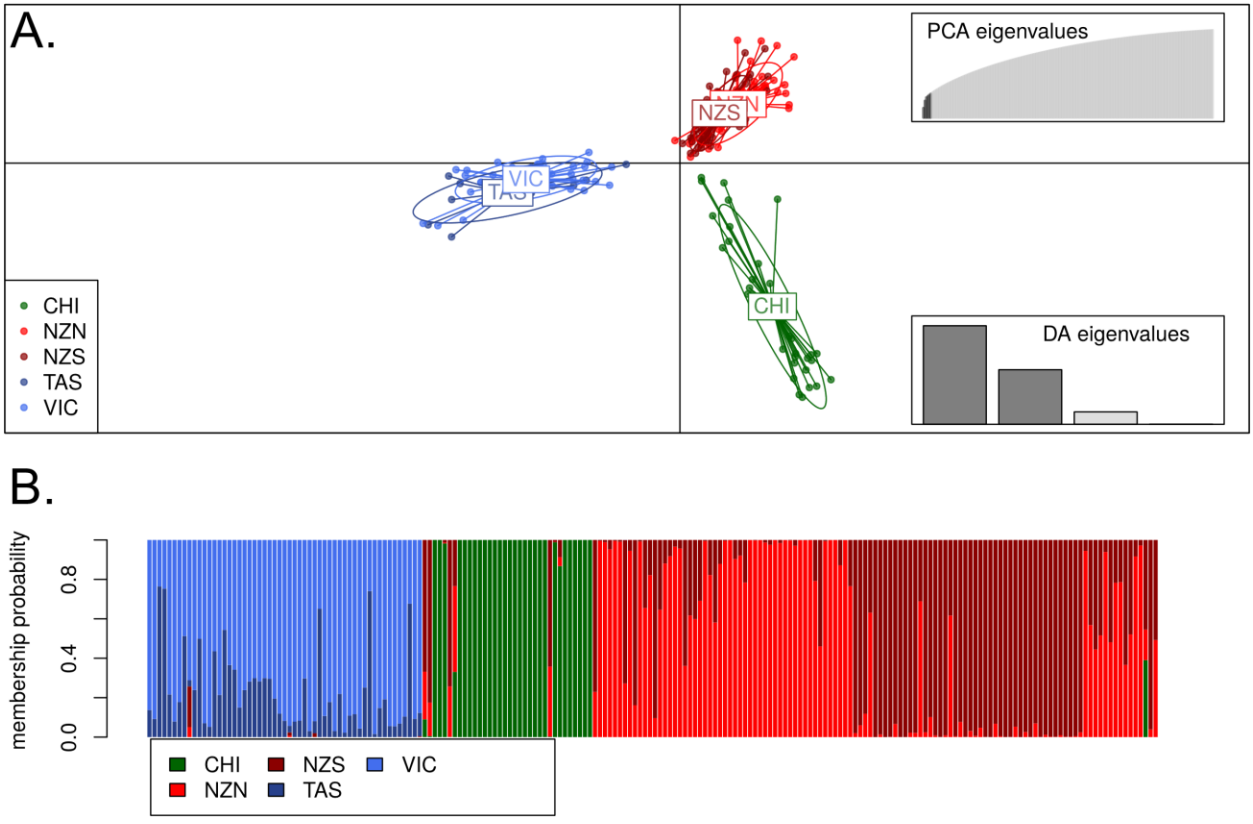


Figure 12. Genomic variation by non-parametric DAPC. (A) DAPC scatter plot of the densities of the populations of *P. glabra* (TAS=dark blue, VIC=light blue, CHI=green, NZN=dark red, NZS=light red) estimated with six PCA and four DA eigenvalues (B) Bar plot of group membership probabilities.

### 4.3.5 Estimation of co-ancestry

The population genetic structure of *P. glabra* samples was assessed using a Bayesian model-based approach with the program fineRADstructure. By converting the pyRAD allele output for fineRADstructure, we reduced the dataset to 1,618 unlinked SNPs with a minimum coverage of 101 samples per locus (50% samples per locus). Results from co-ancestry analysis in Figure 13 provided additional information about ancestry between individuals and revealed patterns consistent with the ML phylogenetic analysis in Figure 11A and the DAPC in Figure 12 but also showed finer-scale differences as well. In particular, five major blocks stood out corresponding to (1, lower-left) the individuals from New Zealand and Chile that clustered in Clade A of the ML phylogeny (2, middle-left) a block containing Australian individuals corresponding to the well-supported clade from Clade B of the ML phylogeny, (3, middle-right) a block containing New Zealand samples from Clade B of the ML phylogeny, (4) four individuals from Victoria, Australia which were early divergent in the ML phylogeny, and (5, upper-right) the Chilean individuals from Clade B in the ML phylogeny. In general, the resulting clustered co-ancestry matrix showed that *P. glabra* samples from Australia (TAS and VIC), Chile (CHI) and New Zealand (NZN and NZS) shared more co-ancestry within each other than between countries. As in the phylogenetic tree (Figure 11A) samples collected in New Zealand formed two clusters with samples found in Clade B sharing less co-ancestry than those from Clade A. The New Zealand and Chile clusters in the upper-right of the matrix have shared co-ancestry which reflects the clustering in the ML phylogeny. Some samples showed the highest degrees of co-ancestry (dark blue and red subblocks) demonstrating very close relatedness, such as sister or clonal relationships. These results agreed with the ML inference (Figure 11A) in which the same specimens were close sister taxa.

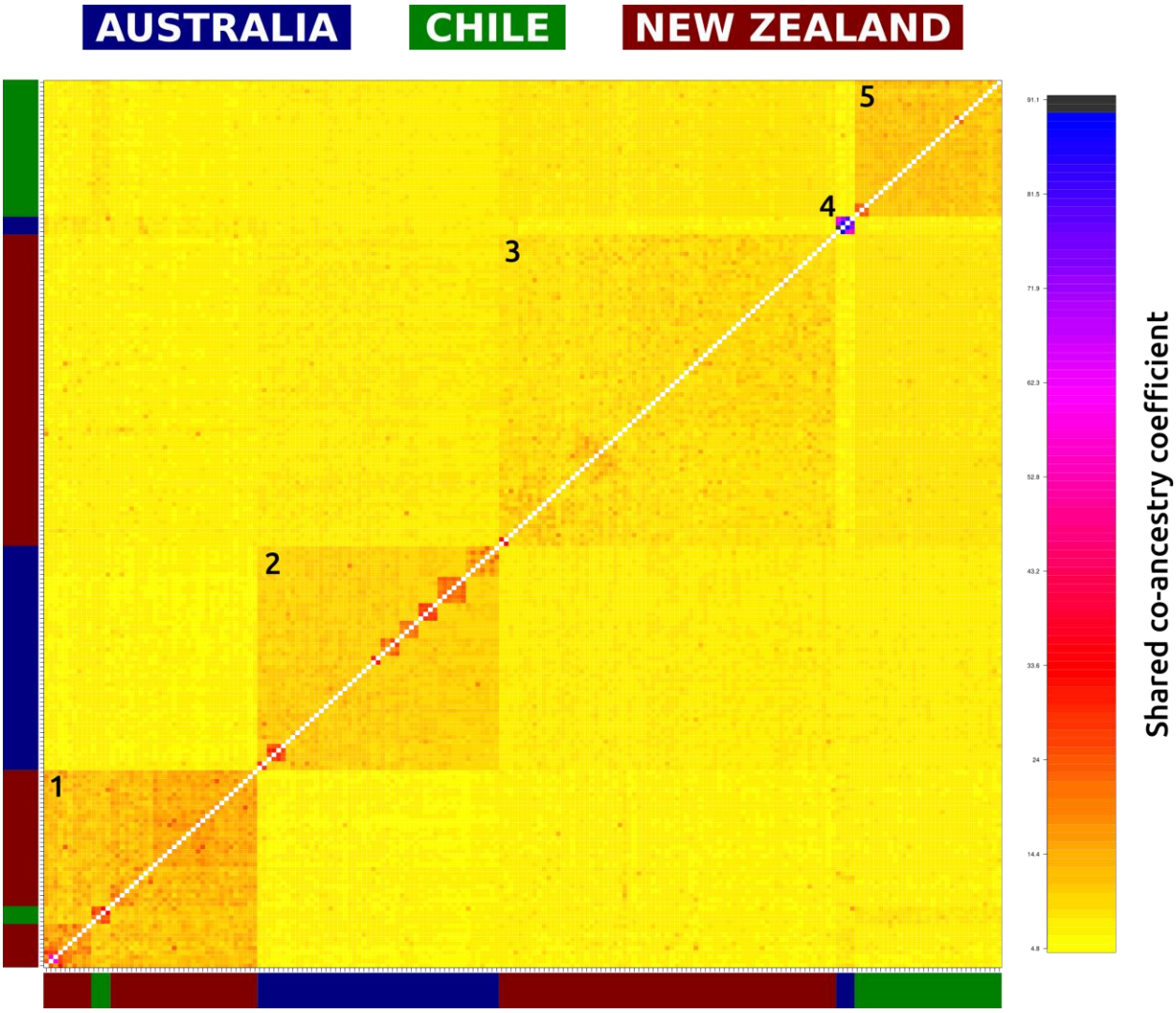


Figure 13.Clustered fineRADstructure co-ancestry matrix estimated from the 1000min_no_PHO dataset including 216 *P. glabra* samples. The heatmap shows pairwise co-ancestry between individuals, with black, blue and purple representing the highest levels, red and orange indicating intermediate levels, and yellow representing the lowest levels of shared coancestry.

## 4.4 Discussion

Our study results implied that the vast water bodies separating continents of the Southern Hemisphere do not form a disruptive barrier to gene flow among populations of the lichenized fungus *P. glabra* where geographically distant individuals may share more recent ancestry that geographically proximate ones, although statistically detectable genetic structure does exist (based on DAPC). This study corroborated the biology of the species, where lichenized fungi with small-size and a large-quantity of reproductive propagules tend to dispersal well and the disjunct distribution of *P. glabra* can be explained by recent dispersal events (Galloway 2008, 2008, 1991).

Our ML results (Figure 11A) recovered *P. glabra* as a distinct clade sister to the 13 outgroup *P. homoeophylla* samples. The two species have been suggested to be a species pair (Galloway and James 1980) and our RADseq results are consistent with them being distinct lineages. Species pairs are common in lichens and consist of one sexual and one asexual species (Tehler 1982; Mattsson and Lumbsch 1989; Poelt 1972). The asexual species form structures that propagate the fungal and photosynthetic partner simultaneously. Otherwise, species in species pairs are morphologically identical, but were traditionally regarded as distinct species due to their different reproductive modes (Poelt 1972). Each species form distinct groupings in both ML and population genomic analyses (Figure 3A and Figure 23, Appendix C). Samples of *P. glabra* formed multiple distinct lineages and did not show clear geographic structure. Individuals of *P. glabra* from all major landmasses were polyphyletic, but most samples from Chile and Australia formed well-supported clades. New Zealand samples are polyphyletic suggesting a greater genetic variability in New Zealand. This could be due to a longer residency on New Zealand and more ancestral polymorphism. Our own collection experience (Widhelm personal observation)

also suggests that the New Zealand population can grow in more forest types and on many different substrates that were not observed in any other populations.

Our population genomic results from the RADseq dataset clearly delimited *P. glabra* into three populations (Figures 12 and 13). This confirms that populations separated by large bodies of water, such as the Tasman Sea and Pacific Ocean are genetically differentiated. Relatively smaller bodies of water, such as the Bass Strait (separating TAS and VIC) and Cook Strait (separating NZN and NZS), are not sufficiently large enough to isolate populations and dispersal is homogenizing the populations. Alternatively, it could be that the Bass and Cook Straits were land bridges during the last glacial maximum (Lambeck and Chappell 2001; Proctor and Carter 1989) and not enough time has passed for populations on each side to become genetically differentiated. The sister species *P. homoeophylla* is genetically isolated from *P. glabra*, even though the two species live in sympatry on both islands of New Zealand (Figure 23, Appendix C). Admixture between New Zealand and Chile was detected in the STRUCTURE-like plot of the DAPC analysis (Figure 12B). Seven samples from Chile were assigned to the genetic cluster containing the New Zealand specimens which could be caused by relatively recent long-distance dispersal. This result agrees with the ML phylogeny, where samples from each country clustered together in well-supported clades and with the co-ancestry matrix, where samples from Chile and New Zealand had relatively high levels of co-ancestry. There was slightly less admixture between New Zealand and Australia samples. Only three Australian samples were assigned to the New Zealand genetic cluster. This could possibly be due to east-to-west dispersal across the Tasman Sea. Some cyclonic weather systems are able to disperse east-to-west. Although the prevailing wind pattern is west-to-east at high altitudes, lower altitudes provide opportunities for east-to-west dispersal, and birds are also capable of carrying spores against the dominant wind

patterns (Wardle 1978).

The co-ancestry matrix in Figure 13 indicated that samples originating from a particular landmass shared more co-ancestry than they did with samples from other landmasses. However, based on the fineRADstructure analysis, there was more shared ancestry among samples originating from New Zealand and Chile than between New Zealand and Australia, which is surprising because of the proximity of Australia to New Zealand. The patterns found in the co-ancestry matrix, which are similar to the ML phylogeny, show that multiple independent lineages of *P. glabra* are found in all landmass, suggesting that all lineages have been or are still undergoing long-distance dispersal.

The biogeography of the Southern Hemisphere has intrigued scientists for hundreds of years. When Joseph Hooker visited these areas during an Antarctic Expedition between 1839 and 1843 he was impelled to write Charles Darwin to explain the biological similarities of Australia, New Zealand, and Southern South America (Skottsberg and Pantin 1960). Hooker became convinced that these affinities were only partly explained by dispersal and more so by a fragmented great Southern Continent (Galloway 1988). This idea was supported later by Wegener's theory of continental drift (Wegener 1966) and later by plate tectonics. The breakup of Gondwana did indeed isolate many groups of organisms, including lichens and these ideas dominated the views and explanations of disjunct distributions of species by biogeographers for many years (Swenson, Hill, and McLoughlin 2001; Raven and Axelrod 1972; Brundin 1966). Today, however, dispersal is seen as the primary mechanism for the disjunct distribution at the species level (Sanmartín and Ronquist 2004; McGlone 2005; Moreira-Muñoz 2007). The first sources of data that suggested long-distance dispersal was an important force in the southern hemisphere were palynological where temporal differences in the first appearance of shared taxa

(i.e. Australia first, New Zealand second, etc.) were observed. The pollen fossil record suggests that transoceanic dispersal occurred throughout the Tertiary (Macphail 1997; M. Pole 1994; M. S. Pole 2001; Mildenhall 1980). Once molecular methods were developed, studies on plant taxa with eastward dispersal were determined by phylogeny: (Table 1 in Winkworth et al., 2002) and as shown in many previous molecular-based studies, our results showed that dispersal rather than vicariance better explained the genetic pattern of currently disjunct distributed *P. glabra*.

We recently (Widhelm et al. – Chapter 2 in this dissertation) estimated divergence times in the former family Lobariaceae. The family is now considered the lobarioid clade of Peltigeraceae based on a temporal banding approach that reclassified higher-level taxonomic groups in the Lecanoromycetes (Kraichak et al. 2018). The time-tree estimated a crown age for this clade around 70 Mya (Widhelm et al. – Chapter 2 in this dissertation). This time-tree included one sample each of the closely related species *P. glabra*, *P. homoeophylla*, and P. freycinetii. The divergence estimates were around 13 Mya for the branching of P. freycinetii and around 3 Mya for *P. glabra* from *P. homoeophylla*. If the estimates are accurate, the entire lobarioid clade diversified rapidly at the end and after the breakup of Gondwana (155-80 Mya, Stevens, 1980) and *P. glabra*, *P. homoeophylla*, and *P. freycinetii* evolved relatively recently when the continents were very close to their present configuration. The result from the study by (Widhelm et al – Chapter 2 in this dissertation) is in line with the dispersal hypotheses proposed by previous literature (Sanmartín and Ronquist 2004; McGlone 2005; Moreira-Muñoz 2007). The dominant wind patterns that form a West-to-East directional flow (i.e. West Wind Drift) are probably facilitating the migrations of wind dispersing organisms (Muñoz et al. 2004; Galloway 1991). Similarly, birds such as the migratory albatross and shearwaters could be other possible vectors that carry propagules and spores in both directions (Gillespie et al. 2012).

## 4.5 Conclusion

Populations of *P. glabra* occur in Australia, Chile, and New Zealand and are genetically structured. They also show that samples of *P. glabra* from all landmasses form a lineage that is distinct from the *P. homoeophylla* lineage that only occurs in New Zealand. Although the origin of *P. glabra* remains unclear, long-distance dispersal, via the dominant wind patterns and possibly by migratory birds has established populations on landmasses between -20S and -60S degrees latitude around Antarctica. The relatively wide ecological tolerance and ability to occur in a variety of habitats and substrates (Galloway 2007) may allow *P. glabra* to be more successful at long-distance dispersal than closely related *Pseudocyphellaria* species, such as *P. homoeophylla* and *P. freycinetii* which are only found in New Zealand and Chile respectively. This study is the first to utilize the power of RADseq to understand the intercontinental distribution of a lichenized fungus at this level and the results suggest that wind patterns and possibly migratory birds can keep populations connected enough to maintain a single species that is divided by large barriers like the Pacific Ocean and the Tasman Sea.

## 4.6 References

Bankevich, Anton, Sergey Nurk, Dmitry Antipov, Alexey A. Gurevich, Mikhail Dvorkin, Alexander S. Kulikov, Valery M. Lesin et al. "SPAdes: A new genome assembly algorithm and its applications to single-cell sequencing." *Journal of Computational Biology* 19, no. 5 (2012): 455-477.

Bolger, Anthony M., Marc Lohse, and Bjoern Usadel. "Trimmomatic: A flexible trimmer for Illumina sequence data." *Bioinformatics* 30, no. 15 (2014): 2114-2120.

Brundin, L. “Transantarctic relationships and their significance, as evidenced by chironomid midges.” In *Kunglige Svenska Velenskapsakademiens Handlinger. Fjärde Series* 11, Stockholm: Almqvist & Wiksell (1966): 1-472.

Burbridge, N. T. The phytogeography of the australian region.” *Australian Journal of Botany* 8: (1960): 75–212.

Chakraborty, Ranajit. "Analysis of genetic structure of populations: Meaning, methods, and implications." In *Human Population Genetics*. Boston: Springer. (1993): 189-206.

Danecek, Petr, Adam Auton, Goncalo Abecasis, Cornelis A. Albers, Eric Banks, Mark A. DePristo, Robert E. Handsaker et al. "The variant call format and VCFtools." *Bioinformatics* 27, no. 15 (2011): 2156-2158.

Davey, JohnW, and Mark L. Blaxter. "RADSeq: Next-generation population genetics." *Brief. Funct. Genomics* 10, no. 2 (2011): 108.

Eaton, Deren., and I. Overcast. "Ipyrad: Interactive assembly and analysis of RADseq data sets." (2016).

Eaton, Deren, and Richard H. Ree. "Inferring phylogeny and introgression using RADseq data: An example from flowering plants (*Pedicularis*: Orobanchaceae)." *Systematic Biology* 62, no. 5 (2013): 689-706.

Elshire, Robert J., Jeffrey C. Glaubitz, Qi Sun, Jesse A. Pol, Ken Kawamoto, and Edward S. Buckler. "A robust, simple genotyping-by-sequencing (GBS) approach for high diversity species.” *PLOS ONE* 6 (2011): e19379.

Excoffier, L. “Analysis of Population Subdivision.” In *Handbook of Statistical Genetics*. Edited by D. J. Balding, M. Bishop, and C. Cannings. Chichester: John Wiley & Sons. (2004).

Galloway, D. J., and P. W. James. "Nomenclatural notes on *Pseudocyphellaria* in New Zealand." *The Lichenologist* 12, no. 3 (1980): 291-303.

Galloway, D. J. *Flora of New Zealand Lichens. Revised second edition including lichen-forming and lichenicolous fungi. Volumes 1 and 2*. Lincoln: Manaaki Whenua Press. (2007).

Galloway, D. J. "Phytogeography of southern hemisphere lichens." In *Quantitative Approaches to Phytogeography*. Edited by Pier Luigi Nimis and T.J. Crovello. Dordrecht: Springer. (1991): 233-262.

Galloway, D. J. “Austral lichenology: 1690–2008.” *New Zealand Journal of Botany* 46 no. 4 (2008) 433–521.

Galloway, D. J. "Plate tectonics and the distribution of cool temperate Southern Hemisphere macrolichens." *Botanical Journal of the Linnean Society* 96, no. 1 (1988): 45-55.

Galloway, D. J. “Lichen biogeography.” In *Lichen Biology*, Cambridge: Cambridge University Press. (2008). 315–35.

Gillespie, Rosemary G., Bruce G. Baldwin, Jonathan M. Waters, Ceridwen I. Fraser, Raisa Nikula, and George K. Roderick. "Long-distance dispersal: A framework for hypothesis testing." *Trends in Ecology & Evolution* 27, no. 1 (2012): 47-56.

Grewe, Felix, Jen-Pen Huang, Steven D. Leavitt, and H. Thorsten Lumbsch. "Reference-based RADseq resolves robust relationships among closely related species of lichen-forming fungi using metagenomic DNA." *Scientific Reports* 7, no. 1 (2017): 9884.

Grewe, Felix, Elisa Lagostina, Huini Wu, Christian Printzen, and H. Thorsten Lumbsch. "Population genomic analyses of RAD sequences resolves the phylogenetic relationship of the lichen-forming fungal species *Usnea antarctica* and *Usnea aurantiacoatra*." *MycoKeys* 43 (2018): 91-113.

Hedrick, Philip W. "A standardized genetic differentiation measure." *Evolution* 59, no. 8 (2005): 1633-1638.

Jombart, Thibaut, Sébastien Devillard, and François Balloux. "Discriminant analysis of principal components: A new method for the analysis of genetically structured populations." *BMC Genetics* 11, no. 1 (2010): 94.

Jost, L. O. U. "GST and its relatives do not measure differentiation." *Molecular Ecology* 17, no. 18 (2008): 4015-4026.

Kraichak, Ekaphan, Jen-Pan Huang, Matthew Nelsen, Steven D. Leavitt, and H. Thorsten Lumbsch. "A revised classification of orders and families in the two major subclasses of Lecanoromycetes (Ascomycota) based on a temporal approach." *Botanical Journal of the Linnean Society* 188, no. 3 (2018): 233-249.

Lambeck, Kurt, and John Chappell. "Sea level change through the last glacial cycle." *Science* 292, no. 5517 (2001): 679-686.

Langmead, Ben, and Steven L. Salzberg. "Fast gapped-read alignment with Bowtie 2." *Nature Methods* 9, no. 4 (2012): 357.

Lawson, Daniel John, Garrett Hellenthal, Simon Myers, and Daniel Falush. "Inference of population structure using dense haplotype data." *PLoS Genetics* 8, no. 1 (2012): e1002453.

Macphail, M K. “Correspondence: The importance of dispersal and recent speciation in the flora of New Zealand.” *Journal of Biogeography* 26, no. 1. (1997): 113–17.

Malinsky, Milan, Emiliano Trucchi, Daniel John Lawson, and Daniel Falush. "RADpainter and fineRADstructure: Population inference from RADseq data." *Molecular Biology and Evolution* 35, no. 5 (2018): 1284-1290.

Mattsson, Jan-Eric, and H. Thorsten Lumbsch. "The use of the species pair concept in lichen taxonomy." *Taxon* (1989): 238-241.

McGlone, Matt S. "Goodbye Gondwana." *Journal of Biogeography* 32, no. 5 (2005): 739-740.

Mildenhall, Dallas C. "New Zealand Late Cretaceous and Cenozoic plant biogeography: A contribution." *Palaeogeography, Palaeoclimatology, Palaeoecology* 31 (1980): 197-233.

Miller, H. A. “Bryophyte evolution and geography.” *Biological Journal of the Linnean Society* 18 no. 2 (1982): 145–96.

Moncalvo, Jean-Marc, and Peter K. Buchanan. "Molecular evidence for long distance dispersal across the Southern Hemisphere in the *Ganoderma applanatum-australe* species complex (Basidiomycota)." *Mycological Research* 112, no. 4 (2008): 425-436.

Moreira-Muñoz, A. "The Austral floristic realm revisited." *Journal of Biogeography* 34, no. 10 (2007): 1649-1660.

Muñoz, Jesús, Ángel M. Felicísimo, Francisco Cabezas, Ana R. Burgaz, and Isabel Martínez. "Wind as a long-distance dispersal vehicle in the Southern Hemisphere." *Science* 304, no. 5674 (2004): 1144-1147.

Nash, Thomas H. *Lichen Biology*. Cambridge: Cambridge University Press. (2008).

Nei, Masatoshi. "Analysis of gene diversity in subdivided populations." *Proceedings of the National Academy of Sciences* 70, no. 12 (1973): 3321-3323.

Parris, Barbara S. "Circum-Antarctic continental distribution patterns in pteridophyte species." *Brittonia* 53, no. 2 (2001): 270-283.

Poelt, J. "Taxonomische Behandlung von Artenpaaren bei den Flechten." *Botaniska Notiser* (1972).

Pole, Mike. "The New Zealand flora - entirely long-distance dispersal?." *Journal of Biogeography* (1994): 625-635.

Pole, Mike S. "Can long-distance dispersal be inferred from the New Zealand plant fossil record?." *Australian Journal of Botany* 49, no. 3 (2001): 357-366.

Proctor, Roger, and Lionel Carter. "Tidal and sedimentary response to the late Quaternary closure and opening of Cook Strait, New Zealand: Results from numerical modeling." *Paleoceanography and Paleoclimatology* 4, no. 2 (1989): 167-180.

Raven, Peter H. "Evolution of subalpine and alpine plant groups in New Zealand." *New Zealand Journal of Botany* 11, no. 2 (1973): 177-200.

Raven, Peter H., and Daniel I. Axelrod. "Plate tectonics and Australasian paleobiogeography." *Science* 176, no. 4042 (1972): 1379-1386.

Sanmartín Isabel, and Fredrik Ronquist. "Southern hemisphere biogeography inferred by event-based models: Plant versus animal patterns." *Systematic Biology* 53, no. 2 (2004): 278-298.

Skottsberg, Carl Johan Fredrik. "Remarks on the plant geography of the southern cold temperate zone." *Proceedings of the Royal Society of London. Series B. Biological Sciences* 152, no. 949 (1960): 447-457.

Stamatakis, Alexandros. "RAxML version 8: A tool for phylogenetic analysis and post-analysis of large phylogenies." *Bioinformatics* 30, no. 9 (2014): 1312-1313.

Stanke, Mario, and Burkhard Morgenstern. "AUGUSTUS: A web server for gene prediction in eukaryotes that allows user-defined constraints." *Nucleic Acids Research* 33, (2005): W465-W467.

Stevens, G. R. "Southwest Pacific faunal palaeobiogeography in Mesozoic and Cenozoic times: A review." *Palaeogeography, Palaeoclimatology, Palaeoecology* 31 (1980): 153-196.

Strous, Marc, Beate Kraft, Regina Bisdorf, and Halina Tegetmeyer. "The binning of metagenomic contigs for microbial physiology of mixed cultures." *Frontiers in microbiology* 3 (2012): 410.

Swenson, Ulf, Robert S. Hill, and Stephen McLoughlin. "Biogeography of *Nothofagus* supports the sequence of Gondwana break-up." *Taxon* (2001): 1025-1041.

Tehler, Anders. "The species pair concept in lichenology." *Taxon* (1982): 708-714.

Wardle, P. "Origin of the New Zealand mountain flora, with special reference to trans-Tasman relationships." *New Zealand Journal of Botany* 16, no. 4 (1978): 535-550.

Wegener, Alfred. *The origin of continents and oceans*. Chelmsford: Courier Corporation. (1966).

Werth, Silke. "Population genetics of lichen-forming fungi–A review." *The Lichenologist* 42, no. 5 (2010): 499-519.

Whitlock, Michael C. “G’ST and D do not replace FST.” *Molecular Ecology* 20, no. 6 (2011): 1083–91.

Winkworth, Richard C., Steven J. Wagstaff, David Glenny, and Peter J. Lockhart. "Plant dispersal news from New Zealand." *Trends in Ecology & Evolution* 17, no. 11 (2002): 514-520.

Winkworth, Richard C., Françoise Hennion, Andreas Prinzing, and Steven J. Wagstaff. "Explaining the disjunct distributions of austral plants: The roles of Antarctic and direct dispersal routes." *Journal of Biogeography* 42, no. 7 (2015): 1197-1209.

Winter, David J. "MMOD: An R library for the calculation of population differentiation statistics." *Molecular Ecology Resources* 12, no. 6 (2012): 1158-1160.

## 5. Picking holes in traditional species delimitations: an integrative taxonomic reassessment of the *Parmotrema perforatum* group (Parmeliaceae, Ascomycota)

Todd J. Widhelm, Robert S. Egan, Francesca R. Bertoletti, Matt J. Asztalos, Ekaphan Kraichak, Steven D. Leavitt and H. Thorsten Lumbsch

This chapter is a reprint (with minimal formatting) of an original article published in the *Botanical Journal of the Linnean Society*. The citation is as follows:

Widhelm, Todd J., Robert S. Egan, Francesca R. Bertoletti, Matt J. Asztalos, Ekaphan Kraichak, Steven D. Leavitt, and H. Thorsten Lumbsch. "Picking holes in traditional species delimitations: an integrative taxonomic reassessment of the *Parmotrema perforatum* group (Parmeliaceae, Ascomycota)." *Botanical Journal of the Linnean Society* 182, no. 4 (2016): 868-884.

### 5.1 Introduction

Species delimitation is the process of discovering species boundaries and new species and the recognition of species figures prominently into biodiversity assessments and conservation programs (Mace 2004), and ecological and biogeographical studies frequently use species as basic units. Furthermore, delimiting species is important in the context of understanding many evolutionary mechanisms and processes (Sites and Marshall 2003). Inaccurate species delimitation can lead to erroneous inferences and confound our understanding of nature (Bickford et al. 2007).

A number of species concepts have been proposed, but it is generally accepted that

species can be more accurately delimited if their origins are better understood (Padial et al. 2010). The commonly employed general lineage concept (GLC) recognizes that species are metapopulations that represent distinct evolutionary lineages that can be delimited using any of several criteria associated with lineage formation (Sites and Marshall 2003; Mayden 1997; Knowles and Carstens 2007; de Queiroz 2007; Lumbsch and Leavitt 2011). However, deciding on operational criteria can be daunting (de Queiroz 2007). The application of multiple species delimitation methods all too often leads to incongruent species boundaries, rendering researchers unable to decide how many species they are working with (Sites and Marshall 2003, 2004; Rannala 2015; Mishler, Donoghue, and Farris 1982). Additionally, taxonomic uncertainty can result if researchers are inconsistent in their application of operational species concepts (Agapow et al. 2004). On the other hand, some scientists suggest using all available methods and only delimiting species if congruence is observed in most approaches (Carstens et al. 2013). With the large variety of methods and differences in operational protocols, the development of a uniting integrative approach to species delimitation that combines morphological, chemical, ecological, geographic and phylogenetic data to recognize species level linages is of utmost importance for future taxonomic studies (Padial et al. 2010; Dayrat 2005) .

During the past decade, there has been an increased interest in integrative species delimitation that combines multiple lines of evidence (Sites and Marshall 2003; Padial et al. 2010). However, integrating traditional morphological data with molecular data can be challenging due to a number of issues such as the presence of cryptic species (Bickford et al. 2007; Leavitt et al. 2011; Singh et al. 2015) and effects of adaptive radiations (Shaffer and Thomson 2007; Maddison 1997). Traditional phenotype-based methods may fail to detect species boundaries in cryptic lineages resulting in an underestimate of the true number of species

relative to other kinds of data (Bickford et al. 2007). In the case of adaptive radiations, incomplete lineage sorting and hybridization confound genetic inferences and can lead to incorrect interpretations of species boundaries (Maddison 1997; Nosil, Harmon, and Seehausen 2009). Additionally, single-locus barcoding efforts can be useful for initially establishing operational taxonomic units which require further validation with an integrative taxonomic approach (Kekkonen et al. 2015).

With recent advances in DNA sequencing technology, the ability to gather data from multiple unlinked genetic loci has become the standard approach and coalescent-based analytical methods now account for incomplete lineage sorting (Balding, Bishop, and Cannings 2008). Coalescent theory is now being widely applied to empirically delimit species, and many methods are available (Fujita et al. 2012). In lichenized fungi the use of coalescent-based methods has been widely used to delimit species (Singh et al. 2015; Parnmen et al. 2012; Leavitt, Esslinger, et al. 2013; Leavitt et al. 2015; Saag et al. 2014; Kraichak et al. 2015).

Lichens are assemblages of fungi, photosynthetic green alga or cyanobacteria, and many non-photosynthetic bacteria. Therefore, lichens can be considered the symbiotic phenotype of miniature ecological systems rather than individual organisms. Despite their complexity, the taxonomy of lichens has traditionally focused on the fungal partner, and current estimates of 13,500 to 28,000 species of lichen-forming fungi have been proposed (Hawksworth 2001; Feuerer and Hawksworth 2007). With the wide range of species estimates in lichenized fungi, it is clear that there is a need for a standard species delimitation protocol (Lumbsch and Leavitt 2011). Parmeliaceae is the largest family of lichenized fungi (Jaklitsch et al. 2016) and has been the focus of many ecological, geographical, and taxonomic studies (Leavitt et al. 2015; Saag et al. 2014; Thell et al. 2004; Crespo et al. 2010; Amo de Paz et al. 2011, 2012; Del-Prado et al.

2013). One of the largest genera in the Parmeliaceae, *Parmotrema* A. Massal. includes over 350 species distributed primarily in tropical to subtropical regions worldwide. These loosely-attached, large-lobed, foliose lichens display a wide variety of chemical variation and reproductive strategies (Blanco et al. 2005).

The *Parmotrema perforatum* group is a complex of species that serves as an excellent model for two controversial topics in species delimitation in lichenized fungi. The first is the species pairs concept, where pairs of taxa that are morphologically and chemically identical differ in their predominant reproductive modes: one taxon is assumed to reproduce sexually (producing apothecia), the other asexually (producing thalloid fragments called lobules, isidia, or soredia) (Mattsson and Lumbsch 1989). The other is the chemospecies concept, where different chemotypes of morphologically identical individuals are classified as distinct species if the chemical differences are correlated with geographical, or ecological differences (Egan 1986).

The *Parmotrema perforatum* group has been extensively studied and delimitation of species in this group has been highly debated (Culberson 1973; Robinson 1975; Culberson and Culberson 1973; Lendemer, Allen, and Noell 2015). The most recent classification recognizes six species in North America (Esslinger n.d.) based on the hypothesis of Culberson & Culberson (1973) who proposed three evolutionary species pairs in the North American group (Figure 14), each with its own distinct chemical profile and biogeography. Each pair has the same secondary lichen chemistry and two reproductive forms, one sexually reproducing form with apothecia (referred to as the primary species) and the other asexually reproducing with soredia (secondary species). He interpreted the three chemically distinct apotheciate species to be sibling species, reproductively isolated but still morphologically identical. He hypothesized that each apotheciate species gave rise, by parallel evolution, to a chemically identical sorediate species.

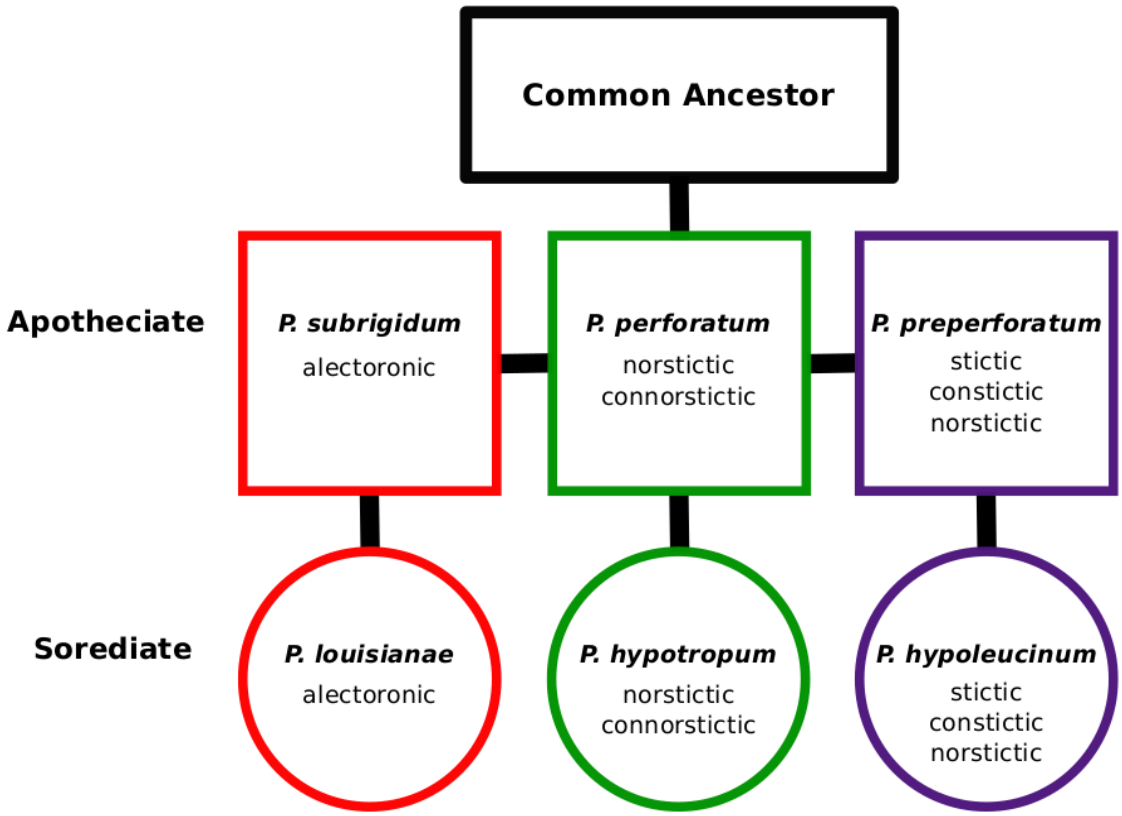


Figure 14. Species delimitation and evolutionary relationships in the *Parmotrema perforatum* group as hypothesized by W. L. Culberson (1973). Each sorediate species (circles) is descended from an apotheciate species (squares) with the same secondary chemistry. Diagnostic secondary lichen acid composition is represented by color (green = norstictic acid only, red = alectoronic acid, purple = norstictic+stictic acid).

We investigated species boundaries in the North American *Parmotrema perforatum* group using population level sampling in Eastern Texas and Western Louisiana where all six currently accepted species occur in sympatry. Using an integrative species delimitation approach, we combined DNA sequence data from seven nuclear loci, differences in reproductive strategies, secondary metabolite variation, and newly discovered variation in conidial morphology to

delimit species in the *Parmotrema perforatum* group. We used a suite of empirical approaches to test the traditional hypotheses of species boundaries, including maximum likelihood, Bayesian, and coalescent-based species tree phylogenetic reconstruction approaches, along with a multi-species coalescent model to estimate speciation probabilities.

## 5.2 Materials and methods

### 5.2.1 Taxon sampling

All six members of the North American *Parmotrema perforatum* group occur in the southeastern United States, and our sampling focused on 25 sites in Oklahoma, Texas, Louisiana, and Arkansas (Figure 15). At each site, *Parmotrema* specimens were indiscriminately collected during the summer of 2006. At each site, small #2 paper bags were filled with available thalli, providing a site-specific perspective of species diversity and relative abundance. The substrate tree was recorded as "conifer" or "hardwood". Mass collections from two sites in Texas (Lake Limestone, 17 thalli; Fort Parker, 9 thalli) and two sites in Louisiana (Pelican, 10 thalli; Vivian, 8 thalli) are included in the present study (Figures 14 and 15, Table XIV). These four sites were selected because they had the highest species diversity among the 25 sites sampled. Two closely related samples of *P. hypoleucinum* from Spain were also included to test for geographic differentiation of disjunct populations.

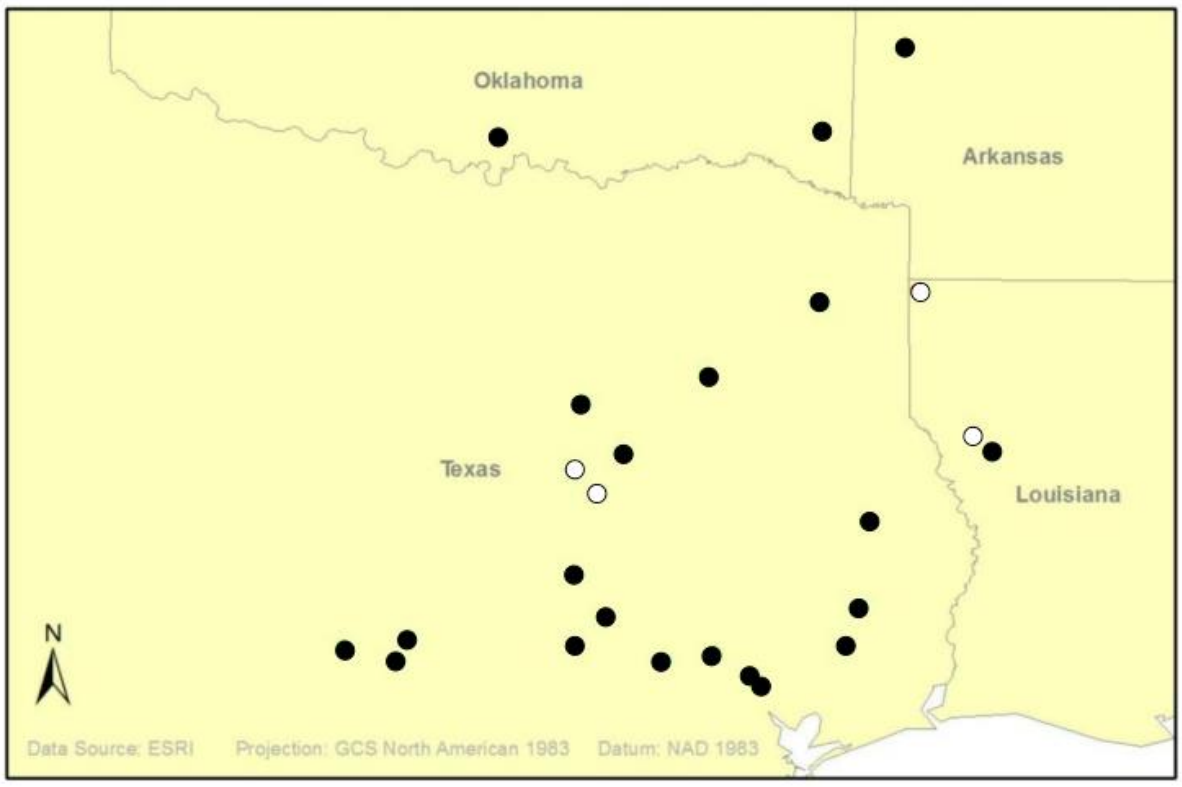


Figure 15. Twenty-five sites sampled in 2006. White dots indicate samples selected for this study.

TABLE XIV. SITES AND POPULATIONS SAMPLED IN THIS STUDY, LIST OF THE SPECIES COLLECTED AT EACH LOCATION, AND VOUCHER SPECIMENS. ALL VOUCHERS ARE DEPOSITED AT OMA. TAXA MARKED WITH AN ASTERISK WERE PRESENT, BUT SPECIMENS DID NOT YIELD A PCR PRODUCT. MULTIPLE THALLI SEQUENCED FROM A SINGLE COLLECTION ARE INDICATED WITH, E.G. "-A, B, C", AFTER THE COLLECTION NUMBER.

| Site | Taxa present | Specimen voucher |
|---|---|---|
| Texas, Limestone County: Ft. Parker State Park on the east side of Springfield Lake; 9.7 Kilometers N of Groesbeck; 31°35.831' N, 96°32.143' W. 19-July-06 [Populations 1 and 2] | *P. perforatum* | Widhelm & Egan 606 |
| | *P. hypotropum* | Widhelm & Egan 607-A, B, C, D, E |
| | *P. preperforatum* | Widhelm & Egan 609 |
| | *P. hypoleucinum** | Widhelm & Egan 608-A, B |
| | *P. subrigidum* | |
| Texas, Limestone County: west of Lake Limestone; 17.7 Kilometers SE of Groesbeck; 31°25.733' N, 96°22.550' W. 19-July-06 [Populations 3 and 4] | | Widhelm & Egan 611-A, B |
| | | Widhelm & Egan 615-A, B |
| | *P. perforatum* | Widhelm & Egan 612 |
| | *P. hypotropum* | Widhelm & Egan 616 |
| | *P. preperforatum* | Widhelm & Egan 614-A, B, C |
| | *P. hypoleucinum* | Widhelm & Egan 618-A, B, C |
| | *P. subrigidum* | Widhelm & Egan 619 |
| | | Widhelm & Egan 613-A, B, C |
| | | Widhelm & Egan 617 |
| Louisiana, Desoto Parish: 5.6 Kilometers SE of Pelican on Route 175; 31°51.647' N, 93°33.335' W. 21-July-06 [Populations 5 and 6] | *P. perforatum* | Widhelm & Egan 653-A, B |
| | *P. hypotropum* | Widhelm & Egan 655 |
| | *P. preperforatum* | Widhelm & Egan 656 |
| | *P. hypoleucinum** | Widhelm & Egan 654a |
| | *P. subrigidum* | Widhelm & Egan 654-AA, C, D |
| | *P. louisianae* | Widhelm & Egan 657 |
| | | Widhelm & Egan 661 |
| Louisiana, Caddo Parish: 9.7 Kilometers NNE of Vivian along Route 769 on Black Bayou Lake; edge of a cypress swamp; 32°55.928' N, 93°58.240' W. 21-July-06 [Populations 7 and 8] | *P. perforatum* | Widhelm & Egan 663-A, B, C |
| | *P. hypotropum* | Widhelm & Egan 664 |
| | *P. hypoleucinum* | Widhelm & Egan 666-A, B |
| | *P. louisianae* | Widhelm & Egan 665-A, B |
| Spain | *P. hypoleucinum* | Crespo |
| | *P. hypoleucinum* | Crespo |

Presence of secondary metabolites in each individual thallus was determined with thin layer chromatography (TLC) in solvent A (Culberson 1972). Each thallus was scored for presence or absence of norstictic acid, stictic acid, alectoronic acid, soredia, and apothecia. Constictic and connorstictic acids were not scored because they are difficult to distinguish from each other using our TLC method. Based on these five characters, each thallus was identified to one of the six currently accepted species in this complex (Culberson 1973). Herbarium packets were filled with one to many conspecific thalli from each location and assigned a collection number. All voucher specimens are deposited at OMA (Table XIV).

From these collections, a total of forty-four thalli representing the six species of the *Parmotrema perforatum* group in North America north of Mexico were selected for the phylogenetic component of this study: *P. perforatum* (Jacq.) A. Massal (11 specimens), *P. hypotropum* (Nyl.) Hale (9), *P. preperforatum* (Culb.) Hale (8), *P. hypoleucinum* (Steiner) Hale (3), *P. subrigidum* Egan (10) and *P. louisianae* (Hale) Hale (3) (Tables XIV and XV). Mass collections from two sites in Texas (Lake Limestone, 17 thalli; Fort Parker, 9 thalli) and two sites in Louisiana (Pelican, 10 thalli; Vivian, 8 thalli) are included in the present study (Figures 14 and 15, Table XIV). These four sites were selected because they had the highest species diversity among the 25 sites sampled. Two samples of *P. hypoleucinum* from Spain were also included to determine if geographic isolation has been long enough for differentiation to occur. Sequences from *Parmotrema fistulatum, P. reticulatum, P. cetratum, P. perlatum P. pilosum, P. haitiense* and *P. crinitum* were used as out-groups to root the allele tree (Genbank accession numbers in Tables XV and XVI).

TABLE XV. COLLECTION NUMBERS WITH CORRESPONDING ALLELE NUMBER AND GENBANK ACCESSION NUMBER OF ALL INGROUP SPECIMENS INCLUDED IN THE ANALYSIS.

| Collection data | F.M. DNA # | Species | *GPD* | IGS | ITS | MS456 (*Mcm7*) | nuLSU | *RPB1* | MS277 (*Tsr1*) |
|---|---|---|---|---|---|---|---|---|---|
| Widhelm & Egan 606 | 2965 | *P. perforatum* | EU665274 | KX246410 | KX246569 | KX246605 | KX246449 | KX246490 | KX246530 |
| Widhelm & Egan 607-A | 2966 | *P. hypotropum* | EU665270 | KX246411 | KX246570 | KX246606 | — | KX246491 | KX246531 |
| Widhelm & Egan 607-B | 2967 | *P. hypotropum* | EU665271 | KX246412 | KX246571 | KX246607 | KX246450 | KX246492 | KX246532 |
| Widhelm & Egan 607-C | 2968 | *P. hypotropum* | EU665272 | KX246413 | KX246572 | — | KX246451 | KX246493 | KX246533 |
| Widhelm & Egan 607-D | 2969 | *P. hypotropum* | EU665273 | KX246414 | KX246573 | KX246608 | KX246452 | KX246494 | KX246534 |
| Widhelm & Egan 607-E | 2970 | *P. hypotropum* | EU665299 | KX246415 | KX246574 | KX246609 | KX246453 | KX246495 | KX246535 |
| Widhelm & Egan 608-A | 2971 | *P. subrigidum* | EU665300 | KX246416 | KX246575 | KX246610 | KX246454 | KX246496 | KX246536 |
| Widhelm & Egan 608-B | 2972 | *P. subrigidum* | EU665269 | KX246417 | KX246576 | KX246611 | KX246455 | KX246497 | KX246537 |
| Widhelm & Egan 609 | 2973 | *P. preperforatum* | EU665275 | KX246418 | KX246577 | KX246612 | KX246456 | KX246498 | KX246538 |
| Widhelm & Egan 611-B | 2974 | *P. perforatum* | EU665279 | KX246419 | KX246578 | KX246613 | KX246457 | KX246499 | KX246539 |
| Widhelm & Egan 611-C | 2975 | *P. perforatum* | EU665280 | KX246420 | KX246579 | KX246614 | KX246458 | KX246500 | KX246540 |
| Widhelm & Egan 612 | 2976 | *P. hypotropum* | EU665278 | KX246421 | KX246580 | KX246615 | KX246459 | KX246501 | — |
| Widhelm & Egan 613-A | 2977 | *P. subrigidum* | EU665303 | KX246422 | KX246581 | KX246616 | KX246460 | KX246502 | KX246541 |
| Widhelm & Egan 613-B | 2978 | *P. subrigidum* | EU665288 | KX246423 | KX246582 | KX246617 | KX246461 | KX246503 | KX246542 |
| Widhelm & Egan 613-C | 2979 | *P. subrigidum* | EU665304 | KX246424 | KX246583 | KX246618 | KX246462 | KX246504 | — |
| Widhelm & Egan 614-A | 2980 | *P. preperforatum* | EU665283 | KX246425 | KX246584 | KX246619 | KX246463 | KX246505 | KX246543 |
| Widhelm & Egan 614-B | 2981 | *P. preperforatum* | EU665284 | KX246426 | — | KX246620 | KX246464 | KX246506 | KX246544 |
| Widhelm & Egan 614-C | 2982 | *P. preperforatum* | EU665285 | KX246427 | KX246585 | KX246621 | KX246465 | — | KX246545 |
| Widhelm & Egan 615-A | 2983 | *P. perforatum* | EU665281 | KX246428 | — | KX246622 | KX246466 | KX246507 | — |
| Widhelm & Egan 615-B | 2984 | *P. perforatum* | EU665282 | KX246429 | KX246586 | KX246623 | KX246467 | KX246508 | KX246546 |
| Widhelm & Egan 616 | 2985 | *P. hypotropum* | EU665301 | KX246430 | — | KX246624 | KX246468 | KX246509 | KX246547 |
| Widhelm & Egan 617 | 2986 | *P. subrigidum* | EU665276 | KX246431 | KX246587 | — | KX246469 | KX246510 | — |
| Widhelm & Egan 618-A | 2987 | *P. preperforatum* | EU665286 | — | KX246588 | KX246625 | KX246470 | KX246511 | KX246548 |
| Widhelm & Egan 618-B | 2988 | *P. preperforatum* | EU665287 | KX246432 | KX246589 | KX246626 | KX246471 | KX246512 | KX246549 |
| Widhelm & Egan 618-C | 2989 | *P. preperforatum* | EU665302 | KX246433 | KX246590 | KX246627 | KX246472 | KX246513 | KX246550 |
| Widhelm & Egan 619 | 2990 | *P. hypoleucinum* | EU665277 | KX246434 | — | KX246628 | KX246473 | KX246514 | KX246551 |
| Widhelm & Egan 653-B | 2991 | *P. perforatum* | EU665258 | — | — | KX246629 | — | — | KX246552 |
| Widhelm & Egan 653-C | 2992 | *P. perforatum* | EU665305 | — | — | — | KX246474 | KX246515 | — |

Table XV, CONTINUED

| Collection data | F.M. DNA # | Species | *GPD* | IGS | ITS | MS456 (Mcm7) | nuLSU | *RPB1* | MS277 (*Tsr1*) |
|---|---|---|---|---|---|---|---|---|---|
| Widhelm & Egan 654-AA | 2993 | *P. subrigidum* | EU665261 | KX246435 | KX246591 | KX246630 | KX246475 | KX246516 | KX246553 |
| Widhelm & Egan 654-C | 2994 | *P. subrigidum* | EU665306 | KX246436 | KX246592 | KX246631 | — | KX246517 | KX246554 |
| Widhelm & Egan 654-D | 2995 | *P. subrigidum* | EU665307 | KX246437 | KX246593 | KX246632 | — | KX246518 | KX246555 |
| Widhelm & Egan 654a | 2996 | *P. preperforatum* | EU665260 | — | KX246594 | — | KX246476 | KX246519 | KX246556 |
| Widhelm & Egan 655 | 2997 | *P. perforatum* | EU665259 | — | KX246595 | KX246633 | KX246477 | KX246520 | KX246557 |
| Widhelm & Egan 656 | 2998 | *P. hypotropum* | EU665257 | KX246438 | KX246596 | KX246634 | KX246478 | KX246521 | KX246558 |
| Widhelm & Egan 657 | 2999 | *P. subrigidum* | EU665268 | KX246439 | KX246597 | KX246635 | KX246479 | KX246522 | KX246559 |
| Widhelm & Egan 661 | 3000 | *P. louisianae* | EU665256 | KX246440 | KX246598 | KX246636 | KX246480 | KX246523 | KX246560 |
| Widhelm & Egan 663-A | 3001 | *P. perforatum* | EU665308 | KX246441 | KX246599 | KX246637 | KX246481 | — | KX246561 |
| Widhelm & Egan 663-B | 3002 | *P. perforatum* | EU665265 | KX246442 | KX246600 | KX246638 | KX246482 | KX246524 | KX246562 |
| Widhelm & Egan 663-C | 3003 | *P. perforatum* | EU665266 | — | KX246601 | KX246639 | KX246483 | — | KX246563 |
| Widhelm & Egan 664 | 3004 | *P. hypotropum* | EU665262 | KX246443 | KX246602 | — | KX246484 | — | KX246564 |
| Widhelm & Egan 665-A | 3005 | *P. louisianae* | EU665263 | KX246444 | — | — | KX246485 | KX246525 | KX246565 |
| Widhelm & Egan 665-B | 3006 | *P. louisianae* | EU665264 | — | KX246603 | KX246640 | KX246486 | KX246526 | KX246566 |
| Widhelm & Egan 666-B | 3007 | *P. hypoleucinum* | EU665290 | KX246445 | — | KX246641 | — | KX246527 | KX246567 |
| Widhelm & Egan 666-C | 3008 | *P. hypoleucinum* | EU665289 | KX246446 | KX246604 | — | KX246487 | KX246528 | KX246568 |
| Crespo & Sergio 4a | 3311 | *P. hypoleucinum* | — | KX246447 | — | — | KX246488 | — | — |
| Crespo & Sergio 4b | 3312 | *P. hypoleucinum* | — | KX246448 | — | — | KX246489 | KX246529 | — |

TABLE XVI. SAMPLE IDENTIFICATION AND GENBANK ACCESSION NUMBERS FOR LOCI FROM OUTGROUP TAXA.

| Species | Sample ID | ITS | nuLSU | *RPB1* | *Mcm7* | *Tsr1* | *GPD* |
|---|---|---|---|---|---|---|---|
| ***Parmotrema cetratum*** | Uruguay: Maldonado, Osorio 9424 (MVM, MAF-Lich 7649) | AY586576 | AY584847 | EF092143 | KR995649 | — | — |
| ***Parmotrema crinitum*** | Portugal: Lisboa, Crespo s.n. (MAF-Lich 6061) | AY586565 | AY584837 | GU994723 | KR995650 | — | — |
| ***Parmotrema crinitum*** | Spain: Tenerife, Crespo & Divakar s.n. (MAF-Lich 16119) | — | — | — | — | KP888272 | |
| ***Parmotrema fistulatum*** | — | — | — | — | — | — | AY249621 |
| ***Parmotrema fistulatum*** | Uruguay: Maldonado, Geymonat, 9423 (MVM, MAF -Lich 7655) | AY581057 | AY578920 | GU994724 | KR995651 | KP888273 | — |
| ***Parmotrema haitiense*** | Australia: Australian Capital Territory, Lowhoff et al. s.n. (MAF-Lich 7657) | AY581055 | AY578918 | EF092144 | KR995652 | KP888274 | — |
| ***Parmotrema perlatum*** | Portugal: Sintra, Crespo et al. s.n. (MAF-Lich 6965) | AY586566 | AY584838 | EF092146 | — | — | — |
| ***Parmotrema perlatum*** | Spain: Tenerife, Crespo & Divakar s.n. (MAF-Lich 16122) | — | — | — | KR995656 | KP888277 | — |
| ***Parmotrema perlatum*** | — | — | — | — | — | — | AY249618 |
| ***Parmotrema pilosum*** | Uruguay: Maldonado, Sacarabino (MAF-Lich 7656) | AY581056 | AY578919 | GU994728 | KR995657 | KP888278 | — |
| ***Parmotrema reticulatum*** | Portugal: Lisboa, Crespo s.n. (MAF-Lich 6067) | AY586579 | AY584850 | GU994729 | KR995658 | — | — |
| ***Parmotrema reticulatum*** | | — | — | — | — | — | AY249617 |

### 5.2.2 Molecular methods

Total genomic DNA was isolated from a ca. 30 mg fragment of each thallus using the DNeasy Plant Mini kit (Qiagen, Valencia, CA) following the manufacturer's instructions except grinding was done with 50 µL of lysis buffer and a pinch of sand in a porcelain mortar and pestle. If apothecia were present on the thallus, DNA was extracted from a fragment that was approximately 50-100% apothecia by mass. On thalli without apothecia, lobes were used for DNA isolation. Fungal specific primers (Table XVII) were used to amplify seven nuclear loci. Of these, three were ribosomal loci: the whole internal transcribed spacer (ITS: ITS1, 5.8S, ITS2), a portion of the intergenic spacer (IGS), and a portion of the large subunit (nuLSU). The other four were low-copy protein coding genes, including glyceraldehyde-3-phosphate-dehydrogenase (*GPD*), DNA replication licensing factor (*Mcm7*), ribosome biogenesis protein (*Tsr1*), and the largest subunit of RNA polymerase II (*RPB1*). Parameters for amplifying the ITS followed Blanco *et al.* (Blanco et al. 2005), and amplification of IGS and nuLSU employed a 66 °–56 ° C touchdown cycle (Lindblom and Ekman 2006). For *GPD*, part of the protein coding region spanning three exons and three introns were PCR-amplified using the parameters described in Myllys, Lohtander, & Tehler (Myllys, Lohtander, and Tehler 2001). The *Mcm7*, *Tsr1,* and *RPB1* loci were amplified as in Schmitt *et al.*, (Schmitt et al. 2009). Unincorporated dNTP and primers for all amplified loci were removed enzymatically by adding 5 units ExoI (Promega) and 0.5 unit shrimp alkaline phosphatase (Promega) to 5 µL of PCR product. The reaction was incubated at 37°C for 45 minutes and 80°C for 15 minutes to deactivate the enzymes. PCR products were used as templates for direct forward and reverse sequencing with BigDyeTerminator v3.1 chemistry. The *GPD* sequencing reactions were run on an ABI 3730 48-capillary electrophoresis DNA analyzer sequencer (Applied Biosystems, Foster City, CA) at the DNA Sequencing and

Genotyping Core Facility (University of Nebraska Medical Center, Omaha, NE). The other genes (ITS, nuLSU, IGS, *RPB1*, *Mcm7*, *Tsr1*) were sequenced on the ABI 3730 48-capillary electrophoresis DNA analyzer sequencer in the Pritzker Laboratory at the Field Museum.

TABLE XVII. PRIMERS USED FOR PCR AMPLIFICATION AND SEQUENCING NUCLEAR RIBOSOMAL IGS, ITS, NULSU AND PROTEIN CODING GENES *GPD, MCM7, RPB1,* AND *TSR1*.

| Marker | Primer name | Forward primer sequence | Annealing temperature °C | Reference |
|---|---|---|---|---|
| IGS | XIGS_F | 5′-GCCGMTGGCTATCATTATCC-3′ | 56–65 (touchdown) | This study |
| | XIGS_R | 5′-TACTGGCAGAATCARCCAGG-3′ | | Leavitt *et al.* (2011) |
| ITS | ITS1F | 5′-CTTGGTCATTTAGAGGAAGTAA-3′ | 56–65 (touchdown) | Gardes & Bruns (1993) White *et al.* (1990) |
| | ITS4a | 5′-TCCTCCGCTTATTGATATGC-3′ | | |
| nuLSU | AL2R | 5′-GCGAGTGAAGCGGCAACAGCTC-3′ | 56–65 (touchdown) | Mangold *et al.* (2008) |
| | LR3 | 5′-CCGTGTTTCAAGACGGG-3′ | | Vilgalys & Hester (1990) |
| *GPD* | GPD1-LM | 5′-ATTGGCCGCATCGTCTTCCGCAA-3′ | 60 | Myllys *et al.* (2002) |
| *Mcm7* | GPD2-LM | 5′-CCCACTCGTTGTCGTACCA-3′ | 56 | Myllys *et al.* (2002) |
| | Mcm7-709F | 5′-ACIMGIGTITCVGAYGTHAARCC-3′ | | Schmitt *et al.* (2009) |
| | Mcm7-1348R | 5′-GAYTTDGCIACICCIGGRTCWCCCAT-3′ | | Schmitt *et al.* (2009) |
| *RPB1* | 9RPB1-A | 5′-GARTGYCCDGGDCAY-3′ | 50 | Stiller & Hall (1997) Matheny *et al.* (2002) |
| *Tsr1* | fRPB1-C | 5′-CCNGCDATNTCRTTRTCCATRTA-3′ | 49 | Schmitt *et al.* (2009) |
| | Tsr1-1459for | 5′-CCIGAYGARATYGARCTICAYCC-3′ | | |
| | Tsr1-2308rev | 5′-CTTRAARTAICCRTGIGTICC-3′ | | Schmitt *et al.* (2009) |

### 5.2.3 Sequence alignment and phylogenetic analysis

Contigs were assembled with Vector NTI 10.1.1 (Invitrogen, Carlsbad, CA) and Geneious 8.1.7 (Biomatters, Auckland, New Zealand). Traces were carefully examined for double peaks. If a base call was ambiguous in one read but unambiguous in the complementary

strand sequence, the nucleotide was called as unambiguous. Sequences were aligned with default settings by MUSCLE implemented in Geneious 8.1.7. Data matrix concatenation was also performed in Geneious 8.1.7.

Phylogenetic relationships were inferred using maximum likelihood (ML) and Bayesian inference (BI), in addition to the multispecies coalescent species tree approach. Analyses of individual gene tree topologies yielded no well-supported (≥ 70% bootstrap values) conflicts, thus phylogenetic relationships were estimated from a seven locus concatenated data matrix using a total-evidence approach (Kluge 1989). The data matrix had approximately 14% missing data; however, phylogenetic analyses have been shown to accurately infer relationships if many characters are sampled overall (Wiens and Morrill 2011). For the ML analysis, we used RAxML v8.0.0 (Stamatakis 2014) to reconstruct the concatenated ML gene-tree. We implemented the GTRGAMMA model and evaluated nodal support using 1000 bootstrap pseudoreplicates. PartitionFinder v1.1.1 (Lanfear et al. 2012) was used to infer the best-fitting partitioning scheme. The input file contained a total of 32 partitions, corresponding to ribosomal RNA genes (5.8s, nuLSU) and spacer regions (IGS, ITS1, ITS2) in the ribosomal repeat regions, introns in protein coding genes (three in *GPD* and two in *RPB1*) and first, second, and third codon positions of each exon of the protein coding genes (*GPD, Mcm7, RPB1, Tsr1*). We used the "greedy" algorithm (heuristic search) with branch lengths estimated as "linked" implemented in PartitionFinder where only one underlying set of branch lengths is estimated. We used the Bayesian Information Criterion (BIC) as implemented in PartitionFinder. We also reconstructed phylogenetic relationships using the concatenated matrix under a Bayesian approach using BEAST v1.8.0 (A J Drummond and Rambaut 2007). The same partitioning scheme that was used in the ML analysis was also used in the Bayesian analysis. We ran two independent Markov

Chain Monte Carlo (MCMC) chains for 20 million generations, implementing a relaxed lognormal clock and a constant coalescent speciation process prior. The first 25% of generations were discarded as burn-in and the remaining trees from the two runs were combined in the program LogCombiner v2.0 (Alexei J. Drummond et al. 2012).

### 5.2.4 Inference of putative populations

We used the Bayesian clustering program STRUCTURE v.2.3.2 to identify genetic groups without a priori knowledge within the *P. perforatum* group. While STRUCTURE assumes independence of all loci (no linkage), previous studies have demonstrated that single nucleotide polymorphisms (SNPs) from multilocus DNA sequence data can also effectively recover population structure (O'Neill et al. 2013; Altermann et al. 2014). Therefore, we reduced our concatenated, multi-locus dataset to include only polymorphic sites for the STRUCTURE analyses. Indels and 'N's were ignored for the purpose of the SNP identification. We explored the population assignments for K values ranging from 1 to 10, with 10 replicate runs per K value. We used the admixture options, and each mcmc run consisted of 50,000 burn-in generations, followed by 50,000 iterations. Results of the STRUCTURE analyses were evaluated using the Structure Harvester webserver (Earl and vonHoldt 2012), and the optimal number of genetic clusters was inferred using the ΔK method (Evanno, Regnaut, and Goudet 2005).

### 5.2.5 Species tree inference

We used a coalescent-based hierarchical Bayesian model *BEAST implemented in BEAST v2.0.0 (Drummond and Rambaut 2007; Drummond, Xie, and Heled 2009) to estimate species trees. *BEAST incorporates the coalescent process and the uncertainty associated with gene trees and nucleotide substitution model parameters and estimates the species tree directly from the sequence data (Drummond, Xie, and Heled 2009). Population assignments are required

a priori for *BEAST analyses, and we assigned each individual to species based on two putative population hypotheses: 1) the traditional classification of reproductive mode and chemical profile determined by TLC for a total of six different populations and 2) the three species scenario inferred from the STRUCTURE analysis. We employed bModelTest (Bouckaert 2015), a Bayesian approach implemented in BEAUti, to estimate nucleotide site substitution model for each of the six sequence alignments which were treated as separate partitions (*GPD*, ITS, *Mcm7*, nuLSU, *RPB1* and *Tsr1*) in the *BEAST analysis. Two independent MCMC runs of 100 million generations were executed with sampling at every 2000 steps. Chain mixing and convergence were evaluated in Tracer v1.6 (Rambaut et al. 2014) making sure that ESS values were greater than 200. We discarded the first 25% of trees as burn-in and the remaining trees from the two runs were combined in the program LogCombiner v2.0 (Drummond et al. 2012), and the final MCC tree was estimated from the combined posterior distribution of the trees using TreeAnnotator v2 (Drummond et al. 2012). Likelihood values of each species tree (three-species and six-species) were compared with a likelihood ratio test in R, to see which model better describes the data.

### 5.2.6 Species delimitation

The program BP&P v3.2 (Yang and Rannala 2010) was used to estimate Bayesian posterior probability distributions for alternative models of species delimitation (speciation probabilities). For the BP&P analysis we tested the two hypotheses of species inference found in STRUCTURE (three species scenario) and the traditional circumscription (six species scenario) by using the *BEAST species trees as guide trees from each analysis. In the six species scenario, the six currently accepted taxa were taken as putative species and two starting tree topologies, one representing the traditional hypothetical relationships and the other representing the

*BEAST species tree, were used for each analysis. The gamma prior G (2, 2000) was used on the population size parameters and on sequence divergence, while the Dirichlet prior was assigned to other divergence time parameters. Each was run twice to confirm consistency between runs.

## 5.3 Results

### 5.3.1 Sympatry of *Parmotrema perfomatum* group species

Collection data from 25 sites showed that the distributions of all six species in the *P. perforatum* group species overlap in a ca. 15,000 $km^2$ area in eastern Texas and western Louisiana. All specimens were collected on hardwood tree species; none were found on conifers at these sites. Four to six species co-occurred within an area of ca. 100 m2 at each of our four sampled sites (Table XIV). Differences in abundance and combination of taxa varied at different sites. Such extensive co-occurrence of the North American species of the *Parmotrema perforatum* group was unexpected, having never been reported before. All specimens were collected on hardwood tree species.

### 5.3.2 Sequences and alignment

We generated 276 new sequences from seven loci for this study. The data set of 46 individuals produced a concatenated alignment that spanned 4726 bp. All sequences were submitted to Genbank (Table XV). Approximately 14% of sequences were missing from the concatenated matrix.

### 5.3.3 Phylogenetic analysis

The ML phylogeny estimated from the concatenated 7-locus dataset (Figure 16) recovered three well-supported, major clades in the *P. perforatum* group individuals sampled. Clade A was comprised of all *P. perforatum s. str*. specimens and a single specimen identified as *P. hypotropum*; all these specimens contain only norstictic acid. Clade B included all specimens

identified as *P. subrigidum* and *P. louisianae*, all of which produce alectoronic acid. Clade C, was comprised of all *P. preperforatum* and *P. hypoleucinum* specimens and all but one specimen of *P. hypotropum* specimens. Clade C has a mixture of chemical profiles, including individuals with stictic and norstictic acids and individuals with only norstictic acid. All specimens of *P. perforatum s. str*. were recovered as monophyletic, but its hypothetical species pair, *P. hypotropum* was polyphyletic, appearing in both Clades A and C. The species pair of *P. subrigidum* and *P. louisianae* clustered together in one monophyletic clade, but neither of these was recovered as monophyletic within Clade B. In Clade C, *P. preperforatum* was paraphyletic and *P. hypoleucinum* was polyphyletic with some of the *P. hypoleucinum* individuals intermixed with the *P. preperforatum* clade and the other two, from Europe, clustering with specimens of *P. hypotropum*. Each clade contained both apotheciate and sorediate specimens. The BI topology inferred from the concatenated seven-locus data matrix in BEAST was congruent with the ML topology.

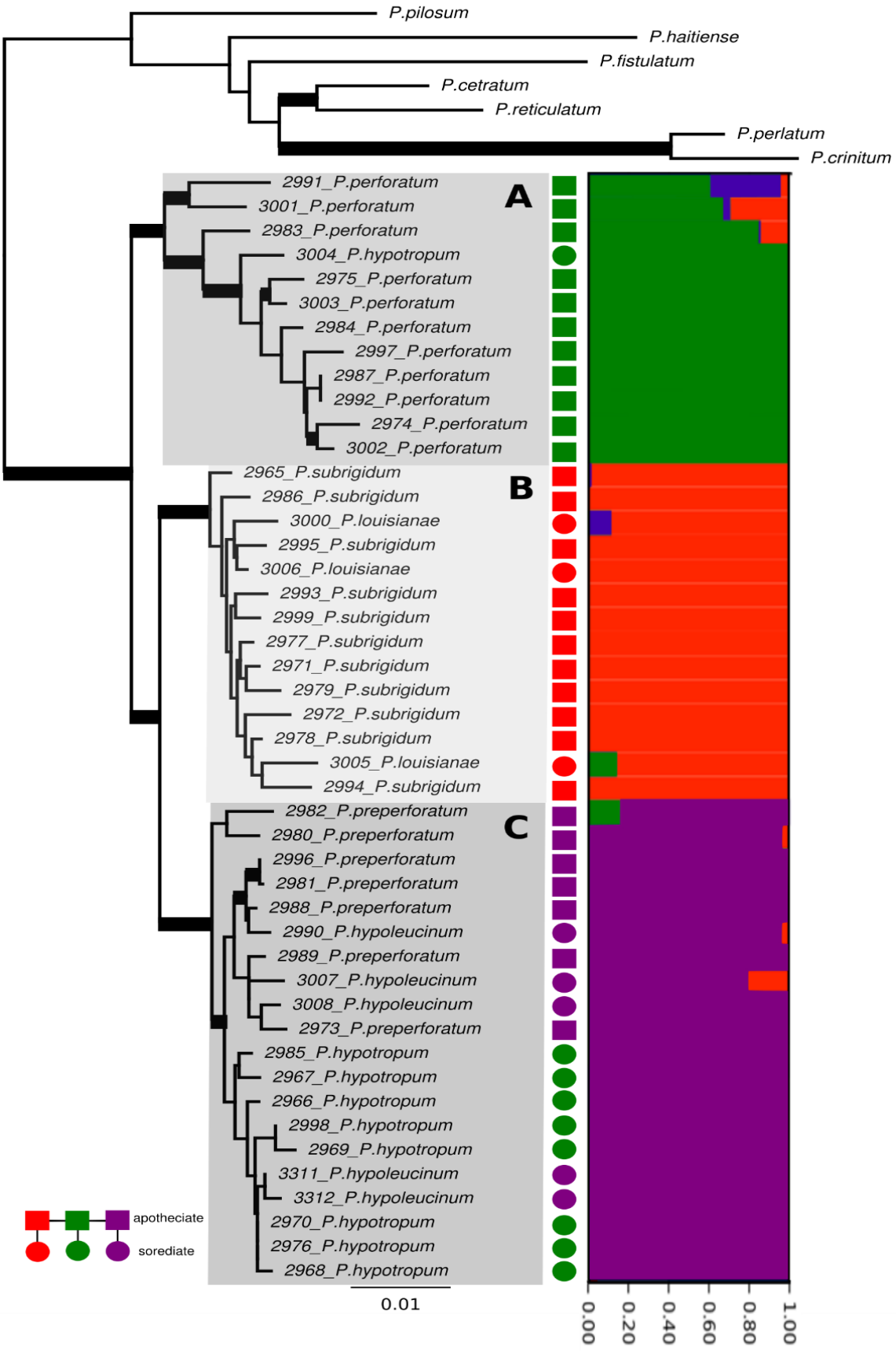
P.pilosum
P.haitiense
P.fistulatum
P.cetratum
P.reticulatum
P.perlatum
P.crinitum
A
2991_P.perforatum
3001_P.perforatum
2983_P.perforatum
3004_P.hypotropum
2975_P.perforatum
3003_P.perforatum
2984_P.perforatum
2997_P.perforatum
2987_P.perforatum
2992_P.perforatum
2974_P.perforatum
3002_P.perforatum
B
2965_P.subrigidum
2986_P.subrigidum
3000_P.louisianae
2995_P.subrigidum
3006_P.louisianae
2993_P.subrigidum
2999_P.subrigidum
2977_P.subrigidum
2971_P.subrigidum
2979_P.subrigidum
2972_P.subrigidum
2978_P.subrigidum
3005_P.louisianae
2994_P.subrigidum
C
2982_P.preperforatum
2980_P.preperforatum
2996_P.preperforatum
2981_P.preperforatum
2988_P.preperforatum
2990_P.hypoleucinum
2989_P.preperforatum
3007_P.hypoleucinum
3008_P.hypoleucinum
2973_P.preperforatum
2985_P.hypotropum
2967_P.hypotropum
2966_P.hypotropum
2998_P.hypotropum
2969_P.hypotropum
3311_P.hypoleucinum
3312_P.hypoleucinum
2970_P.hypotropum
2976_P.hypotropum
2968_P.hypotropum
apotheciate
sorediate
0.01
0.00
0.20
0.40
0.60
0.80
1.00

Figure 16. Phylogeny of the *Parmotrema perforatum* group with other *Parmotrema* species selected as outgroup inferred from a seven locus data set as the most likely tree in a ML analysis which was congruent with the BEAST BI. Support was evaluated with ML bootstrap proportions (BS) and bayesian posterior probabilities (BPP) which are mapped onto the branches. Support is depicted as the bold branches: (ML-BS>75 / BPP>95). Colours represent chemical composition of the sample collected inferred by TLC (green = norstictic acid only, red = alectoronic acid, purple = norstictic+stictic acid). Apotheciate (sexual) species are depicted as squares while sorediate (asexual) species are shown as circles.

The partitioning strategy inferred with PartitionFinder resulted in three partitions: (I) the first codon position in the first exon, the third codon position in the second exon, and the second codon position of the third exon and all three introns for *GPD*; all of IGS, 18S, ITS1, and ITS2; the third codon position for *Mcm7*; the second codon in the first exon and third codon in the second exon and both introns for *RPB1*; and the first and third codon positions for *Tsr1*; (ii) the second and third codon positions of the first exon, and the first position in the second exon of *GPD*; the first and second codon positions of *Mcm7*; the first codon position of the first and second exons in *RPB1*; the second codon position of *Tsr1*; and all of the nuLSU; and (iii) the 5.8s gene; the second codon position of the second exon and the first and third codon positions of the third exon in *GPD*; and the third codon position of the first exon and the second codon position of the second exon in *RPB1*. The GTR+G model was used for the first and third partitions while the GTR+I+G was used for the second partition as these were found to be the best fitting nucleotide substitution models in PartitionFinder.

### 5.3.4 Inference of putative population clusters

Bayesian clustering using STRUCTURE resulted in strong support for three distinct populations, congruent with the concatenated ML and Bayesian phylogenetic clades A, B, and C.

Most individuals showed little evidence of admixed genomes (probability of assignment to a single genetic cluster >0.95), although a limited number of individuals showed evidence of admixture (Figure 16). Likelihood values in the STRUCTURE analysis peaked at K=3, and the ad hoc ΔK approach supported a three population model as well (Evanno, Regnaut, and Goudet 2005) (Figure 17).

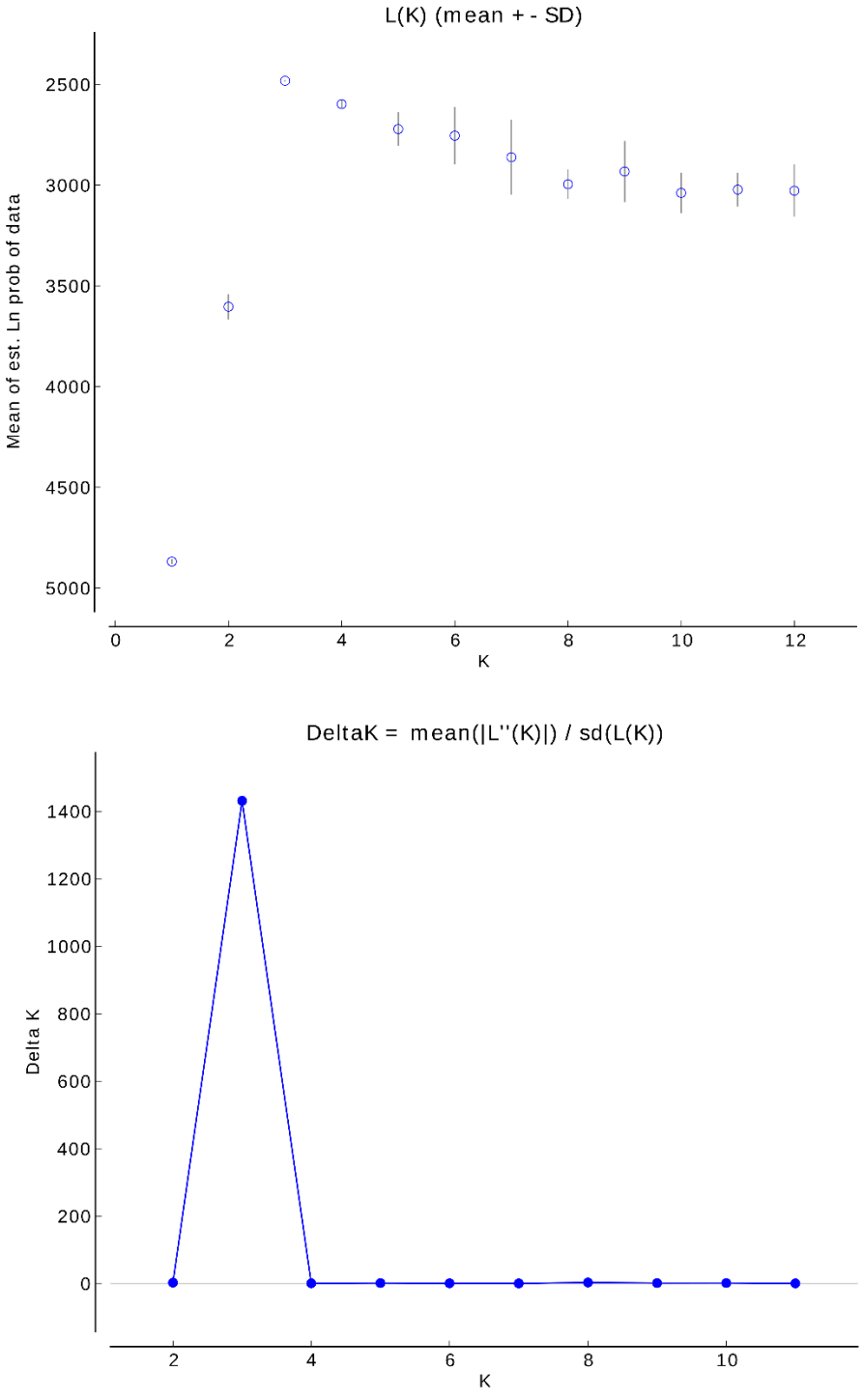


Figure 17. A, Mean L(K) (±SD) over ten runs for each K value. B, ΔK calculated as ΔK = m|L”(K)|/s[L(K)]. The modal value of this distribution is the true K(*) or the uppermost level of structure, here three clusters.

### 5.3.5 Species tree inference

In both *BEAST analyses, run lengths generated effective sample size (ESS) values in the thousands and tree topologies were congruent across independent runs. Figure 16 shows the results of the three species scenario, where asterisks denote the topology recovered by *BEAST. The three species tree is congruent with the backbone branches of the concatenated phylogeny and recovering the three species A, B, and C with PP support greater than 90 on all branches. Figure 18 shows the MCC species tree with PP support from the *BEAST analysis indicated in above the branches. In Figure 18, BP&P species delimitation PP values are shown in italics by the names of putative species and in the nodes to show the PP of combined putative species. The topology of the species tree mirrors the backbone of the ML tree in Figure 17. The *P. perforatum* group was inferred as monophyletic and all branches were highly supported (PP >90) except the clade of *P. preperforatum* and *P. hypoleucinum* (PP = 0.87), which was sister to *P. hypotropum*. Sister to this clade was the clade of the alectoronic acid containing species *P. subrigidum* and *P. louisianae* and sister to the rest of the group was *P. perforatum*.

The likelihood values of the species trees inferred in *BEAST was -10568.3934 and -10575.2822 for the three- and six-species trees respectively. A chi-squared test of the likelihood ratio had a *p*-value=0, indicating that the three-species model is significantly better than the six-species model at explaining the model.

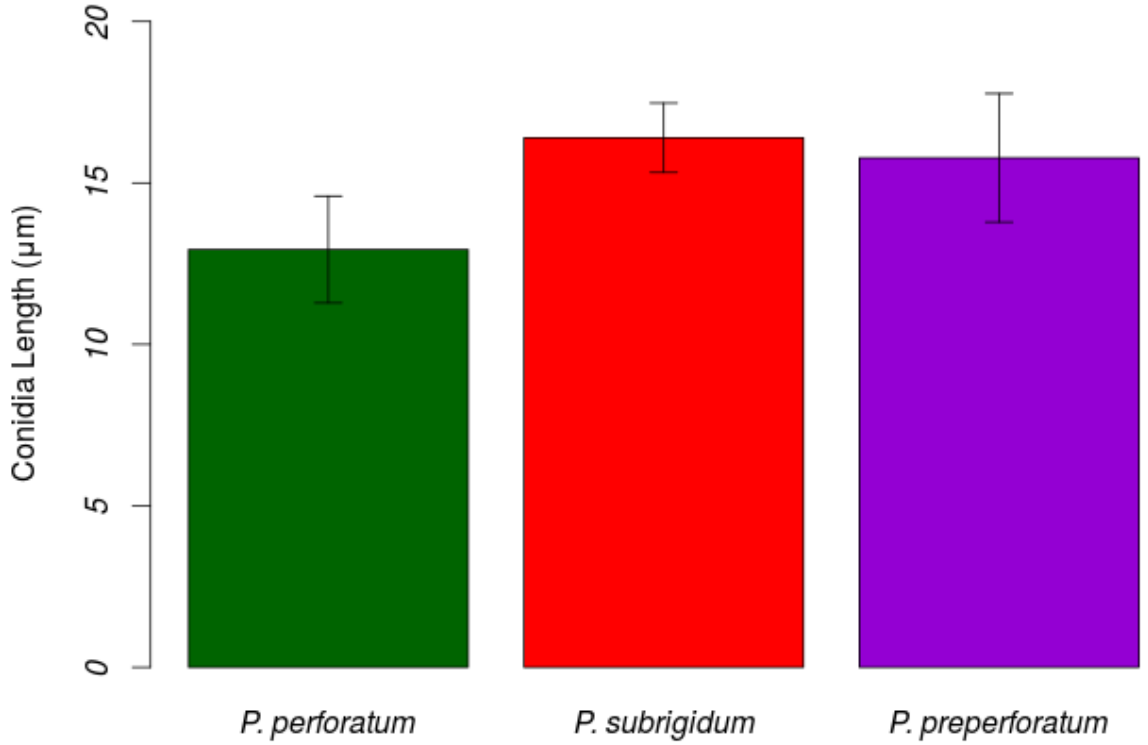


Figure 18. Average conidia length of apotheciate (sexually reproducing) species of the PPG.

### 5.3.6 Species delimitation analysis

In the three species scenario, BP&P inferred a final species tree that was congruent with the *BEAST three-species tree. It is depicted in Figure 16 by asterisks above the branches. BP&P delimited the three species A, B, and C all with PP = 1.

Despite the difference in starting tree topologies in the six species scenario, BP&P consistently inferred a final species tree topology that was congruent with the *BEAST species tree in Figure 18. Each run consistently delimited four previously described species (*P.*

*perforatum, P. hypotropum, P. subrigidum*, and *P. louisianae*) and combined *P. preperforatum* and *P. hypoleucinum* into one species. All species were delimited with high speciation probabilities (PP > 95).

### 5.3.7 Micromophological measurements

In total, 143 conidia from the sexually reproducing specimens of the *P. perforatum* group were measured. Average conidia length was 12.9 ± 1.7 µm, 16.4 ± 1.1 µm and 15.8 ± 2.0 µm for *P. perforatum*, *P. subrigidum* and *P. preperforatum*, respectively (Figure 19).

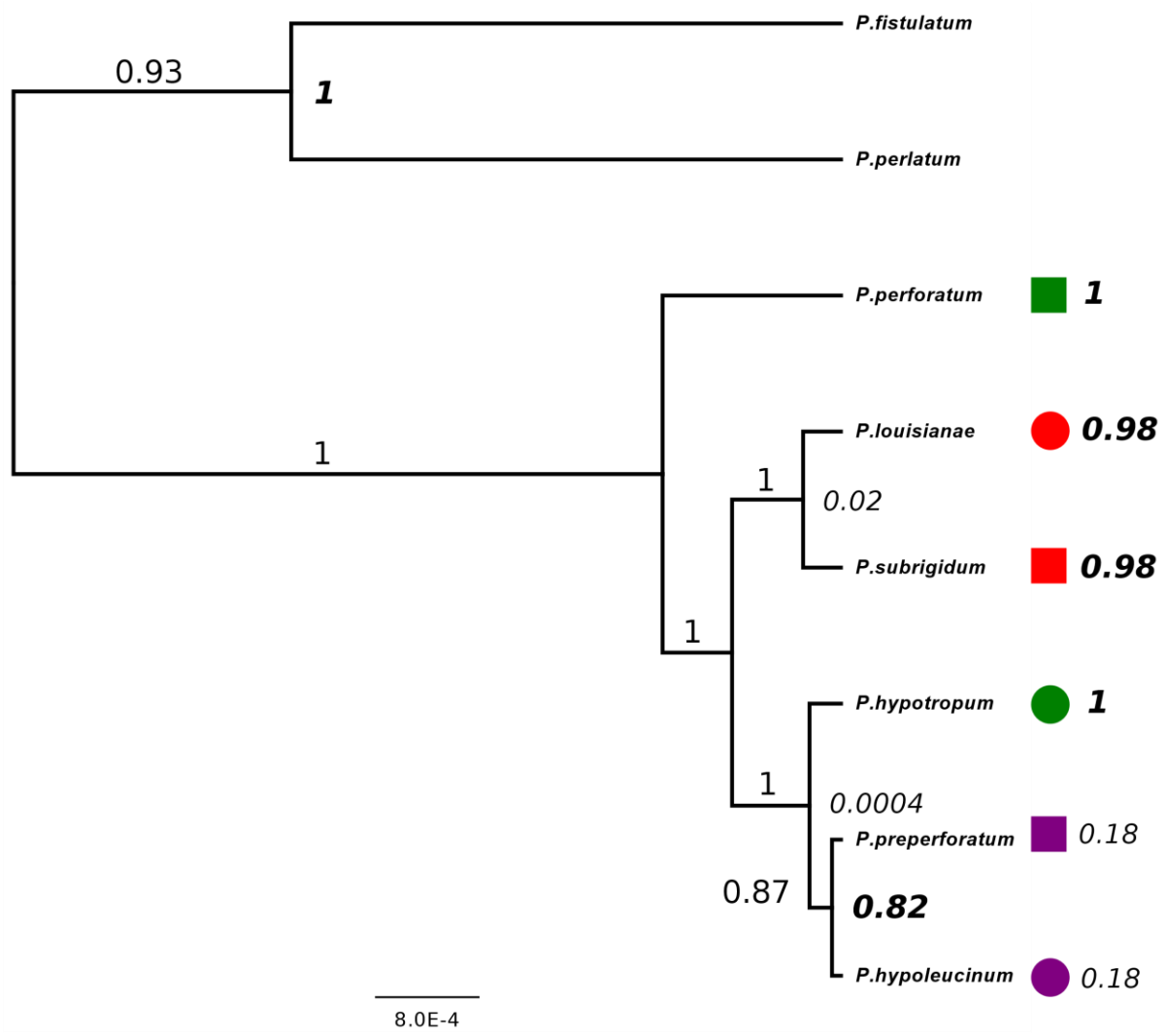


Figure 19. *BEAST species tree for the *Parmotrema perforatum* group. Posterior probabilities at branches indicate support from the *BEAST analysis. The posterior probability of each delimited species calculated by BP&P are indicated in italics in front of each putative species or in the node indicating the support if the two species are combined by BP&P. The highly supported BP&P posterior probabilities are shown in bold.

## 5.4 Discussion

Our study provides an important case study highlighting the importance of considering independent lines of evidence and analytical approaches for effectively delimiting species in taxonomically challenging groups. An integrative approach incorporating phenotypic characters (secondary metabolite variation, differences in reproductive strategies, and conidial size), analyses of molecular sequence data using Bayesian clustering, ML and BI phylogenetic inference and a coalescent-based species-tree method, and empirical species delimitation analysis in BP&P, provides unprecedented insight into species boundaries and evolutionary relationships in the *P. perforatum* group. We approached the delimitation of species in two ways. The first employed the Bayesian clustering algorithm STRUCTURE to infer putative populations. This approach was congruent with the concatenated phylogeny, inferring three populations that corresponded with the three major clades A, B, and C (Figure 16). Individuals were then assigned to their population for inferring a *BEAST species tree. This tree was used as a starting topology in BP&P for species delimitation. The three-species scenario was highly supported by all analysis methods (Figure 16). The second approach used a six-species scenario assigning individuals to their traditional circumscribed species to infer a *BEAST species tree (Figure 18). This topology was used as a starting tree in the BP&P species delimitation. This approach supported the distinctiveness of the traditionally recognized taxa *P. perforatum*, *P. hypotropum, P. subrigidum* and *P. louisianae*, while *P. preperforatum* and *P. hypoleucinum* were found to be conspecific. Although our results highlight the fact that secondary metabolite variation and differences in reproductive mode can serve as taxonomically relevant characters in *Parmotrema*, traditional species pair concepts and chemotaxonomy are not reflected in evolutionary relationships.

Before secondary chemistry was integrated into the taxonomic treatment of the *P. perforatum* group, only two species, *Parmelia perforata* (apotheciate-fertile) and *P. hypotropa* (sorediate-sterile) were recognized as distinct, based solely on reproductive strategy. However, inclusion of secondary chemical data revealed six diagnosable populations. Culberson (1973) discussed what he considered to be the best taxonomic treatment of species in the *P. perforatum* group and claimed that all the chemical races of the apotheciate morph were sister species, each with a sorediate counterpart considered a secondary species. Based on this interpretation, he described a number of new species (Culberson 1973). By incorporating multilocus sequence data, we have added another valuable resource for species delimitation.

### 5.4.1 Evolutionary relationships

The ML and BI concatenated phylogenies and the Bayesian clustering program STRUCTURE (Figure 16) recovered well-supported clades that corresponded to the secondary chemistry of specimens, providing support for Culberson's (1973) original hypothesis of chemospecies. For example, all apotheciate-fertile chemically unique specimens were in separate, well-supported clades. However, the relationships among these clades did not correlate with the similarity of secondary chemistries. Alectoronic acid, an orcinol-type depsidone, is distinct from norstictic and stictic acids, which are both β-orcinol-type depsidones; the latter two differ only by the degree of *O*-methylation. Based on the chemical structure of secondary compounds, we would expect that the two clades that contain norstictic acid (Figure 17, Clades A and C) would be sister, but instead, the species containing alectoronic acid (*P. subrigidum* and *P. louisianae*, Figure 16, Clade B) were sister to the clade containing *P. preperforatum* (Figure 16, Clade C). This relationship was also observed in the species trees approach of *BEAST (Figure 18). The BP&P species tree provided the same topology with the highest support of all analyses

even when the starting tree matched the traditional hypothesis proposed by Culberson (1973). The observed evolutionary relationships found in all DNA sequence analyses were further confirmed by conidial length data (Figure 19); conidia from *P. perforatum* were smaller (average conidia length 12.9 ± 1.7 μm) than those of *P. subrigidum* and *P. preperforatum* (average lengths of 16.4 ± 1.1 μm and 15.8 ± 2.0 μm respectively).

Culberson (1973) considered the sorediate taxa (secondary species) to be derived from their apotheciate counterpart (primary species), thus forming closely related species pairs. Most studies that address the issue of species pairs find the two species of the pair to be monophyletic in molecular phylogenies (Myllys, Lohtander, and Tehler 2001; Lohtander, Källersjö, and Tehler 1998; Lohtander et al. 2000; Articus et al. 2002; Cubero et al. 2004; Buschbom and Mueller 2006; Wirtz, Printzen, and Lumbsch 2012; Lohtander et al. 1998). However, of the sorediate-sterile individuals of *P. hypotropum*, which only contains norstictic acid, only one specimen clustered with its primary counterpart *P. perforatum* (Figure 16, Clade A), and most specimens formed a clade that was sister to the stictic acid clade of *P. preperforatum* (Figure 16, Clade C). This was unexpected, since *P. hypotropum* was hypothesized to be a derived sterile species pair from *P. perforatum* (Culberson 1973). This evolutionary relationship was further corroborated using the coalescent-based species tree inference programs *BEAST and BP&P, both of which placed *P. hypotropum* sister to the stictic acid clade (Figure 18).

In the other sorediate-sterile taxon, *P. hypoleucinum*, all specimens collected in North America clustered with chemically similar specimens of the apotheciate counterpart *P. preperforatum*, but the individuals from Europe clustered with the *P. hypotropum* sub-clade in Clade C on the ML phylogeny (Figure 16). In the alectoronic clade, *P. louisianae* was always clustered with chemically similar specimens of apotheciate *P. subrigidum* in their own

monophyletic clade (Clade B, Figure 16) with no support for the two to be distinct species, but *BEAST and BP&P always recovered them as distinct lineages with high PP support (Figure 19).

### 5.4.2 Species delimitation

The analyses of the seven-locus concatenated dataset gave us a first look at the relationships of the individuals in the group, suggesting hypotheses of independently evolving lineages. However, with gene concatenation, there still is the possibility that loci have different evolutionary histories and inaccurate inferences could be drawn (DeGiorgio et al. 2014). Also, species delimitation based on monophyly of clades of genes is usually highly supportive for determining boundaries, but it is not necessary and can potentially lead to inaccurate delimitations (Ross, Murugan, and Li 2008). To address these potential issues, we employed a coalescent-based model to identify well-supported species and to quantify the probability of evolutionary divergence to avoid the possible bias from single-gene or concatenated phylogenies (Knowles and Carstens 2007; Fujita et al. 2012). The species tree generated by the MSC program *BEAST (Figure 18) generally corroborated the topology of the ML phylogeny (Figure 17). This topology was used as a starting tree in the species delimitation program BP&P which is able to detect evolutionary lineages even if they are recently diverged (Yang and Rannala 2010). Using BP&P, all traditional species were delimited with high support values (PP >95%) with the exception of *P. preperforatum* and *P. hypoleucinum* which were consistently combined into one species in multiple analyses.

## 5.5 Conclusions

Our analyses support the presence of three to five distinct species-level lineages in the *Parmotrema perforatum* group in eastern Texas and western Louisiana depending. Using only

DNA sequence data, three populations were inferred with the Bayesian clustering program STRUCTURE and in the concatenated ML and BI phylogenies, corresponding to clades A, B, and C. The MSC methods *BEAST and BP&P both highly supported the three species delimitation. However, when independent chemical and morphological data were included, a more detailed delimitation was the result. In the six-species situation, the currently circumscribed species, *P. perforatum*, *P. hypotropum, P. subrigidum and P. louisianae* were delimited using the MSC method BP&P, with the exception of the chemically identical species pair of *P. preperforatum* and *P. hypoleucinum*, which were consistently recovered as conspecific. Furthermore, these species-level lineages were recovered with strong support in both concatenated and MSC species-tree topologies. Even though the six-species model is more fine-tuned, the likelihood ratio test, showed that the three-species model was significantly better. However, this result is difficult to accept completely at this stage, as we feel that more sampling may be necessary to get a clearer picture of species boundaries in the *P. perforatum* group.

This study provides a detailed investigation of the *P. perforatum* group in the Southern United States, integrating morphology, chemistry, concatenated molecular data and MSC-based methods; however, for a clearer picture of the species boundaries in this group, future studies should include a broader, worldwide sample.

**5.6 References**

Agapow, Paul-Michael, Olaf Bininda-Emonds, Keith A. Crandall, John L. Gittleman, Georgina M. Mace, Jonathon C. Marshall, and Andy Purvis. "The impact of species concept on biodiversity studies." *The Quarterly Review of Biology* 79, no. 2 (2004): 161-179.

Altermann, Susanne, Steven D. Leavitt, Trevor Goward, Matthew P. Nelsen, and H. Thorsten Lumbsch. "How do you solve a problem like *Letharia*? A new look at cryptic species in

lichen-forming fungi using Bayesian clustering and SNPs from multilocus sequence data." *PLOS ONE* 9, no. 5 (2014): e97556.

Amo de Paz, Guillermo, Paloma Cubas, Ana Crespo, John A. Elix, and H. Thorsten Lumbsch. "Transoceanic dispersal and subsequent diversification on separate continents shaped diversity of the *Xanthoparmelia pulla* group (Ascomycota)." *PLOS ONE* 7, no. 6 (2012): e39683.

Amo de Paz, Guillermo, Paloma Cubas, Pradeep K. Divakar, H. Thorsten Lumbsch, and Ana Crespo. "Origin and diversification of major clades in parmelioid lichens (Parmeliaceae, Ascomycota) during the Paleogene inferred by Bayesian analysis." *PLOS ONE* 6, no. 12 (2011): e28161

Articus, Kristina, Jan-Eric Mattsson, Leif Tibell, Martin Grube, and Mats Wedin. "Ribosomal DNA and β-tubulin data do not support the separation of the lichens *Usnea florida* and *U. subfloridana* as distinct species." *Mycological Research* 106, no. 4 (2002): 412-418.

Bickford, David, David J. Lohman, Navjot S. Sodhi, Peter KL Ng, Rudolf Meier, Kevin Winker, Krista K. Ingram, and Indraneil Das. "Cryptic species as a window on diversity and conservation." *Trends in Ecology & Evolution* 22, no. 3 (2007): 148-155.

Blanco, Oscar, Ana Crespo, Pradeep K. Divakar, John A. Elix, and H. Thorsten Lumbsch. "Molecular phylogeny of parmotremoid lichens (Ascomycota, Parmeliaceae)." *Mycologia* 97, no. 1 (2005): 150-159.

Bouckaert, Remco. "bModelTest: Bayesian site model selection for nucleotide data." *BioRxiv* 1 (2015): 20792.

Buschbom, Jutta, and Gregory M. Mueller. "Testing “species pair” hypotheses: evolutionary processes in the lichen-forming species complex *Porpidia flavocoerulescens* and *Porpidia*

*melinodes*." *Molecular Biology and Evolution* 23, no. 3 (2005): 574-586.

Carstens, Bryan C., Tara A. Pelletier, Noah M. Reid, and Jordan D. Satler. "How to fail at species delimitation." *Molecular Ecology* 22, no. 17 (2013): 4369-4383.

Crespo, Ana, Frank Kauff, Pradeep K. Divakar, Ruth del Prado, Sergio Pérez-Ortega, Guillermo Amo de Paz, Zuzana Ferencova et al. "Phylogenetic generic classification of parmelioid lichens (Parmeliaceae, Ascomycota) based on molecular, morphological and chemical evidence." *Taxon* 59, no. 6 (2010): 1735-1753.

Cubero, Oscar F., Ana Crespo, Theodore L. Esslinger, and H. Thorsten Lumbsch. "Molecular phylogeny of the genus *Physconia* (Ascomycota, Lecanorales) inferred from a Bayesian analysis of nuclear ITS rDNA sequences." *Mycological Research* 108, no. 5 (2004): 498-505.

Culberson, Chicita F. "Improved conditions and new data for identification of lichen products by standardized thin-layer chromatographic method." *Journal of Chromatography* 72, no. 1 (1972): 113-125.

Culberson, William Louis. "The *Parmelia perforata* group: niche characteristics of chemical races, speciation by parallel evolution, and a new taxonomy." *The Bryologist* (1973): 20-29.

Culberson, William Louis, and Chicita F. Culberson. "Parallel Evoluton in Lichen-Forming Fungi." *Science* 180, no. 4082 (1973): 196-198.

Dayrat, Benoit. "Towards integrative taxonomy." *Biological Journal of the Linnean Society* 85, no. 3 (2005): 407-417.

DeGiorgio, Michael, John Syring, Andrew J. Eckert, Aaron Liston, Richard Cronn, David B. Neale, and Noah A. Rosenberg. "An empirical evaluation of two-stage species tree inference strategies using a multilocus dataset from North American pines." *BMC*

*Evolutionary Biology* 14, no. 1 (2014): 67.

Del-Prado, Ruth, Oscar Blanco, H. Thorsten Lumbsch, Pradeep K. Divakar, John A. Elix, M. Carmen Molina, and Ana Crespo. "Molecular phylogeny and historical biogeography of the lichen-forming fungal genus *Flavoparmelia* (Ascomycota: Parmeliaceae)." *Taxon* 62, no. 5 (2013): 928-939.

Drummond, Alexei J., and Andrew Rambaut. "BEAST: Bayesian evolutionary analysis by sampling trees." *BMC Evolutionary Biology* 7, no. 1 (2007): 214.

Drummond, Alexei J., Marc A. Suchard, Dong Xie, and Andrew Rambaut. "Bayesian phylogenetics with BEAUti and the BEAST 1.7." *Molecular Biology and Evolution* 29, no. 8 (2012): 1969-1973.

Earl, Dent A. "STRUCTURE HARVESTER: A website and program for visualizing STRUCTURE output and implementing the Evanno method." *Conservation Genetics Resources* 4, no. 2 (2012): 359-361.

Egan, Robert S. "Correlations and non-correlations of chemical variation patterns with lichen morphology and geography." *The Bryologist* (1986): 99-110.

Esslinger, Theodore L. n.d. “A cumulative checklist for the lichen-forming, lichenicolous and allied fungi of the continental United States and Canada.” https://www.ndsu.edu/pubweb/~esslinge/chcklst/chcklst7.htm (Accessed November 30, 2015).

Evanno, Guillaume, Sebastien Regnaut, and Jérôme Goudet. "Detecting the number of clusters of individuals using the software STRUCTURE: A simulation study." *Molecular Ecology* 14, no. 8 (2005): 2611-2620.

Feuerer, Tassilo, and David L. Hawksworth. "Biodiversity of lichens, including a world-wide

analysis of checklist data based on Takhtajan's floristic regions." *Biodiversity and Conservation* 16, no. 1 (2007): 85-98.

Fujita, Matthew K., Adam D. Leaché, Frank T. Burbrink, Jimmy A. McGuire, and Craig Moritz. "Coalescent-based species delimitation in an integrative taxonomy." *Trends in Ecology & Evolution* 27, no. 9 (2012): 480-488.

Gardes, Monique, and Thomas D. Bruns. "ITS primers with enhanced specificity for basidiomycetes‐Application to the identification of mycorrhizae and rusts." *Molecular Ecology* 2, no. 2 (1993): 113-118.

Hawksworth, David L. "The magnitude of fungal diversity: The 1.5 million species estimate revisited." *Mycological Research* 105, no. 12 (2001): 1422-1432.

Heled, Joseph, and Alexei J. Drummond. "Bayesian inference of species trees from multilocus data." *Molecular Biology and Evolution* 27, no. 3 (2009): 570-580.

Jaklitsch, Walter, Hans-Otto Baral, Robert Lücking, H. Thorsten Lumbsch, and Wolfgang Frey. *Syllabus of Plant Families-A. Engler's Syllabus der Pflanzenfamilien Part 1/2*. Edited by Wolfgang Frey. Stuttgart: Borntraeger Science Publishers. (2016).

Kekkonen, Mari, Marko Mutanen, Lauri Kaila, Marko Nieminen, and Paul DN Hebert. "Delineating species with DNA barcodes: A case of taxon dependent method performance in moths." *PLOS ONE* 10, no. 4 (2015): e0122481.

Kluge, Arnold G. "A concern for evidence and a phylogenetic hypothesis of relationships among *Epicrates* (Boidae, Serpentes)." *Systematic Biology* 38, no. 1 (1989): 7-25.

Knowles, L. Lacey, and Bryan C. Carstens. "Delimiting species without monophyletic gene trees." *Systematic Biology* 56, no. 6 (2007): 887-895.

Kraichak, Ekaphan, Robert Lücking, Andre Aptroot, Andreas Beck, Patrick Dornes, Volker

John, James C. Lendemer et al. "Hidden diversity in the morphologically variable script lichen (*Graphis scripta*) complex (Ascomycota, Ostropales, Graphidaceae)." *Organisms Diversity & Evolution* 15, no. 3 (2015): 447-458.

Lanfear, Robert, Brett Calcott, Simon Ho, and Stephane Guindon. "PartitionFinder: Combined selection of partitioning schemes and substitution models for phylogenetic analyses." *Molecular Biology and Evolution* 29, no. 6 (2012): 1695-1701.

Leavitt, Steven D., Pradeep K. Divakar, Yoshihito Ohmura, Li-song Wang, Theodore L. Esslinger, and H. Thorsten Lumbsch. "Who's getting around? Assessing species diversity and phylogeography in the widely distributed lichen-forming fungal genus *Montanelia* (Parmeliaceae, Ascomycota)." *Molecular Phylogenetics and Evolution* 90 (2015): 85-96.

Leavitt, Steven D., Theodore L. Esslinger, Toby Spribille, Pradeep K. Divakar, and H. Thorsten Lumbsch. "Multilocus phylogeny of the lichen-forming fungal genus *Melanohalea* (Parmeliaceae, Ascomycota): Insights on diversity, distributions, and a comparison of species tree and concatenated topologies." *Molecular Phylogenetics and Evolution* 66, no. 1 (2013): 138-152.

Leavitt, Steven D., Johnathon D. Fankhauser, Dean H. Leavitt, Lyndon D. Porter, Leigh A. Johnson, and Larry L. St Clair. "Complex patterns of speciation in cosmopolitan "rock posy" lichens–Discovering and delimiting cryptic fungal species in the lichen-forming *Rhizoplaca melanophthalma* species-complex (Lecanoraceae, Ascomycota)." *Molecular Phylogenetics and Evolution* 59, no. 3 (2011): 587-602.

Leavitt, Steven D., Corrie S. Moreau, and H. Thorsten Lumbsch. "The dynamic discipline of species delimitation: Progress toward effectively recognizing species boundaries in natural populations." In *Recent Advances in Lichenology*, 11-44. New Delhi, Springer. (2015).

Lendemer, James C., Jessica L. Allen, and Nastassja Noell. "The *Parmotrema* acid test: A look at species delineation in the *P. perforatum* group 40 y later." *Mycologia* 107, no. 6 (2015): 1120-1129.

Lindblom, Louise, and Stefan Ekman. "Genetic variation and population differentiation in the lichen-forming ascomycete *Xanthoria parietina* on the island Storfosna, central Norway." *Molecular Ecology* 15, no. 6 (2006): 1545-1559.

Lohtander, Katileena, Mari Källersjö, Roland Moberg, and Anders Tehler. "The family Physciaceae in Fennoscandia: Phylogeny inferred from ITS sequences." *Mycologia* (2000): 728-735.

Lohtander, Katileena, Mari Källersjö, and Anders Tehler. "Dispersal strategies in *Roccellina capensis* (Arthoniales)." *The Lichenologist* 30, no. 4-5 (1998): 341-350.

Lohtander, Katileena, Leena Myllys, Rikard Sundin, Mari Källersjö, and Anders Tehler. "The species pair concept in the lichen *Dendrographa leucophaea* (Arthoniales): Analyses based on ITS sequences." *The Bryologist* (1998): 404-411.

Lumbsch, H. Thorsten, and Steven D. Leavitt. "Goodbye morphology? A paradigm shift in the delimitation of species in lichenized fungi." *Fungal Diversity* 50, no. 1 (2011): 59.

Mangold, Armin, María P. Martín, Robert Lücking, and H. Thorsten Lumbsch. "Molecular phylogeny suggests synonymy of Thelotremataceae within Graphidaceae (Ascomycota: Ostropales)." *Taxon* 57, no. 2 (2008): 476-486.

Matheny, P. Brandon, Yajuan J. Liu, Joseph F. Ammirati, and Benjamin D. Hall. "Using *RPB1* sequences to improve phylogenetic inference among mushrooms (*Inocybe*, Agaricales)." *American Journal of Botany* 89, no. 4 (2002): 688-698.

Mace, Georgina M. "The role of taxonomy in species conservation." *Philosophical Transactions*

*of the Royal Society of London. Series B: Biological Sciences* 359, no. 1444 (2004): 711-719.

Maddison, Wayne P. "Gene trees in species trees." *Systematic Biology* 46, no. 3 (1997): 523-536.

Mattsson, Jan-Eric, and H. Thorsten Lumbsch. "The use of the species pair concept in lichen taxonomy." *Taxon* (1989): 238-241.

Mayden, Richard L. "A hierarchy of species concepts: The denouement in the saga of the species problem." (1997). In *Species: The Units of Diversity*. edited by M. F. Claridge, H. A. Dawah & M. R. Wilson. London: Chapman & Hall (1997): 381–423.

Mishler, Brent D., and Michael J. Donoghue. "Species concepts: A case for pluralism." *Systematic Zoology* 31, no. 4 (1982): 491-503.

Myllys, Leena, Katileena Lohtander, and Anders Tehler. "β-tubulin, ITS and group I intron sequences challenge the species pair concept in *Physcia aipolia* and *P. caesia*." *Mycologia* (2001): 335-343.

Nosil, Patrik, Luke J. Harmon, and Ole Seehausen. "Ecological explanations for (incomplete) speciation." *Trends in Ecology & Evolution* 24, no. 3 (2009): 145-156.

O'Neill, Eric M., Rachel Schwartz, C. Thomas Bullock, Joshua S. Williams, H. Bradley Shaffer, X. Aguilar-Miguel, Gabriela Parra-Olea, and David W. Weisrock. "Parallel tagged amplicon sequencing reveals major lineages and phylogenetic structure in the North American tiger salamander (*Ambystoma tigrinum*) species complex." *Molecular Ecology* 22, no. 1 (2013): 111-129.

Padial, José M., Aurélien Miralles, Ignacio De la Riva, and Miguel Vences. "The integrative future of taxonomy." *Frontiers in Zoology* 7, no. 1 (2010): 16.

Parnmen, Sittiporn, Achariya Rangsiruji, Pachara Mongkolsuk, Kansri Boonpragob, Aparna

Nutakki, and H. Thorsten Lumbsch. "Using phylogenetic and coalescent methods to understand the species diversity in the *Cladia aggregata* complex (Ascomycota, Lecanorales)." *PLOS ONE* 7, no. 12 (2012): e52245.

de Queiroz, Kevin. "Species concepts and species delimitation." *Systematic Biology* 56, no. 6 (2007): 879-886.

Rambaut, Andrew, M. A. Suchard, D. Xie, and A. J. Drummond. 2014. "Tracer v1.6." http://beast.bio.ed.ac.uk/Tracer.

Rannala, Bruce. "The art and science of species delimitation." *Current Zoology* 61, no. 5 (2015): 846-853.

Robinson, Harold. "Considerations on the evolution of lichens." *Phytologia (USA)* (1975).

Ross, Howard A., Sumathi Murugan, and Wai Lok Sibon Li. "Testing the reliability of genetic methods of species identification via simulation." *Systematic Biology* 57, no. 2 (2008): 216-230.

Saag, Lauri, Kristiina Mark, Andres Saag, and Tiina Randlane. "Species delimitation in the lichenized fungal genus *Vulpicida* (Parmeliaceae, Ascomycota) using gene concatenation and coalescent-based species tree approaches." *American Journal of Botany* 101, no. 12 (2014): 2169-2182.

Schmitt, I., A. Crespo, P. K. Divakar, J. D. Fankhauser, E. Herman-Sackett, K. Kalb, M. P. Nelsen et al. "New primers for promising single-copy genes in fungal phylogenetics and systematics." *Persoonia* 23 (2009): 35.

Shaffer, H. Bradley, and Robert C. Thomson. "Delimiting species in recent radiations." *Systematic Biology* 56, no. 6 (2007): 896-906.

Singh, Garima, Francesco Dal Grande, Pradeep K. Divakar, Jürgen Otte, Steven D. Leavitt,

Katarzyna Szczepanska, Ana Crespo et al. "Coalescent-based species delimitation approach uncovers high cryptic diversity in the cosmopolitan lichen-forming fungal genus *Protoparmelia* (Lecanorales, Ascomycota)." *PLOS ONE* 10, no. 5 (2015): e0124625.

Sites Jr, Jack W., and Jonathon C. Marshall. "Delimiting species: A Renaissance issue in systematic biology." *Trends in Ecology & Evolution* 18, no. 9 (2003): 462-470.

Sites Jr, Jack W., and Jonathon C. Marshall. "Operational criteria for delimiting species." *Annual Review of Ecology, Evolution, and Systematics.* 35 (2004): 199-227.

Stamatakis, Alexandros. "RAxML version 8: A tool for phylogenetic analysis and post-analysis of large phylogenies." *Bioinformatics* 30, no. 9 (2014): 1312-1313.

Stiller, John W., and Benjamin D. Hall. "The origin of red algae: Implications for plastid evolution." *Proceedings of the National Academy of Sciences* 94, no. 9 (1997): 4520-4525.

Thell, Arne, Tassilo Feuerer, Ingvar Kärnefelt, Leena Myllys, and Soili Stenroos. "Monophyletic groups within the Parmeliaceae identified by ITS rDNA, β-tubulin and GAPDH sequences." *Mycological Progress* 3, no. 4 (2004): 297-314.

Vilgalys, Rytas, and Mark Hester. "Rapid genetic identification and mapping of enzymatically amplified ribosomal DNA from several *Cryptococcus* species." *Journal of bacteriology* 172, no. 8 (1990): 4238-4246.

White, Thomas J., Thomas Bruns, S. J. W. T. Lee, and J. L. Taylor. "Amplification and direct sequencing of fungal ribosomal RNA genes for phylogenetics." In *PCR Protocols: A Guide to Methods and Applications*. London: Academic Press. (1990): 315-322.

Wiens, John J., and Matthew C. Morrill. "Missing data in phylogenetic analysis: Reconciling results from simulations and empirical data." *Systematic Biology* 60, no. 5 (2011): 719-731.

Wirtz, Nora, Christian Printzen, and H. Thorsten Lumbsch. "Using haplotype networks,

estimation of gene flow and phenotypic characters to understand species delimitation in fungi of a predominantly Antarctic *Usnea* group (Ascomycota, Parmeliaceae)." *Organisms Diversity & Evolution* 12, no. 1 (2012): 17-37.

Yang, Ziheng, and Bruce Rannala. "Bayesian species delimitation using multilocus sequence data." *Proceedings of the National Academy of Sciences* 107, no. 20 (2010): 9264-9269.

# APPENDICES

## APPENDIX A

TABLE XVIII. HYBPIPER BLASTX STATS.

| Name | ReadsMapped | GenesMapped | GenesWithContigs | GenesWithSeqs | GenesAt25pct | GenesAt50pct | GenesAt75pct | Genesat150pct | ParalogWarnings |
|---|---|---|---|---|---|---|---|---|---|
| *15880-Sticta-fuliginosa* | 16247 | 395 | 244 | 242 | 240 | 214 | 182 | 0 | 2 |
| *4005-Ricasolia-amplissima* | 43711 | 394 | 378 | 378 | 378 | 375 | 366 | 0 | 10 |
| *15878-Pseudocyphellaria-pubescens* | 77434 | 389 | 378 | 377 | 377 | 375 | 368 | 0 | 12 |
| *15871-Sticta-caulescens* | 66202 | 396 | 377 | 376 | 375 | 375 | 363 | 0 | 14 |
| *14538-Sticta-scabrosa* | 104206 | 393 | 380 | 379 | 379 | 376 | 370 | 0 | 15 |
| *15885-Pseudocyphellaria-hirsuta* | 49919 | 387 | 365 | 365 | 365 | 362 | 353 | 0 | 20 |
| *15881-Sticta-fuliginosa* | 22895 | 386 | 311 | 310 | 307 | 294 | 256 | 0 | 8 |
| *15682-Ricasolia-sp* | 67366 | 393 | 382 | 382 | 382 | 381 | 371 | 0 | 14 |
| *14850-Pseudocyphellaria-rubrina* | 212630 | 396 | 387 | 387 | 386 | 385 | 381 | 0 | 29 |
| *15156-Sticta-sp* | 34842 | 384 | 344 | 343 | 339 | 332 | 307 | 0 | 8 |
| *15848-Pseudocyphellaria-freycinetii* | 65127 | 391 | 374 | 374 | 374 | 372 | 366 | 0 | 12 |
| *15678-Yoshimuriella-sp* | 23494 | 390 | 277 | 276 | 274 | 269 | 255 | 0 | 8 |
| *15879-Sticta-latifrons* | 40643 | 387 | 359 | 358 | 358 | 352 | 335 | 0 | 9 |
| *15890-Pseudocyphellaria-carpoloma* | 99794 | 394 | 377 | 376 | 376 | 374 | 369 | 0 | 11 |
| *15686-Lobaria-sp* | 25823 | 390 | 301 | 299 | 298 | 292 | 266 | 0 | 15 |
| *15895-Pseudocyphellaria-degelii* | 106741 | 392 | 380 | 380 | 380 | 378 | 376 | 0 | 16 |
| *15272-Dendriscosticta-affwrightii* | 67788 | 392 | 383 | 383 | 383 | 383 | 375 | 0 | 13 |
| *15253-Dendriscosticta-kurokawae* | 84925 | 392 | 386 | 385 | 385 | 383 | 374 | 0 | 18 |
| *15275-Lobariella-sp* | 89805 | 393 | 383 | 382 | 382 | 380 | 361 | 0 | 22 |
| *14492-Sticta-beauvoisii* | 165286 | 394 | 381 | 380 | 380 | 379 | 376 | 0 | 15 |
| *9930-Lobaria-pulmonaria* | 317874 | 400 | 398 | 398 | 398 | 398 | 398 | 0 | 19 |
| *15874-Pseudocyphellaria-haywardiosum* | 27024 | 381 | 312 | 312 | 312 | 310 | 295 | 0 | 8 |
| *15873-Sticta-scabrosa* | 140166 | 390 | 380 | 379 | 379 | 376 | 373 | 0 | 23 |
| *15155-Sticta-sp* | 31980 | 392 | 344 | 343 | 339 | 329 | 301 | 0 | 9 |
| *15892-Pseudocyphellaria-chloroluca* | 140011 | 390 | 375 | 375 | 374 | 371 | 365 | 0 | 13 |

TABLE XVIII. CONTINUED

| Name | ReadsMapped | GenesMapped | GenesWithContigs | GenesWithSeqs | GenesAt25pct | GenesAt50pct | GenesAt75pct | Genesat150pct | ParalogWarnings |
|---|---|---|---|---|---|---|---|---|---|
| *15897-Pseudocyphellaria-episticta* | 76645 | 394 | 376 | 376 | 376 | 376 | 370 | 0 | 12 |
| *15683-Ricasolia-sp* | 59859 | 390 | 379 | 379 | 379 | 377 | 370 | 0 | 14 |
| *15688-Nephroma-sp* | 37009 | 381 | 292 | 286 | 284 | 250 | 206 | 0 | 10 |
| *14657-Sticta-affsublimbatoides* | 12791 | 381 | 199 | 195 | 194 | 179 | 143 | 0 | 2 |
| *15901-Sticta-latifrons* | 181353 | 393 | 383 | 382 | 382 | 378 | 374 | 0 | 19 |
| *15899-Pseudocyphellaria-rufovirescens* | 105510 | 393 | 376 | 374 | 373 | 371 | 367 | 0 | 14 |
| *15276-Lobariella-sp* | 53711 | 392 | 378 | 378 | 375 | 364 | 339 | 1 | 23 |
| *15280-Yoshimuriella-peltigera* | 85126 | 393 | 382 | 381 | 380 | 378 | 371 | 1 | 17 |
| *15882-Sticta-cinereoglauca* | 7929 | 386 | 79 | 78 | 74 | 54 | 32 | 0 | 0 |
| *15884-Pseudocyphellaria-sp* | 69857 | 390 | 374 | 374 | 374 | 374 | 367 | 0 | 14 |
| *15257-Lobaria-sp* | 72323 | 397 | 395 | 395 | 395 | 393 | 392 | 0 | 16 |
| *15876-Pseudocyphellaria-cinnamomea* | 40418 | 390 | 364 | 364 | 362 | 357 | 347 | 0 | 9 |
| *15258-Nephroma-antarcticum* | 62403 | 384 | 341 | 333 | 330 | 297 | 249 | 0 | 6 |
| *15847-Pseudocyphellaria-berberina* | 95431 | 391 | 381 | 380 | 380 | 380 | 377 | 0 | 13 |
| *14840-Pseudocyphellaria-neglecta* | 87835 | 389 | 374 | 374 | 374 | 373 | 371 | 0 | 15 |
| *15869-Pseudocyphellaria-intricata* | 51376 | 390 | 370 | 369 | 369 | 367 | 359 | 0 | 11 |
| *15894-Pseudocyphellaria-crocatagroup* | 73117 | 393 | 375 | 375 | 375 | 373 | 370 | 0 | 15 |
| *15844-Pseudocyphellaria-crocata* | 91425 | 387 | 375 | 375 | 0 | 0 | 0 | 0 | 14 |
| *15684-Lobaria-sp* | 20432 | 387 | 253 | 250 | 249 | 243 | 231 | 0 | 7 |
| *15679-Yoshimuriella-sp* | 39663 | 390 | 353 | 352 | 352 | 351 | 337 | 0 | 18 |
| *15893-Pseudocyphellaria-corbettii* | 68465 | 390 | 375 | 374 | 373 | 371 | 363 | 0 | 10 |
| *15898-Pseudocyphellaria-montagnei* | 172716 | 393 | 383 | 383 | 381 | 379 | 375 | 0 | 16 |
| *15902-Sticta-lacera-livida* | 115924 | 393 | 384 | 383 | 383 | 381 | 374 | 0 | 19 |
| *15277-Lobariella-sp* | 88480 | 391 | 385 | 385 | 384 | 380 | 359 | 1 | 17 |
| *15685-Lobaria-sp* | 26296 | 390 | 320 | 318 | 318 | 309 | 284 | 0 | 11 |
| *15896-Pseudocyphellaria-disimilis* | 63765 | 389 | 373 | 373 | 373 | 368 | 357 | 0 | 10 |
| *15279-Yoshimuriella-peltigera* | 175762 | 395 | 385 | 385 | 385 | 382 | 374 | 0 | 18 |
| *15903-Sticta-martinii* | 154510 | 394 | 381 | 380 | 379 | 375 | 370 | 0 | 10 |
| *10048-Sticta-afffuliginosa* | 36811 | 384 | 349 | 349 | 347 | 343 | 333 | 0 | 13 |
| *14665-Sticta-densiphyllidata* | 63900 | 392 | 378 | 377 | 377 | 374 | 362 | 0 | 16 |
| *15891-Pseudocyphellaria-carpoloma* | 73265 | 390 | 376 | 376 | 376 | 375 | 370 | 0 | 10 |

TABLE XVIII. CONTINUED

| Name | ReadsMapped | GenesMapped | GenesWithContigs | GenesWithSeqs | GenesAt25pct | GenesAt50pct | GenesAt75pct | Genesat150pct | ParalogWarnings |
|---|---|---|---|---|---|---|---|---|---|
| *14830-Pseudocyphellaria-billardierei* | 82895 | 391 | 378 | 376 | 376 | 374 | 372 | 0 | 12 |
| *15877-Pseudocyphellaria-lividofusa* | 81644 | 388 | 372 | 372 | 372 | 369 | 363 | 0 | 9 |
| *15875-Pseudocyphellaria-affintricata* | 28950 | 386 | 324 | 324 | 324 | 320 | 310 | 0 | 8 |
| *15843-Pseudocyphellaria-obvoluta* | 69568 | 388 | 375 | 375 | 374 | 372 | 366 | 0 | 15 |
| *15886-Pseudocyphellaria-sp* | 121706 | 391 | 379 | 378 | 377 | 376 | 371 | 0 | 14 |
| *15889-Nephroma-australe* | 58436 | 387 | 319 | 314 | 313 | 296 | 259 | 0 | 7 |
| *14532-Sticta-weigelii* | 30708 | 387 | 345 | 345 | 345 | 338 | 315 | 0 | 11 |
| *15841-Pseudocyphellaria-granulata* | 80330 | 392 | 374 | 373 | 373 | 373 | 369 | 0 | 15 |
| *15274-Lobarina-oregana* | 103892 | 398 | 389 | 389 | 389 | 387 | 383 | 0 | 16 |
| *14493-Sticta-carolinensis* | 119992 | 390 | 383 | 380 | 380 | 380 | 376 | 0 | 17 |
| *15256-Lobaria-sp* | 91578 | 399 | 398 | 398 | 398 | 398 | 396 | 0 | 18 |
| *10049-Sticta-afflimbata* | 37025 | 390 | 352 | 351 | 350 | 342 | 334 | 0 | 11 |
| *15887-Pseudocyphellaria-vaccina* | 87740 | 390 | 378 | 377 | 377 | 375 | 369 | 0 | 24 |
| *15850-Yarrumia-coronata* | 92707 | 393 | 383 | 383 | 382 | 381 | 375 | 0 | 31 |
| *15851-Yarrumia-colensoi* | 74045 | 392 | 377 | 377 | 377 | 376 | 366 | 0 | 30 |
| *15254-Lobaria-linita* | 69494 | 397 | 392 | 392 | 392 | 392 | 390 | 0 | 16 |
| *15317-Yarrumia-coronata* | 78530 | 395 | 376 | 376 | 376 | 373 | 365 | 0 | 34 |
| *15681-Yoshimuriella-sp* | 43085 | 390 | 361 | 361 | 361 | 360 | 350 | 0 | 16 |
| *15900-Sticta-filix* | 145328 | 396 | 385 | 384 | 383 | 381 | 376 | 0 | 18 |
| *15144-Pseudocyphellaria-homoeophylla* | 84774 | 394 | 377 | 376 | 376 | 375 | 368 | 0 | 14 |
| *15271-Anomalobaria-anomala* | 47259 | 396 | 385 | 384 | 383 | 382 | 379 | 0 | 13 |
| *15868-Pseudocyphellaria-coriifolia* | 19578 | 392 | 261 | 258 | 258 | 254 | 232 | 0 | 5 |
| *15278-Yoshimuriella-subdissecta* | 167360 | 393 | 386 | 386 | 386 | 386 | 380 | 1 | 20 |
| *15273-Nephroma-plumbeum* | 43210 | 381 | 294 | 290 | 287 | 250 | 181 | 0 | 4 |
| *15687-Nephroma-sp* | 50277 | 388 | 306 | 300 | 298 | 275 | 224 | 0 | 8 |
| *15872-Sticta-sp* | 70932 | 392 | 377 | 376 | 376 | 375 | 368 | 0 | 18 |
| *15904-Sticta-subcaperata* | 156960 | 393 | 385 | 381 | 381 | 380 | 377 | 0 | 18 |
| *15870-Sticta-hypochra* | 56609 | 389 | 372 | 370 | 370 | 365 | 357 | 0 | 13 |
| *15316-Yarrumia-colensoi* | 100375 | 390 | 381 | 381 | 381 | 379 | 370 | 0 | 28 |
| *15680-Yoshimuriella-sp* | 54282 | 390 | 374 | 374 | 374 | 371 | 363 | 0 | 19 |
| *15888-Crocodia-aurata-poculifera* | 67681 | 386 | 370 | 370 | 369 | 367 | 360 | 0 | 13 |
| *14835-Pseudocyphellaria-crocata* | 52660 | 387 | 367 | 367 | 367 | 365 | 359 | 0 | 11 |

TABLE XVIII. CONTINUED

| Name | ReadsMapped | GenesMapped | GenesWithContigs | GenesWithSeqs | GenesAt25pct | GenesAt50pct | GenesAt75pct | Genesat150pct | ParalogWarnings |
|---|---|---|---|---|---|---|---|---|---|
| *15849-Pseudocyphellaria-flavicans* | 81891 | 390 | 377 | 376 | 376 | 375 | 365 | 0 | 13 |
| *14829-Pseudocyphellaria-dissimilis* | 34235 | 388 | 348 | 348 | 348 | 347 | 333 | 0 | 10 |
| *15842-Pseudocyphellaria-lecheri* | 45146 | 387 | 367 | 367 | 366 | 365 | 358 | 0 | 12 |
| *15845-Pseudocyphellaria-crocata* | 63722 | 387 | 372 | 372 | 372 | 372 | 363 | 0 | 12 |
| *14681-Pseudocyphellaria-glabra* | 169690 | 395 | 380 | 379 | 379 | 378 | 372 | 0 | 15 |
| *15313-Crocodia-aurata-poculifera* | 87348 | 389 | 369 | 369 | 369 | 369 | 362 | 0 | 14 |
| *15261-Dendriscosticta-sp* | 76478 | 392 | 384 | 384 | 384 | 382 | 374 | 0 | 18 |
| *14845-Pseudocyphellaria-granulata* | 70414 | 390 | 376 | 376 | 376 | 375 | 371 | 0 | 14 |

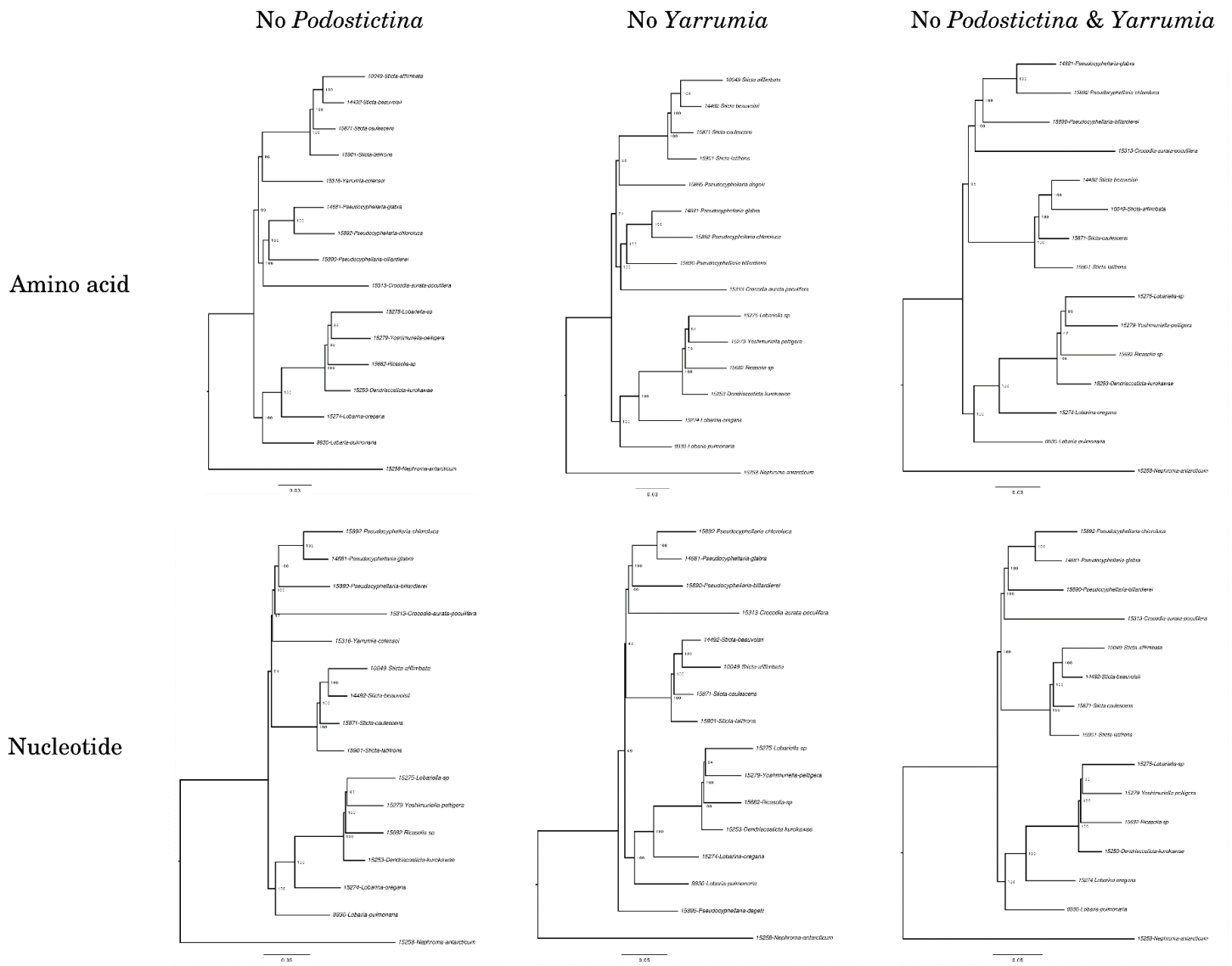


Figure 20. Maximum likelihood analyses conducted without *Podostictina*, *Yarrumia*, or both. Bootstrap support is depicted at the nodes.

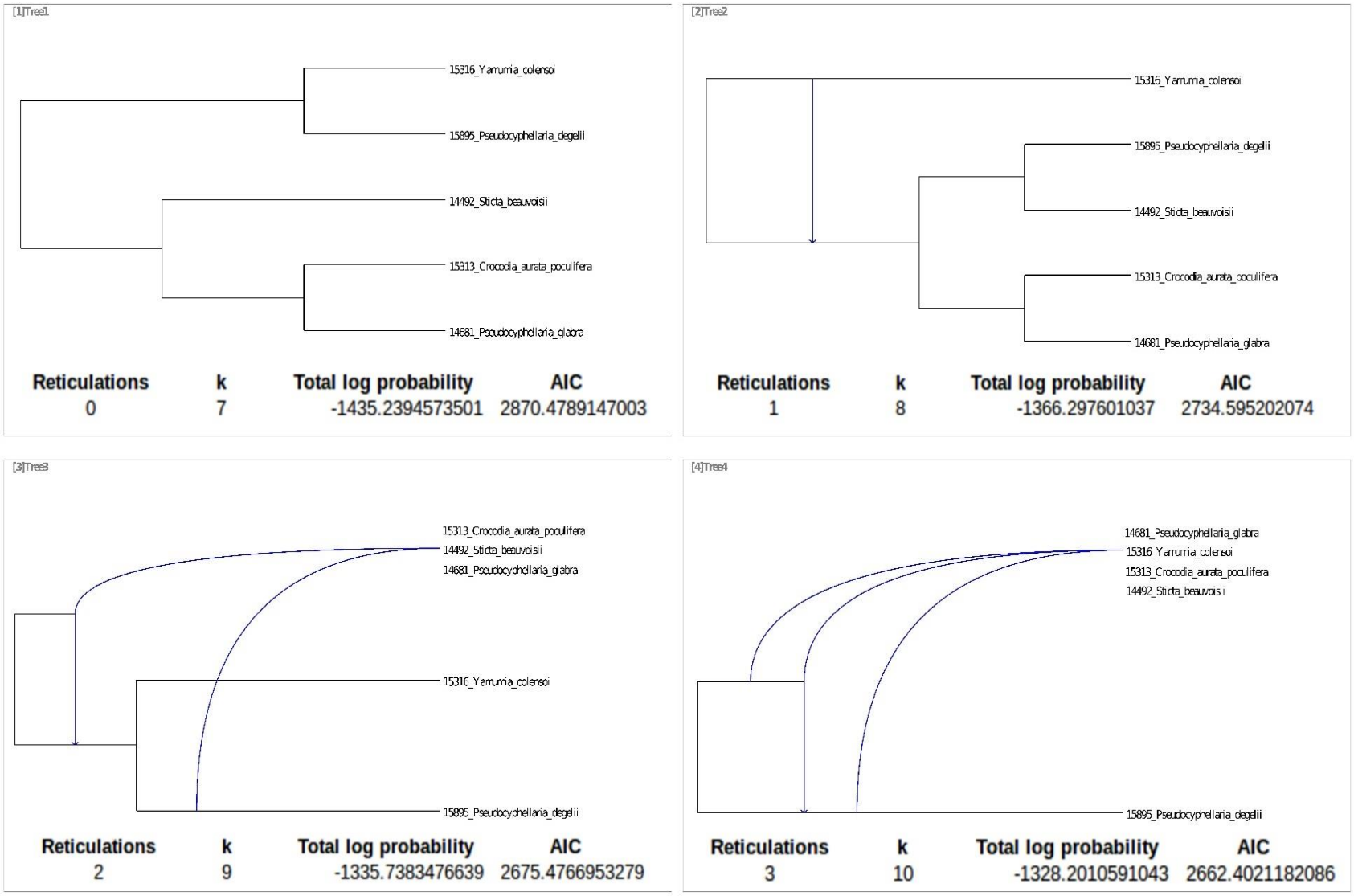


Figure 21. PhyloNet ML networks for five taxa. For each reticulation scenario, the log likelihood and AIC are reported under the networks.

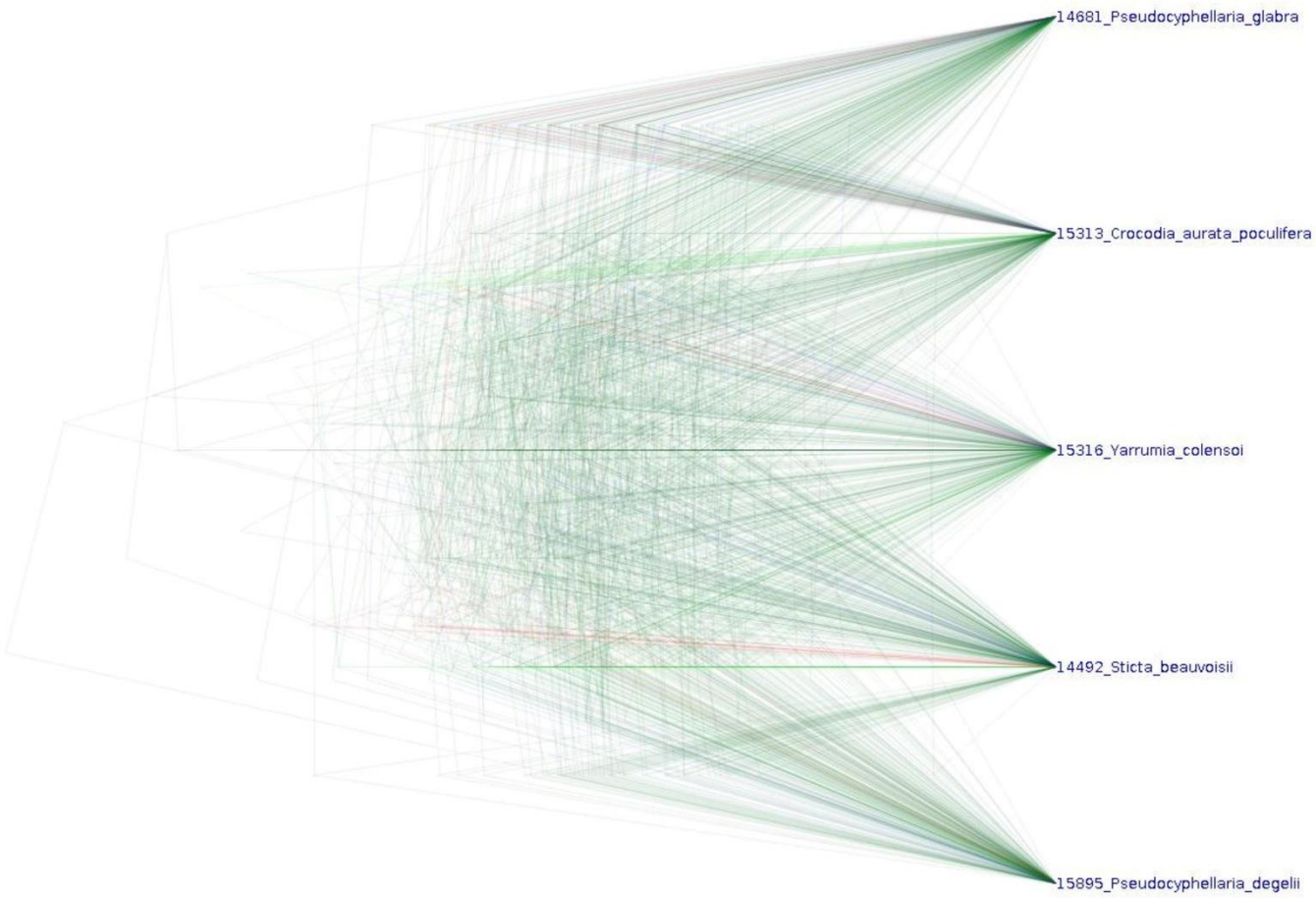


Figure 22. A DensiTree plot of 297 gene trees used to produce the five-taxa datasets.

## APPENDIX B

TABLE XIX. BISSE_TYPE1_ERROR_FS_OUTPUT_TAB.

| Free speciation lnlik | MK1 lnlink | P-value |
|---|---|---|
| -453.0334598 | -461.7208293 | 0 |
| -446.3326743 | -456.185631 | 0 |
| -452.5660204 | -467.5487094 | 0 |
| -448.4409255 | -461.3138182 | 0 |
| -453.6635799 | -465.7078711 | 0 |
| -455.9191195 | -467.3026283 | 0 |
| -446.0415487 | -456.4762503 | 0 |
| -449.5841757 | -464.1176214 | 0 |
| -450.8700521 | -465.4754459 | 0 |
| -452.3660765 | -460.3896314 | 0 |
| -450.7616996 | -459.8537142 | 0 |
| -449.8442364 | -458.7617392 | 0 |
| -453.6934017 | -465.8725579 | 0 |
| -445.6139216 | -461.2685178 | 0 |
| -444.0935829 | -454.3989049 | 0 |
| -451.8448645 | -459.7662793 | 0 |
| -451.0659349 | -460.7121476 | 0 |
| -453.3167867 | -466.5992442 | 0 |
| -450.8216473 | -463.2256214 | 0 |
| -454.5652604 | -464.4101676 | 0 |
| -447.3915685 | -461.3266474 | 0 |
| -448.3718325 | -462.0114557 | 0 |
| -450.8164039 | -465.6550844 | 0 |
| -451.1254287 | -461.9698401 | 0 |
| -447.5236554 | -462.4288391 | 0 |
| -455.4425802 | -467.62042 | 0 |
| -455.3030599 | -464.9832458 | 0 |
| -451.5266883 | -461.0797044 | 0 |
| -454.0690699 | -460.9851401 | 0 |
| -453.7837261 | -466.3863684 | 0 |
| -456.4439032 | -464.1782996 | 0 |
| -452.5886863 | -464.8115485 | 0 |
| -455.3462546 | -467.555996 | 0 |
| -452.6577318 | -459.1921188 | 0 |
| -448.7469549 | -464.2869391 | 0 |
| -450.0374357 | -462.0024233 | 0 |
| -454.8846111 | -469.2394012 | 0 |
| -447.1342458 | -458.2591833 | 0 |
| -447.8587455 | -461.2984439 | 0 |

TABLE XIX, CONTINUED

| Free speciation lnlik | MK1 lnlink | P-value |
|---|---|---|
| -448.4619439 | -462.1481918 | 0 |
| -457.380102 | -468.4114798 | 0 |
| -452.6609261 | -466.8633401 | 0 |
| -455.4424234 | -466.7421559 | 0 |
| -451.4709334 | -460.3633978 | 0 |
| -451.5263038 | -465.6229023 | 0 |
| -449.8606003 | -461.2490985 | 0 |
| -455.7666675 | -469.5249455 | 0 |
| -451.9548528 | -465.7059072 | 0 |
| -450.8977848 | -463.3416954 | 0 |
| -447.3934143 | -459.5833944 | 0 |
| -455.1805463 | -463.9582022 | 0 |
| -448.7488602 | -455.84619 | 0 |
| -448.3761209 | -463.3279683 | 0 |
| -453.0425525 | -461.9766297 | 0 |
| -451.4677978 | -466.2318968 | 0 |
| -453.9177097 | -460.6274286 | 0 |
| -446.8090171 | -458.04367 | 0 |
| -454.9673838 | -468.107789 | 0 |
| -449.7360873 | -459.5800885 | 0 |
| -447.6974974 | -460.7253019 | 0 |
| -455.9017229 | -467.415531 | 0 |
| -452.0642301 | -461.8601719 | 0 |
| -446.7125528 | -461.5351495 | 0 |
| -456.9196818 | -466.0913466 | 0 |
| -452.1450082 | -464.849112 | 0 |
| -454.6015616 | -464.0264228 | 0 |
| -456.0166208 | -468.5122848 | 0 |
| -455.3833113 | -466.6295235 | 0 |
| -449.2016536 | -463.9196176 | 0 |
| -459.6439668 | -465.9251738 | 0 |
| -446.3824782 | -456.5757055 | 0 |
| -455.4596005 | -463.6446678 | 0 |
| -451.30943 | -459.3674819 | 0 |
| -446.2914156 | -460.0073126 | 0 |
| -452.1954654 | -464.9073486 | 0 |
| -450.9364752 | -465.7347841 | 0 |
| -448.9170153 | -462.6276464 | 0 |
| -447.837001 | -459.4924811 | 0 |
| -449.8782375 | -462.8482498 | 0 |
| -456.9163264 | -468.0234727 | 0 |

TABLE XIX, CONTINUED

| Free speciation lnlik | MK1 lnlink | P-value |
|---|---|---|
| -446.3685496 | -457.5448217 | 0 |
| -453.8613322 | -466.4610184 | 0 |
| -451.2545293 | -463.3265159 | 0 |
| -451.0210337 | -465.6431369 | 0 |
| -443.0621573 | -455.6499227 | 0 |
| -453.9367158 | -461.4010071 | 0 |
| -448.9466754 | -459.3651761 | 0 |
| -449.0100985 | -458.442455 | 0 |
| -454.4492425 | -464.243407 | 0 |
| -448.8482683 | -459.776057 | 0 |
| -452.7891062 | -461.614043 | 0 |
| -453.2894109 | -468.0184465 | 0 |
| -454.1267704 | -464.9674751 | 0 |
| -457.4564447 | -471.1969709 | 0 |
| -447.3807104 | -457.7797761 | 0 |
| -448.3956568 | -457.7946038 | 0 |
| -453.6424531 | -464.6784383 | 0 |
| -452.0953149 | -464.5017164 | 0 |
| -455.1594986 | -466.9571553 | 0 |
| -451.8008581 | -461.1797339 | 0 |
| -452.1568911 | -458.0616056 | 0 |
| -459.279603 | -466.830471 | 0 |
| -451.7807074 | -461.5477279 | 0 |
| -449.5798994 | -459.2920984 | 0 |
| -449.7228739 | -461.4392315 | 0 |
| -452.2342542 | -461.2441771 | 0 |
| -451.3536489 | -465.7475725 | 0 |
| -453.2001298 | -462.6662996 | 0 |
| -455.5872674 | -468.4051691 | 0 |
| -451.6269374 | -456.6432309 | 0 |
| -453.0494336 | -462.7623455 | 0 |
| -457.8438034 | -466.457251 | 0 |
| -451.9779309 | -466.162925 | 0 |
| -451.0276745 | -459.0969013 | 0 |
| -445.094549 | -458.9558586 | 0 |
| -452.478129 | -462.1544474 | 0 |
| -451.9341203 | -460.547119 | 0 |
| -450.5314788 | -459.1741365 | 0 |
| -458.1162129 | -466.5935136 | 0 |
| -446.9977665 | -461.3104821 | 0 |
| -450.0429297 | -461.4308079 | 0 |

TABLE XIX, CONTINUED

| Free speciation lnlik | MK1 lnlink | P-value |
|---|---|---|
| -450.1443846 | -462.7870193 | 0 |
| -447.3929874 | -455.7093001 | 0 |
| -453.3866674 | -464.4983199 | 0 |
| -452.2546776 | -464.2230343 | 0 |
| -448.3537262 | -461.2633217 | 0 |
| -449.5049955 | -463.9641971 | 0 |
| -451.4205447 | -465.0976336 | 0 |
| -448.8335492 | -459.989035 | 0 |
| -455.2850831 | -464.9440792 | 0 |
| -454.5316297 | -468.486296 | 0 |
| -449.0806078 | -458.1481399 | 0 |
| -454.4781239 | -466.5417603 | 0 |
| -449.1114152 | -460.2027004 | 0 |
| -447.499664 | -459.212637 | 0 |
| -448.9689136 | -457.3652081 | 0 |
| -451.2824903 | -464.026768 | 0 |
| -448.8818944 | -461.5328124 | 0 |
| -449.5225119 | -459.8508041 | 0 |
| -447.8838331 | -459.966532 | 0 |
| -450.6780422 | -462.5317461 | 0 |
| -455.5615876 | -466.7569992 | 0 |
| -446.8940686 | -461.7825037 | 0 |
| -445.9240609 | -456.106823 | 0 |
| -451.6506109 | -459.5839731 | 0 |
| -451.471989 | -462.8444467 | 0 |
| -451.5688282 | -461.3574422 | 0 |
| -449.5823033 | -464.1319732 | 0 |
| -454.3007209 | -466.3780492 | 0 |
| -447.846218 | -459.6391116 | 0 |
| -452.837424 | -466.2215119 | 0 |
| -447.5565858 | -460.7538609 | 0 |
| -450.5965784 | -460.4297268 | 0 |
| -450.6605104 | -463.0416604 | 0 |
| -451.9508502 | -462.5833625 | 0 |
| -447.7388188 | -463.0055746 | 0 |
| -450.5885569 | -464.0618918 | 0 |
| -451.9497275 | -462.8100295 | 0 |
| -451.6820864 | -466.3649863 | 0 |
| -449.9263214 | -462.7078009 | 0 |
| -452.266663 | -463.185565 | 0 |
| -448.3873423 | -459.1092683 | 0 |

TABLE XIX, CONTINUED

| Free speciation lnlik | MK1 lnlink | P-value |
|---|---|---|
| -453.0923859 | -461.3170612 | 0 |
| -456.3332817 | -465.8512744 | 0 |
| -450.8913949 | -463.4323076 | 0 |
| -455.4396522 | -464.2696916 | 0 |
| -450.2562107 | -464.1503911 | 0 |
| -454.6448503 | -462.434081 | 0 |
| -447.1028636 | -456.2289491 | 0 |
| -446.9352749 | -457.1458794 | 0 |
| -452.5263742 | -465.1376855 | 0 |
| -446.8958678 | -461.3790117 | 0 |
| -455.9223054 | -465.7770914 | 0 |
| -450.7366421 | -463.341783 | 0 |
| -450.6957068 | -464.2821535 | 0 |
| -445.6585074 | -457.9619156 | 0 |
| -448.2226678 | -461.7016205 | 0 |
| -450.3752659 | -463.1717692 | 0 |
| -455.1798279 | -466.7815911 | 0 |
| -449.9487899 | -458.2851392 | 0 |
| -451.8137863 | -459.8980165 | 0 |
| -451.6267714 | -458.2239435 | 0 |
| -449.2167382 | -463.2325056 | 0 |
| -450.6240453 | -461.6009328 | 0 |
| -454.351143 | -465.4603333 | 0 |
| -454.0057248 | -461.8287871 | 0 |
| -455.2808224 | -464.2346189 | 0 |
| -446.4225341 | -458.4165807 | 0 |
| -452.6494478 | -463.09464 | 0 |
| -452.1082432 | -466.1034849 | 0 |
| -444.544176 | -458.240619 | 0 |
| -451.8660917 | -464.8918006 | 0 |
| -450.3043758 | -462.8340727 | 0 |
| -450.9663808 | -460.5905295 | 0 |
| -448.7561 | -459.9892828 | 0 |
| -451.4560882 | -462.1016322 | 0 |
| -453.2746398 | -460.1144152 | 0 |
| -451.1188177 | -459.2284182 | 0 |
| -451.2281028 | -464.3941102 | 0 |
| -451.744558 | -460.4350256 | 0 |
| -455.8694528 | -465.6526444 | 0 |
| -452.2677449 | -467.6664661 | 0 |
| -452.1210746 | -460.5038289 | 0 |

TABLE XIX, CONTINUED

| Free speciation lnlik | MK1 lnlink | P-value |
|---|---|---|
| -449.6672097 | -463.5618559 | 0 |
| -448.7383786 | -463.7889265 | 0 |
| -453.9538021 | -460.7516698 | 0 |
| -450.4792244 | -457.2552908 | 0 |
| -453.8021702 | -465.8076768 | 0 |
| -447.6236987 | -455.5641351 | 0 |
| -453.6302355 | -465.4907785 | 0 |
| -452.8639873 | -458.147202 | 0 |
| -450.9268265 | -462.948657 | 0 |
| -453.9263866 | -465.9282186 | 0 |
| -445.9999478 | -456.8385327 | 0 |
| -451.1801521 | -464.3273722 | 0 |
| -457.1460428 | -467.2438763 | 0 |
| -449.4639307 | -461.0853916 | 0 |
| -451.2599495 | -463.8410268 | 0 |
| -453.9820049 | -463.5871027 | 0 |
| -450.2566125 | -462.0397739 | 0 |
| -452.1193367 | -462.2244713 | 0 |
| -453.7001413 | -464.5042316 | 0 |
| -449.9805514 | -457.1248922 | 0 |
| -449.8047779 | -460.3405069 | 0 |
| -452.7961746 | -465.5164502 | 0 |
| -451.9071772 | -462.5102883 | 0 |
| -453.8619102 | -465.2531088 | 0 |
| -446.4652704 | -457.1966751 | 0 |
| -456.9210002 | -466.7341529 | 0 |
| -450.4878809 | -462.7566165 | 0 |
| -451.1226798 | -462.5473055 | 0 |
| -453.3536984 | -460.064388 | 0 |
| -448.1687549 | -460.7252742 | 0 |
| -450.557697 | -462.0625545 | 0 |
| -453.0931901 | -465.3572884 | 0 |
| -455.3582574 | -466.3189448 | 0 |
| -452.7282054 | -465.1853541 | 0 |
| -449.3848832 | -464.7623552 | 0 |
| -445.6889946 | -456.8179441 | 0 |
| -449.8203878 | -463.3524337 | 0 |
| -450.9046089 | -462.3246539 | 0 |
| -450.3356075 | -462.4801032 | 0 |
| -453.644544 | -466.9891646 | 0 |
| -449.0721569 | -460.8682775 | 0 |

TABLE XIX, CONTINUED

| Free speciation lnlik | MK1 lnlink | P-value |
|---|---|---|
| -447.6279661 | -457.0614027 | 0 |
| -453.2821075 | -463.2793679 | 0 |
| -448.0320889 | -462.4277266 | 0 |
| -450.135772 | -465.6886535 | 0 |
| -449.018654 | -463.0003305 | 0 |
| -458.4172263 | -465.8410669 | 0 |
| -448.8420416 | -461.2426729 | 0 |
| -448.6841964 | -461.3580127 | 0 |
| -449.7311061 | -458.6609864 | 0 |
| -448.5850969 | -460.1738681 | 0 |
| -457.754427 | -469.6834763 | 0 |
| -450.3049802 | -463.8584413 | 0 |
| -452.3272445 | -466.5404459 | 0 |
| -450.9994314 | -459.94859 | 0 |
| -455.1509147 | -464.2198152 | 0 |
| -452.0509377 | -464.9095607 | 0 |
| -454.0067362 | -465.2667638 | 0 |
| -451.5647978 | -463.2097897 | 0 |
| -451.54038 | -464.960496 | 0 |
| -449.4747857 | -459.9678376 | 0 |
| -451.526962 | -463.6162215 | 0 |
| -452.6744496 | -466.0750049 | 0 |
| -451.5626876 | -465.6201051 | 0 |
| -450.3066345 | -460.6131005 | 0 |
| -446.4784406 | -457.3018122 | 0 |
| -455.398142 | -464.489883 | 0 |
| -450.3697755 | -459.532449 | 0 |
| -457.1628095 | -468.9440571 | 0 |
| -455.2850061 | -464.5088639 | 0 |
| -459.9806977 | -468.6341095 | 0 |
| -449.2598849 | -459.1886468 | 0 |
| -452.7320791 | -462.4057572 | 0 |
| -451.0907881 | -459.8959825 | 0 |
| -450.1510659 | -459.1505219 | 0 |
| -456.3284776 | -466.4320561 | 0 |
| -456.8942148 | -464.1807968 | 0 |
| -457.1012307 | -466.8651577 | 0 |
| -452.0389165 | -464.9460455 | 0 |
| -447.5217439 | -461.333209 | 0 |
| -452.7428878 | -465.9438403 | 0 |
| -453.4089934 | -467.7932071 | 0 |

TABLE XIX, CONTINUED

| Free speciation lnlik | MK1 lnlink | P-value |
|---|---|---|
| -453.7450867 | -465.3661749 | 0 |
| -451.6997536 | -464.1692602 | 0 |
| -451.364277 | -461.9453162 | 0 |
| -447.7027253 | -459.3257612 | 0 |
| -456.0384162 | -467.516911 | 0 |
| -449.8505535 | -462.0428748 | 0 |
| -451.3128597 | -466.1685694 | 0 |
| -456.1992855 | -466.9178737 | 0 |
| -453.0176933 | -465.1309394 | 0 |
| -444.1248899 | -454.0059724 | 0 |
| -453.9425024 | -463.0236863 | 0 |
| -449.2981906 | -463.0715684 | 0 |
| -449.6012415 | -462.2677412 | 0 |
| -456.4720522 | -470.5948563 | 0 |
| -451.3143521 | -465.0984991 | 0 |
| -451.3657606 | -462.9244641 | 0 |
| -455.483409 | -465.6470692 | 0 |
| -453.9879467 | -467.6824601 | 0 |
| -453.3141616 | -464.5166589 | 0 |
| -449.5010217 | -458.6296314 | 0 |
| -452.9212287 | -459.6995149 | 0 |
| -451.8405045 | -461.2159881 | 0 |
| -454.1016671 | -467.6780542 | 0 |
| -457.0980188 | -470.2158085 | 0 |
| -448.8570564 | -458.4287066 | 0 |
| -446.7921755 | -461.4716628 | 0 |
| -455.9057658 | -467.2560565 | 0 |
| -456.080819 | -467.7243321 | 0 |
| -452.3462461 | -465.6351246 | 0 |
| -452.4790499 | -464.4308538 | 0 |
| -450.1987684 | -461.7051799 | 0 |
| -450.7102383 | -464.4188126 | 0 |
| -449.6519002 | -460.340023 | 0 |
| -454.5659567 | -464.9359547 | 0 |
| -453.9397425 | -465.9029993 | 0 |
| -448.9059303 | -460.013144 | 0 |
| -448.2770333 | -461.2661979 | 0 |
| -447.7943526 | -459.7353571 | 0 |
| -455.8398803 | -463.5314023 | 0 |
| -453.2841348 | -464.7390694 | 0 |
| -448.10257 | -462.1169067 | 0 |

TABLE XIX, CONTINUED

| Free speciation lnlik | MK1 lnlink | P-value |
|---|---|---|
| -449.4511173 | -460.2563784 | 0 |
| -457.2597219 | -469.1734878 | 0 |
| -453.4708024 | -468.1390107 | 0 |
| -447.9280231 | -458.2303078 | 0 |
| -450.3977788 | -458.5096675 | 0 |
| -454.29082 | -467.3883089 | 0 |
| -452.1528771 | -466.7615411 | 0 |
| -450.058851 | -462.9840808 | 0 |
| -453.9692616 | -468.852776 | 0 |
| -451.2816186 | -461.4678 | 0 |
| -443.5786452 | -455.3207166 | 0 |
| -455.1436444 | -463.6606249 | 0 |
| -448.534043 | -462.8788716 | 0 |
| -446.8711114 | -461.1474991 | 0 |
| -455.0289652 | -466.5381001 | 0 |
| -452.1855082 | -462.6467861 | 0 |
| -448.1692608 | -459.7654526 | 0 |
| -451.0950898 | -459.8438025 | 0 |
| -449.5044178 | -462.3792759 | 0 |
| -452.7388717 | -463.9867695 | 0 |
| -452.6461523 | -462.5289825 | 0 |
| -455.9223202 | -462.7932688 | 0 |
| -452.105378 | -465.4501331 | 0 |
| -453.3924506 | -463.7013004 | 0 |
| -451.5265171 | -465.1805253 | 0 |
| -451.2880253 | -459.7728892 | 0 |
| -454.2447486 | -467.3708094 | 0 |
| -449.7182666 | -457.3547096 | 0 |
| -452.7728672 | -461.4085695 | 0 |
| -447.9708853 | -456.1737649 | 0 |
| -454.7300625 | -470.2952329 | 0 |
| -450.808366 | -462.2404407 | 0 |
| -445.6261039 | -457.9325944 | 0 |
| -453.7900363 | -458.2221401 | 0 |
| -451.8507546 | -461.3866394 | 0 |
| -448.2082252 | -462.4290848 | 0 |
| -449.8821933 | -463.5038484 | 0 |
| -454.0987857 | -465.7008371 | 0 |
| -453.2329223 | -467.0656634 | 0 |
| -455.7692188 | -465.9509972 | 0 |
| -447.6499867 | -461.9518489 | 0 |

TABLE XIX, CONTINUED

| Free speciation lnlik | MK1 lnlink | P-value |
|---|---|---|
| -456.5899917 | -472.1976789 | 0 |
| -451.9012497 | -460.395346 | 0 |
| -449.8948401 | -460.6452467 | 0 |
| -449.932856 | -465.574787 | 0 |
| -454.0333635 | -461.5148657 | 0 |
| -458.4445617 | -470.7660012 | 0 |
| -453.7286295 | -469.3910788 | 0 |
| -452.167333 | -463.1688816 | 0 |
| -456.7260744 | -467.140607 | 0 |
| -450.7098344 | -461.4329508 | 0 |
| -446.2422063 | -458.1752932 | 0 |
| -453.7027152 | -467.730229 | 0 |
| -454.9173788 | -466.7819684 | 0 |
| -451.0098001 | -460.4233765 | 0 |
| -451.5772185 | -463.1592818 | 0 |
| -450.004609 | -464.3011801 | 0 |
| -450.3599462 | -463.4298817 | 0 |
| -447.9967014 | -458.9452744 | 0 |
| -449.524956 | -464.8453361 | 0 |
| -449.703755 | -465.321002 | 0 |
| -453.9089796 | -468.1253116 | 0 |
| -450.9536495 | -465.2867985 | 0 |
| -452.8943435 | -466.7084987 | 0 |
| -453.4319457 | -464.8724456 | 0 |
| -455.0458025 | -465.6754112 | 0 |
| -449.2841786 | -458.9835008 | 0 |
| -452.7207496 | -461.388292 | 0 |
| -447.8171227 | -457.7599461 | 0 |
| -448.5956323 | -459.3260343 | 0 |
| -452.4736695 | -462.0276592 | 0 |
| -451.8005816 | -460.118923 | 0 |
| -443.9548488 | -454.3342113 | 0 |
| -457.2337025 | -471.5569175 | 0 |
| -450.6370662 | -464.9172277 | 0 |
| -454.1295055 | -465.9470139 | 0 |
| -454.9456831 | -462.6900812 | 0 |
| -452.8247709 | -460.675113 | 0 |
| -453.1891127 | -459.5060059 | 0 |
| -448.6372539 | -463.1506819 | 0 |
| -449.5210883 | -462.2771865 | 0 |
| -455.4042601 | -462.3066636 | 0 |

TABLE XIX, CONTINUED

| Free speciation lnlik | MK1 lnlink | P-value |
|---|---|---|
| -452.1262196 | -461.7895631 | 0 |
| -453.3413845 | -467.688765 | 0 |
| -453.7987362 | -466.1003556 | 0 |
| -453.548008 | -466.9833351 | 0 |
| -454.3053794 | -468.0043821 | 0 |
| -452.2548283 | -467.9984657 | 0 |
| -455.2410769 | -462.2125709 | 0 |
| -455.8747541 | -469.78487 | 0 |
| -453.4796713 | -468.0266984 | 0 |
| -444.0939397 | -456.9683702 | 0 |
| -450.4385043 | -463.3445036 | 0 |
| -448.3835333 | -461.538537 | 0 |
| -452.4784552 | -462.4620435 | 0 |
| -452.035133 | -466.3906086 | 0 |
| -452.9058534 | -461.5433659 | 0 |
| -453.6892687 | -463.6439146 | 0 |
| -451.8457316 | -467.0439001 | 0 |
| -451.5113729 | -458.5581635 | 0 |
| -443.6773104 | -454.2170042 | 0 |
| -445.7959534 | -460.8722069 | 0 |
| -452.5070409 | -462.5650421 | 0 |
| -457.7647961 | -470.4466009 | 0 |
| -458.8030414 | -469.0121826 | 0 |
| -454.271888 | -463.5710662 | 0 |
| -453.4898733 | -464.7107904 | 0 |
| -453.0252641 | -461.325648 | 0 |
| -448.7505168 | -461.4919284 | 0 |
| -451.218309 | -464.047261 | 0 |
| -452.7735607 | -459.9994762 | 0 |
| -447.6323023 | -462.3178526 | 0 |
| -442.6052397 | -456.929988 | 0 |
| -449.4034148 | -457.5484872 | 0 |
| -444.6995979 | -452.2162459 | 0 |
| -450.9587241 | -462.7929001 | 0 |
| -451.5817505 | -463.7461501 | 0 |
| -453.6465293 | -459.4183929 | 0 |
| -445.2514434 | -455.7656509 | 0 |
| -455.7515577 | -462.236334 | 0 |
| -452.5311603 | -458.3706069 | 0 |
| -452.0467815 | -464.965338 | 0 |
| -452.2901775 | -462.0736017 | 0 |

TABLE XIX, CONTINUED

| Free speciation lnlik | MK1 lnlink | P-value |
|---|---|---|
| -452.90015 | -465.4709041 | 0 |
| -450.8337055 | -465.1931738 | 0 |
| -453.7383508 | -464.1311739 | 0 |
| -449.5033127 | -459.3833583 | 0 |
| -450.3102926 | -457.0957866 | 0 |
| -447.4847273 | -459.329979 | 0 |
| -450.102028 | -464.0022249 | 0 |
| -455.2677139 | -467.0568679 | 0 |
| -455.5957286 | -469.3443976 | 0 |
| -452.0691707 | -460.6475596 | 0 |
| -450.2784641 | -459.7812587 | 0 |
| -450.8795351 | -466.6446234 | 0 |
| -450.3770632 | -464.648734 | 0 |
| -450.7633411 | -461.8934298 | 0 |
| -452.445138 | -465.1707873 | 0 |
| -449.7850646 | -460.1163187 | 0 |
| -454.677513 | -463.754009 | 0 |
| -454.383832 | -466.0305125 | 0 |
| -451.1042764 | -462.5720393 | 0 |
| -450.5920666 | -464.9110168 | 0 |
| -454.4616583 | -461.4098332 | 0 |
| -451.4983949 | -462.2686028 | 0 |
| -450.2726077 | -462.8826772 | 0 |
| -452.0819749 | -466.2356645 | 0 |
| -454.1037932 | -469.3239325 | 0 |
| -453.9843622 | -463.2214179 | 0 |
| -453.269521 | -467.3218089 | 0 |
| -450.3836971 | -459.0722699 | 0 |
| -449.285439 | -459.6267727 | 0 |
| -451.8856712 | -465.3012156 | 0 |
| -452.6979381 | -464.2542173 | 0 |
| -455.4352964 | -469.8048726 | 0 |
| -451.682171 | -464.1563622 | 0 |
| -454.2609689 | -466.0596523 | 0 |
| -454.3560441 | -463.6298443 | 0 |
| -454.6696032 | -465.9641632 | 0 |
| -448.5008081 | -462.0836308 | 0 |
| -456.3026131 | -465.2025172 | 0 |
| -451.3773105 | -462.6953795 | 0 |
| -451.2224356 | -459.9371853 | 0 |
| -447.3297256 | -459.5169828 | 0 |

TABLE XIX, CONTINUED

| Free speciation lnlik | MK1 lnlink | P-value |
|---|---|---|
| -451.8228208 | -461.3136536 | 0 |
| -447.309059 | -458.1565107 | 0 |
| -453.4054273 | -466.0346403 | 0 |
| -446.7734846 | -458.6450426 | 0 |
| -451.85258 | -460.9629584 | 0 |
| -449.2476648 | -459.4463775 | 0 |
| -459.9703132 | -468.0916156 | 0 |
| -447.1472254 | -455.1002452 | 0 |
| -450.2015091 | -458.4443277 | 0 |
| -454.3483605 | -469.1819002 | 0 |

TABLE XX. BISSE_TYPE1_ERROR_ANDES_Q01_TAB.

| no q01 lnlik | MK1 lnlik | P-value |
|---|---|---|
| -489.8016292 | -476.2167454 | 0.999999814 |
| -491.4000487 | -476.4162103 | 0.999999956 |
| -487.2179832 | -476.3088207 | 0.999997003 |
| -479.3683717 | -476.3902813 | 0.985334223 |
| -488.6215127 | -476.3901397 | 0.999999242 |
| -489.68726 | -476.4409781 | 0.999999735 |
| -486.479672 | -476.3946673 | 0.999992915 |
| -490.7683527 | -476.3955541 | 0.999999918 |
| -478.4404028 | -476.3955253 | 0.956856109 |
| -477.0715122 | -476.8762219 | 0.468005554 |
| -486.3227429 | -476.2583955 | 0.99999276 |
| -474.0174911 | -476.383348 | 0 |
| -487.00004 | -474.4468631 | 0.999999458 |
| -492.9587782 | -476.4013586 | 0.999999991 |
| -482.871719 | -473.6713165 | 0.999982102 |
| -494.038642 | -475.9568 | 0.999999998 |
| -487.7234775 | -476.3968844 | 0.99999806 |
| -485.0620141 | -475.9186719 | 0.999980997 |
| -479.6807468 | -476.394875 | 0.989638961 |
| -490.5831884 | -476.3773877 | 0.999999902 |
| -494.658378 | -475.9970842 | 0.999999999 |
| -486.0909565 | -476.380759 | 0.999989512 |
| -490.3499809 | -476.386874 | 0.999999874 |
| -476.8863046 | -474.4115216 | 0.973902781 |
| -484.6046622 | -476.3912878 | 0.999949433 |
| -488.575398 | -476.3077155 | 0.99999927 |
| -478.2973156 | -474.2562251 | 0.995529739 |
| -486.094944 | -474.7629315 | 0.999998071 |
| -490.2298238 | -476.3982005 | 0.999999856 |
| -495.2019504 | -476.3947271 | 0.999999999 |
| -488.0468935 | -476.3960052 | 0.999998615 |
| -489.7409904 | -476.3946749 | 0.999999762 |
| -490.4469352 | -476.3963543 | 0.999999885 |
| -490.2697502 | -476.3820607 | 0.999999864 |
| -488.75402 | -476.0008052 | 0.999999559 |
| -486.4063284 | -476.398035 | 0.999992323 |
| -489.7929088 | -476.4000754 | 0.999999773 |
| -492.1231787 | -476.3921772 | 0.99999998 |
| -481.865897 | -476.3793722 | 0.999075535 |
| -487.6562697 | -475.7504775 | 0.999998938 |
| -487.9073582 | -475.977028 | 0.999998964 |
| -486.3738286 | -476.3892709 | 0.99999213 |
| -487.4589996 | -476.1151718 | 0.999998094 |
| -485.3631159 | -476.2917443 | 0.999979505 |
| -480.1323865 | -475.03606 | 0.998589987 |
| -476.7271184 | -474.9394086 | 0.941359368 |
| -487.3254954 | -476.4126901 | 0.999997014 |
| -487.6483661 | -476.3955937 | 0.999997905 |
| -488.4677525 | -476.3948371 | 0.999999107 |
| -490.1153814 | -476.3969346 | 0.999999838 |
| -496.8744778 | -476.400374 | 1 |
| -484.9418026 | -476.2747437 | 0.999968649 |
| -489.1850381 | -476.4481959 | 0.999999552 |
| -495.30897 | -476.0697776 | 0.999999999 |
| -491.7205833 | -476.3335614 | 0.999999971 |
| -492.5978032 | -476.3983606 | 0.999999987 |
| -491.3712104 | -476.3912567 | 0.999999956 |
| -487.1595542 | -475.4346902 | 0.999998718 |
| -490.4649303 | -476.400825 | 0.999999887 |
| -488.8783492 | -476.3947201 | 0.999999417 |

TABLE XX, CONTINUED

| no q01 lnlik | MK1 lnlik | P-value |
|---|---|---|
| -484.572387 | -476.389377 | 0.999947787 |
| -488.8936691 | -476.182465 | 0.99999954 |
| -487.2596843 | -476.3955284 | 0.999996859 |
| -482.0402575 | -475.3239439 | 0.999752714 |
| -486.975879 | -476.3948673 | 0.99999578 |
| -485.497146 | -476.1129568 | 0.999985241 |
| -480.7396523 | -476.3964518 | 0.99679407 |
| -487.5032374 | -476.3947399 | 0.999997565 |
| -481.3673825 | -476.3430723 | 0.998475379 |
| -472.9530584 | -474.8843589 | 0 |
| -494.2299807 | -476.3955325 | 0.999999998 |
| -493.3955975 | -476.4215207 | 0.999999994 |
| -488.4559791 | -476.3955222 | 0.999999095 |
| -483.3996987 | -475.6315174 | 0.999919067 |
| -493.1330686 | -476.4820061 | 0.999999992 |
| -494.411138 | -476.413998 | 0.999999998 |
| -495.0571435 | -476.3963432 | 0.999999999 |
| -489.2808239 | -476.394775 | 0.999999616 |
| -489.5608476 | -475.9267565 | 0.999999823 |
| -486.2347333 | -476.3955247 | 0.999990837 |
| -486.2666542 | -476.2834843 | 0.999992118 |
| -487.7243152 | -476.3480582 | 0.999998157 |
| -483.6238016 | -476.3955307 | 0.999856569 |
| -483.1791173 | -476.1024911 | 0.999831495 |
| -489.9134306 | -476.3955464 | 0.9999998 |
| -493.9020939 | -476.3583746 | 0.999999997 |
| -482.5548856 | -476.1369002 | 0.999659981 |
| -479.1688663 | -476.3955253 | 0.981484246 |
| -481.3970005 | -476.3915966 | 0.998443758 |
| -487.3481373 | -475.1826927 | 0.999999189 |
| -490.7126825 | -476.4002943 | 0.999999912 |
| -492.7380104 | -476.3538789 | 0.99999999 |
| -488.1826301 | -476.3934789 | 0.999998801 |
| -482.1472757 | -476.1783931 | 0.999449926 |
| -487.9713002 | -476.2731344 | 0.999998682 |
| -488.0942543 | -476.3955306 | 0.999998683 |
| -493.8685926 | -476.4403653 | 0.999999997 |
| -492.6272882 | -476.3955264 | 0.999999988 |
| -487.6152292 | -476.0096018 | 0.999998549 |
| -485.1246611 | -475.6318742 | 0.999986829 |

## APPENDIX C

TABLE XXI. SPECIMEN VOUCHER INFORMATION.

| Date | Country | DNA number | Latitude | Altitude | Longitude | Collected by | Collection. no. |
|---|---|---|---|---|---|---|---|
| 01/14/16 | Australia | 14682_TAS | -41.15 | 110 m | 145.1 | H.T. Lumbsch, T. Widhelm & F. Grewe | 2046 B |
| 01/14/16 | Australia | 14687_TAS | -41.1333 | 210 m | 145.06667 | H.T. Lumbsch, T. Widhelm & F. Grewe | 2072 D |
| 01/14/16 | Australia | 14689_TAS | -41.1333 | 210 m | 145.06667 | H.T. Lumbsch, T. Widhelm & F. Grewe | 2076 B |
| 01/14/16 | Australia | 14690_TAS | -41.1333 | 210 m | 145.06667 | H.T. Lumbsch, T. Widhelm & F. Grewe | 2076 C |
| 01/14/16 | Australia | 14693_TAS | -41.1333 | 210 m | 145.06667 | H.T. Lumbsch, T. Widhelm & F. Grewe | 2077 C |
| 01/15/16 | Australia | 14696_TAS | -41.4667 | 350 m | 145.26667 | H.T. Lumbsch, T. Widhelm & F. Grewe | 2096 B |
| 01/15/16 | Australia | 14702_TAS | -41.4667 | 350 m | 145.26667 | H.T. Lumbsch, T. Widhelm & F. Grewe | 2096 H |
| 01/16/16 | Australia | 14706_TAS | -42.6833 | 1050 m | 146.58333 | H.T. Lumbsch, T. Widhelm & F. Grewe | 2144 B |
| 01/16/16 | Australia | 14708_TAS | -42.6833 | 1050 m | 146.58333 | H.T. Lumbsch, T. Widhelm & F. Grewe | 2144 D |
| 01/16/16 | Australia | 14709_TAS | -42.6833 | 700 m | 146.66667 | H.T. Lumbsch, T. Widhelm & F. Grewe | 2172 A |
| 01/16/16 | Australia | 14711_TAS | -42.6833 | 700 m | 146.66667 | H.T. Lumbsch, T. Widhelm & F. Grewe | 2172 C |
| 01/16/16 | Australia | 14712_TAS | -42.6833 | 700 m | 146.66667 | H.T. Lumbsch, T. Widhelm & F. Grewe | 2172 D |
| 01/16/16 | Australia | 14718_TAS | -42.6833 | 700 m | 146.66667 | H.T. Lumbsch, T. Widhelm & F. Grewe | 2172 J |
| 01/17/16 | Australia | 14720_TAS | -42.8167 | 390 m | 146.65 | H.T. Lumbsch, T. Widhelm & F. Grewe | 2201 |
| 01/21/16 | Australia | 14725_VIC | -37.7 | 740 m | 145.7 | T. Widhelm & F. Grewe | 2259 B |
| 01/21/16 | Australia | 14727_VIC | -37.7 | 1149 m | 145.66667 | T. Widhelm & F. Grewe | 2272 |
| 01/21/16 | Australia | 14728_VIC | -37.7 | 1149 m | 145.66667 | T. Widhelm & F. Grewe | 2272 A |
| 01/21/16 | Australia | 14729_VIC | -37.7 | 1149 m | 145.66667 | T. Widhelm & F. Grewe | 2272 B |
| 01/21/16 | Australia | 14731_VIC | -37.7 | 1149 m | 145.66667 | T. Widhelm & F. Grewe | 2272 D |
| 01/21/16 | Australia | 14732_VIC | -37.7167 | 993 m | 145.6 | T. Widhelm & F. Grewe | 2282 A |
| 01/21/16 | Australia | 14735_VIC | -37.7167 | 993 m | 145.6 | T. Widhelm & F. Grewe | 2282 D |
| 01/21/16 | Australia | 14743_VIC | -37.7 | 976 m | 145.61667 | T. Widhelm & F. Grewe | 2290 G |
| 01/21/16 | Australia | 14747_VIC | -37.7 | 976 m | 145.61667 | T. Widhelm & F. Grewe | 2290 K |
| 01/21/16 | Australia | 14749_VIC | -37.7 | 1070 m | 145.65 | T. Widhelm & F. Grewe | 2293 A |
| 01/21/16 | Australia | 14753_VIC | -37.7 | 1070 m | 145.65 | T. Widhelm & F. Grewe | 2293 E |
| 01/21/16 | Australia | 14755_VIC | -37.7 | 1070 m | 145.65 | T. Widhelm & F. Grewe | 2293 G |
| 01/21/16 | Australia | 14756_VIC | -37.7 | 1070 m | 145.65 | T. Widhelm & F. Grewe | 2293 H |
| 01/21/16 | Australia | 14757_VIC | -37.7 | 1070 m | 145.65 | T. Widhelm & F. Grewe | 2293 I |
| 01/21/16 | Australia | 14758_VIC | -37.7 | 1070 m | 145.65 | T. Widhelm & F. Grewe | 2293 J |

Table XXI, CONTINUED

| Date | Country | DNA number | Latitude | Altitude | Longitude | Collected by | Collection. no. |
|---|---|---|---|---|---|---|---|
| 01/22/16 | Australia | 14759_VIC | -37.5167 | 888 m | 145.83333 | T. Widhelm & F. Grewe | 2311 A |
| 01/22/16 | Australia | 14761_VIC | -37.5167 | 888 m | 145.83333 | T. Widhelm & F. Grewe | 2311 C |
| 01/24/16 | Australia | 14762_VIC | -38.1 | 655 m | 147.4 | T. Widhelm & F. Grewe | 2324 A |
| 01/25/16 | Australia | 14763_VIC | -38.45 | 339 m | 146.53333 | T. Widhelm & F. Grewe | 2402 A |
| 01/25/16 | Australia | 14764_VIC | -38.45 | 339 m | 146.53333 | T. Widhelm & F. Grewe | 2402 B |
| 01/25/16 | Australia | 14766_VIC | -38.45 | 339 m | 146.53333 | T. Widhelm & F. Grewe | 2402 D |
| 01/25/16 | Australia | 14767_VIC | -38.45 | 339 m | 146.53333 | T. Widhelm & F. Grewe | 2402 E |
| 01/25/16 | Australia | 14768_VIC | -38.45 | 339 m | 146.53333 | T. Widhelm & F. Grewe | 2402 F |
| 01/25/16 | Australia | 14769_VIC | -38.45 | 339 m | 146.53333 | T. Widhelm & F. Grewe | 2403 A |
| 01/25/16 | Australia | 14770_VIC | -38.45 | 339 m | 146.53333 | T. Widhelm & F. Grewe | 2403 B |
| 01/25/16 | Australia | 14771_VIC | -38.45 | 339 m | 146.53333 | T. Widhelm & F. Grewe | 2403 C |
| 01/25/16 | Australia | 14772_VIC | -38.45 | 339 m | 146.53333 | T. Widhelm & F. Grewe | 2403 D |
| 01/25/16 | Australia | 14776_VIC | -38.45 | 339 m | 146.53333 | T. Widhelm & F. Grewe | 2403 H |
| 01/26/16 | Australia | 14777_VIC | -37.3167 | 1022 m | 148.83333 | T. Widhelm & F. Grewe | 2421 A |
| 01/26/16 | Australia | 14778_VIC | -37.3167 | 1022 m | 148.83333 | T. Widhelm & F. Grewe | 2421 B |
| 01/26/16 | Australia | 14779_VIC | -37.3167 | 1022 m | 148.83333 | T. Widhelm & F. Grewe | 2421 C |
| 01/26/16 | Australia | 14780_VIC | -37.3167 | 1022 m | 148.83333 | T. Widhelm & F. Grewe | 2421 D |
| 01/26/16 | Australia | 14781_VIC | -37.3167 | 1022 m | 148.83333 | T. Widhelm & F. Grewe | 2421 E |
| 01/26/16 | Australia | 14783_VIC | -37.3167 | 1022 m | 148.83333 | T. Widhelm & F. Grewe | 2421 G |
| 01/26/16 | Australia | 14784_VIC | -37.3167 | 1022 m | 148.83333 | T. Widhelm & F. Grewe | 2421 H |
| 01/26/16 | Australia | 14785_VIC | -37.3167 | 1022 m | 148.83333 | T. Widhelm & F. Grewe | 2421 I |
| 01/26/16 | Australia | 14786_VIC | -37.3167 | 1022 m | 148.83333 | T. Widhelm & F. Grewe | 2421 J |
| 01/26/16 | Australia | 14787_VIC | -37.3167 | 1022 m | 148.83333 | T. Widhelm & F. Grewe | 2421 K |
| 01/26/16 | Australia | 14789_VIC | -37.3167 | 1022 m | 148.83333 | T. Widhelm & F. Grewe | 2421 M |
| 01/26/16 | Australia | 14790_VIC | -37.3167 | 1022 m | 148.83333 | T. Widhelm & F. Grewe | 2421 N |
| 01/26/16 | Australia | 14791_VIC | -37.3167 | 1022 m | 148.83333 | T. Widhelm & F. Grewe | 2421 O |
| 01/26/16 | Australia | 14792_VIC | -37.3167 | 1022 m | 148.83333 | T. Widhelm & F. Grewe | 2421 P |
| 01/26/16 | Australia | 14793_VIC | -37.3167 | 1022 m | 148.83333 | T. Widhelm & F. Grewe | 2421 Q |
| 01/26/16 | Australia | 14796_VIC | -37.3167 | 1022 m | 148.83333 | T. Widhelm & F. Grewe | 2421 T |
| 01/26/16 | Australia | 14798_VIC | -37.3167 | 1022 m | 148.83333 | T. Widhelm & F. Grewe | 2421 V |
| 01/26/16 | Australia | 14799_VIC | -37.3167 | 1022 m | 148.83333 | T. Widhelm & F. Grewe | 2421 W |

Table XXI, CONTINUED

| Date | Country | DNA number | Latitude | Altitude | Longitude | Collected by | Collection. no. |
|---|---|---|---|---|---|---|---|
| 01/26/16 | Australia | 14800_VIC | -37.3167 | 1022 m | 148.83333 | T. Widhelm & F. Grewe | 2421 X |
| 01/13/16 | Australia | 14810_VIC | -41.5 | 1240 m | 147.66667 | H.T. Lumbsch, T. Widhelm & F. Grewe | 2030 F |
| 01/13/16 | Australia | 14811_VIC | -41.5 | 1240 m | 147.66667 | H.T. Lumbsch, T. Widhelm & F. Grewe | 2030 HO |
| 01/13/16 | Australia | 14812_VIC | -41.5 | 1240 m | 147.66667 | H.T. Lumbsch, T. Widhelm & F. Grewe | 2030 HO A |
| 01/14/16 | Australia | 14814_VIC | -41.1333 | 210 m | 145.06667 | H.T. Lumbsch, T. Widhelm & F. Grewe | 2076 |
| 01/14/16 | Australia | 14815_VIC | -41.1333 | 210 m | 145.06667 | H.T. Lumbsch, T. Widhelm & F. Grewe | 2076 D |
| 01/21/16 | Australia | 14816_VIC | -37.6333 | 554 m | 145.71667 | T. Widhelm & F. Grewe | 2287 A |
| 01/21/16 | Australia | 14818_VIC | -37.6333 | 554 m | 145.71667 | T. Widhelm & F. Grewe | 2287 C |
| 12/16/17 | Chile | 15514_CHI | -41.1906 | 111.16 m | -72.532718 | Todd Widhelm, Matt von Konrat, Juan Larrain | 4322 |
| 12/16/17 | Chile | 15516_CHI | -41.1906 | 111.16 m | -72.532718 | Todd Widhelm, Matt von Konrat, Juan Larrain | 4324 |
| 12/16/17 | Chile | 15517_CHI | -41.1906 | 111.16 m | -72.532718 | Todd Widhelm, Matt von Konrat, Juan Larrain | 4326 |
| 12/16/17 | Chile | 15518_CHI | -41.1906 | 111.16 m | -72.532718 | Todd Widhelm, Matt von Konrat, Juan Larrain | 4327 |
| 12/16/17 | Chile | 15520_CHI | -41.1906 | 111.16 m | -72.532718 | Todd Widhelm, Matt von Konrat, Juan Larrain | 4329 |
| 12/16/17 | Chile | 15521_CHI | -41.1906 | 111.16 m | -72.532718 | Todd Widhelm, Matt von Konrat, Juan Larrain | 4330 |
| 12/16/17 | Chile | 15522_CHI | -41.1906 | 111.16 m | -72.532718 | Todd Widhelm, Matt von Konrat, Juan Larrain | 4331 |
| 12/16/17 | Chile | 15523_CHI | -41.1906 | 111.16 m | -72.532718 | Todd Widhelm, Matt von Konrat, Juan Larrain | 4332 |
| 12/16/17 | Chile | 15524_CHI | -41.1906 | 111.16 m | -72.532718 | Todd Widhelm, Matt von Konrat, Juan Larrain | 4333 |
| 12/16/17 | Chile | 15526_CHI | -41.1906 | 111.16 m | -72.532718 | Todd Widhelm, Matt von Konrat, Juan Larrain | 4338 |
| 12/16/17 | Chile | 15527_CHI | -41.1906 | 111.16 m | -72.532718 | Todd Widhelm, Matt von Konrat, Juan Larrain | 4339 |
| 12/16/17 | Chile | 15528_CHI | -41.1906 | 111.16 m | -72.532718 | Todd Widhelm, Matt von Konrat, Juan Larrain | 4340 |
| 12/16/17 | Chile | 15529_CHI | -41.1906 | 111.16 m | -72.532718 | Todd Widhelm, Matt von Konrat, Juan Larrain | 4341 |
| 12/16/17 | Chile | 15530_CHI | -41.1906 | 111.16 m | -72.532718 | Todd Widhelm, Matt von Konrat, Juan Larrain | 4342 |
| 12/16/17 | Chile | 15535_CHI | -41.1906 | 111.16 m | -72.532718 | Todd Widhelm, Matt von Konrat, Juan Larrain | 4347 |
| 12/16/17 | Chile | 15537_CHI | -41.1739 | 250 m | -72.517188 | Todd Widhelm, Matt von Konrat, Juan Larrain | 4351 |
| 12/16/17 | Chile | 15538_CHI | -41.1739 | 250 m | -72.517188 | Todd Widhelm, Matt von Konrat, Juan Larrain | 4351A |
| 12/16/17 | Chile | 15539_CHI | -41.1739 | 250 m | -72.517188 | Todd Widhelm, Matt von Konrat, Juan Larrain | 4355 |
| 12/16/17 | Chile | 15540_CHI | -41.1388 | 1000 m | -72.536507 | Todd Widhelm, Matt von Konrat, Juan Larrain | 4364 |
| 12/16/17 | Chile | 15541_CHI | -41.1388 | 1000 m | -72.536507 | Todd Widhelm, Matt von Konrat, Juan Larrain | 4365 |
| 12/16/17 | Chile | 15542_CHI | -41.1388 | 1000 m | -72.536507 | Todd Widhelm, Matt von Konrat, Juan Larrain | 4366 |
| 12/16/17 | Chile | 15543_CHI | -41.1388 | 1000 m | -72.536507 | Todd Widhelm, Matt von Konrat, Juan Larrain | 4367 |

Table XXI, CONTINUED

| Date | Country | DNA number | Latitude | Altitude | Longitude | Collected by | Collection. no. |
|---|---|---|---|---|---|---|---|
| 12/16/17 | Chile | 15544_CHI | -41.1388 | 1000 m | -72.536507 | Todd Widhelm, Matt von Konrat, Juan Larrain | 4368 |
| 12/16/17 | Chile | 15545_CHI | -41.1388 | 1000 m | -72.536507 | Todd Widhelm, Matt von Konrat, Juan Larrain | 4369 |
| 12/16/17 | Chile | 15546_CHI | -41.1388 | 1000 m | -72.536507 | Todd Widhelm, Matt von Konrat, Juan Larrain | 4370 |
| 12/16/17 | Chile | 15547_CHI | -41.1388 | 1000 m | -72.536507 | Todd Widhelm, Matt von Konrat, Juan Larrain | 4371 |
| 12/17/17 | Chile | 15550_CHI | -41.598 | 134.17 m | -72.599706 | Todd Widhelm, Matt von Konrat, Juan Larrain | 4375 |
| 12/17/17 | Chile | 15551_CHI | -41.598 | 134.17 m | -72.599706 | Todd Widhelm, Matt von Konrat, Juan Larrain | 4376 |
| 12/17/17 | Chile | 15552_CHI | -41.598 | 134.17 m | -72.599706 | Todd Widhelm, Matt von Konrat, Juan Larrain | 4377 |
| 12/17/17 | Chile | 15556_CHI | -41.598 | 134.17 m | -72.599706 | Todd Widhelm, Matt von Konrat, Juan Larrain | 4381 |
| 12/17/17 | Chile | 15557_CHI | -41.598 | 134.17 m | -72.599706 | Todd Widhelm, Matt von Konrat, Juan Larrain | 4382 |
| 12/17/17 | Chile | 15559_CHI | -41.598 | 134.17 m | -72.599706 | Todd Widhelm, Matt von Konrat, Juan Larrain | 4384 |
| 12/17/17 | Chile | 15560_CHI | -41.598 | 134.17 m | -72.599706 | Todd Widhelm, Matt von Konrat, Juan Larrain | 4385 |
| 12/17/17 | Chile | 15562_CHI | -41.598 | 134.17 m | -72.599706 | Todd Widhelm, Matt von Konrat, Juan Larrain | 4387 |
| 12/17/17 | Chile | 15563_CHI | -41.598 | 134.17 m | -72.599706 | Todd Widhelm, Matt von Konrat, Juan Larrain | 4388 |
| 12/17/17 | Chile | 15565_CHI | -41.5938 | 138.91 m | -72.593082 | Todd Widhelm, Matt von Konrat, Juan Larrain | 4391 |
| 12/17/17 | Chile | 15567_CHI | -41.5938 | 138.91 m | -72.593082 | Todd Widhelm, Matt von Konrat, Juan Larrain | 4393 |
| 12/17/17 | Chile | 15571_CHI | -41.5938 | 138.91 m | -72.593082 | Todd Widhelm, Matt von Konrat, Juan Larrain | 4397 |
| 12/17/17 | Chile | 15575_CHI | -41.5938 | 138.91 m | -72.593082 | Todd Widhelm, Matt von Konrat, Juan Larrain | 4410 |
| 12/17/17 | Chile | 15578_CHI | -41.5938 | 138.91 m | -72.593082 | Todd Widhelm, Matt von Konrat, Juan Larrain | 4414 |
| 12/17/17 | Chile | 15579_CHI | -41.5938 | 138.91 m | -72.593082 | Todd Widhelm, Matt von Konrat, Juan Larrain | 4415 |
| 12/18/17 | Chile | 15581_CHI | -41.8872 | 32.94 m | -73.672813 | Todd Widhelm, Matt von Konrat, Juan Larrain | 4444 |
| 12/18/17 | Chile | 15586_CHI | -41.8872 | 32.94 m | -73.672813 | Todd Widhelm, Matt von Konrat, Juan Larrain | 4449 |
| 12/18/17 | Chile | 15587_CHI | -41.8872 | 32.94 m | -73.672813 | Todd Widhelm, Matt von Konrat, Juan Larrain | 4450 |
| 12/18/17 | Chile | 15588_CHI | -41.8872 | 32.94 m | -73.672813 | Todd Widhelm, Matt von Konrat, Juan Larrain | 4451 |
| 12/18/17 | Chile | 15589_CHI | -41.8872 | 32.94 m | -73.672813 | Todd Widhelm, Matt von Konrat, Juan Larrain | 4452 |
| 12/18/17 | Chile | 15590_CHI | -41.8872 | 32.94 m | -73.672813 | Todd Widhelm, Matt von Konrat, Juan Larrain | 4453 |
| 12/18/17 | Chile | 15591_CHI | -41.8872 | 32.94 m | -73.672813 | Todd Widhelm, Matt von Konrat, Juan Larrain | 4454 |
| 12/18/17 | Chile | 15592_CHI | -41.8872 | 32.94 m | -73.672813 | Todd Widhelm, Matt von Konrat, Juan Larrain | 4455 |
| 12/18/17 | Chile | 15593_CHI | -41.8872 | 32.94 m | -73.672813 | Todd Widhelm, Matt von Konrat, Juan Larrain | 4456 |
| 12/18/17 | Chile | 15594_CHI | -41.8872 | 32.94 m | -73.672813 | Todd Widhelm, Matt von Konrat, Juan Larrain | 4457 |
| 12/18/17 | Chile | 15595_CHI | -41.8872 | 32.94 m | -73.672813 | Todd Widhelm, Matt von Konrat, Juan Larrain | 4458 |
| 12/19/17 | Chile | 15603_CHI | -42.7122 | 105.41 m | -73.936354 | Todd Widhelm, Matt von Konrat, Juan Larrain | 4472 |

Table XXI, CONTINUED

| Date | Country | DNA number | Latitude | Altitude | Longitude | Collected by | Collection. no. |
|---|---|---|---|---|---|---|---|
| 12/19/17 | Chile | 15605_CHI | -42.7122 | 105.41 m | -73.936354 | Todd Widhelm, Matt von Konrat, Juan Larrain | 4472 |
| 12/19/17 | Chile | 15606_CHI | -42.7122 | 105.41 m | -73.936354 | Todd Widhelm, Matt von Konrat, Juan Larrain | 4475 |
| 12/19/17 | Chile | 15609_CHI | -42.7122 | 105.41 m | -73.936354 | Todd Widhelm, Matt von Konrat, Juan Larrain | 4478 |
| 12/19/17 | Chile | 15611_CHI | -42.7122 | 105.41 m | -73.936354 | Todd Widhelm, Matt von Konrat, Juan Larrain | 4482 |
| 11/07/17 | New Zealand | 15905_NZN | -37.317 | 757 m | 175.44699 | Felix Grewe, Todd Widhelm, Dan Blanchon, Peter de Lange | 3050 |
| 11/07/17 | New Zealand | 15906_NZN | -37.317 | 757 m | 175.44699 | Felix Grewe, Todd Widhelm, Dan Blanchon, Peter de Lange | 3052 |
| 11/07/17 | New Zealand | 15907_NZN | -37.317 | 757 m | 175.44699 | Felix Grewe, Todd Widhelm, Dan Blanchon, Peter de Lange | 3053 |
| 11/07/17 | New Zealand | 15909_NZN | -37.317 | 757 m | 175.44699 | Felix Grewe, Todd Widhelm, Dan Blanchon, Peter de Lange | 3066 |
| 11/07/17 | New Zealand | 15910_PHO | -37.317 | 757 m | 175.44699 | Felix Grewe, Todd Widhelm, Dan Blanchon, Peter de Lange | 3069 |
| 11/07/17 | New Zealand | 15911_PHO | -37.317 | 757 m | 175.44699 | Felix Grewe, Todd Widhelm, Dan Blanchon, Peter de Lange | 3075 |
| 11/07/17 | New Zealand | 15912_NZN | -37.317 | 757 m | 175.44699 | Felix Grewe, Todd Widhelm, Dan Blanchon, Peter de Lange | 3077 |
| 11/07/17 | New Zealand | 15913_NZN | -37.317 | 757 m | 175.44699 | Felix Grewe, Todd Widhelm, Dan Blanchon, Peter de Lange | 3101 |
| 11/07/17 | New Zealand | 15914_NZN | -37.317 | 757 m | 175.44699 | Felix Grewe, Todd Widhelm, Dan Blanchon, Peter de Lange | 3106 |
| 11/07/17 | New Zealand | 15915_NZN | -37.317 | 757 m | 175.44699 | Felix Grewe, Todd Widhelm, Dan Blanchon, Peter de Lange | 3107 |
| 11/07/17 | New Zealand | 15916_PHO | -37.317 | 757 m | 175.44699 | Felix Grewe, Todd Widhelm, Dan Blanchon, Peter de Lange | 3110 |
| 11/07/17 | New Zealand | 15917_NZN | -37.317 | 757 m | 175.44699 | Felix Grewe, Todd Widhelm, Dan Blanchon, Peter de Lange | 3116 |
| 11/07/17 | New Zealand | 15918_NZN | -37.317 | 757 m | 175.44699 | Felix Grewe, Todd Widhelm, Dan Blanchon, Peter de Lange | 3122 |
| 11/09/17 | New Zealand | 15919_NZN | -39.205 | 1154 m | 175.54103 | Felix Grewe, Todd Widhelm | 3143 |
| 11/09/17 | New Zealand | 15920_NZN | -39.205 | 1154 m | 175.54103 | Felix Grewe, Todd Widhelm | 3144 |
| 11/09/17 | New Zealand | 15921_NZN | -39.205 | 1154 m | 175.54103 | Felix Grewe, Todd Widhelm | 3145 |
| 11/09/17 | New Zealand | 15923_NZN | -39.205 | 1154 m | 175.54103 | Felix Grewe, Todd Widhelm | 3147 |
| 11/09/17 | New Zealand | 15924_NZN | -39.205 | 1154 m | 175.54103 | Felix Grewe, Todd Widhelm | 3148 |
| 11/09/17 | New Zealand | 15926_NZN | -39.205 | 1154 m | 175.54103 | Felix Grewe, Todd Widhelm | 3151 |
| 11/09/17 | New Zealand | 15927_NZN | -39.205 | 1154 m | 175.54103 | Felix Grewe, Todd Widhelm | 3152 |

Table XXI, CONTINUED

| Date | Country | DNA number | Latitude | Altitude | Longitude | Collected by | Collection. no. |
|---|---|---|---|---|---|---|---|
| 11/09/17 | New Zealand | 15928_NZN | -39.205 | 1154 m | 175.54103 | Felix Grewe, Todd Widhelm | 3153 |
| 11/09/17 | New Zealand | 15929_NZN | -39.205 | 1154 m | 175.54103 | Felix Grewe, Todd Widhelm | 3154 |
| 11/09/17 | New Zealand | 15930_NZN | -39.205 | 1154 m | 175.54103 | Felix Grewe, Todd Widhelm | 3155 |
| 11/09/17 | New Zealand | 15931_NZN | -39.205 | 1154 m | 175.54103 | Felix Grewe, Todd Widhelm | 3156 |
| 11/09/17 | New Zealand | 15932_NZN | -39.205 | 1154 m | 175.54103 | Felix Grewe, Todd Widhelm | 3157 |
| 11/09/17 | New Zealand | 15934_NZN | -39.205 | 1154 m | 175.54103 | Felix Grewe, Todd Widhelm | 3159 |
| 11/09/17 | New Zealand | 15937_NZN | -39.205 | 1154 m | 175.54103 | Felix Grewe, Todd Widhelm | 3162 |
| 11/09/17 | New Zealand | 15938_NZN | -39.154 | 724 m | 175.82364 | Felix Grewe, Todd Widhelm | 3203 |
| 11/09/17 | New Zealand | 15939_NZN | -39.154 | 724 m | 175.82364 | Felix Grewe, Todd Widhelm | 3204 |
| 11/09/17 | New Zealand | 15940_NZN | -39.154 | 724 m | 175.82364 | Felix Grewe, Todd Widhelm | 3205 |
| 11/09/17 | New Zealand | 15942_NZN | -39.154 | 724 m | 175.82364 | Felix Grewe, Todd Widhelm | 3207 |
| 11/09/17 | New Zealand | 15943_NZN | -39.154 | 724 m | 175.82364 | Felix Grewe, Todd Widhelm | 3212 |
| 11/09/17 | New Zealand | 15944_NZN | -39.154 | 724 m | 175.82364 | Felix Grewe, Todd Widhelm | 3213 |
| 11/09/17 | New Zealand | 15946_NZN | -39.154 | 724 m | 175.82364 | Felix Grewe, Todd Widhelm | 3216 |
| 11/09/17 | New Zealand | 15947_NZN | -39.154 | 724 m | 175.82364 | Felix Grewe, Todd Widhelm | 3218 |
| 11/09/17 | New Zealand | 15948_NZN | -39.154 | 724 m | 175.82364 | Felix Grewe, Todd Widhelm | 3226 |
| 11/09/17 | New Zealand | 15949_NZN | -39.154 | 724 m | 175.82364 | Felix Grewe, Todd Widhelm | 3227 |
| 11/09/17 | New Zealand | 15950_NZN | -39.154 | 724 m | 175.82364 | Felix Grewe, Todd Widhelm | 3228 |
| 11/09/17 | New Zealand | 15951_NZN | -39.154 | 724 m | 175.82364 | Felix Grewe, Todd Widhelm | 3233 |
| 11/09/17 | New Zealand | 15952_NZN | -39.154 | 724 m | 175.82364 | Felix Grewe, Todd Widhelm | 3234 |
| 11/09/17 | New Zealand | 15953_NZN | -39.154 | 724 m | 175.82364 | Felix Grewe, Todd Widhelm | 3235 |
| 11/09/17 | New Zealand | 15954_NZN | -39.154 | 724 m | 175.82364 | Felix Grewe, Todd Widhelm | 3236 |
| 11/09/17 | New Zealand | 15955_NZN | -39.154 | 724 m | 175.82364 | Felix Grewe, Todd Widhelm | 3237 |
| 11/09/17 | New Zealand | 15957_NZN | -39.154 | 724 m | 175.82364 | Felix Grewe, Todd Widhelm | 3239 |
| 11/09/17 | New Zealand | 15958_NZN | -39.154 | 724 m | 175.82364 | Felix Grewe, Todd Widhelm | 3240 |
| 11/09/17 | New Zealand | 15959_NZN | -39.154 | 724 m | 175.82364 | Felix Grewe, Todd Widhelm | 3242 |
| 11/10/17 | New Zealand | 15960_NZN | -40.808 | 290 m | 175.54575 | Felix Grewe, Todd Widhelm | 3275 |
| 11/10/17 | New Zealand | 15963_NZN | -40.808 | 290 m | 175.54575 | Felix Grewe, Todd Widhelm | 3283 |
| 11/10/17 | New Zealand | 15965_NZN | -40.808 | 290 m | 175.54575 | Felix Grewe, Todd Widhelm | 3308 |
| 11/10/17 | New Zealand | 15969_NZN | -40.808 | 290 m | 175.54575 | Felix Grewe, Todd Widhelm | 3313 |
| 11/10/17 | New Zealand | 15971_NZN | -40.808 | 290 m | 175.54575 | Felix Grewe, Todd Widhelm | 3315 |

Table XXI, CONTINUED

| Date | Country | DNA number | Latitude | Altitude | Longitude | Collected by | Collection. no. |
|---|---|---|---|---|---|---|---|
| 11/10/17 | New Zealand | 15972_NZN | -40.808 | 290 m | 175.54575 | Felix Grewe, Todd Widhelm | 3316 |
| 11/10/17 | New Zealand | 15975_NZN | -40.808 | 290 m | 175.54575 | Felix Grewe, Todd Widhelm | 3319 |
| 11/11/17 | New Zealand | 15978_NZN | -41.353 | 33 m and up | 174.91752 | Felix Grewe, Todd Widhelm, Jeremy Rolfe | 3361 |
| 11/11/17 | New Zealand | 15980_NZN | -41.353 | 33 m and up | 174.91752 | Felix Grewe, Todd Widhelm, Jeremy Rolfe | 3363 |
| 11/11/17 | New Zealand | 15981_NZN | -41.353 | 33 m and up | 174.91752 | Felix Grewe, Todd Widhelm, Jeremy Rolfe | 3368 |
| 11/11/17 | New Zealand | 15982_NZN | -41.353 | 33 m and up | 174.91752 | Felix Grewe, Todd Widhelm, Jeremy Rolfe | 3374 |
| 11/11/17 | New Zealand | 15984_NZN | -41.353 | 33 m and up | 174.91752 | Felix Grewe, Todd Widhelm, Jeremy Rolfe | 3377 |
| 11/11/17 | New Zealand | 15986_NZN | -41.353 | 33 m and up | 174.91752 | Felix Grewe, Todd Widhelm, Jeremy Rolfe | 3379 |
| 11/11/17 | New Zealand | 15987_NZN | -41.353 | 33 m and up | 174.91752 | Felix Grewe, Todd Widhelm, Jeremy Rolfe | 3380 |
| 11/11/17 | New Zealand | 15988_NZN | -41.353 | 33 m and up | 174.91752 | Felix Grewe, Todd Widhelm, Jeremy Rolfe | 3381 |
| 11/11/17 | New Zealand | 15991_NZN | -41.353 | 33 m and up | 174.91752 | Felix Grewe, Todd Widhelm, Jeremy Rolfe | 3384 |
| 11/11/17 | New Zealand | 15993_NZN | -41.353 | 33 m and up | 174.91752 | Felix Grewe, Todd Widhelm, Jeremy Rolfe | 3386 |
| 11/11/17 | New Zealand | 15995_NZN | -41.353 | 33 m and up | 174.91752 | Felix Grewe, Todd Widhelm, Jeremy Rolfe | 3388 |
| 11/11/17 | New Zealand | 15996_NZN | -41.353 | 33 m and up | 174.91752 | Felix Grewe, Todd Widhelm, Jeremy Rolfe | 3389 |
| 11/11/17 | New Zealand | 15997_NZN | -41.353 | 33 m and up | 174.91752 | Felix Grewe, Todd Widhelm, Jeremy Rolfe | 3400 |
| 11/13/17 | New Zealand | 15999_NZS | -41.106 | 367 m | 172.72146 | Felix Grewe, Todd Widhelm | 3438 |
| 11/13/17 | New Zealand | 16000_PHO | -41.106 | 367 m | 172.72146 | Felix Grewe, Todd Widhelm | 3439 |
| 11/13/17 | New Zealand | 16002_PHO | -41.106 | 367 m | 172.72146 | Felix Grewe, Todd Widhelm | 3441 |
| 11/13/17 | New Zealand | 16003_PHO | -41.106 | 367 m | 172.72146 | Felix Grewe, Todd Widhelm | 3442 |
| 11/13/17 | New Zealand | 16009_PHO | -41.106 | 367 m | 172.72146 | Felix Grewe, Todd Widhelm | 3448 |
| 11/13/17 | New Zealand | 16010_PHO | -41.106 | 367 m | 172.72146 | Felix Grewe, Todd Widhelm | 3449 |
| 11/13/17 | New Zealand | 16011_NZS | -41.106 | 367 m | 172.72146 | Felix Grewe, Todd Widhelm | 3450 |
| 11/13/17 | New Zealand | 16012_PHO | -41.106 | 367 m | 172.72146 | Felix Grewe, Todd Widhelm | 3451 |
| 11/13/17 | New Zealand | 16014_NZS | -41.106 | 367 m | 172.72146 | Felix Grewe, Todd Widhelm | 3453 |

Table XXI, CONTINUED

| Date | Country | DNA number | Latitude | Altitude | Longitude | Collected by | Collection. no. |
|---|---|---|---|---|---|---|---|
| 11/14/17 | New Zealand | 16017_NZS | -41.807 | 625 m | 172.84679 | Felix Grewe, Todd Widhelm | 3500 |
| 11/14/17 | New Zealand | 16019_NZS | -41.807 | 625 m | 172.84679 | Felix Grewe, Todd Widhelm | 3502 |
| 11/14/17 | New Zealand | 16021_NZS | -41.807 | 625 m | 172.84679 | Felix Grewe, Todd Widhelm | 3504 |
| 11/14/17 | New Zealand | 16022_NZS | -41.807 | 625 m | 172.84679 | Felix Grewe, Todd Widhelm | 3505 |
| 11/14/17 | New Zealand | 16024_NZS | -41.807 | 625 m | 172.84679 | Felix Grewe, Todd Widhelm | 3508 |
| 11/14/17 | New Zealand | 16025_NZS | -41.807 | 625 m | 172.84679 | Felix Grewe, Todd Widhelm | 3509 |
| 11/14/17 | New Zealand | 16026_NZS | -41.807 | 625 m | 172.84679 | Felix Grewe, Todd Widhelm | 3510 |
| 11/14/17 | New Zealand | 16027_NZS | -41.807 | 625 m | 172.84679 | Felix Grewe, Todd Widhelm | 3511 |
| 11/14/17 | New Zealand | 16034_NZS | -41.807 | 625 m | 172.84679 | Felix Grewe, Todd Widhelm | 3519 |
| 11/14/17 | New Zealand | 16035_NZS | -41.807 | 625 m | 172.84679 | Felix Grewe, Todd Widhelm | 3520 |
| 11/14/17 | New Zealand | 16036_NZS | -41.807 | 625 m | 172.84679 | Felix Grewe, Todd Widhelm | 3521 |
| 11/14/17 | New Zealand | 16037_NZS | -41.807 | 625 m | 172.84679 | Felix Grewe, Todd Widhelm | 3522 |
| 11/14/17 | New Zealand | 16039_NZS | -41.767 | 139 m | 172.19267 | Felix Grewe, Todd Widhelm | 3525 |
| 11/14/17 | New Zealand | 16040_NZS | -41.767 | 139 m | 172.19267 | Felix Grewe, Todd Widhelm | 3526 |
| 11/14/17 | New Zealand | 16042_NZS | -41.767 | 139 m | 172.19267 | Felix Grewe, Todd Widhelm | 3528 |
| 11/14/17 | New Zealand | 16043_NZS | -41.767 | 139 m | 172.19267 | Felix Grewe, Todd Widhelm | 3529 |
| 11/14/17 | New Zealand | 16045_NZS | -41.767 | 139 m | 172.19267 | Felix Grewe, Todd Widhelm | 3531 |
| 11/14/17 | New Zealand | 16046_NZS | -41.767 | 139 m | 172.19267 | Felix Grewe, Todd Widhelm | 3532 |
| 11/14/17 | New Zealand | 16050_NZS | -41.767 | 139 m | 172.19267 | Felix Grewe, Todd Widhelm | 3536 |
| 11/14/17 | New Zealand | 16056_NZS | -41.767 | 139 m | 172.19267 | Felix Grewe, Todd Widhelm | 3542 |
| 11/14/17 | New Zealand | 16057_NZS | -41.767 | 139 m | 172.19267 | Felix Grewe, Todd Widhelm | 3543 |
| 11/15/17 | New Zealand | 16067_NZS | -42.919 | 851 m | 171.55832 | Felix Grewe, Todd Widhelm | 3597 |
| 11/15/17 | New Zealand | 16068_NZS | -42.919 | 851 m | 171.55832 | Felix Grewe, Todd Widhelm | 3598 |
| 11/15/17 | New Zealand | 16069_NZS | -42.919 | 851 m | 171.55832 | Felix Grewe, Todd Widhelm | 3599 |
| 11/15/17 | New Zealand | 16070_NZS | -42.919 | 851 m | 171.55832 | Felix Grewe, Todd Widhelm | 3600 |
| 11/15/17 | New Zealand | 16072_NZS | -42.919 | 851 m | 171.55832 | Felix Grewe, Todd Widhelm | 3602 |
| 11/15/17 | New Zealand | 16073_NZS | -42.919 | 851 m | 171.55832 | Felix Grewe, Todd Widhelm | 3603 |
| 11/15/17 | New Zealand | 16074_NZS | -42.919 | 851 m | 171.55832 | Felix Grewe, Todd Widhelm | 3604 |
| 11/15/17 | New Zealand | 16075_NZS | -42.919 | 851 m | 171.55832 | Felix Grewe, Todd Widhelm | 3605 |
| 11/15/17 | New Zealand | 16076_NZS | -42.919 | 851 m | 171.55832 | Felix Grewe, Todd Widhelm | 3606 |
| 11/15/17 | New Zealand | 16077_NZS | -42.919 | 851 m | 171.55832 | Felix Grewe, Todd Widhelm | 3607 |

Table XXI, CONTINUED

| Date | Country | DNA number | Latitude | Altitude | Longitude | Collected by | Collection. no. |
|---|---|---|---|---|---|---|---|
| 11/15/17 | New Zealand | 16078_NZS | -42.919 | 851 m | 171.55832 | Felix Grewe, Todd Widhelm | 3608 |
| 11/15/17 | New Zealand | 16079_NZS | -42.919 | 851 m | 171.55832 | Felix Grewe, Todd Widhelm | 3609 |
| 11/15/17 | New Zealand | 16080_NZS | -42.919 | 851 m | 171.55832 | Felix Grewe, Todd Widhelm | 3610 |
| 11/15/17 | New Zealand | 16081_NZS | -42.919 | 851 m | 171.55832 | Felix Grewe, Todd Widhelm | 3611 |
| 11/15/17 | New Zealand | 16082_NZS | -42.919 | 851 m | 171.55832 | Felix Grewe, Todd Widhelm | 3612 |
| 11/15/17 | New Zealand | 16084_NZS | -42.919 | 851 m | 171.55832 | Felix Grewe, Todd Widhelm | 3614 |
| 11/15/17 | New Zealand | 16089_NZS | -42.745 | 129 m | 171.4202 | Felix Grewe, Todd Widhelm | 3651 |
| 11/15/17 | New Zealand | 16091_NZS | -42.745 | 129 m | 171.4202 | Felix Grewe, Todd Widhelm | 3653 |
| 11/15/17 | New Zealand | 16092_NZS | -42.718 | 63 m | 171.24679 | Felix Grewe, Todd Widhelm | 3662 |
| 11/15/17 | New Zealand | 16093_NZS | -42.718 | 63 m | 171.24679 | Felix Grewe, Todd Widhelm | 3665 |
| 11/17/17 | New Zealand | 16094_NZS | -43.449 | 100 m | 169.9701 | Felix Grewe, Todd Widhelm | 3671 |
| 11/17/17 | New Zealand | 16096_NZS | -43.449 | 100 m | 169.9701 | Felix Grewe, Todd Widhelm | 3673 |
| 11/17/17 | New Zealand | 16097_NZS | -43.449 | 100 m | 169.9701 | Felix Grewe, Todd Widhelm | 3674 |
| 11/17/17 | New Zealand | 16099_NZS | -43.449 | 100 m | 169.9701 | Felix Grewe, Todd Widhelm | 3676 |
| 11/17/17 | New Zealand | 16100_NZS | -43.449 | 100 m | 169.9701 | Felix Grewe, Todd Widhelm | 3677 |
| 11/17/17 | New Zealand | 16101_NZS | -43.449 | 100 m | 169.9701 | Felix Grewe, Todd Widhelm | 3678 |
| 11/17/17 | New Zealand | 16102_NZS | -43.449 | 100 m | 169.9701 | Felix Grewe, Todd Widhelm | 3679 |
| 11/17/17 | New Zealand | 16103_NZS | -43.449 | 100 m | 169.9701 | Felix Grewe, Todd Widhelm | 3680 |
| 11/17/17 | New Zealand | 16104_NZS | -43.449 | 100 m | 169.9701 | Felix Grewe, Todd Widhelm | 3681 |
| 11/17/17 | New Zealand | 16106_NZS | -43.449 | 100 m | 169.9701 | Felix Grewe, Todd Widhelm | 3683 |
| 11/17/17 | New Zealand | 16107_NZS | -43.449 | 100 m | 169.9701 | Felix Grewe, Todd Widhelm | 3684 |
| 11/17/17 | New Zealand | 16108_NZS | -43.449 | 100 m | 169.9701 | Felix Grewe, Todd Widhelm | 3685 |
| 11/17/17 | New Zealand | 16111_NZS | -43.449 | 100 m | 169.9701 | Felix Grewe, Todd Widhelm | 3688 |
| 11/17/17 | New Zealand | 16112_NZS | -43.449 | 100 m | 169.9701 | Felix Grewe, Todd Widhelm | 3689 |
| 11/17/17 | New Zealand | 16113_NZS | -43.449 | 100 m | 169.9701 | Felix Grewe, Todd Widhelm | 3690 |
| 11/17/17 | New Zealand | 16114_NZS | -43.449 | 100 m | 169.9701 | Felix Grewe, Todd Widhelm | 3691 |
| 11/17/17 | New Zealand | 16115_NZS | -43.449 | 100 m | 169.9701 | Felix Grewe, Todd Widhelm | 3692 |
| 11/17/17 | New Zealand | 16116_NZS | -43.449 | 100 m | 169.9701 | Felix Grewe, Todd Widhelm | 3720 |
| 11/19/17 | New Zealand | 16117_NZS | -45.899 | 34 m | 169.49716 | Felix Grewe, Todd Widhelm, John Knight | 3883 |
| 11/19/17 | New Zealand | 16119_NZS | -45.899 | 34 m | 169.49716 | Felix Grewe, Todd Widhelm, John Knight | 3885 |
| 11/19/17 | New Zealand | 16120_NZS | -45.899 | 34 m | 169.49716 | Felix Grewe, Todd Widhelm, John Knight | 3886 |

Table XXI, CONTINUED

| Date | Country | DNA number | Latitude | Altitude | Longitude | Collected by | Collection. no. |
|---|---|---|---|---|---|---|---|
| 11/19/17 | New Zealand | 16121_NZS | -45.899 | 34 m | 169.49716 | Felix Grewe, Todd Widhelm, John Knight | 3887 |
| 11/19/17 | New Zealand | 16122_NZS | -45.899 | 34 m | 169.49716 | Felix Grewe, Todd Widhelm, John Knight | 3888 |
| 11/19/17 | New Zealand | 16123_NZS | -45.899 | 34 m | 169.49716 | Felix Grewe, Todd Widhelm, John Knight | 3889 |
| 11/19/17 | New Zealand | 16124_NZS | -45.899 | 34 m | 169.49716 | Felix Grewe, Todd Widhelm, John Knight | 3890 |
| 11/19/17 | New Zealand | 16125_NZS | -45.899 | 34 m | 169.49716 | Felix Grewe, Todd Widhelm, John Knight | 3891 |
| 11/19/17 | New Zealand | 16126_NZS | -45.899 | 34 m | 169.49716 | Felix Grewe, Todd Widhelm, John Knight | 3892 |
| 11/19/17 | New Zealand | 16127_NZS | -45.899 | 34 m | 169.49716 | Felix Grewe, Todd Widhelm, John Knight | 3893 |
| 11/19/17 | New Zealand | 16128_NZS | -45.899 | 34 m | 169.49716 | Felix Grewe, Todd Widhelm, John Knight | 3894 |
| 11/19/17 | New Zealand | 16129_NZS | -45.899 | 34 m | 169.49716 | Felix Grewe, Todd Widhelm, John Knight | 3895 |
| 11/19/17 | New Zealand | 16130_NZS | -45.899 | 34 m | 169.49716 | Felix Grewe, Todd Widhelm, John Knight | 3896 |
| 11/19/17 | New Zealand | 16131_NZS | -45.899 | 34 m | 169.49716 | Felix Grewe, Todd Widhelm, John Knight | 3897 |
| 11/19/17 | New Zealand | 16132_NZS | -45.899 | 34 m | 169.49716 | Felix Grewe, Todd Widhelm, John Knight | 3898 |
| 11/19/17 | New Zealand | 16133_NZS | -45.899 | 34 m | 169.49716 | Felix Grewe, Todd Widhelm, John Knight | 3899 |
| 11/19/17 | New Zealand | 16134_NZS | -45.899 | 34 m | 169.49716 | Felix Grewe, Todd Widhelm, John Knight | 3900 |
| 11/19/17 | New Zealand | 16135_NZS | -45.899 | 34 m | 169.49716 | Felix Grewe, Todd Widhelm, John Knight | 3901 |
| 11/07/17 | New Zealand | 16138_PHO | -37.317 | 757 m | 175.44699 | Felix Grewe, Todd Widhelm, Dan Blanchon, Peter de Lange | 3051 |
| 11/07/17 | New Zealand | 16139_PHO | -37.317 | 757 m | 175.44699 | Felix Grewe, Todd Widhelm, Dan Blanchon, Peter de Lange | 3070 |
| 11/07/17 | New Zealand | 16140_PHO | -37.317 | 757 m | 175.44699 | Felix Grewe, Todd Widhelm, Dan Blanchon, Peter de Lange | 3103 |
| 11/07/17 | New Zealand | 16141_PHO | -37.317 | 757 m | 175.44699 | Felix Grewe, Todd Widhelm, Dan Blanchon, Peter de Lange | 3112 |
| 12/14/17 | Chile | 16142_CHI | -54.9774 | 313 m | -67.674222 | Felix Grewe, Todd Widhelm, Matt von Konrat, Juan Larrain | 4268 |
| 01/07/18 | New Zealand | 17204_CAM | -52.5378 | 20-200 m | 169.1497 | A. Knight | 70993 |
| 01/08/18 | New Zealand | 17205_NZN | -50.8117 | 50 m | 166.0908 | A. Knight | 70992 |
| 01/06/18 | New Zealand | 17206_NZS | -50.4961 | 25 m | 166.2789 | A. Knight | 70988 |
| 11/16/17 | New Zealand | 17208_NZS | -45.8167 | 560 m | 170.5439 | A. Knight | 69177 |

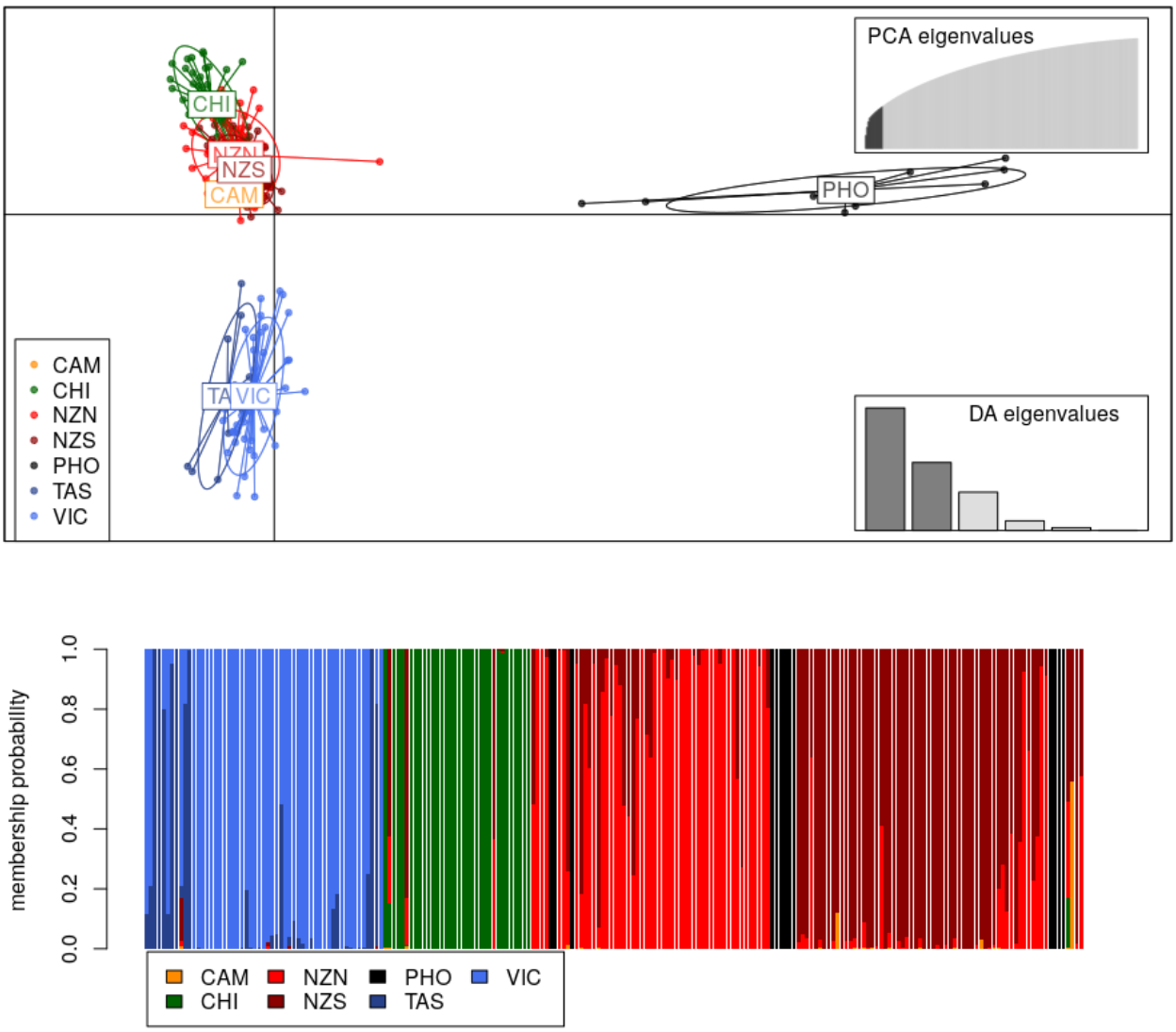


Figure 23. Genomic variation by non-parametric DAPC. (A) DAPC scatter plot of the densities of the populations of *P. glabra* (TAS=dark blue, VIC=light blue, CHI=green, NZN=dark red, NZS=light red, CAM=orange, PHO=black) estimated with 14 PCA and six DA eigenvalues (B) Bar plot of group membership probabilities.

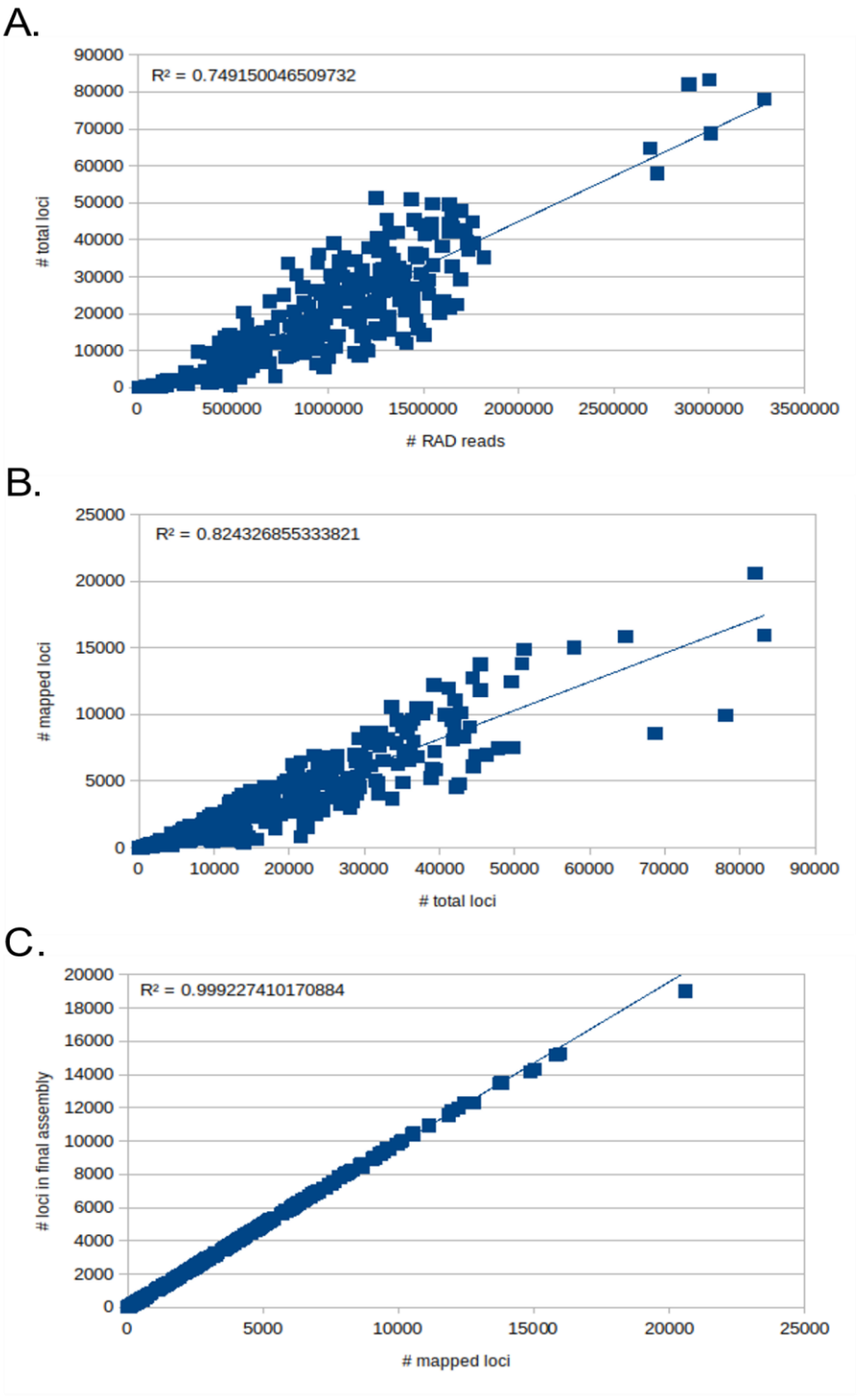


Figure 24. Reference-based RADseq assembly statistics. (A) The strong, positive, linear association between the number of RADseq reads and total RAD loci assembled. (B) The strong, positive, linear association between the number of total RAD loci assembled and those mapped to the reference genome. (C) The very strong, positive, linear association between the number of mapped loci and the total number of loci in the final assembly.

TABLE XXII. STATISTICS ON THE NUMBER OF RADESQ READS, TOTAL UNMAPPED LOCI ASSEMBLED IN PYRAD, LOCI MAPPED TO THE REFERENCE GENOME WITH BOWTIE2, AND LOCI IN THE 1000MIN DATASET.

| sample_name | n_reads | n_total_loci | n_mapped_loci | % loci mapped | n_assembled_loci | 1000min_dataset |
|---|---|---|---|---|---|---|
| 14682_TAS | 1305804 | 17934 | 3813 | 21.26% | 3756 | 3756 |
| 14687_TAS | 1473828 | 15724 | 2682 | 17.06% | 2661 | 2661 |
| 14689_TAS | 831680 | 30502 | 7830 | 25.67% | 7828 | 7828 |
| 14690_TAS | 984352 | 23891 | 6072 | 25.42% | 6045 | 6045 |
| 14693_TAS | 1293865 | 15579 | 3541 | 22.73% | 3483 | 3483 |
| 14696_TAS | 976359 | 5333 | 824 | 15.45% | 793 | |
| 14702_TAS | 878723 | 9286 | 2267 | 24.41% | 2230 | 2230 |
| 14706_TAS | 385699 | 1124 | 181 | 16.10% | 177 | |
| 14708_TAS | 484668 | 663 | 25 | 3.77% | 27 | |
| 14709_TAS | 1605770 | 23280 | 5390 | 23.15% | 5357 | 5357 |
| 14711_TAS | 1651796 | 32714 | 8091 | 24.73% | 8062 | 8062 |
| 14712_TAS | 859785 | 17657 | 4577 | 25.92% | 4560 | 4560 |
| 14718_TAS | 1506181 | 41256 | 11985 | 29.05% | 11809 | 11809 |
| 14720_TAS | 2690816 | 64767 | 15843 | 24.46% | 15173 | 15173 |
| 14725_VIC | 782498 | 12226 | 1889 | 15.45% | 1849 | 1849 |
| 14727_VIC | 691438 | 6796 | 543 | 7.99% | 534 | |
| 14728_VIC | 463814 | 1769 | 64 | 3.62% | 59 | |
| 14729_VIC | 723291 | 3132 | 177 | 5.65% | 173 | |
| 14731_VIC | 583556 | 4244 | 191 | 4.50% | 182 | |
| 14732_VIC | 877672 | 13736 | 434 | 3.16% | 416 | |
| 14735_VIC | 1417236 | 21891 | 1674 | 7.65% | 1644 | 1644 |
| 14743_VIC | 1580485 | 21528 | 816 | 3.79% | 777 | |
| 14747_VIC | 1456408 | 35938 | 6608 | 18.39% | 6554 | 6554 |
| 14749_VIC | 1245019 | 20448 | 4367 | 21.36% | 4371 | 4371 |
| 14753_VIC | 3006808 | 68705 | 8602 | 12.52% | 8584 | 8584 |
| 14755_VIC | 1176617 | 31872 | 4860 | 15.25% | 4852 | 4852 |
| 14756_VIC | 1049268 | 25409 | 3719 | 14.64% | 3702 | 3702 |
| 14757_VIC | 1178418 | 27097 | 3463 | 12.78% | 3448 | 3448 |
| 14758_VIC | 447083 | 10385 | 2421 | 23.31% | 2387 | 2387 |
| 14759_VIC | 798059 | 16876 | 3603 | 21.35% | 3531 | 3531 |
| 14761_VIC | 1488375 | 36168 | 7328 | 20.26% | 7170 | 7170 |
| 14762_VIC | 1164755 | 21570 | 6441 | 29.86% | 6401 | 6401 |
| 14763_VIC | 2728019 | 57949 | 15025 | 25.93% | 14326 | 14326 |
| 14764_VIC | 1518728 | 41717 | 9600 | 23.01% | 9550 | 9550 |
| 14766_VIC | 1402244 | 31376 | 8077 | 25.74% | 8094 | 8094 |
| 14767_VIC | 458809 | 12044 | 3274 | 27.18% | 3250 | 3250 |
| 14768_VIC | 1349460 | 26368 | 6900 | 26.17% | 6862 | 6862 |
| 14769_VIC | 562702 | 5777 | 1416 | 24.51% | 1386 | 1386 |
| 14770_VIC | 963716 | 10313 | 2459 | 23.84% | 2438 | 2438 |
| 14771_VIC | 1216447 | 14913 | 2330 | 15.62% | 2281 | 2281 |
| 14772_VIC | 383453 | 1383 | 253 | 18.29% | 223 | |
| 14776_VIC | 1634386 | 21335 | 5146 | 24.12% | 5118 | 5118 |
| 14777_VIC | 795078 | 8573 | 2145 | 25.02% | 2104 | 2104 |

TABLE XXII, CONTINUED

| sample_name | n_reads | n_total_loci | n_mapped_loci | % loci mapped | n_assembled_loci | 1000min_dataset |
|---|---|---|---|---|---|---|
| 14778_VIC | 604752 | 5914 | 1461 | 24.70% | 1440 | 1440 |
| 14779_VIC | 1549084 | 33159 | 8153 | 24.59% | 8107 | 8107 |
| 14780_VIC | 365582 | 1177 | 181 | 15.38% | 170 | |
| 14781_VIC | 1161929 | 8518 | 1723 | 20.23% | 1693 | 1693 |
| 14783_VIC | 802292 | 16746 | 4618 | 27.58% | 4605 | 4605 |
| 14784_VIC | 1527992 | 25286 | 6826 | 27.00% | 6810 | 6810 |
| 14785_VIC | 1109095 | 19606 | 5090 | 25.96% | 5052 | 5052 |
| 14786_VIC | 1042293 | 20486 | 4992 | 24.37% | 4968 | 4968 |
| 14787_VIC | 665833 | 9746 | 2285 | 23.45% | 2273 | 2273 |
| 14789_VIC | 983316 | 14044 | 3925 | 27.95% | 3878 | 3878 |
| 14790_VIC | 1374252 | 23513 | 5330 | 22.67% | 5300 | 5300 |
| 14791_VIC | 1735343 | 37061 | 6854 | 18.49% | 6800 | 6800 |
| 14792_VIC | 1543533 | 41771 | 8084 | 19.35% | 8057 | 8057 |
| 14793_VIC | 1345674 | 28918 | 6458 | 22.33% | 6423 | 6423 |
| 14796_VIC | 1195161 | 22177 | 3679 | 16.59% | 3682 | 3682 |
| 14798_VIC | 1285540 | 32046 | 7616 | 23.77% | 7541 | 7541 |
| 14799_VIC | 1394096 | 29572 | 6298 | 21.30% | 6264 | 6264 |
| 14800_VIC | 1404040 | 20973 | 4110 | 19.60% | 4077 | 4077 |
| 14810_VIC | 1393288 | 13204 | 3243 | 24.56% | 3238 | 3238 |
| 14811_VIC | 71160 | 209 | 20 | 9.57% | 18 | |
| 14812_VIC | 1716669 | 42597 | 4780 | 11.22% | 4758 | 4758 |
| 14814_VIC | 931884 | 26345 | 6021 | 22.85% | 5990 | 5990 |
| 14815_VIC | 589474 | 14318 | 2785 | 19.45% | 2779 | 2779 |
| 14816_VIC | 1034601 | 11649 | 783 | 6.72% | 776 | |
| 14818_VIC | 955999 | 18801 | 2450 | 13.03% | 2394 | 2394 |
| 15514_CHI | 1204098 | 10006 | 528 | 5.28% | 519 | |
| 15516_CHI | 765990 | 25113 | 6231 | 24.81% | 6160 | 6160 |
| 15517_CHI | 173875 | 2140 | 318 | 14.86% | 310 | |
| 15518_CHI | 317169 | 9700 | 2507 | 25.85% | 2476 | 2476 |
| 15520_CHI | 483821 | 14498 | 3691 | 25.46% | 3692 | 3692 |
| 15521_CHI | 1141522 | 9498 | 721 | 7.59% | 691 | |
| 15522_CHI | 43524 | 209 | 27 | 12.92% | 23 | |
| 15523_CHI | 152937 | 1946 | 299 | 15.36% | 286 | |
| 15524_CHI | 54075 | 297 | 33 | 11.11% | 23 | |
| 15526_CHI | 95698 | 857 | 144 | 16.80% | 132 | |
| 15527_CHI | 153019 | 453 | 8 | 1.77% | 8 | |
| 15528_CHI | 6901 | 9 | 0 | 0.00% | 0 | |
| 15529_CHI | 429485 | 12268 | 3484 | 28.40% | 3440 | 3440 |
| 15530_CHI | 44377 | 30 | 1 | 3.33% | 1 | |
| 15535_CHI | 371991 | 9315 | 2361 | 25.35% | 2332 | 2332 |
| 15537_CHI | 251979 | 4323 | 1100 | 25.45% | 1079 | 1079 |
| 15538_CHI | 1251984 | 51242 | 14880 | 29.04% | 14143 | 14143 |
| 15539_CHI | 147206 | 1595 | 353 | 22.13% | 340 | |
| 15540_CHI | 135844 | 1662 | 343 | 20.64% | 323 | |
| 15541_CHI | 458031 | 13616 | 4008 | 29.44% | 3994 | 3994 |
| 15542_CHI | 24906 | 59 | 4 | 6.78% | 1 | |
| 15543_CHI | 81484 | 591 | 74 | 12.52% | 68 | |

TABLE XXII, CONTINUED

| sample_name | n_reads | n_total_loci | n_mapped_loci | % loci mapped | n_assembled_loci | 1000min_dataset |
|---|---|---|---|---|---|---|
| 15544_CHI | 129692 | 1351 | 223 | 16.51% | 211 | |
| 15545_CHI | 790120 | 33595 | 10564 | 31.45% | 10336 | 10336 |
| 15546_CHI | 1059953 | 34323 | 9580 | 27.91% | 9489 | 9489 |
| 15547_CHI | 1636141 | 42036 | 11129 | 26.47% | 10943 | 10943 |
| 15550_CHI | 692966 | 23332 | 6930 | 29.70% | 6895 | 6895 |
| 15551_CHI | 2891795 | 82044 | 20591 | 25.10% | 19017 | 19017 |
| 15552_CHI | 820990 | 20668 | 6021 | 29.13% | 5988 | 5988 |
| 15556_CHI | 555083 | 20411 | 6235 | 30.55% | 6227 | 6227 |
| 15557_CHI | 165175 | 1798 | 288 | 16.02% | 275 | |
| 15559_CHI | 1597329 | 38205 | 10535 | 27.57% | 10397 | 10397 |
| 15560_CHI | 1060689 | 32225 | 8612 | 26.72% | 8591 | 8591 |
| 15562_CHI | 1543762 | 44439 | 12759 | 28.71% | 12291 | 12291 |
| 15563_CHI | 1306708 | 45440 | 13754 | 30.27% | 13449 | 13449 |
| 15565_CHI | 1029363 | 39231 | 12214 | 31.13% | 11968 | 11968 |
| 15567_CHI | 1264822 | 37019 | 10542 | 28.48% | 10471 | 10471 |
| 15571_CHI | 576311 | 17258 | 4366 | 25.30% | 4366 | 4366 |
| 15575_CHI | 1253619 | 40729 | 9975 | 24.49% | 9807 | 9807 |
| 15578_CHI | 1436944 | 50989 | 13810 | 27.08% | 13513 | 13513 |
| 15579_CHI | 890797 | 14829 | 4327 | 29.18% | 4328 | 4328 |
| 15581_CHI | 1175460 | 8673 | 1210 | 13.95% | 1194 | 1194 |
| 15586_CHI | 1443125 | 21977 | 2489 | 11.33% | 2497 | 2497 |
| 15587_CHI | 1270923 | 14482 | 811 | 5.60% | 777 | |
| 15588_CHI | 1677445 | 22496 | 1504 | 6.69% | 1465 | 1465 |
| 15589_CHI | 1318664 | 15657 | 615 | 3.93% | 591 | |
| 15590_CHI | 999579 | 8087 | 625 | 7.73% | 615 | |
| 15591_CHI | 1210293 | 9839 | 414 | 4.21% | 388 | |
| 15592_CHI | 1178245 | 13923 | 387 | 2.78% | 361 | |
| 15593_CHI | 437925 | 4418 | 211 | 4.78% | 192 | |
| 15594_CHI | 1409637 | 12068 | 534 | 4.42% | 518 | |
| 15595_CHI | 1241913 | 23498 | 2541 | 10.81% | 2514 | 2514 |
| 15603_CHI | 1635832 | 49574 | 12445 | 25.10% | 12301 | 12301 |
| 15605_CHI | 739692 | 19384 | 4905 | 25.30% | 4877 | 4877 |
| 15606_CHI | 1083965 | 35151 | 9111 | 25.92% | 8991 | 8991 |
| 15609_CHI | 953819 | 36157 | 9319 | 25.77% | 9216 | 9216 |
| 15611_CHI | 1010247 | 25628 | 5855 | 22.85% | 5856 | 5856 |
| 15905_NZN | 635453 | 14629 | 2562 | 17.51% | 2534 | 2534 |
| 15906_NZN | 1647253 | 46240 | 6988 | 15.11% | 6939 | 6939 |
| 15907_NZN | 1072907 | 30070 | 6734 | 22.39% | 6671 | 6671 |
| 15909_NZN | 1182530 | 28846 | 6469 | 22.43% | 6441 | 6441 |
| 15910_PHO | 1362241 | 42008 | 8643 | 20.57% | 8551 | 8551 |
| 15911_PHO | 1322625 | 41899 | 9660 | 23.06% | 9548 | 9548 |
| 15912_NZN | 827881 | 19984 | 3869 | 19.36% | 3807 | 3807 |
| 15913_NZN | 1652612 | 43228 | 8281 | 19.16% | 8237 | 8237 |
| 15914_NZN | 511931 | 5214 | 452 | 8.67% | 445 | |
| 15915_NZN | 946410 | 10463 | 1314 | 12.56% | 1293 | 1293 |
| 15916_PHO | 1159461 | 25674 | 4442 | 17.30% | 4443 | 4443 |
| 15917_NZN | 550604 | 13306 | 3753 | 28.21% | 3726 | 3726 |

TABLE XXII, CONTINUED

| sample_name | n_reads | n_total_loci | n_mapped_loci | % loci mapped | n_assembled_loci | 1000min_dataset |
|---|---|---|---|---|---|---|
| 15918_NZN | 616738 | 12402 | 2205 | 17.78% | 2213 | 2213 |
| 15919_NZN | 392997 | 4041 | 268 | 6.63% | 265 | |
| 15920_NZN | 1423653 | 25984 | 4663 | 17.95% | 4634 | 4634 |
| 15921_NZN | 1319506 | 18156 | 1387 | 7.64% | 1374 | 1374 |
| 15923_NZN | 1270438 | 28077 | 2951 | 10.51% | 2932 | 2932 |
| 15924_NZN | 909372 | 12369 | 1047 | 8.46% | 1034 | 1034 |
| 15926_NZN | 1164119 | 22685 | 2861 | 12.61% | 2831 | 2831 |
| 15927_NZN | 930918 | 16610 | 2933 | 17.66% | 2898 | 2898 |
| 15928_NZN | 1665311 | 42267 | 4534 | 10.73% | 4521 | 4521 |
| 15929_NZN | 1253352 | 28363 | 3461 | 12.20% | 3435 | 3435 |
| 15930_NZN | 1275234 | 31885 | 4038 | 12.66% | 4004 | 4004 |
| 15931_NZN | 1001044 | 22164 | 3590 | 16.20% | 3562 | 3562 |
| 15932_NZN | 1402105 | 20747 | 2672 | 12.88% | 2672 | 2672 |
| 15934_NZN | 1582775 | 20043 | 2691 | 13.43% | 2638 | 2638 |
| 15937_NZN | 1144809 | 17565 | 2974 | 16.93% | 2931 | 2931 |
| 15938_NZN | 1469036 | 35255 | 6867 | 19.48% | 6821 | 6821 |
| 15939_NZN | 1042169 | 10960 | 881 | 8.04% | 858 | |
| 15940_NZN | 974044 | 17740 | 2487 | 14.02% | 2469 | 2469 |
| 15942_NZN | 779188 | 8095 | 1161 | 14.34% | 1156 | 1156 |
| 15943_NZN | 1108641 | 28911 | 4070 | 14.08% | 4031 | 4031 |
| 15944_NZN | 1759768 | 44805 | 6956 | 15.53% | 6912 | 6912 |
| 15946_NZN | 1765626 | 39051 | 5952 | 15.24% | 5866 | 5866 |
| 15947_NZN | 447493 | 6582 | 415 | 6.31% | 405 | |
| 15948_NZN | 1446135 | 24441 | 2763 | 11.30% | 2734 | 2734 |
| 15949_NZN | 831614 | 16906 | 1875 | 11.09% | 1850 | 1850 |
| 15950_NZN | 705615 | 12033 | 1850 | 15.37% | 1830 | 1830 |
| 15951_NZN | 3002039 | 83290 | 15965 | 19.17% | 15236 | 15236 |
| 15952_NZN | 1360447 | 31473 | 5060 | 16.08% | 5036 | 5036 |
| 15953_NZN | 3286909 | 78041 | 9951 | 12.75% | 9827 | 9827 |
| 15954_NZN | 1323095 | 19215 | 4529 | 23.57% | 4484 | 4484 |
| 15955_NZN | 1313325 | 27695 | 5226 | 18.87% | 5204 | 5204 |
| 15957_NZN | 1426632 | 26321 | 4200 | 15.96% | 4162 | 4162 |
| 15958_NZN | 986805 | 20312 | 4241 | 20.88% | 4195 | 4195 |
| 15959_NZN | 1726385 | 39353 | 7238 | 18.39% | 7174 | 7174 |
| 15960_NZN | 216205 | 1679 | 24 | 1.43% | 12 | |
| 15963_NZN | 1009462 | 30470 | 8652 | 28.40% | 8412 | 8412 |
| 15965_NZN | 383041 | 2786 | 566 | 20.32% | 562 | |
| 15969_NZN | 119492 | 343 | 21 | 6.12% | 23 | |
| 15971_NZN | 300588 | 3566 | 628 | 17.61% | 614 | |
| 15972_NZN | 114420 | 772 | 75 | 9.72% | 71 | |
| 15975_NZN | 629056 | 12309 | 2966 | 24.10% | 2927 | 2927 |
| 15978_NZN | 439530 | 2568 | 363 | 14.14% | 355 | |
| 15980_NZN | 1317839 | 36520 | 8011 | 21.94% | 7970 | 7970 |
| 15981_NZN | 957736 | 25333 | 6497 | 25.65% | 6425 | 6425 |
| 15982_NZN | 1140007 | 34290 | 7852 | 22.90% | 7778 | 7778 |
| 15984_NZN | 396622 | 6727 | 1650 | 24.53% | 1628 | 1628 |
| 15986_NZN | 850060 | 11357 | 2710 | 23.86% | 2685 | 2685 |

TABLE XXII, CONTINUED

| sample_name | n_reads | n_total_loci | n_mapped_loci | % loci mapped | n_assembled_loci | 1000min_dataset |
|---|---|---|---|---|---|---|
| 15987_NZN | 1209196 | 37763 | 10094 | 26.73% | 9944 | 9944 |
| 15988_NZN | 1454547 | 35682 | 8575 | 24.03% | 8481 | 8481 |
| 15991_NZN | 1482568 | 44076 | 9047 | 20.53% | 8921 | 8921 |
| 15993_NZN | 1025297 | 26874 | 4224 | 15.72% | 4188 | 4188 |
| 15995_NZN | 1291444 | 26186 | 4797 | 18.32% | 4712 | 4712 |
| 15996_NZN | 31968 | 105 | 5 | 4.76% | 4 | |
| 15997_NZN | 740794 | 11890 | 1796 | 15.11% | 1759 | 1759 |
| 15999_NZS | 484988 | 4552 | 448 | 9.84% | 437 | |
| 16000_PHO | 919747 | 17850 | 2878 | 16.12% | 2823 | 2823 |
| 16002_PHO | 1449485 | 45402 | 11853 | 26.11% | 11555 | 11555 |
| 16003_PHO | 1077454 | 25893 | 6043 | 23.34% | 5941 | 5941 |
| 16009_PHO | 1266737 | 24619 | 5268 | 21.40% | 5253 | 5253 |
| 16010_PHO | 760345 | 12550 | 1705 | 13.59% | 1669 | 1669 |
| 16011_NZS | 79766 | 154 | 2 | 1.30% | 2 | |
| 16012_PHO | 1118812 | 25542 | 5700 | 22.32% | 5636 | 5636 |
| 16014_NZS | 446577 | 4520 | 805 | 17.81% | 782 | |
| 16017_NZS | 332318 | 3194 | 595 | 18.63% | 577 | |
| 16019_NZS | 243762 | 994 | 142 | 14.29% | 137 | |
| 16021_NZS | 940094 | 6454 | 564 | 8.74% | 553 | |
| 16022_NZS | 1518607 | 27826 | 3520 | 12.65% | 3499 | 3499 |
| 16024_NZS | 413290 | 1732 | 129 | 7.45% | 117 | |
| 16025_NZS | 1270669 | 20963 | 3232 | 15.42% | 3174 | 3174 |
| 16026_NZS | 534657 | 2564 | 184 | 7.18% | 180 | |
| 16027_NZS | 151004 | 536 | 43 | 8.02% | 43 | |
| 16034_NZS | 988880 | 18539 | 2738 | 14.77% | 2676 | 2676 |
| 16035_NZS | 439725 | 3071 | 327 | 10.65% | 307 | |
| 16036_NZS | 251664 | 1731 | 154 | 8.90% | 137 | |
| 16037_NZS | 1422823 | 22805 | 4133 | 18.12% | 4094 | 4094 |
| 16039_NZS | 1296703 | 29275 | 8215 | 28.06% | 8160 | 8160 |
| 16040_NZS | 702807 | 16367 | 3476 | 21.24% | 3423 | 3423 |
| 16042_NZS | 1458468 | 36432 | 9626 | 26.42% | 9533 | 9533 |
| 16043_NZS | 1641151 | 42791 | 10127 | 23.67% | 10031 | 10031 |
| 16045_NZS | 408694 | 5469 | 1158 | 21.17% | 1128 | 1128 |
| 16046_NZS | 1315574 | 35372 | 9423 | 26.64% | 9336 | 9336 |
| 16050_NZS | 131056 | 1049 | 136 | 12.96% | 113 | |
| 16056_NZS | 1170807 | 21067 | 5892 | 27.97% | 5844 | 5844 |
| 16057_NZS | 502248 | 6625 | 1487 | 22.45% | 1445 | 1445 |
| 16067_NZS | 925207 | 16783 | 2645 | 15.76% | 2605 | 2605 |
| 16068_NZS | 1545634 | 49722 | 7511 | 15.11% | 7418 | 7418 |
| 16069_NZS | 717712 | 12164 | 2088 | 17.17% | 2045 | 2045 |
| 16070_NZS | 691421 | 12231 | 1485 | 12.14% | 1448 | 1448 |
| 16072_NZS | 527922 | 5657 | 435 | 7.69% | 413 | |
| 16073_NZS | 1163050 | 18696 | 2469 | 13.21% | 2431 | 2431 |
| 16074_NZS | 1117320 | 26201 | 4303 | 16.42% | 4242 | 4242 |
| 16075_NZS | 1129674 | 24156 | 3744 | 15.50% | 3687 | 3687 |
| 16076_NZS | 633782 | 10053 | 1443 | 14.35% | 1428 | 1428 |
| 16077_NZS | 1080014 | 23765 | 4863 | 20.46% | 4796 | 4796 |

TABLE XXII, CONTINUED

| sample_name | n_reads | n_total_loci | n_mapped_loci | % loci mapped | n_assembled_loci | 1000min_dataset |
|---|---|---|---|---|---|---|
| 16078_NZS | 1050421 | 14151 | 1180 | 8.34% | 1184 | 1184 |
| 16079_NZS | 1637419 | 44502 | 6123 | 13.76% | 6052 | 6052 |
| 16080_NZS | 838323 | 11896 | 2558 | 21.50% | 2521 | 2521 |
| 16081_NZS | 1462655 | 18096 | 2365 | 13.07% | 2310 | 2310 |
| 16082_NZS | 376360 | 2885 | 449 | 15.56% | 436 | |
| 16084_NZS | 1819134 | 35140 | 4909 | 13.97% | 4885 | 4885 |
| 16089_NZS | 1343610 | 34509 | 6277 | 18.19% | 6250 | 6250 |
| 16091_NZS | 1372859 | 32511 | 6539 | 20.11% | 6497 | 6497 |
| 16092_NZS | 1441475 | 26800 | 3258 | 12.16% | 3225 | 3225 |
| 16093_NZS | 1695182 | 29326 | 4538 | 15.47% | 4517 | 4517 |
| 16094_NZS | 1257733 | 27705 | 4816 | 17.38% | 4794 | 4794 |
| 16096_NZS | 1527435 | 29165 | 5376 | 18.43% | 5322 | 5322 |
| 16097_NZS | 487029 | 9009 | 1300 | 14.43% | 1263 | 1263 |
| 16099_NZS | 1136123 | 29528 | 7046 | 23.86% | 6959 | 6959 |
| 16100_NZS | 562435 | 11522 | 1900 | 16.49% | 1874 | 1874 |
| 16101_NZS | 1489631 | 30918 | 6157 | 19.91% | 6103 | 6103 |
| 16102_NZS | 597913 | 9643 | 520 | 5.39% | 401 | |
| 16103_NZS | 554532 | 6523 | 815 | 12.49% | 806 | |
| 16104_NZS | 1189517 | 13903 | 1396 | 10.04% | 1360 | 1360 |
| 16106_NZS | 1305004 | 28606 | 7003 | 24.48% | 6920 | 6920 |
| 16107_NZS | 892152 | 16390 | 2546 | 15.53% | 2518 | 2518 |
| 16108_NZS | 916286 | 15213 | 2990 | 19.65% | 2972 | 2972 |
| 16111_NZS | 969153 | 26163 | 4039 | 15.44% | 4010 | 4010 |
| 16112_NZS | 873571 | 17989 | 2927 | 16.27% | 2932 | 2932 |
| 16113_NZS | 819249 | 14448 | 2374 | 16.43% | 2338 | 2338 |
| 16114_NZS | 1251298 | 27278 | 4495 | 16.48% | 4465 | 4465 |
| 16115_NZS | 526740 | 13500 | 1976 | 14.64% | 1950 | 1950 |
| 16116_NZS | 1192267 | 21068 | 3301 | 15.67% | 3269 | 3269 |
| 16117_NZS | 656004 | 14990 | 2507 | 16.72% | 2478 | 2478 |
| 16119_NZS | 906322 | 19575 | 3162 | 16.15% | 3088 | 3088 |
| 16120_NZS | 355744 | 4654 | 476 | 10.23% | 463 | |
| 16121_NZS | 260353 | 870 | 39 | 4.48% | 40 | |
| 16122_NZS | 506995 | 12022 | 2113 | 17.58% | 2064 | 2064 |
| 16123_NZS | 809748 | 8917 | 1098 | 12.31% | 1057 | 1057 |
| 16124_NZS | 872816 | 23206 | 4717 | 20.33% | 4649 | 4649 |
| 16125_NZS | 364959 | 2484 | 225 | 9.06% | 211 | |
| 16126_NZS | 568246 | 8175 | 1154 | 14.12% | 1128 | 1128 |
| 16127_NZS | 350201 | 2775 | 256 | 9.23% | 237 | |
| 16128_NZS | 901233 | 22162 | 4132 | 18.64% | 4092 | 4092 |
| 16129_NZS | 461994 | 3559 | 370 | 10.40% | 357 | |
| 16130_NZS | 837556 | 10140 | 1320 | 13.02% | 1269 | 1269 |
| 16131_NZS | 1246214 | 16131 | 2525 | 15.65% | 2509 | 2509 |
| 16132_NZS | 548384 | 8779 | 1406 | 16.02% | 1365 | 1365 |
| 16133_NZS | 292028 | 2470 | 426 | 17.25% | 426 | |
| 16134_NZS | 1109089 | 18442 | 2882 | 15.63% | 2847 | 2847 |
| 16135_NZS | 1441725 | 23782 | 3081 | 12.96% | 3033 | 3033 |
| 16138_PHO | 865446 | 27221 | 4309 | 15.83% | 4278 | 4278 |

TABLE XXII, CONTINUED

| sample_name | n_reads | n_total_loci | n_mapped_loci | % loci mapped | n_assembled_loci | 1000min_dataset |
|---|---|---|---|---|---|---|
| 16139_PHO | 1029367 | 38850 | 5235 | 13.47% | 5175 | 5175 |
| 16140_PHO | 1281728 | 39505 | 5842 | 14.79% | 5801 | 5801 |
| 16141_PHO | 945414 | 33745 | 3675 | 10.89% | 3645 | 3645 |
| 16142_CHI | 792246 | 11055 | 1530 | 13.84% | 1501 | 1501 |
| 17204_CAM | 1020705 | 29943 | 5668 | 18.93% | 5598 | 5598 |
| 17205_NZN | 660624 | 6753 | 827 | 12.25% | 794 | |
| 17206_NZS | 1699635 | 47798 | 7451 | 15.59% | 7419 | 7419 |
| 17208_NZS | 1503607 | 14241 | 1028 | 7.22% | 1012 | 1012 |
| **AVE** | **994,295.95** | **20,357.12** | **3,966.98** | **17.27%** | **3,910.36** | **5,073.16** |
| **STDEV** | **535,452.64** | **15,128.82** | **3,584.49** | **7.17%** | **3,498.41** | **3,263.88** |

# VITA

**NAME**:

Todd J. Widhelm

**EDUCATION**:

| | | |
|---|---|---|
| B.S. | 2005 | Environmental Studies, University of Nebraska at Omaha, Omaha, NE |
| M.S. | 2008 | Biology, University of Nebraska at Omaha, Omaha, NE |
| Ph.D. | 2019 | Biological Sciences, University of Illinois at Chicago, Chicago, IL |

**PUBLICATIONS**:


Egan, Robert S, Robert Harms, and Todd Widhelm. 2005. "Studies on the Lichen *Parmotrema rigidum* s. Lat. from North and South America." *The Bryologist* 108 (3).

Fey, Paul D, Jennifer L Endres, Vijaya Kumar Yajjala, Todd J Widhelm, Robert J Boissy, Jeffrey L Bose, and Kenneth W Bayles. 2013. "A Genetic Resource for Rapid and Comprehensive Phenotype Screening of Nonessential *Staphylococcus aureus* Genes." *MBio* 4 (1).

Laabei, Maisem, Mario Recker, Justine K Rudkin, Mona Aldeljawi, Zeynep Gulay, Tim J Sloan, Paul Williams, et al. 2014. "Predicting the Virulence of MRSA from Its Genome Sequence." *Genome Research* 24 (5).

Leavitt, Steven D., Felix Grewe, Todd Widhelm, Lucia Muggia, Brian Wray, and H. Thorsten Lumbsch. 2016. "Resolving Evolutionary Relationships in Lichen-Forming Fungi Using Diverse Phylogenomic Datasets and Analytical Approaches." *Scientific Reports* 6.

Sadykov, Marat R, Jong-Sam Ahn, Todd J Widhelm, Valerie M Eckrich, Jennifer L Endres, Adam Driks, Gregory E Rutkowski, Kevin L Wingerd, and Kenneth W Bayles. 2017. "Poly (3-hydroxybutyrate) Fuels the Tricarboxylic Acid Cycle and de Novo Lipid Biosynthesis during *Bacillus anthracis* Sporulation." *Molecular Microbiology* 104 (5): 793–803.

Sadykov, Marat R, Vinai C Thomas, Darrell D Marshall, Christopher J Wenstrom, Derek E Moormeier, Todd J Widhelm, Austin S Nuxoll, Robert Powers, and Kenneth W Bayles. 2013. "Inactivation of the Pta-AckA Pathway Causes Cell Death in *Staphylococcus aureus*." *Journal of Bacteriology* 195 (13).

Schmitt, I., A. Crespo, P.K. Divakar, J.D. Fankhauser, E. Herman-Sackett, K. Kalb, M.P. Nelsen, et al. 2009. "New Primers for Promising Single-Copy Genes in Fungal Phylogenetics and Systematics." *Persoonia - Molecular Phylogeny and Evolution of Fungi* 23 (1): 35–40.

Thomas, Vinai Chittezham, Marat R Sadykov, Sujata S Chaudhari, Joselyn Jones, Jennifer L Endres, Todd J Widhelm, Jong-Sam Ahn, Randeep S Jawa, Matthew C Zimmerman, and Kenneth W Bayles. 2014. "A Central Role for Carbon-Overflow Pathways in the

Modulation of Bacterial Cell Death." *PLoS Pathog* 10 (6).

Widhelm, Todd J., Francesca R. Bertoletti, Matt J. Asztalos, Joel A. Mercado-Díaz, Jen-Pan Huang, Bibiana Moncada, Robert Lücking, et al. 2018. "Oligocene Origin and Drivers of Diversification in the Genus *Sticta* (Lobariaceae, Ascomycota)." *Molecular Phylogenetics and Evolution* 126. 58–73.

Widhelm, Todd J, Robert S Egan, Francesca R Bertoletti, Matt J Asztalos, Ekaphan Kraichak, Steven D Leavitt, and H Thorsten Lumbsch. 2016. "Picking Holes in Traditional Species Delimitations: An Integrative Taxonomic Reassessment of the *Parmotrema perforatum* Group (Parmeliaceae, Ascomycota)." *Botanical Journal of the Linnean Society* 182 (4).

Widhelm, Todd J, Vijay Kumar Yajjala, Jennifer L Endres, Paul D Fey, and Kenneth W Bayles. 2014. "Methods to Generate a Sequence-Defined Transposon Mutant Library in *Staphylococcus epidermidis* Strain 1457." In *Methods in Molecular Biology (Clifton, N.J.)*, 1106:135–42.

Widhelm, Todd, and H. Thorsten Lumbsch. 2011. "The Phylogenetic Placement of Miltideaceae Inferred from Ribosomal DNA Sequence Data." *Bibl Lichenologica*, no. 106: 365–73.

Yajjala, Vijaya Kumar, Todd J Widhelm, Jennifer L Endres, Paul D Fey, and Kenneth W Bayles. 2016. "Generation of a Transposon Mutant Library in *Staphylococcus aureus* and *Staphylococcus epidermidis* Using *bursa aurealis*." *The Genetic Manipulation of Staphylococci* 1353: 103–10.

**CONFERENCE PRESENTATIONS**:

Assessing evolutionary relationships in Lobariaceae using target capture; American Bryological and Lichenological Society meeting, Nederland, Colorado, August 2018

Miocene radiation and the effect of photobiont association on diversification in the genus *Sticta* (Lobariaceae); Botany Conference, Fort Worth, Texas, June 2017

Picking holes in traditional species delimitations: an integrative taxonomic reassessment of *Parmotrema perforatum* group (Parmeliaceae, Ascomycota); International Association for Lichenology, Helsinki, Finland, August 2016

A Defined Transposon-Mutant Library for the *Staphylococcus aureus* Research Community; Wind River Conference on Prokaryotic Biology, Estes Park, Colorado; 2011 Jun

A Defined Transposon-Mutant Library for the *Staphylococcus aureus* Research Community; American Society for Microbiology Annual Meeting of the Missouri Valley Branch, Lincoln, Nebraska; March 2011

Testing Species Delimitations in the *Parmotrema peforatum* group (Parmeliaceae, Ascomycota) in Eastern North America; Botany and Mycology 2009, Snowbird, Utah; July 2009

Testing Species Delimitations in the *Parmotrema perforatum* Group in Eastern North America;

International Association on Lichenology/American Bryological and Lichenological Society joint meeting, Asilomar Conference grounds, Monterey California; July 2008

Phylogenetic Relationships in the *Parmotrema perforatum* Group in North America based on the glyceraldehyde-3-phosphate dehydrogenase (*GPD*) gene; American Bryological and Lichenological Society meeting, Xalapa, Veracruz, Mexico; August 2007

The *Parmotrema perforatum* group: A New Look at an Old Problem in Lichen Taxonomy; Nebraska Academy of Sciences Annual Meeting, Lincoln, NE; April 2007

**GRANTS AND AWARDS**:

Armour Fellowship, Field Museum
American Bryological and Lichenological Society student travel award
Culberson & Hale Award, American Bryological and Lichenological Society
UIC LAS Student Travel Award
UIC BIOS Student Travel Award
UIC Student Presenter Award
UIC Graduate Student Council travel award
British Lichen Society Travel Grant for IAL8
UIC Liberal Arts and Sciences travel funds
NSF and the Society for Systematic Biology Travel Award, Phylogenetics Symposium
UIC Bodmer Award for International Travel
UIC Elmer Hadley Award
A. J. Sharp Award, American Brylogical and Lichenological Society
University of Nebraska at Omaha, University Committee on Research Travel Award
American Bryological and Lichenological Society
Thelotremataceae Lichen Workshop Travel Award, Thailand
American Bryological and Lichenological Society
UNO Summer Graduate Scholarship
NASA Nebraska Space Grant Program
Philadelphia Botanical Club Bayard Long Award
University of Nebraska at Omaha Biology Department Grant
Outstanding Undergraduate in Environmental Studies
Seasonal Employee of the Year, US Fish and Wildlife Service, Crescent Lake NWR

**TEACHING EXPERIENCE**:

Computational Biology at the Field Museum Workshop (assisted teaching)
General Microbiology Laboratory (Bios 351), University of Illinois at Chicago
Biology of Cell and Organisms Laboratory (Bios 100), University of Illinois at Chicago
SERTs Tutorial at the Field Museum, Northwestern University
Lichenology Laboratory, University of Nebraska at Omaha
Microbial Physiology Laboratory, University of Nebraska at Omaha

Biology of Fungi Laboratory, University of Nebraska at Omaha
Flora of the Great Plains, University of Nebraska at Omaha
Biology 1450, Biology I Laboratory, University of Nebraska at Omaha

**ACADEMIC SERVICE**:

University of Nebraska at Omaha, Graduate Student Representative, Graduate Program Committee
Article peer reviewer for Evolution

**PROFESSIONAL AFFILIATIONS**:

American Bryological and Lichenological Society
British Lichen Society

**SCIENTIFIC OUTREACH**:

Field Museum Dozin with The Dinos
Field Museum Talk to a Scientist
Field Museum This is How We Science
Field Museum Members' Night

# PERMISSION TO REPRINT

**OXFORD UNIVERSITY PRESS LICENSE**
**TERMS AND CONDITIONS**

Jan 19, 2019

This Agreement between Todd J Widhelm ("You") and Oxford University Press ("Oxford University Press") consists of your license details and the terms and conditions provided by Oxford University Press and Copyright Clearance Center.

| | |
|---|---|
| License Number | 4512550098133 |
| License date | Jan 19, 2019 |
| Licensed content publisher | Oxford University Press |
| Licensed content publication | Botanical Journal of the Linnean Sociey |
| Licensed content title | Picking holes in traditional species delimitations: an integrative taxonomic reassessment of the *Parmotrema perforatum* group (Parmeliaceae, Ascomycota) |
| Licensed content author | Widhelm, Todd J.; Egan, Robert S. |
| Licensed content date | Nov 14, 2016 |
| Type of Use | Thesis/Dissertation |
| Institution name | |
| Title of your work | Systematics of lichenized fungi from families to populations |
| Publisher of your work | University of Illinois at Chicago |
| Expected publication date | Mar 2019 |
| Permissions cost | 0.00 USD |
| Value added tax | 0.00 USD |
| Total | 0.00 USD |
| Title | Systematics of lichenized fungi from families to populations |
| Institution name | University of Illinois at Chicago |
| Expected presentation date | Mar 2019 |
| Requestor Location | Todd J Widhelm<br>Field Museum<br>1400 S Lake Shore Dr<br><br>CHICAGO, IL 60605<br>United States<br>Attn: Todd J Widhelm |
| Publisher Tax ID | GB125506730 |
| Billing Type | Invoice |
| Billing Address | Todd J Widhelm<br>Field Museum<br>1400 S Lake Shore Dr<br><br>CHICAGO, IL 60605<br>United States<br>Attn: Todd J Widhelm |
| Total | 0.00 USD |
| Terms and Conditions | |

**STANDARD TERMS AND CONDITIONS FOR REPRODUCTION OF MATERIAL FROM AN OXFORD UNIVERSITY PRESS JOURNAL**